2022

Ionic liquids as a versatile tool to study antimicrobial strategies of and against filamentous fungi.

Maika Clara Rothkegel

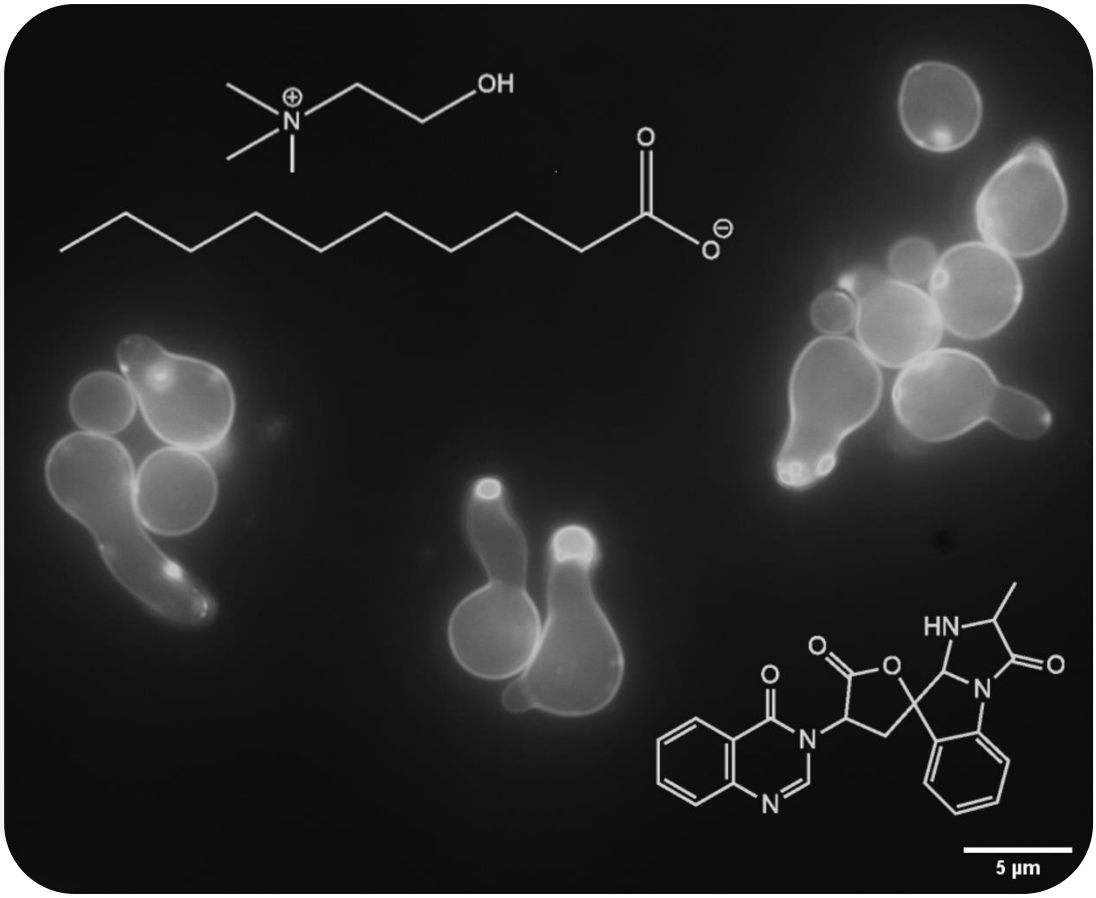

Dissertation presented to obtain the **Ph.D degree in Biochemistry.**

Molecular Biosciences PhD Programme

Oeiras, May, 2022

Ionic liquids as a versatile tool to study antimicrobial strategies of and against filamentous fungi.

Maika Clara Rothkegel

Dissertation presented to obtain the PhD degree in Biochemistry.

Instituto de Tecnologia Química e Biológica António Xavier | Universidade Nova de Lisboa

Oeiras, May 2022

I declare that the work presented in this thesis, except where otherwise stated, is based on my own research. It was supervised by Doctor Cristina Silva Pereira. The work was mainly performed in *Instituto de Tecnologia Química e Biológica*, *Universidade Nova de Lisboa*, between May 2016 and August 2021.

I am grateful for the financial support provided by *Fundação para a Ciência e Tecnologia* for the fellowship PD / BD / 113989 / 2015 and the project "PinusResina" (reference PDR2020-101-031905 financed by PDR2020) for the fellowship 017/BI/2021. I also acknowledge funding support from the European Research Council through grant ERC 2014-CoG-647928.

Acknowledgements

The completion of this thesis was only possible with the help of several people, to whom I wish to acknowledge.

First, I wish to thank my supervisor Cristina Silva Pereira for making this work possible. Cristina, thank you for your continuous support and believe in the project, for looking forward and finding solutions with me. I thank you for always finding the time to talk, no matter how many issues you had to deal with at the same time. Your resourcefulness, creativity and optimism are inspiring!

Of course, I would not have made it without the great help of all the lab members. My deepest gratitude goes to Patrícia Gonçalves, Patrícia Sequeira and Diego Hartmann. Without your practical and emotional support, I would never have finished this work! I will never forget our wonderful time together and all the good food we shared! A special thanks also goes to Isabel Martins, Cristina Leitão and André Cairrão for their valuable help in various projects.

I want to thank Pedro Lima for the collaborative project with Sea4us, expanding my scientific repertoire. Particularly for the opportunity to join the BlueBioValue Startup accelerator and his support throughout the program, which has been a great learning experience.

Not to forget the ITQB community and my colleagues from the MolBios program, especially Eleonora Marini, Filipa Sena, Joana Dias and Catarina Gaspar. But also, the Covid-19 volunteer group, the shifts were always fun and a welcome change to the everyday lab life. I always felt welcomed and grateful for the time I got to spend in such an amazing country and city!

Finally, I want to thank my family and friends outside of ITQB. The wonderful friendships I have made in Lisbon and all the dear people who came to visit and to support our family. I cannot name them all, but my dearest thanks go to Moritz, for always believing in me, and Emil, my greatest joy!

Table of contents

Summary

Life threatening microbial infections caused by pathogenic bacteria or fungi are becoming an increasing concern for our society, due to the increasing appearance of antimicrobial (multi-)resistant strains and the lack of appropriate treatment options. In the case of fungal infections, *Aspergillus* spp. can lead to severe invasive infections with *Aspergillus fumigatus* being the main cause, especially in severely immunocompromised patients. On the other hand, filamentous fungi harbor a vast number of biosynthetic backbone genes for secondary metabolites. Fungal secondary metabolites have been studied intensively for their antibiotic and antifungal potential, as well as their role during pathogenesis to identify virulence factors, potential targets for drug development and biomarkers. Media supplementation with ionic liquids, salts with a melting point below a temperature of 100°C, have been shown to induce diverse stress responses in filamentous fungi, including the production and secretion of otherwise cryptic secondary metabolites. This thesis aimed to investigate different approaches to identify novel strategies against microbial infections with a focus on *A. fumigatus* as a pathogen but also as a producer of bioactive compounds, combining fungal biology and secondary metabolism with the versatile applications of ionic liquids.

Owing to their toxic nature against filamentous fungi, ionic liquids can be exploited as antimicrobial drugs themselves (Chapter II). We combined an anionic form of the widely used antifungal drug Amphotericin B ([AmB]), with several cations to form ionic liquids as a novel formulation to overcome problems of other formulations such as low solubility and permeability. Susceptibility assays, gene expression analyses and molecular dynamic simulations revealed that the formulations with cholinium ([chol][AmB]) and cetylpyridinium ([C16py][AmB]) provide increased antifungal activity against *Aspergillus fumigatus* as well as *Aspergillus terreus*, while maintaining the mechanism of action of Amphotericin B. Furthermore, the combination with

cetylpyridinium - an antiseptic in clinical use - showed preservation of antibacterial properties, suggesting that ionic formulations of combined drugs maintain both, antifungal and antibiotic, functionalities while potentially improving administration, efficacy and safety.

Aiming to identify bioactive secondary metabolites from filamentous fungi, cholinium based ionic liquids were exploited. Ionic liquid supplemented cultures showed an altered diversity of secreted secondary metabolites in *Aspergillus fumigatus*, *Neurospora crassa* and *Aspergillus nidulans,* shown by the resulting fingerprints of secreted compounds in liquid chromatography and mass spectrometry analyses (Chapter III & IV). Short term exposure of *A. fumigatus* to sub-lethal concentrations of the ionic liquid led to the presence of growth and germination enhancing compounds in the spent medium. Compounds of the ergot alkaloid class were identified, specifically tryptoquivaline F which proved to be capable of inducing germination (Chapter III). Exposure to other toxic agents, including antifungal drugs, recapitulated the phenomenon, indicating a stress response involving growth inducing signaling molecules. Identifying such compounds that allow fungi to coordinate specific developmental stages creates the opportunity to develop strategies to counteract detrimental fungal growth. Longer exposure of *A. fumigatus* and *N. crassa* to sub-lethal concentrations of ionic liquids led to the production and secretion of metabolites with potent activity against *Escherichia coli* and *Staphylococcus aureus* (Chapter IV). Liquid chromatography and mass spectrometry analyses indicated the presence of peptides containing various non proteinogenic amino acids, macrolides and (cyclic) depsipeptides, compounds with valuable characteristics for the development of potent antimicrobial drugs.

The work in this thesis contributes to the array of approaches available to study antimicrobial strategies with emphasis on combining the versatility of ionic liquids with fungal biology.

Sumário

As infecções microbianas com risco de vida estão a tornar-se uma preocupação crescente, devido as estirpes antimicrobianas (multi-) resistentes e à falta de opções de tratamento adequados. No caso de infecções fúngicas, *Aspergillus* spp., principalmente o *A. fumigatus*, podem levar a infecções invasivas graves, especialmente em pacientes gravemente imunocomprometidos. Por outro lado, os fungos filamentosos comportam um grande número de genes de biossíntese para metabólitos secundários. Estes compostos têm sido estudados intensivamente devido ao potencial antibiótico e antifúngico, bem como o seu papel durante a patogénese para identificar fatores de virulência. A suplementação de meios com líquidos iónicos, sais com um ponto de fusão abaixo de 100°C, demonstrou induzir diversas respostas em fungos filamentosos, incluindo a produção e secreção de metabolitos secundários crípticos. Este trabalho investigou diferentes abordagens para identificar estratégias contra infecções microbianas com foco em *A. fumigatus* como patógeno, mas também como produtor de compostos bioativos, combinando a biologia fúngica e o metabolismo secundário com as aplicações versáteis de líquidos iónicos.

Devido à sua natureza tóxica contra fungos filamentosos, os líquidos iónicos podem ser explorados como compostos antimicrobianos (Capítulo II). Combinamos uma forma aniónica do composto antifúngico amplamente utilizado Anfotericina B ([AmB]), com vários catiões para formar líquidos iónicos para superar problemas de outras formulações, como baixa solubilidade e permeabilidade. Ensaios de suscetibilidade, análises de expressão génica e simulações de dinâmica molecular revelaram que as formulações com colínio ([chol][AmB]) e cetilpiridínio ([C16py][AmB]) proporcionam maior atividade antifúngica contra *A. fumigatus* e *A. terreus*, mantendo o mecanismo de ação da Anfotericina B. Além disso, a combinação com cetilpiridínio - um antisséptico em uso clínico - mostrou

preservação das propriedades antibacterianas, sugerindo que a combinação de formulações iónicas com medicamentos mantêm as respectivas funcionalidades, enquanto potencialmente melhoram a administração.

Com o objetivo de identificar metabolitos secundários bioativos de fungos filamentosos, foram explorados líquidos iónicos à base do catião colínio. As culturas suplementadas com líquido iónico mostraram uma diversidade alterada de metabólitos secundários secretados em *A. fumigatus*, *N. crassa* e *A. nidulans*, demonstrando diferentes perfis de compostos secretados através de cromatografia líquida e análises de espectrometria de massa (Capítulo III e IV). A exposição de curto prazo de *A. fumigatus* a concentrações sub-letais do líquido iónico levou à presença de compostos no meio sobrenadante que melhoram o crescimento e a germinação no próprio fungo. Foi identificado a alcalóid triptoquivalina F que mostrou ser capaz de induzir a germinação (Capítulo III). A exposição a outros agentes tóxicos, incluindo compostos antifúngicos, replicou o fenómeno, indicando que a resposta ao stresse envolve moléculas sinalizadoras indutoras de crescimento. A identificação de tais compostos que permitem que os fungos coordenem estágios específicos de desenvolvimento cria a oportunidade de desenvolver estratégias para neutralizar o crescimento fúngico de forma descontrolada. A exposição mais prolongada de *A. fumigatus* e *N. crassa* a concentrações sub-letais de líquidos iónicos levou à produção e secreção de metabolitos com eficaz atividade contra *E. coli* e *S. aureus* (Capítulo IV). Análises por cromatografia líquida e espectrometria de massa indicaram a presença de peptidos contendo diversos aminoácidos não proteinogénicos, macrolides e depsipeptidos (cíclicos), metabolitos com características vantajosas para o desenvolvimento de compostos antimicrobianos eficazes.

O trabalho desenvolvido nesta tese contribui para a variedade de abordagens para estudar estratégias antimicrobianas com ênfase na combinação da versatilidade de líquidos iónicos com a biologia fúngica.

List of acronyms

ACC	1-Aminocyclopropane-1-carboxylic acid
Aib	2-Aminoisobutyric acid / α-aminoisobutyric acid
AmB	Amphotericin B
C_{16}py	Cetylpyridinium
CAS	Caspofungin
ChoCl	Cholinium chloride
ChoDec	Choline decanoate
Chol	Cholinium
CoA	Coenzyme A
DKP	2,5-diketopiperazine
DNA	Deoxyribonucleic acid
GNPS	Global Natural Product Social Molecular Networking
GST	Glutathione S-transferase
HPLC	High-performance liquid chromatography
HRMS	High resolution mass spectrometry
IC_{50}	Half-maximal inhibitory concentration
IL	Ionic liquid
ITC	Itraconazole
LC	Liquid chromatography
MeOH	Methanol
MIC	Minimal inhibitory concentration
MS	Mass spectrometry

MTT	3-(4,5-dimethylthiazol-2-yl)-2,5-diphenyl tetrazolium bromide
NaDec	Sodium decanoate
NPAA	Non-proteinogenic amino acid
NRP	Non-ribosomal peptide
NRPS	Non-ribosomal peptide synthetase
OD	Optical density
$P_{6\,6\,6\,14}$	Trihexyltetradecylphosphonium
PCR	Polymerase chain reaction
Phe	Phenylalanine
PK	Polyketide
PKS	Polyketide synthase
qRT-PCR	Quantitative Real-Time PCR
QSM	Quorum sensing molecule
RiPP	Ribosomally synthesized and post-translationally modified peptide
RNA	Ribonucleic acid
ROS	Reactive oxygen species
Ser	Serine
SM	Secondary Metabolite
SME	Spent medium extract
SPE	Solid Phase Extraction
spp.	Species
UPLC	Ultra Performance Liquid Chromatography

Chapter I

Introduction

Introduction

Fungi

“Fungi are everywhere and affect our lives every day, from mushrooms to industrially important products to plant helpers to plant pathogens to human diseases” Thomas J. Volk[1].

Fungi, Mycota, can be found in virtually all environments, as they are heterotrophic organisms, thriving on all kind of organic matter by nutrient adsorption and exhibiting high tolerance towards pH, temperature and water availability. They are eukaryotic organisms, like animals and plants they possess membrane-bound organelles, such as a nucleus, vacuoles, endoplasmic reticulum, Golgi apparatus and mitochondria, as well as cellular features like chromatin and 80S ribosomes[1,2]. They distinguish themselves through their cell wall, composed of chitin, α- and β- linked glucans, glycoproteins, and pigments, which is different from the cellulose-rich cell wall of plants. In contrast to other eukaryotes, fungi are usually haploid, and exhibit vegetative growth in form of filaments extending from their hyphal tips. Though some fungi can grow as single-cell yeasts or switch between both phases, called dimorphic fungi.

Fungi are among the oldest habitants of earth, with estimates of their origin ranging from 760 million years to 1.06 billion years ago[3]. Without them life on earth couldn´t exist, as they have important roles in almost all ecosystems. Fungi produce a diverse range of enzymes and acids, able to break down all kinds of polymeric molecules. The released nutrients are absorbed by the fungi, enabling them to grow on a variety of substrates. Different fungi are adapted to decompose different types of polymers, often living in mixed communities complementing each other’s enzymatic capabilities. Based on their nutrient uptake, fungi can be grouped into saprotrophs, symbionts and parasites. Saprotrophs live on dead organic matter, decomposing it and making it available to other members of the ecosystem. Some saprotrophs

can pose a threat, as they grow on stored food and produce mycotoxins, such as aflatoxins, which are known to be carcinogenic. Symbionts are part of mutualistic associations, for example on plant roots as mycorrhizae, or with algae and cyanobacteria in form of lichen[1]. Parasitic fungi, pathogens, endanger plants and humans. More than 70% of crop diseases are caused by fungi resulting in the loss of billions of dollars' worth of economic crops every year. Some major epidemics have been caused by necrotrophic fungi, like the dutch elm disease, an ongoing pandemic since the 1970s, caused by *Ophiostoma* spp., leading to the decimation of most forest and urban elm populations in North America and Europe. or the mass mortalities of amphibians, bees and bats[4,5]. Human pathogens are especially dangerous for patients with compromised immune systems, e.g. due to organ transplantations, treatments for AIDS, cancer and diabetes, which can lead to life threatening fungal infections with mortality rates up to 90%[6]. Among human pathogens causing nosocomial infections *Candida* spp., *Cryptococcus* spp. and *Aspergillus* spp. are the most prevalent. Despite the downsides, the physiological and ecological features of fungi have encouraged the exploration of their biotechnological potential. They are used in the production of fermented foods, as factories to commercially produce enzymes and compounds relevant for medical purposes, e.g. the antibiotic penicillin, and as easily manipulated models for genetics and cell biology of lower eukaryotes[7–9].

Fungal taxonomy is still evolving and has been subject to many changes and debate. The current taxonomy of known true fungi comprises nine major phyla, the Opisthosporidia, Chytridiomycota, Neocallimastigomycota, Blastocladiomycota, Zoopagomycota, Mucoromycota, Glomeromycota, Ascomycota and Basidiomycota (Figure 1)[10]. The Basidiomycota and Ascomycota are grouped into the subkingdom Dikarya, as they produce cells with two nuclei (di-karyon). The Ascomycota is the largest phylum of fungi encompassing more than ~64,000 known species and a vast number of

undescribed fungi, including yeasts, filamentous fungi, symbionts, saprotrophs, and pathogens[11]. The sexual organs formed by ascomycetes are called ascomata, which contain the characteristic spore-producing cells of the phylum called asci.

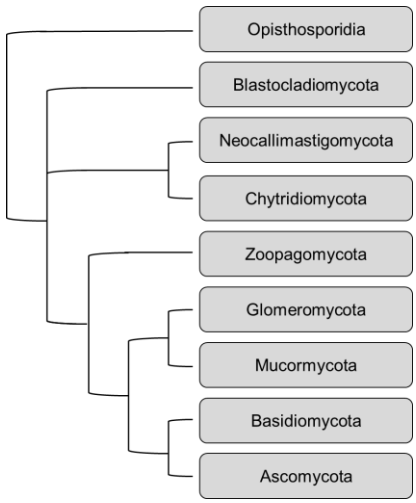

Figure 1 Phylogeny of true fungi

Within the *Ascomycota*, three subphyla have been defined, the *Taphrinomycotina*, *Saccharomycotina* and *Pezizomycotina*[10]. A prominent species within the *Taphrinomycotina* is the fission yeast *Schizosaccharomyces pombe*, widely used as a model organism in cell biology of eukaryotes[12]. Within the subphylum *Saccharomycotina* the budding yeast *Saccharomyces cerevisiae,* widely used for fermentation processes[13] and the species of the genus *Candida*, important human pathogens[14] are well known representatives. The subphylum *Pezizomycotina* contains the filamentous *Ascomycota*, such as the famous *Penicillium rubens,* which led to the discovery of penicillin[7,15], *Neurospora crassa*, an important model organism[16], and the species of the *Aspergillus* genus. The *Aspergillus* genus is one of the most abundant and widespread

on earth including over 185 species, such as *Aspergillus nidulans,* a prominent model organism, and *Aspergillus fumigatus*, a major human pathogen responsible for severe lung infections.

Ascomycota life cycle

Filamentous fungi grow in form of hyphae, a tubular form of 3-10 µm diameter[1]. External factors such as light, nutrients, oxygen, agitation, etc. can change the morphology and physiology of a fungal culture. Under stress or starvation conditions the fungus can switch from a vegetative growth to the formation of sexual or asexual structures[17].

Ascomycota colonies usually start from asexual spores, the conidia. These structures can survive in a state of quiescence for many months. To break their dormancy, cues like water, nutrients and oxygen are required; the specific mechanisms remain unclear though[18,19]. Germination does not require *de novo* RNA synthesis, as active transcripts of one third of the genome are present in the spores[20,21]. When germinating, conidia lose their hydrophobic melanin coating and enter the isotropic growth phase, increasing their diameter twofold or more by taking up water, thereby decreasing viscosity of the cytoplasm[22]. In the next phase, a germ tube emerges, elongating by polarized growth into hyphae (Figure 2).

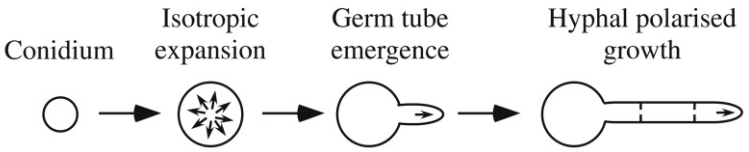

Figure 2 The phases of a germinating conidium, isotropic expansion followed by polarized growth of the germ tube into the hyoha[23]*.*

Those germ tubes elongate into long filaments, which start branching and fusing to form the typical interconnected hyphal network, called mycelium. The tips are the most dynamic area of hyphae, controlling nutrient uptake, secretion, hyphal extension, cell wall synthesis as well as polarized

growth[24,25]. The so called Spitzenkörper, an agglomeration of secretory vesicles just beneath the apical plasma membrane, assembles *de novo* in the emerging tips of germlings and branching hyphae[26] and directs hyphal tip growth in response to external factors by varying its morphology and behaviour[27,28]. The Spitzenkörper can be considered as a supply center, receiving, and distributing signaling molecules and secretory vesicles. Those vesicles provide enzymes and material for cell wall synthesis and plasma membrane expansion, which occurs mainly at expanding hyphal tips[1,29–31]. Around 20-30% of the biomass are constituted by the hyphal cell wall, composed of an inner layer of rigid fibrous polysaccharides and an outer layer of gel-like polymers. It is responsible for maintaining the cell shape and controlling the interactions with the environment, such as acquisition of scarce nutrients, protection against harmful factors, as well as building the interface between fungal pathogens and their hosts[32–34].

Hyphal cells are usually binuclear, hence the name Dikarya, whereas apical hyphae are multinuclear[35,36]. Cell division within the hyphae is called septation. Compartmentalization is achieved through cell wall formation at the division site, called septum, characterized by a composition different from the lateral cell wall[37]. This septum remains permeable, allowing the exchange of cytoplasm, organelles and other cellular components, such as nutrients and signaling molecules along the hyphal network (Figure 3)[38].

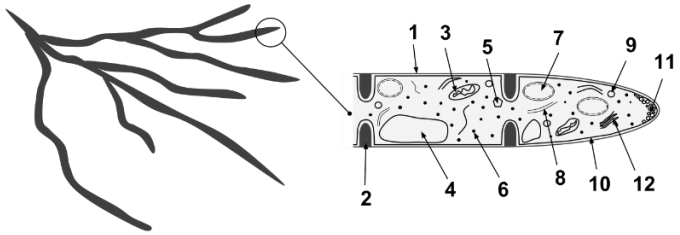

Figure 3 Fungal Hyphae Cells 1- Hyphal wall 2- Septum 3- Mitochondrion 4- Vacuole 5- Crystal 6- Ribosome 7- Nucleus 8- Endoplasmic reticulum 9- Lipid body 10- Plasma membrane 11- Spitzenkörper/growth tip and vesicles 12- Golgi apparatus (credit Wikimedia Commons[39])

Under stress or starvation conditions, vegetative growth switches to either sexual or asexual propagation (Figure 4). Filamentous fungi usually propagate via spores, which are transmitted through the air or water or disseminated by insects[40]. Sporulation can be triggered by various factors - nutrient limitations, light, oxygen availability, temperature variations and other external stress factors. These factors also influence the type of spore being produced, sexual (ascospore) or asexual (conidia). Conidia are more adapted for dispersal, whereas ascospores are specialized to survive harsh conditions with less potential to disseminate. Conidia are highly hydrophobic, due to a hydrophobin coating, and rise above the mycelial mat. Wind, physical contact or splashing raindrops can lead to their release into the air, where they can be transported over large distances to reach new grounds with favorable growth conditions[41].

Whereas colonies growing in nature, can reach new sources of nutrients by hyphal extension, nutrient supply in fungal cultures is limited. When grown on solid medium, fungi form radial colonies; when grown in static liquid, they build a mat of hyphae at the surface of the liquid, whereas agitation usually results in submerged fungal pellets. Submerged fungal cultures initiated from spores can be roughly characterized by four stages. The lag phase, the time it takes to break dormancy and germination to start, followed by the exponential phase, where biomass increases exponentially at a specific growth rate[42]. Finally, cultures enter the stationary phase, when nutrients in the medium are depleted and the maximum biomass is achieved. When the stationary phase is reached, cell death and autolysis occur, releasing nutrients that can lead to new cell growth. When the rate of cell death exceeds the growth rate, overall biomass is reduced, and the organism enters the decline phase[43,44]. The individual shape of the growth curve largely depend on the initial inoculum and the nutrient composition of the medium[42].

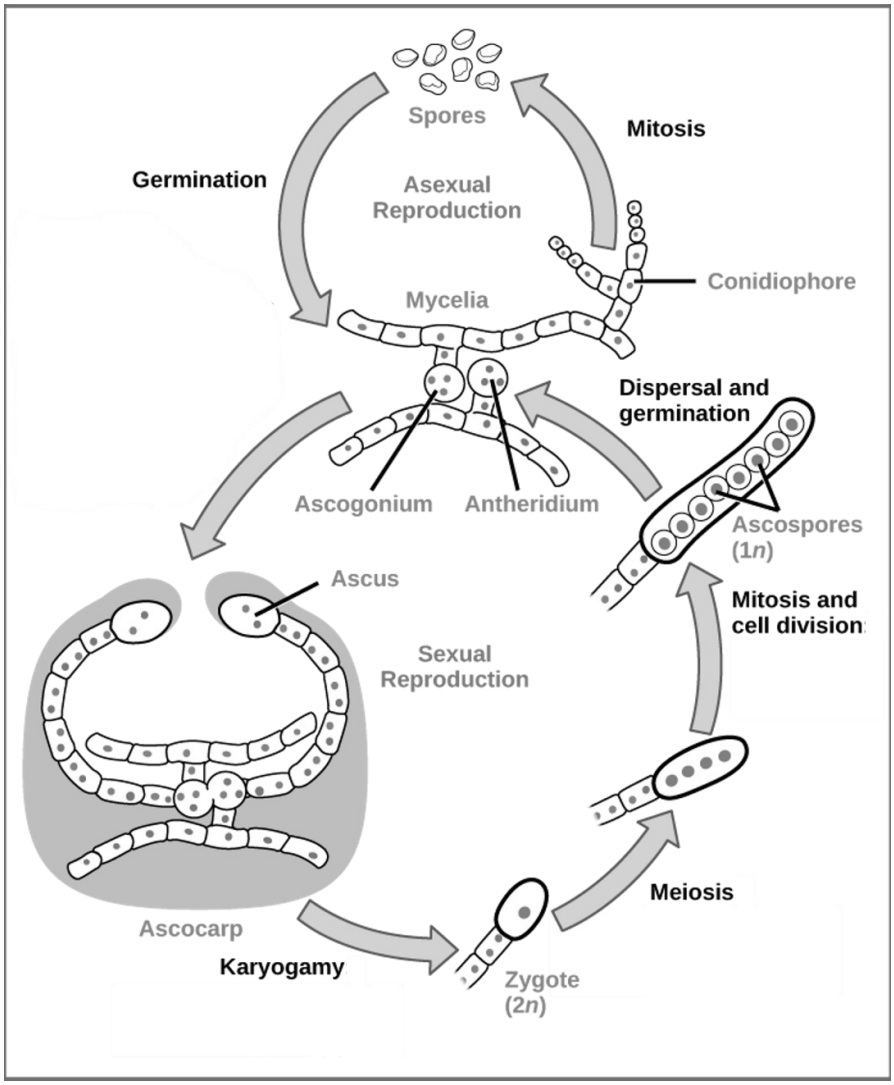

Figure 4 Ascomycota life cycle (Source: OpenStax Microbiology)

Neurospora crassa

Neurospora crassa (*N. crassa*) is commonly observed growing on burned wood after a forest fire. It was first described as a contaminant in French bakeries (champignons rouges)[45]. Nearly one century after the initial description of the "red-bread mold", it was classified as the new genus *Neurospora* based on the observation of a complete sexual cycle (Figure 5)[46]. To date, at least 43 species are recognized, of which 13 are heterothallic

(sexual reproduction requiring two distinct mating types), 28 are homothallic (spores are self-fertile, both mating types are combined in one single genome) and 2 are pseudohomothallic (self-fertility results from two independent, opposite mating type nuclei within a single spore)[47–50]. *Neurospora crassa* attributes, such as its minimal requirements, its incredibly fast growth (~3 mm/h), a short life cycle, and its haploid genetics, make it an attractive model organism for genetic studies. It was first developed as an experimental organism by Dodge and later adopted by Beadle and Tatum for their famous “one gene–one protein” studies linking biochemistry and genetics[51,52]. *Neurospora crassa* has been especially useful for studies on photobiology, circadian rhythms, population biology, morphogenesis, mitochondrial import, DNA repair and recombination, DNA methylation, and other epigenetic processes, that are applicable for fungi, as well as across all kingdoms of life[53,54].

Neurospora crassa has two mating types (*A* and *a*), which are morphologically indistinguishable from each other. The vegetative phase is initiated when either a sexual spore (ascospore) or an asexual spore (conidium) germinates. Whereas conidial cells germinate spontaneously, ascospore germination is activated by heat, either by a fire in the wild or heat shock in the laboratory. After the mycelium is well established, two types of asexual sporulation can occur, which are usually triggered by circadian rhythms[55]. The hyphae can differentiate into microconidia, which are uninucleate and have lower viability or into conidiophores leading to the production of multinucleated macroconidia with a characteristic orange color due to the presence of carotenoids[1,53].

The conidia, which contain one to several nuclei each, can either establish new vegetative cultures or fertilize strains of the opposite mating type (Figure 5). Each colony can produce both male and female structures but mating only occurs between colonies that encode opposite mating types. If nutrients

are limited or upon changes in light and temperature, the sexual phase is initiated by producing nascent fruiting bodies ("protoperithecia"). When a specialized hypha ("trichogyne") chemotropically grows from the protoperithecium towards a "male" cell of the opposite mating type, cell fusion can occur, and an acquired "male" nucleus is transported back to the protoperithecium[56]. The two haploid nuclei undergo repeated divisions within a developing dikaryotic ascogenous hyphae and form the crozier, where cell fusion occurs, which ultimately becomes an ascus containing the eight meiotic ascospores[57,58]. This process is replicated many times, resulting in hundreds of asci within a single fruiting body.

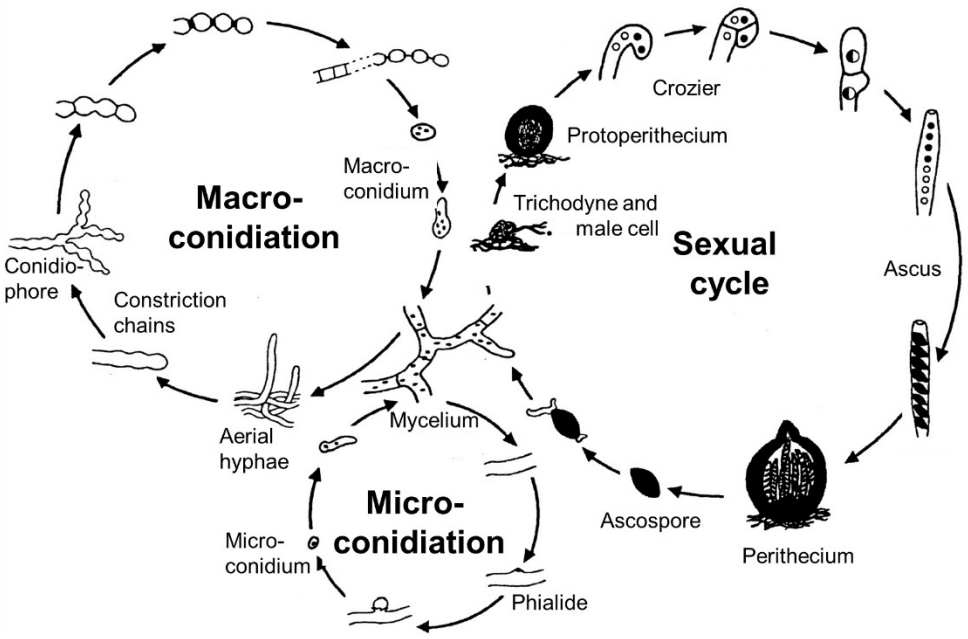

Figure 5 Neurospora crassa life cycle, adopted from Borkovich et al.[53]

Aspergillus nidulans and *Aspergillus fumigatus*

The generic name *Aspergillus* is derived from the Latin aspergillum, a mop for distributing holy water and refers to the appearance of the mature conidiophores[59]. *Aspergilli* are normally haploid but can also grow as heterokaryons or vegetative diploids. Both asexual spores (conidia) and

sexual spores (ascospores), which are usually released from the conidiophore or the ascocarp (cleistothecium), can be produced (Figure 4). A conidiophore grows perpendicular from the mycelium and starts swelling at the tip, forming the vesicle. From the vesicle arise numerous tubular outgrowths, the phialides, which can carry conidia, or they may branch to give further phialides with conidia. *Aspergillus* conidia have a characteristic dark color due to melanin or melanin-like pigments in their cell wall. They are highly stress resistant and rest in a state of dormancy, preventing them from germinating prematurely. Most *Aspergillus species* are homothallic, self-fertile; therefore, any two strains can mate and enter the sexual stage. When sexual reproduction is triggered, hyphae fuse to produce dikaryotic hyphae, the ascogonium and antheridium, which further develop into the cleistothecia, approximately spherical closed ascocarps. Thick-walled Hülle cells may surround the developing cleistothecia to protect them during their development providing nutrients and protection[17,60]. The fertile hyphae within the cleistothecium undergo differentiation and form asci, containing ascospores[55]. Ascospores are released upon physical rupture of cleistothecia[1].

The model filamentous fungus *Aspergillus nidulans (A. nidulans)*, a common soil organism, has had an important role in the development of genetics, e.g. utilized by Pontecorvo to establish that genetic analysis could be carried out in self-fertile organisms, and is one of the most well studied fungi regarding secondary metabolism[61,62].

Aspergillus fumigatus (A. fumigatus) is a thermotolerant, extremely common fungus. It can grow at temperatures between 12°C and 52°C and can be found in a wide range of environments. It grows commonly in composts, on moldy grain, and on other decaying organic matter. But it is also known for infecting humans, colonizing the respiratory tract if conditions are favorable[63].

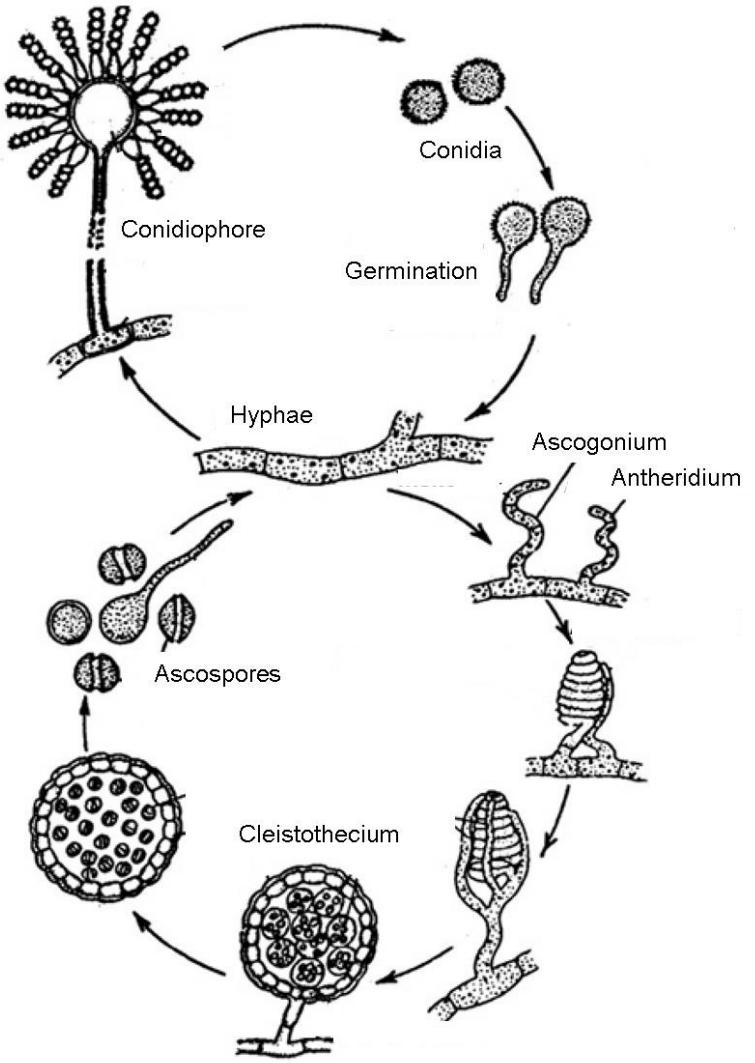

Figure 6 The Aspergillus nidulans life cycle, adapted from Diano et al.[64]

Aspergillosis

Few species among the Aspergillus genus can be a threat to humans and animals. About 90% of infections are caused by A. fumigatus, but other species, mainly A. flavus, A. niger, A. terreus and A. nidulans, in this order, are frequently isolated from patients as well[65–67]. Those air-borne infections are caused by the asexual conidia produced by the fungus, which are inhaled by the host organism. Usually, conidia are eliminated by the innate immune

system, but in immunocompromised hosts, they can become opportunistic and lead to allergic aspergillosis, chronic aspergillosis or invasive aspergillosis. When conidia germinate in the lung, fungal hyphae can invade the pulmonary arterioles and lung parenchyma and when entering the blood stream even reach distant organs such as kidneys, liver, spleen, sinuses and central nervous system[68,69]. Invasive pulmonary aspergillosis is a community-acquired pneumonia that predominantly occurs in stem cell and solid organ transplant recipients, but increasingly as well in patients suffering from cancer, autoimmune or inflammatory diseases[70–72]. Mortality rates in severely immunocompromised patients can reach up to 50% or, if untreated, even up to 100%[63,73]. Such high mortality rates are in large part due to a limited number of antifungal options available as well as insufficient diagnostics, but at the same time derives from a lack of understanding the complex mechanisms underlying host colonization and development of infection[63].

Aspergillus pathogenicity is a multifactorial trait (Figure 7)[74]. Being a saprophytic fungus, it had to evolve many strategies to acquire nutrients in niche environments and resist microbial enemies, thus developing great flexibility[74,75]. *Aspergillus fumigatus* pathogenicity does not derive from specific virulence factors, but from the overall adaptation to its host environment. Especially for disease persistence and progression, many key pathways are still insufficiently defined and need further analysis. Nutrient acquisition and subsequent metabolic processes are crucial for initial host colonization and promote invasion as well as long-term survival within the host[76]. Several anabolic and metabolic traits are fungal specific and absent in higher eukaryotes, thus posing an interesting target for antifungal drugs[77,78].

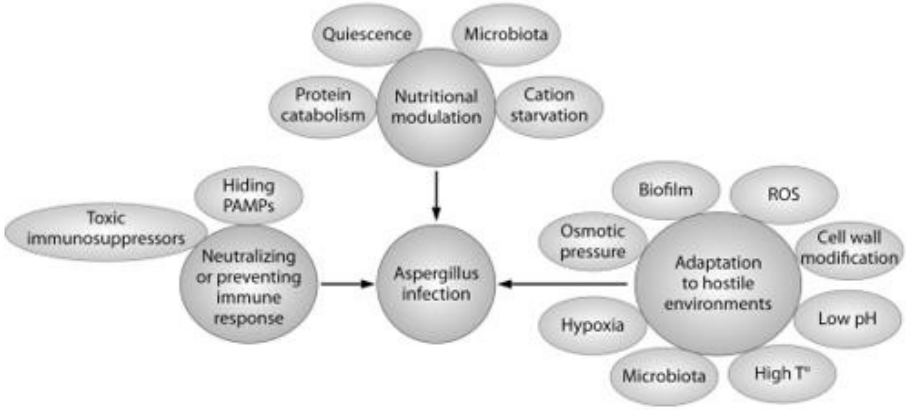

Figure 7 Adopted from Latgé et al.[63] *A. fumigatus multifactorial virulence.*

Antifungals

Currently there are only three classes of antifungal drugs available to treat aspergillosis, polyenes, azoles and echinocandins (Figure 8). Polyenes represent the oldest class, whereas the first compound to be discovered was amphotericin B, being the only polyene used to treat aspergillosis. Amphotericin B binds to ergosterol, the major component unique to fungal membranes, leading to membrane leakage and therefore cell death[79]. It is the most broad-spectrum antifungal on the market. Azoles also target ergosterol by inhibiting its biosynthesis pathway. They are the most widely used antifungal drug class and considered first-line agents for the treatment of invasive fungal infections, especially voriconazole and posaconazole[80]. *Aspergillus fumigatus* is susceptible towards most azoles, whereas it has an intrinsic resistance towards others, such as fluconazole[81,82]. The fungicidal activity is caused by the inhibition of the lanosterol 14-α-demethylase (*CYP51)*, a key enzyme in the ergosterol biosynthesis pathway, inducing a compensatory cell wall stress. This leads to the formation of carbohydrate patches that penetrate the plasma membrane, thereby causing sudden cell integrity failure and fungal death[83]. The last and relatively most recent class of drugs are the echinocandins, which are used as second-line therapy for invasive aspergillosis, namely caspofungin, micafungin, and anidulafungin.

They inhibit noncompetitively the β-1,3-glucan synthase, a key enzyme responsible for the synthesis of the major fungal cell wall carbohydrate β-1,3-glucan. Echinocandins are fungistatic, except caspofungin that showed to be fungicidal towards *A. fumigatus*[84]. Flucytosine constitutes a fourth class of antifungals, a pyrimidine, inhibiting DNA and RNA biosynthesis. It is mostly restricted to the treatment of cryptococcal meningitis and not applied against invasive aspergillosis[85].

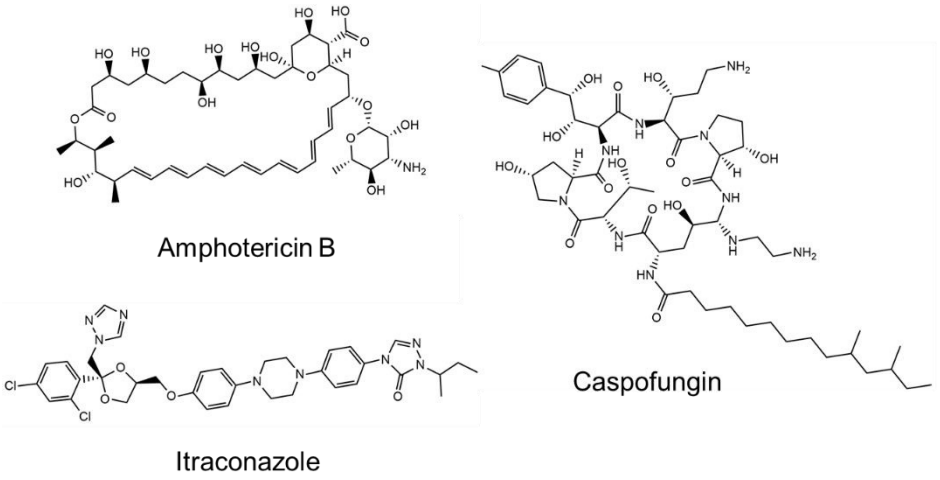

Figure 8 Structures of common antifungal drugs applied against invasive aspergillosis. The polyene Amphotericin B, the azole Itraconazole and Caspofungin, an echinocandin.

In vitro susceptibility tests show an echinocandin-specific, so-called paradoxical effect, which has been observed for *Candida* spp. as well as *Aspergillus* spp. This effect is characterized by a complete susceptibility towards the fungal drug at low and very high concentrations, but at moderate to high concentrations inhibition is incomplete and fungal growth reconstituted[86]. Approximately 2-3 days after treatment, paradoxically growing hyphae emerge, which show fast growth, normal morphology, reconstituted β-1,3-glucan synthesis and normalized levels of cell wall chitin[87]. The clinical impact of the paradoxical effect remains highly debated, though there are several studies suggesting an impact *in vivo* as well[87–89].

Resistance and antifungal drug development

Resistance of *Aspergillus* spp. against azole treatments, in contrast to echinocandins and amphotericin B, is growing and case reports show that infections with azole resistant strains are linked with higher mortality rates[90,91]. This can be explained by increased drug use for prophylactic reasons and long-term treatments, as well as agricultural fungicides with similar targets as medically relevant antifungals leading to environmental reservoirs of resistant *Aspergillus* spp.[91–93]. A lack of novel antifungals targeting unique fungal traits might cause future challenges fighting resistant invasive infections.

Unfortunately, antifungal drug discovery has not been keeping up with the evolving emergence of resistance. All four classes of antifungals available to date, have been already introduced (azoles, polyenes, flucytosine) or at least discovered (echinocandins) before 1980[94]. Big pharmaceutical companies are reluctant to develop new antifungal therapeutics, since clinical trials are expensive, and the expected financial returns are not covering the discovery expenses. Antifungal drug discovery is thus left to smaller biotech companies with more limited resources[95]. One limitation in this research line are the potential targets, since fungi, like humans, are eukaryotic organisms and cytotoxicity is a high risk[95]. For this reason, most of the agents currently under development are also targeting ergosterol or the β-1,3-glucan synthase[95]. Some innovative antifungal drug candidates include an inhibitor of glycosylphosphatidylinositol (GPI)-anchored protein maturation (fosmanogepix), an inhibitor of the *de novo* pyrimidine biosynthesis (Olorofim) and Aureobasidin A, a cyclic peptide that inhibits fungal sphingolipid biosynthesis[96–98]. With limited research efforts of pharmaceutical companies, academic research is the major source for the identification of potential antifungal agents with novel mode of actions and targets. Some promising targets under investigation include the calcineurin and RAS pathways, sphingolipid biosynthesis, as well as the trehalose biosynthetic

pathway[99]. Furthermore, understanding pathogenesis mechanisms in more detail can lead to the identification of specific anti-virulence agents[100]. Apart from studying fungal biology to identify potential targets for antifungal drug development, natural products screening is the most common approach to identify antifungal compounds[101]. Most antimicrobial agents to date have their origin in other living organisms. Polyenes are derived from bacteria whereas echinocandins are derivatives of fungal compounds[102,103]. Screenings for bioactive compounds commonly investigate bacteria, fungi, and plants. While for a long time, the focus has been on terrestrial organisms, as they were more accessible, since the 1980s a large number of research has been conducted on marine organisms, identifying a whole new range of promising molecules[104,105].

Secondary metabolism and signaling molecules

Filamentous fungi produce a wide range of secondary metabolites (SMs). They are low-molecular mass molecules that are non-essential for growth, reproduction or development[106]. Fungal SMs are usually produced when the fungus is not actively growing anymore and under specific environmental conditions. They are thought to play an important role for survival by providing the fungus with competitive advantages in its ecological niche, such as nutrient acquisition, self-protection and defense, inhibition of competing microorganisms and communication with their biotic environment[106–109].

SMs from fungi, but also all kind of other organisms, plants, marine organisms, and bacteria, have been studied intensively for their diverse bioactive properties as they can have valuable biotechnological or clinical applications. Fungi, especially those belonging to the *Ascomycota* phylum, are known to produce compounds used as antibiotics (e.g. penicillin), immunosuppressants (e.g. cyclosporine) and antitumor agents (*e.g.* camptothecin), among others[7,110]. A major constraint in the discovery of novel

fungal bioactive SMs is the fact that SMs often remain cryptic under standard laboratory conditions. As the particular stimuli leading to their activation are largely unknown and not given in this setting, they are not being synthesized[110–112]. Different strategies have thus been proposed to induce secondary metabolism production. Co-cultivation with other fungal or bacterial strains to promote inter-species interactions, or genome engineering such as activating key regulators of the biosynthesis backbone genes are some examples[110,113,114]. A more simple and rapid approach is media supplementation with exogenous agents to cause diverse stimuli leading to the activation of biosynthetic genes[115]. Sequencing analyses strongly indicate a significant gap between the number of fungal SM biosynthesis backbone genes and the isolated molecules to date, suggesting that the majority of secondary metabolites have yet to be discovered[110,116]. Those genes are usually located in clusters, encoding extremely large multidomain, multimodular enzymes[110]. The enzymes responsible for the production of SMs or at least the first step of biosynthesis, are one of the following: polyketide synthases (PKSs), nonribosomal peptide synthetases (NRPSs), hybrid NRPS–PKS enzymes, prenyltransferases and terpene cyclases[110,117].

Those enzymes produce the five main classes of secondary metabolites, polyketides, non-ribosomal peptides, ribosomally synthesized and post translationally modified peptides (RiPPs), indole alkaloids (or shikimic acid derived compounds) and terpenes, as well as some hybrid combinations like NRP-PKs, which involve more than one type of biosynthesis enzyme[118–121].

Polyketides (PKs) comprise the largest class of fungal secondary metabolites with a high degree of structural diversity, although they are synthesized from simple acyl building blocks, such as acetyl-CoA and malonyl-CoA[110,122]. Polyketide synthases consist of several modules, each in turn containing several domains, which are responsible for one chain

elongation by addition of a carboxylic acid building block. The polyketide scaffold can then be further modified by oxygenases, glycosyltransferase and other transferases[110]. Several polyketides were already successfully linked to their corresponding biosynthetic gene cluster, for example monodictyphenone[123] and orsellinic acid[124]. Just like their high structural diversity, polyketides display diverse biological activities, as antibiotics (griseofulvin)[125], immunosuppressants (mycophenolic acid)[126], cholesterol-lowering (lovastatin)[127] and antitumoral agents (emodin)[128].

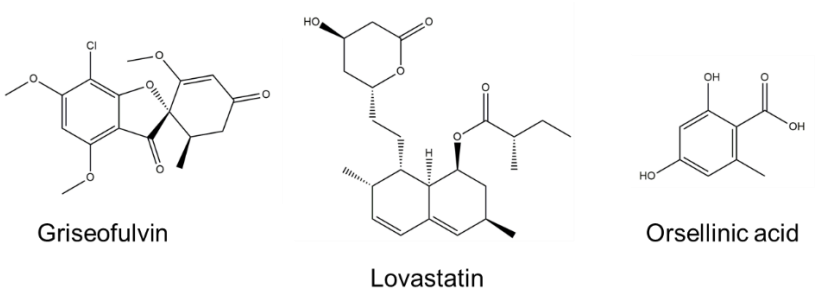

Figure 9 Examples of polyketides, the antibiotic griseofulvin[125], the cholesterol-lowering agent lovastatin[127] and orsellinic acid[124].

Nonribosomal peptides (NRPs) are the second largest group of secondary metabolites. They are linear or cyclic peptides containing proteinogenic, as well as non-proteinogenic amino acids with potential modifications[129]. NRPSs, like PKSs, contain modules comprising several domains as well, which assemble the NRPs successively[110,129]. NRPs are for example the antibiotic echinocandin B, the immunosuppressant cyclosporin A, siderophores like ferricrocin and some toxins[130–132]. A particularly interesting group within the NRPs are peptaibiotics, named according to their broad antibiotic activities. They usually consist of five to twenty amino acid residues with an acetylated N-terminus and a molecular weight of 0.5-2.2 kDa. Characteristic is the occurrence of several α-aminoisobutyric acid (Aib) residues within those compounds, as well as other nonproteinogenic and lipoamino acid moieties[133,134]. Peptaibiotics can be further divided into

peptaibols, efrapeptins and neofrapeptins. Peptaibols, which are mainly synthesized by *Trichoderma* species, feature an alcohol group at the C-terminus and may carry isovaline[134,135]. Efrapeptins have pipecolic acid and cationic bicycle amine modification at the C-terminus and have been reported in *Tolypocladium* species[136]. Neofrapeptins, which have been isolated from *Geotrichum candidum*, contain the 1-Aminocyclopropane-1-carboxylic acid (ACC) and in some cases 3-methylproline[134,137].

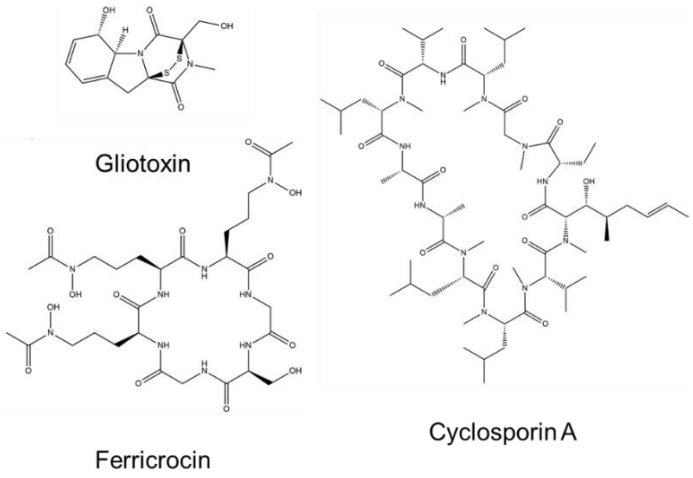

Figure 10 Examples of NRPs, one of the most wildly studied fungal toxins gliotoxin[138], the siderophore ferricrocin[130] and the immunosuppressant cyclosporin A[132].

RiPPs are peptides with a vast structural diversity, many of which are cyclized providing them with several advantages, such as avoiding degradation by exopeptidases, structural rigidity that enhances binding affinity and biological activity, as well as denaturation upon heating[119]. Common representatives are amatoxins, phallotoxins and phomopsins mostly isolated from fungal species other than the Ascomycota[139–141]. At least 94 sets of precursor genes were computationally identified and classified though, indicating that RiPPs are likely to be widespread in the Ascomycota as well[142]. Specifically in *A. flavus,* ustiloxins, cyclic peptides that are derived

from a Tyr-Val/Ala-Ile-Gly tetrapeptide and the bicyclic peptide asperipin-2a were identified[142,143].

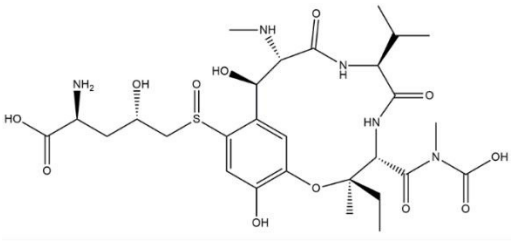

Ustiloxin A

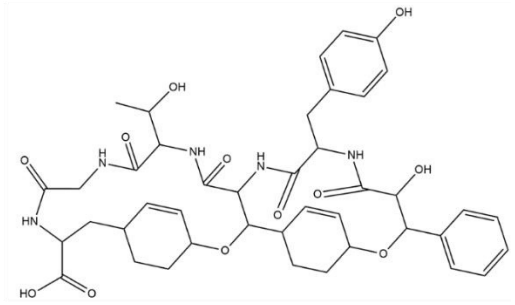

Asperipin – 2a

Figure 11 Examples of RIPPs, ustiloxin A[144] and Asperipin-2a[142].

Terpenes are synthetized from the five-carbon precursor molecules isopentenyl diphosphate and/or dimethylallyl diphosphate, derived from acetyl-CoA[145]. Condensation of those precursor monomers results in branched hydrocarbon termed geranyl pyrophosphate (C_{10}), farnesyl pyrophosphate (C_{15}), geranylgeranyl pyrophosphate (C_{20}), squalene (C_{30}), and phytoene/lycopene (C_{40}). These linear prenyl chains are further processed by prenyl transferases, terpene cyclases, and terpene synthases into linear or cyclic terpenoid compounds[146]. Fungal terpenes comprise diterpenes, aristolochenes, carotenoids, gibberellins and the trichothecenes[147–150].

Indole alkaloids are derived from the aromatic amino acid L-tryptophan. L-Tryptophan is most commonly prenylated by the 4-dimethylallyl tryptophan synthase to produce 4-dimethylallyl tryptophan[151,152]. Several cyclization

steps then lead to the formation of an ergoline ring, which is the basic module of ergot alkaloids[153]. Alternatively, L-tryptophan can be decarboxylated to yield tryptamine, which is a widely used in the biosynthesis of plant indole alkaloids. Some fungal indole alkaloids, also show indole moieties derived from tryptamine, although the direct biosynthesis has never been demonstrated[154]. Some diterpenes are synthesized from a precursor of L-tryptophan, indole-3-glycerol-phosphate[155].

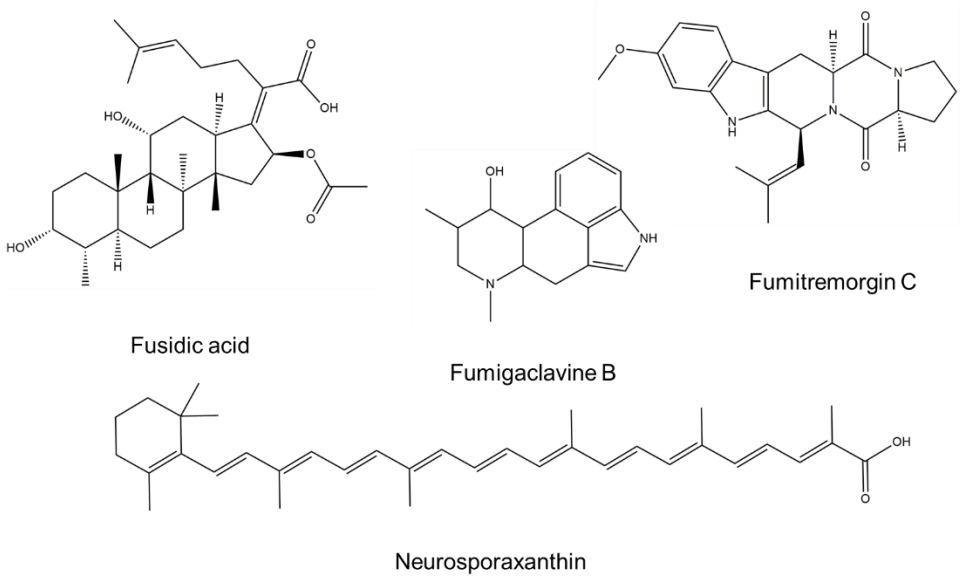

Figure 12 Examples of terpenes and alkaloids. Fusidic acid[156] *is a triterpene and neurosporaxanthin a carotenoid from N. crassa*[157]*. The alkaloids fumigacalvine B and fumitremorgin C have both been isolated from A. fumigatus*[158,159]*.*

The complexity and variety of SMs is further increased by the combination of different structural components, which can be synthetized by the hybrid enzymes PKS-NRPS or by different synthases subsequently. Next to the PKs-NRPs compounds exist NRPs-terpenes, polyketide-NRPs, indole diterpenes, or indole alkaloids incorporated into NRPs and polyketide-NRPs[110,152].

Secondary metabolites as signaling molecules

This following section aims to introduce fungal secondary metabolites that can act as extracellular signaling molecules, with an emphasis on Aspergillus spp.

Some fungal secondary metabolites have been found to act as signaling molecules. They are usually produced during specific developmental stages such as germination, formation of the mycelial network, coordination of colony development and both sexual and asexual reproduction[160]. Three types of cell-to-cell signaling can be distinguished: the coordination of a response depending on cell density and concentration of the signaling molecule (quorum sensing), communication between intrinsically different cells (paracrine signaling), like mating types, and finally sensing between identical cells, like hyphal fusion (autocrine signaling)[161]. The extracellular signals are species specific and largely unknown. A variety of chemical substances like small peptides and pheromones[160], MAP kinase signaling[162,163], ROS signaling, a multi-subunit signaling complex, homologous to the human striatin-interacting phosphatase and kinase (STRIPAK) complex[164] and many other factors are crucial for the development of fungi.

Quorum sensing, a well-studied phenomenon in prokaryotes, is increasingly being investigated in eukaryotes, especially in *Candida albicans, Saccharomyces cerevisiae and Cryptococcus neoformans*[165]*.* The first quorum sensing molecule (QSM), or auto-inducer, to be discovered and the best studied so far is farnesol, which has been shown to block hyphal formation, affect morphological pathways and inhibit biofilm formation in *Candida albicans (C. albicans)*, but also to influence hyphal morphology, conidiation and germination in some other fungal species[166,167]. Since then, other QSMs have been discovered, including lipids (oxylipins), peptides (pheromones), alcohols (tyrosol, tryptophol), acetaldehydes and some

volatiles which are involved in pathogenesis, morphogenesis and filamentation[168–171].

Studies on quorum sensing in other fungal species most often involve the exposure of fungal species to known QSMs and the subsequent analysis of their effects[166]. Farnesol has thus been labelled a QSM with activity in many fungal species; in *A. fumigatus* for example it has been shown to perturb the cell wall organization. Since farnesol production in *A. fumigatus* is minimal and has not been directly linked with self-modulating activity, such QSM denominations should be considered with caution[172,173]. Actually, no true QSM has been discovered in *A. fumigatus* thus far and only few QS mechanisms have been identified for the *Aspergillus* species[165]. Oxylipins seem to coordinate conidium and sclerotium formation in a cell-density dependent manner in *A. flavus*[174]; in *A. nidulans,* γ-heptalactone was shown to accumulate in the extracellular matrix at high cell densities. Cell-free extracts containing γ-heptalactone led to a reduction of the lag-phase in *A. nidulans* cultures, which could be confirmed by the addition of commercial γ-heptalactone[175]. External addition of butyrolactone to *A. terreus* increased the production of lovastatin as well as its own endogenous production[176]. In another study the culture medium of *Aspergillus terreus* was supplemented with linoleic acid, also an oxylipin, to successfully increase lovastatin production as well[177]. Autoinducer capabilities suggest that butyrolactone and linoleic acid can be QSMs, although no cell density dependent production has been shown.

According to Albuquerque and Casadevall, to be classified as a self-signaling molecule or QSM, the compound should fulfill the following five criteria: (I) accumulation in the extracellular environment during microbial growth; (II) at a concentration proportional to cell density, restricted to a specific growth phase; (III) lead to a coordinated response across the population, which is not simply the metabolization or detoxification of the molecule itself (IV)

reproduce the QS phenotype when being added exogenously; (V) it is not merely a by-product of microbial catabolism[165,168]. Those criteria should be taken into consideration when studying QS mechanism.

Intraspecies cell-cell signaling does not only occur as a quorum sensing mechanism, secreted signaling molecules play a versatile role for the growth and development of fungal cultures[160]. In *N. crassa* pheromones mediate cell fusion during sexual reproduction and germling and hyphal tip fusion during vegetative growth seems to be directed by the signaling proteins MAK-2 and SOFT[56,178]. In *Aspergillus* spp. the outwards growth of mycelial colonies is influenced by the secretion of growth inhibitors just behind the growing front, the molecule has not been isolated though[179]. The two oxylipins psiA and psiB, promote fruiting body formation and inhibit conidiation in *A. nidulans,* while the oxylipin psiC promotes conidiation[180,181].

Despite the studies mentioned, our overall knowledge of the fungal chemical language remains scarce. The study of QS or intercellular signaling mechanisms is of importance, as it provides information about the adaptation of organisms to external cues and growth coordination. If those compounds are identified, inhibiting strategies can be designed to counteract detrimental fungal growth. Inhibition can be achieved by three methods: inhibiting the production of the compound itself; degradation by enzymes; or blocking their receptors[165].

Choline based Ionic Liquids

The following paragraph is focused on the properties of cholinium based ionic liquids and their effects especially towards Aspergillus spp. and to some extent towards Neurospora crassa.

Ionic liquids are defined as salts which are liquid below a temperature of 100°C[182]. Due to the enormous diversity of anions and cations, ionic liquids have broad chemical properties and are highly tunable. Our group was the

first to study the interactions of ionic liquids and filamentous fungi, such as toxicity, biodegradation, stress responses and metabolic changes[183–186]. Especially cholinium based ionic liquids and their alkanoates have been analyzed in detail[185,187]. The cholinium cation does not exhibit great toxicity, which is rather induced and tuned by the variable length of the alkanoate anion[187]. Increasing chain length of the anion enhances their toxic effects towards filamentous fungi such as *Aspergillus* and *Penicillium* species, as long as their water solubility is still given[183,186,187]. Another feature of cholinium based ionic liquids is that their ionic components are easily degradable[187–189].

Our group has intensively investigated the effect of ionic liquids on stress response and metabolic changes in filamentous fungi. In contrast to some other ionic liquids, such as imidazolium based ones, cholinium alkanoates do not permeabilize the fungal plasma membrane of *A. nidulans*, potentially because their alkyl chains are negatively charged and therefore repelled by the likewise negatively charged phospholipids of the plasma membrane[186]. Another study showed that cholinium decanoate activated the sphingolipid biosynthetic pathway. But, in contrast to 1-decyl-3-methylimidazolium chloride, it does not lead to the accumulation of an unknown free sphingoid base, which is believed to act as a signaling molecule[190].

Transcriptomic, proteomic and metabolomic analyses have shown that sub-lethal concentrations of cholinium chloride ionic liquids, among others, cause ubiquitous alterations of the primary and secondary metabolism of *A. nidulans* and *N. crassa*[184,185]. Overall, it can be stated that cholinium chloride supplementation upregulates primary metabolism. Cholinium chloride, also known as choline, is usually biosynthesized endogenously as it constitutes part of the vitamin B complex. It can be taken up from the medium as source of carbon and nitrogen and has been shown to induce morphological changes like reduced branching in some filamentous

fungi[191,192]. *Aspergillus nidulans* seems to metabolize choline via the glycine, serine, threonine pathway, where it enters the primary metabolism in form of betain aldehyde and betaine, which is then further metabolized to glycine[184,185]. Choline led to an upregulation of most genes involved in the TCA cycle and glyoxylate shunt, as well as some involved in glycolysis/ gluconeogenesis, potentially due to the increased availability of carbohydrates[184,185].

Choline supplementation of *A. nidulans* cultures led to increased levels of EngA, a protein involved in autolysis[193,194]. In the study, choline did not seem to trigger cell death, but instead led to more robust mycelia and the development of sexual Hülle cells. This might be correlated to an overall increase of protein biosynthesis and up-regulated genes involved in amino acid metabolism upon choline exposure[184,185]. Specifically, cysteine, methionine, aspartate, alanine, asparagine; branched and aromatic amino acids, glutamate, glutamine and proline, among others. Choline chloride also led to a decrease of CpcB, the repressor of the cross-pathway control of amino acid synthesis, which is activated upon amino acid starvation[195]. CpcB depletion is potentially correlated to the formation of Hülle cells[195]. Furthermore an accumulation of the heat shock protein 70 could be observed under choline supplementation, probably in response to the development of ROS, which play important roles as signaling molecules in several stress responses and morphological transitions[184,196]. The accumulation of cyanase, an enzyme mediating the mineralization of the toxic compound cyanide[197], may indicate cyanide production and partially explain the growth inhibition due to choline exposure.

In *N. crassa* cultures, choline supplementation led to a decrease of the Rho-1 GTPase, which is involved in cellular morphogenesis, cell wall integrity and hyphal polarisation[198]. Whereas NDK-1, a nucleoside diphosphate kinase thought to be involved in the control of branching, aerial hyphae formation,

and conidiation, was increased[199]. Nevertheless, in contrast to other filamentous fungi, choline did not lead to obvious alterations in the morphology[191]. Microscopic analysis only showed that choline induced conidiation within two days, in contrast to the control which only showed conidiation after 7 days of incubation. In fact, Cat-3 was increased, a catalase associated with vegetative growth and the onset of conidiation[200].

Apart from primary metabolism, choline chloride increased diversity of secondary metabolites, as shown by chromatographic profiling and transcriptomic analysis. In *A. nidulans* it stimulates the production of acetyl-CoA, a key precursor in the synthesis of numerous SMs[201] and upregulated nine of the sixty six predicted backbone genes[185,202]. Among the newly biosynthesized metabolites, some have shown anti-carcinoma potential and it can be expected that many others exhibit diverse bioactive properties. For *N. crassa* an interesting finding is the increased expression of the 1-aminocyclopropane-1-carboxylate deaminase (NCU04657) under the choline stimulus, which mediates the formation of 1-aminocyclopropane-1-carboxylate (ACC)[184]. Higher ACC levels have been linked to the production of neofrapeptins and acretocins, compounds belonging to the class of peptaibiotics, in some fungi[134,203]. The potential production of peptaibiotics by *N. crassa*, which have been shown to have valuable antimicrobial properties, would provide a new source for novel antimicrobial compounds.

Throughout the following study cholinium decanoate and cholinium chloride were used (Figure 13), as they are taken up and degraded by the fungus. This avoids secondary effects of residual ionic liquid when bioactive compounds in the spent medium of fungal cultures are being investigated. Choline decanoate additionally shows high toxicity due to the long alkyl chain, thus very little amounts are needed for effective medium supplementation, avoiding secondary effects due to carbon sources or high salinity. Even longer alkyl chains have not been considered, since cholinium

dodecanoate has been shown to be less toxic due to reduced water solubility[187].

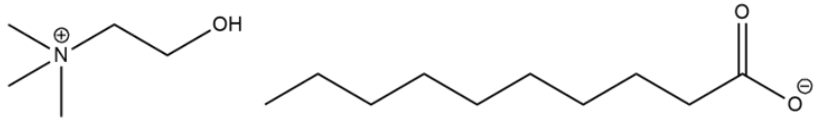

Figure 13 Cholinium decanoate structure, choline chloride comprises of a chloride ion instead of the decanoate anion.

Objectives

In this work ionic liquids and filamentous fungi were being combined in three different experimental settings to investigate novel antimicrobial strategies. The toxicity of ionic liquids themselves towards filamentous fungi served as the basis for the first study. An anionic form of the commonly used antifungal Amphotericin B was combined with different cations to form ionic liquids. Those novel formulations were investigated for their antifungal as well as antibiotic potential, to set the ground for antifungal formulations that could overcome limitations of common formulations such as solubility and bioavailability.

On the other hand, ionic liquids were utilized as growth medium supplements to activate and diversify the production of bioactive secondary metabolites in fungal cultures. Previous studies of the laboratory have shown to successfully induce and alter secondary metabolite biosynthesis of otherwise cryptic genes with this approach[185]. Two different aspects were being investigated. Secondary metabolites that act as intercellular signaling molecules and secondary metabolites with antimicrobial properties.

Potential intercellular signaling metabolites were being investigated within the pathogenic fungus *A. fumigatus.* Understanding signals that influence the growth and dissemination of this opportunistic fungus may provide useful information to design counteracting strategies limiting its growth or even

pathogenicity. Here we attempted the stimulation of cryptic secondary metabolite production and tested the spent medium extracts for their ability to induce changes in the fungal life cycle.

Filamentous fungi are known to produce secondary metabolites with antimicrobial properties. Furthermore, our laboratory has preliminary results suggesting the production of peptaibiotics by *N. crassa.* Another objective of this thesis was therefore to study the potential production of antimicrobial metabolites in the three model organisms *N. crassa, A. nidulans* and *A. fumigatus.* Ionic liquid medium supplementation was again employed to stimulate the biosynthesis of such compounds, as it had been shown to alter the fungal proteome[184].

References

1. Carlile, M. J., Watkinson, S. C. & Gooday, G. W. The Fungi 2nd. *Sci. Acad. Press. San Diego* (2001).
2. Bourett, T. M., James, S. W. & Howard, R. J. The Endomembrane System of the Fungal Cell. in *Biology of the Fungal Cell* (2007). doi:10.1007/978-3-540-70618-2_1
3. Butterfield, N. J. Probable Proterozoic fungi. *Paleobiology* **31**, 165–182 (2005).
4. Gibbs, J. N. & Wainhouse, D. Spread of Forest Pests and Pathogens in the Northern Hemisphere. For. An Int. J. For. Res. 59, 141–153 (1986).
5. Fisher, M. C. *et al.* Emerging fungal threats to animal, plant and ecosystem health. *Nature* **484**, 186–194 (2012).
6. Drgona, L. *et al.* Clinical and economic burden of invasive fungal diseases in Europe: focus on pre-emptive and empirical treatment of Aspergillus and Candida species. *Eur. J. Clin. Microbiol. Infect. Dis.* **33**, 7–21 (2014).
7. Fleming, A. The discovery of Penicillin. *Br Med Bull* **2**, 4–5 (1944).

8. HeeSoo, P., SangCheol, J., KapHoon, H., SeungBeom, H. & JaeHyuk, Y. Chapter Three - Diversity, Application, and Synthetic Biology of Industrially Important Aspergillus Fungi. in *Advances in Applied Microbiology* (2017).
9. Nielsen, J. Yeast Systems Biology: Model Organism and Cell Factory. *Biotechnol. J.* **14**, 1800421 (2019).
10. Naranjo-Ortiz, M. A. & Gabaldón, T. Fungal evolution: diversity, taxonomy and phylogeny of the Fungi. Biol. Rev. 94, 2101–2137 (2019).
11. Bennett, R. J. & Turgeon, B. G. Fungal Sex: The Ascomycota. *Microbiol. Spectr.* **4**, (2016).
12. Yanagida, M. The model unicellular eukaryote, Schizosaccharomyces pombe. *Genome Biol.* **3**, COMMENT2003 (2002).
13. Karathia, H., Vilaprinyo, E., Sorribas, A. & Alves, R. Saccharomyces cerevisiae as a Model Organism: A Comparative Study. *PLoS One* **6**, e16015 (2011).
14. Borkovich, K. A. & Ebbole, D. J. *Cellular and Molecular Biology of Filamentous Fungi*. *Cellular and Molecular Biology of Filamentous Fungi* (ASM Press, 2010). doi:10.1128/9781555816636
15. Houbraken, J., Frisvad, J. C. & Samson, R. A. Fleming's penicillin producing strain is not Penicillium chrysogenum but P. rubens. *IMA Fungus* **2**, 87–95 (2011).
16. Davis, R. H. & Perkins, D. D. Neurospora: a model of model microbes. *Nat. Rev. Genet.* **3**, 397–403 (2002).
17. Dyer, P. S. & O'Gorman, C. M. Sexual development and cryptic sexuality in fungi: insights from Aspergillus species. *FEMS Microbiol. Rev.* **36**, 165–92 (2012).
18. Osherov, N. The molecular mechanisms of conidial germination. *FEMS Microbiol. Lett.* **199**, 153–160 (2001).
19. Baltussen, T. J. H., Zoll, J., Verweij, P. E. & Melchers, W. J. G.

Molecular Mechanisms of Conidial Germination in Aspergillus spp. *Microbiol. Mol. Biol. Rev.* **84**, 1–31 (2020).

20. Novodvorska, M. *et al.* Metabolic activity in dormant conidia of Aspergillus niger and developmental changes during conidial outgrowth. *Fungal Genet. Biol.* **94**, 23–31 (2016).
21. Baltussen, T. J. H., Coolen, J. P. M., Zoll, J., Verweij, P. E. & Melchers, W. J. G. Gene co-expression analysis identifies gene clusters associated with isotropic and polarized growth in Aspergillus fumigatus conidia. *Fungal Genet. Biol.* **116**, 62–72 (2018).
22. Dijksterhuis, J., Nijsse, J., Hoekstra, F. A. & Golovina, E. A. High Viscosity and Anisotropy Characterize the Cytoplasm of Fungal Dormant Stress-Resistant Spores. *Eukaryot. Cell* **6**, 157–170 (2007).
23. Ursula, K. & Reinhard, F. *Growth, differentiation & sexuality, (The Mycota, Vol. 1),*. (2010).
24. Gooday, G. W. The dynamics of hyphal growth. *Mycol. Res.* **99**, 385–394 (1995).
25. Roberson, R. W. Subcellular structure and behaviour in fungal hyphae. *J. Microsc.* **280**, 75–85 (2020).
26. Riquelme, M. & Bartnicki-Garcia, S. Key differences between lateral and apical branching in hyphae of Neurospora crassa. *Fungal Genet. Biol.* **41**, 842–851 (2004).
27. Lopez-Franco, R. & Bracker, C. E. Diversity and dynamics of the Spitzenkörper in growing hyphal tips of higher fungi. *Protoplasma* **195**, 90–111 (1996).
28. Brand, A. & Gow, N. A. Mechanisms of hypha orientation of fungi. *Curr. Opin. Microbiol.* **12**, 350–357 (2009).
29. Bartnicki-Garcia, S. & Lippman, E. Fungal Morphogenesis: Cell Wall Construction in Mucor rouxii. *Science (80-.).* **165**, 302–304 (1969).
30. Yamazaki, H., Tanaka, A., Kaneko, J., Ohta, A. & Horiuchi, H. Aspergillus nidulans ChiA is a glycosylphosphatidylinositol (GPI)-

anchored chitinase specifically localized at polarized growth sites. *Fungal Genet. Biol.* **45**, 963–972 (2008).

31. Riquelme, M. & Sánchez-León, E. The Spitzenkörper: a choreographer of fungal growth and morphogenesis. *Curr. Opin. Microbiol.* **20**, 27–33 (2014).
32. Latgé, J. The cell wall: a carbohydrate armour for the fungal cell. *Mol. Microbiol.* **66**, 279–290 (2007).
33. Klis, F. M., Ram, A. F. J. & De Groot, P. W. J. A Molecular and Genomic View of the Fungal Cell Wall. in *Biology of the Fungal Cell* 97–120 (Springer Berlin Heidelberg, 2007). doi:10.1007/978-3-540-70618-2_4
34. de Groot, P. W. J. *et al.* Comprehensive genomic analysis of cell wall genes in Aspergillus nidulans. *Fungal Genet. Biol.* **46**, S72–S81 (2009).
35. Yuill, E. The numbers of nuclei in conidia of aspergilli. *Trans. Br. Mycol. Soc.* **33**, 324-IN10 (1950).
36. MARUYAMA, J., NAKAJIMA, H. & KITAMOTO, K. Visualization of Nuclei in Aspergillus oryzae with EGFP and Analysis of the Number of Nuclei in Each Conidium by FACS. *Biosci. Biotechnol. Biochem.* **65**, 1504–1510 (2001).
37. Hunsley, D. & Gooday, G. W. The structure and development of septa inNeurospora crassa. *Protoplasma* **82**, 125–146 (1974).
38. Deacon, J. *Fungal Biology*. *Fungal Biology: 4th Edition* (Wiley, 2005). doi:10.1002/9781118685068
39. Wikimedia Commons Contributors. File:HYPHAE.png. *Wikimedia Commons, the free media repository* Available at: https://commons.wikimedia.org/w/index.php?title=File:HYPHAE.png&oldid=486195866. (Accessed: 13th November 2021)
40. Dahlberg, K. R. & Etten, J. L. V. Physiology and Biochemistry of Fungal Sporulation. *Annu. Rev. Phytopathol.* **20**, 281–301 (1982).

41. Money, N. P. Spore Production, Discharge, and Dispersal. in *The Fungi* 67–97 (Elsevier, 2016). doi:10.1016/B978-0-12-382034-1.00003-7
42. Vrabl, P., Schinagl, C. W., Artmann, D. J., Heiss, B. & Burgstaller, W. Fungal Growth in Batch Culture – What We Could Benefit If We Start Looking Closer. *Front. Microbiol.* **10**, 2391 (2019).
43. Werner-Washburne, M., Braun, E., Johnston, G. C. & Singer, R. A. Stationary phase in the yeast Saccharomyces cerevisiae. *Microbiol. Rev.* **57**, 383–401 (1993).
44. Moore, D., Robson, G. D. & Trinci, A. P. J. *21st Century Guidebook to Fungi*. *21st Century Guidebook to Fungi* (2000). doi:10.1017/cbo9780511977022
45. Payen, A. Extrait d'un rapport adresse a M. Le Marechal Duc de Dalmatie, Ministre de la Guerre, President du Conseil, sur une alteration extraordinaire du pain de munition. *Ann. Chim. Phys.* **9**, 5–21 (1843).
46. Shear, C. L. & Dodge, B. O. Life histories and heterothallism of the red bread-mold fungi of the Monilia sitophila group. *J. Agric. Res.* **34**, 1019–1042 (1927).
47. Davis, R. H. Neurospora – Contributions of a Model Organism. *Oxford Univ. Press* (2000). doi:10.1017/s0016672301215080
48. Dettmann, A., Heilig, Y., Valerius, O., Ludwig, S. & Seiler, S. Fungal Communication Requires the MAK-2 Pathway Elements STE-20 and RAS-2, the NRC-1 Adapter STE-50 and the MAP Kinase Scaffold HAM-5. *PLoS Genet.* **10**, (2014).
49. Nygren, K. *et al.* A comprehensive phylogeny of Neurospora reveals a link between reproductive mode and molecular evolution in fungi. *Mol. Phylogenet. Evol.* **59**, 649–663 (2011).
50. Wilson, A. M. *et al.* Homothallism: an umbrella term for describing diverse sexual behaviours. *IMA Fungus* **6**, 207–214 (2015).

51. Dodge, B. O. Heterocaryotic Vigor in Neurospora. *Bull. Torrey Bot. Club* **69**, 75 (1942).
52. Davis, R. H. & de Serres, F. J. [4] Genetic and microbiological research techniques for Neurospora crassa. in *Methods in Enzymology* 79–143 (1970). doi:10.1016/0076-6879(71)17168-6
53. Borkovich, K. A. *et al.* Lessons from the Genome Sequence of Neurospora crassa : Tracing the Path from Genomic Blueprint to Multicellular Organism. *Microbiol. Mol. Biol. Rev.* **68**, 1–108 (2004).
54. Roche, C. M., Loros, J. J., McCluskey, K. & Glass, N. L. Neurospora crassa: Looking back and looking forward at a model microbe. *Am. J. Bot.* **101**, 2022–2035 (2014).
55. Whiteway, M. & Bachewich, C. Fungal Genetics. in *Fungi* 37–65 (Wiley, 2011). doi:10.1002/9781119976950.ch2
56. Kim, H. & Borkovich, K. A. Pheromones Are Essential for Male Fertility and Sufficient To Direct Chemotropic Polarized Growth of Trichogynes during Mating in Neurospora crassa. *Eukaryot. Cell* **5**, 544–554 (2006).
57. Raju, N. B. Meiosis and ascospore genesis in Neurospora. *Eur. J. Cell Biol.* **23**, 208–23 (1980).
58. Fleißner, A., Simonin, A. R. & Glass, N. L. Cell Fusion in the Filamentous Fungus, Neurospora crassa. in *Methods in Molecular Biology* 21–38 (2008). doi:10.1007/978-1-59745-250-2_2
59. Bennett, J. W. An overview of the genus Aspergillus. in Aspergillus: Molecular Biology and Genomics (Caister Academic Press, U.K., 2010).
60. Krijgsheld, P. *et al.* Development in aspergillus. *Stud. Mycol.* **74**, 1–29 (2013).
61. Pontecorvo, G., Roper, J. A., Chemmons, L. M., Macdonald, K. D. & Bufton, A. W. J. The Genetics of Aspergillus nidulans. in *Advances in Genetics* 141–238 (1953). doi:10.1016/S0065-2660(08)60408-3

62. Maggio-Hall, L. A., Hammond, T. M. & Keller, N. P. Chapter ten Aspergillus nidulans as a model system to study secondary metabolism. in *Recent Advances in Phytochemistry* 197–222 (2004). doi:10.1016/S0079-9920(04)80011-X
63. Latgé, J.-P. & Chamilos, G. Aspergillus fumigatus and Aspergillosis in 2019. *Clin. Microbiol. Rev.* **33**, (2019).
64. Diano, A., Dynesen, J. Ø., & Nielsen, J. Physiology of Aspergillus niger under oxygen limitation. *Tech. Univ. DENMARK* (2007).
65. Perfect, J. R. *et al.* The Impact of Culture Isolation of Aspergillus Species: A Hospital-Based Survey of Aspergillosis. *Clin. Infect. Dis.* **33**, 1824–1833 (2001).
66. Enoch, D. A., Ludlam, H. A. & Brown, N. M. Invasive fungal infections: a review of epidemiology and management options. *J. Med. Microbiol.* **55**, 809–818 (2006).
67. Paulussen, C. *et al.* Ecology of aspergillosis: insights into the pathogenic potency of Aspergillus fumigatus and some other Aspergillus species. *Microb. Biotechnol.* **10**, 296–322 (2016).
68. Stergiopoulou, T. *et al.* Host-Dependent Patterns of Tissue Injury in Invasive Pulmonary Aspergillosis. *Am. J. Clin. Pathol.* **127**, 349–355 (2007).
69. Lehrnbecher, T. *et al.* Trends in the postmortem epidemiology of invasive fungal infections at a university hospital. *J. Infect.* **61**, 259–265 (2010).
70. Alangaden, G. J., Wahiduzzaman, M. & Chandrasekar, P. H. Aspergillosis: The Most Common Community-Acquired Pneumonia with Gram-Negative Bacilli as Copathogens in Stem Cell Transplant Recipients with Graft-versus-Host Disease. *Clin. Infect. Dis.* **35**, 659–664 (2002).
71. Pappas, P. G. *et al.* Invasive Fungal Infections among Organ Transplant Recipients: Results of the Transplant-Associated Infection

Surveillance Network (TRANSNET). *Clin. Infect. Dis.* **50**, 1101–1111 (2010).

72. Herbrecht, R., Bories, P., Moulin, J.-C., Ledoux, M.-P. & Letscher-Bru, V. Risk stratification for invasive aspergillosis in immunocompromised patients. *Ann. N. Y. Acad. Sci.* **1272**, 23–30 (2012).
73. Taccone, F. S. *et al.* Epidemiology of invasive aspergillosis in critically ill patients: clinical presentation, underlying conditions, and outcomes. *Crit. Care* **19**, 7 (2015).
74. Tekaia, F. & Latgé, J.-P. Aspergillus fumigatus: saprophyte or pathogen? *Curr. Opin. Microbiol.* **8**, 385–392 (2005).
75. Amich, J. & Krappmann, S. Deciphering metabolic traits of the fungal pathogen Aspergillus fumigatus: Redundancy vs. Essentiality. *Front. Microbiol.* **3**, 2008–2013 (2012).
76. Nicolas, L. *et al.* Nutritional heterogeneity among aspergillus fumigatus strains has consequences for virulence in a strain- And host-dependent manner. *Front. Microbiol.* **10**, 1–20 (2019).
77. Andersen, M. R. Elucidation of primary metabolic pathways in Aspergillus species: Orphaned research in characterizing orphan genes. *Brief. Funct. Genomics* **13**, 451–455 (2014).
78. Sasse, A., Hamer, S. N., Amich, J., Binder, J. & Krappmann, S. Mutant characterization and in vivo conditional repression identify aromatic amino acid biosynthesis to be essential for Aspergillus fumigatus virulence. *Virulence* **7**, 56–62 (2016).
79. Gray, K. C. *et al.* Amphotericin primarily kills yeast by simply binding ergosterol. *Proc. Natl. Acad. Sci.* **109**, 2234–2239 (2012).
80. Lass-Flörl, C. Triazole Antifungal Agents in Invasive Fungal Infections. *Drugs* **71**, 2405–2419 (2011).
81. Gregson, L. et al. In vitro susceptibility of Aspergillus fumigatus to isavuconazole: correlation with itraconazole, voriconazole, and posaconazole. Antimicrob. Agents Chemother. 57, 5778–5780

(2013).

82. Leonardelli, F. *et al.* Aspergillus fumigatus Intrinsic Fluconazole Resistance Is Due to the Naturally Occurring T301I Substitution in Cyp51Ap. *Antimicrob. Agents Chemother.* **60**, 5420 (2016).
83. Geißel, B. *et al.* Azole-induced cell wall carbohydrate patches kill Aspergillus fumigatus. *Nat. Commun.* **9**, 3098 (2018).
84. Bowman, J. C. *et al.* The Antifungal Echinocandin Caspofungin Acetate Kills Growing Cells of Aspergillus fumigatus In Vitro. *Antimicrob. Agents Chemother.* **46**, 3001–3012 (2002).
85. Vermes, A., Guchelaar, H. J. & Dankert, J. Flucytosine: A review of its pharmacology, clinical indications, pharmacokinetics, toxicity and drug interactions. *J. Antimicrob. Chemother.* **46**, 171–179 (2000).
86. Stevens, D. A., Espiritu, M. & Parmar, R. Paradoxical Effect of Caspofungin: Reduced Activity against Candida albicans at High Drug Concentrations. *Antimicrob. Agents Chemother.* **48**, 3407–3411 (2004).
87. Wagener, J. & Loiko, V. Recent Insights into the Paradoxical Effect of Echinocandins. *J. Fungi* **4**, 5 (2017).
88. Walker, L. A., Lee, K. K., Munro, C. A. & Gow, N. A. R. Caspofungin treatment of Aspergillus fumigatus results in ChsG-dependent upregulation of chitin synthesis and the formation of chitin-rich microcolonies. *Antimicrob. Agents Chemother.* **59**, 5932–5941 (2015).
89. Moreno-Velásquez, S. D., Seidel, C., Juvvadi, P. R., Steinbach, W. J. & Read, N. D. Caspofungin-mediated growth inhibition and paradoxical growth in Aspergillus fumigatus involve fungicidal hyphal tip lysis coupled with regenerative intrahyphal growth and dynamic changes in β-1,3-glucan synthase localization. *Antimicrob. Agents Chemother.* **61**, (2017).
90. Howard, S. J. *et al.* Frequency and Evolution of Azole Resistance in Aspergillus fumigatus Associated with Treatment Failure1. *Emerg.*

Infect. Dis. **15**, 1068–1076 (2009).

91. Verweij, P. E. *et al.* In-host adaptation and acquired triazole resistance in Aspergillus fumigatus : a dilemma for clinical management. *Lancet Infect. Dis.* **16**, e251–e260 (2016).
92. Perlin, D. S., Rautemaa-Richardson, R. & Alastruey-Izquierdo, A. The global problem of antifungal resistance: prevalence, mechanisms, and management. *Lancet Infect. Dis.* **17**, e383–e392 (2017).
93. Chowdhary, A., Sharma, C. & Meis, J. F. Azole-Resistant Aspergillosis: Epidemiology, Molecular Mechanisms, and Treatment. *J. Infect. Dis.* **216**, S436–S444 (2017).
94. Butts, A. & Krysan, D. J. Antifungal drug discovery: Something old and something new. *PLoS Pathog* **8**, e1002870 (2012).
95. Wall, G. & Lopez-Ribot, J. L. Current antimycotics, new prospects, and future approaches to antifungal therapy. *Antibiotics* **9**, 445 (2020).
96. Berkow, E. L. & Lockhart, S. R. Activity of novel antifungal compound APX001A against a large collection of Candida auris. *J. Antimicrob. Chemother.* **73**, 3060–3062 (2018).
97. Oliver, J. D. *et al.* F901318 represents a novel class of antifungal drug that inhibits dihydroorotate dehydrogenase. *Proc. Natl. Acad. Sci. U. S. A.* **113**, 12809–12814 (2016).
98. Takesako, K. *et al.* Biological properties of aureobasidin A, a cyclic depsipeptide antifungal antibiotic. *J. Antibiot. (Tokyo).* **46**, 1414–1420 (1993).
99. Perfect, J. R. The antifungal pipeline: A reality check. *Nat. Rev. Drug Discov.* **16**, 603–616 (2017).
100. Romo, J. A. *et al.* Development of anti-virulence approaches for candidiasis via a novel series of small-molecule inhibitors of Candida albicans filamentation. *MBio* **8**, (2017).
101. Heard, S. C., Wu, G. & Winter, J. M. Antifungal natural products. *Curr. Opin. Biotechnol.* **69**, 232–241 (2021).

102. Oura, M., Sternberg, T. H. & Wright, E. T. A new antifungal antibiotic, amphotericin B. *Antibiot. Annu.* **3**, 566–73 (1955).
103. Onishi, J. *et al.* Discovery of Novel Antifungal (1,3)-β- D -Glucan Synthase Inhibitors. *Antimicrob. Agents Chemother.* **44**, 368–377 (2000).
104. Liu, M. *et al.* Potential of marine natural products against drug-resistant bacterial infections. *Lancet Infect. Dis.* **19**, e237–e245 (2019).
105. El-Hossary, E. M. *et al.* Antifungal potential of marine natural products. *Eur. J. Med. Chem.* **126**, 631 (2017).
106. Fox, E. M. & Howlett, B. J. Secondary metabolism: regulation and role in fungal biology. *Curr. Opin. Microbiol.* **11**, 481–487 (2008).
107. Demain, A. L. & Fang, A. The Natural Functions of Secondary Metabolites. in *Advances in biochemical engineering/biotechnology* 1–39 (2000). doi:10.1007/3-540-44964-7_1
108. Calvo, A. M., Wilson, R. A., Bok, J. W. & Keller, N. P. Relationship between Secondary Metabolism and Fungal Development. *Microbiol. Mol. Biol. Rev.* **66**, 447–459 (2002).
109. Keller, N. P. Fungal secondary metabolism: regulation, function and drug discovery. *Nat. Rev. Microbiol.* **17**, 167–180 (2019).
110. Brakhage, A. A. Regulation of fungal secondary metabolism. *Nat. Rev. Microbiol.* **11**, 21–32 (2013).
111. Smith, D. J. *et al.* Beta-lactam antibiotic biosynthetic genes have been conserved in clusters in prokaryotes and eukaryotes. *EMBO J.* **9**, 741–7 (1990).
112. Bok, J. W. & Keller, N. P. LaeA, a regulator of secondary metabolism in Aspergillus spp. *Eukaryot. Cell* **3**, 527–535 (2004).
113. Bok, J. W. *et al.* VeA and MvlA repression of the cryptic orsellinic acid gene cluster in Aspergillus nidulans involves histone 3 acetylation. *Mol. Microbiol.* **89**, 963–974 (2013).

114. Begani, J., Lakhani, J. & Harwani, D. Current strategies to induce secondary metabolites from microbial biosynthetic cryptic gene clusters. *Ann. Microbiol.* **68**, 419–432 (2018).
115. Bode, H. B., Bethe, B., Höfs, R. & Zeeck, A. Big Effects from Small Changes: Possible Ways to Explore Nature's Chemical Diversity. *ChemBioChem* **3**, 619 (2002).
116. Bergmann, S. *et al.* Genomics-driven discovery of PKS-NRPS hybrid metabolites from Aspergillus nidulans. *Nat. Chem. Biol.* **3**, 213–217 (2007).
117. Khaldi, N. *et al.* SMURF: Genomic mapping of fungal secondary metabolite clusters. *Fungal Genet. Biol.* **47**, 736–741 (2010).
118. Pusztahelyi, T., Holb, I. J. & PÃ³csi, I. Secondary metabolites in fungus-plant interactions. *Front. Plant Sci.* **6**, (2015).
119. Bills, G. F. & Gloer, J. B. Biologically Active Secondary Metabolites from the Fungi. *Microbiol. Spectr.* **4**, (2016).
120. Arnison, P. G. *et al.* Ribosomally synthesized and post-translationally modified peptide natural products: overview and recommendations for a universal nomenclature. *Nat. Prod. Rep.* **30**, 108–160 (2013).
121. Ortega, M. A. & van der Donk, W. A. New Insights into the Biosynthetic Logic of Ribosomally Synthesized and Post-translationally Modified Peptide Natural Products. *Cell Chem. Biol.* **23**, 31–44 (2016).
122. Hertweck, C. The Biosynthetic Logic of Polyketide Diversity. *Angew. Chemie Int. Ed.* **48**, 4688–4716 (2009).
123. Chiang, Y.-M. *et al.* Characterization of the Aspergillus nidulans Monodictyphenone Gene Cluster. *Appl. Environ. Microbiol.* **76**, 2067–2074 (2010).
124. Sanchez, J. F. *et al.* Molecular genetic analysis of the orsellinic acid/F9775 genecluster of Aspergillus nidulans. *Mol. BioSyst.* **6**, 587–593 (2010).
125. Cacho, R. A., Chooi, Y.-H., Zhou, H. & Tang, Y. Complexity

Generation in Fungal Polyketide Biosynthesis: A Spirocycle-Forming P450 in the Concise Pathway to the Antifungal Drug Griseofulvin. *ACS Chem. Biol.* **8**, 2322–2330 (2013).

126. Bentley, R. Mycophenolic Acid: A One Hundred Year Odyssey from Antibiotic to Immunosuppressant. *Chem. Rev.* **100**, 3801–3826 (2000).
127. Rollini, M. Manzoni, M. Biosynthesis and biotechnological production of statins by filamentous fungi and application of these cholesterol-lowering drugs. *Appl. Microbiol. Biotechnol.* **58**, 555–564 (2002).
128. Srinivas, G., Babykutty, S., Sathiadevan, P. P. & Srinivas, P. Molecular mechanism of emodin action: Transition from laxative ingredient to an antitumor agent. *Med. Res. Rev.* **27**, 591–608 (2007).
129. Keller, N. P., Turner, G. & Bennett, J. W. Fungal Secondary Metabolism - From Biochemistry to Genomics. *Nat. Rev. Microbiol.* **3**, 937–947 (2005).
130. Eisendle, M., Oberegger, H., Zadra, I. & Haas, H. The siderophore system is essential for viability of Aspergillus nidulans: functional analysis of two genes encoding l-ornithine N 5-monooxygenase (sidA) and a non-ribosomal peptide synthetase (sidC). *Mol. Microbiol.* **49**, 359–375 (2003).
131. Cacho, R. A., Jiang, W., Chooi, Y.-H., Walsh, C. T. & Tang, Y. Identification and Characterization of the Echinocandin B Biosynthetic Gene Cluster from Emericella rugulosa NRRL 11440. *J. Am. Chem. Soc.* **134**, 16781–16790 (2012).
132. Bushley, K. E. *et al.* The Genome of Tolypocladium inflatum: Evolution, Organization, and Expression of the Cyclosporin Biosynthetic Gene Cluster. *PLoS Genet.* **9**, e1003496 (2013).
133. Degenkolb, T., Berg, A., Gams, W., Schlegel, B. & Gräfe, U. The occurrence of peptaibols and structurally related peptaibiotics in fungi and their mass spectrometric identification via diagnostic fragment

ions. *J. Pept. Sci.* **9**, 666–678 (2003).

134. Degenkolb, T. & Brückner, H. Peptaibiomics: Towards a myriad of bioactive peptides containing Cα-dialkylamino acids? *Chemistry and Biodiversity* (2008). doi:10.1002/cbdv.200890171
135. Stoppacher, N. *et al.* The Comprehensive Peptaibiotics Database. *Chem. Biodivers.* **10**, 734–743 (2013).
136. Bandani, A. R. *et al.* Production of efrapeptins by Tolypocladium species and evaluation of their insecticidal and antimicrobial properties. *Mycol. Res.* **104**, 537–544 (2000).
137. Fredenhagen, A., Molleyres, L.-P., Böhlendorf, B. & Laue, G. Structure Determination of Neoefrapeptins A to N: Peptides with Insecticidal Activity Produced by the Fungus Geotrichum candidum. *J. Antibiot. (Tokyo).* **59**, 267–280 (2006).
138. Scharf, D. H., Brakhage, A. A. & Mukherjee, P. K. Gliotoxin - bane or boon? *Environ. Microbiol.* **18**, 1096–1109 (2016).
139. Michael Sgambelluri, R. *et al.* Profiling of amatoxins and phallotoxins in the genus Lepiota by liquid chromatography combined with UV absorbance and mass spectrometry. *Toxins (Basel).* **6**, 2336–2347 (2014).
140. Battilani, P. *et al.* Phomopsins: An overview of phytopathological and chemical aspects, toxicity, analysis and occurrence. *World Mycotoxin J.* **4**, 345–359 (2011).
141. Tsukui, T. *et al.* Ustiloxins, fungal cyclic peptides, are ribosomally synthesized in Ustilaginoidea virens. *Bioinformatics* **31**, 981–985 (2015).
142. Nagano, N. *et al.* Class of cyclic ribosomal peptide synthetic genes in filamentous fungi. *Fungal Genet. Biol.* **86**, 58–70 (2016).
143. Umemura, M. *et al.* MIDDAS-M: Motif-Independent De Novo Detection of Secondary Metabolite Gene Clusters through the Integration of Genome Sequencing and Transcriptome Data. *PLoS One* **8**, e84028

(2013).

144. Koiso, Y. *et al.* Ustiloxins, antimitotic cyclic peptides from false smut balls on rice panicles caused by ustilaginoidea virens. *J. Antibiot. (Tokyo).* **47**, 765–773 (1994).
145. Miziorko, H. M. Enzymes of the mevalonate pathway of isoprenoid biosynthesis. *Arch. Biochem. Biophys.* **505**, 131–143 (2011).
146. Schmidt-Dannert, C. Biosynthesis of Terpenoid Natural Products in Fungi. in *Advances in Biochemical Engineering/Biotechnology* 19–61 (2014). doi:10.1007/10_2014_283
147. Nicholson, M. J. *et al.* Identification of Two Aflatrem Biosynthesis Gene Loci in Aspergillus flavus and Metabolic Engineering of Penicillium paxilli To Elucidate Their Function. *Appl. Environ. Microbiol.* **75**, 7469–7481 (2009).
148. Caruthers, J. M., Kang, I., Rynkiewicz, M. J., Cane, D. E. & Christianson, D. W. Crystal Structure Determination of Aristolochene Synthase from the Blue Cheese Mold, Penicillium roqueforti*. *J. Biol. Chem.* **275**, 25533–25539 (2000).
149. KAWAIDE, H. Biochemical and Molecular Analyses of Gibberellin Biosynthesis in Fungi. *Biosci. Biotechnol. Biochem.* **70**, 583–590 (2006).
150. McCormick, S. P., Stanley, A. M., Stover, N. A. & Alexander, N. J. Trichothecenes: From Simple to Complex Mycotoxins. *Toxins (Basel).* **3**, 802–814 (2011).
151. Lee, S.-L., Floss, H. G. & Heinstein, P. Purification and properties of dimethylallylpyrophosphate: Tryptophan dimethylallyl transferase, the first enzyme of ergot alkaloid biosynthesis in Claviceps. sp. SD 58. *Arch. Biochem. Biophys.* **177**, 84–94 (1976).
152. Xu, W., Gavia, D. J. & Tang, Y. Biosynthesis of fungal indole alkaloids. *Nat. Prod. Rep.* **31**, 1474–1487 (2014).
153. Wallwey, C. & Li, S.-M. Ergot alkaloids: structure diversity,

biosynthetic gene clusters and functional proof of biosynthetic genes. *Nat. Prod. Rep.* **28**, 496–510 (2011).

154. Wigley, L. J., Perry, D. A. & Mantle, P. G. An experimental strategy towards optimising directed biosynthesis of communesin analogues by Penicillium marinum in submerged fermentation. *Mycol. Res.* **112**, 131–137 (2008).
155. Tagami, K. *et al.* Reconstitution of Biosynthetic Machinery for Indole-Diterpene Paxilline in Aspergillus oryzae. *J. Am. Chem. Soc.* **135**, 1260–1263 (2013).
156. Fernandes, P. Fusidic acid: A bacterial elongation factor inhibitor for the oral treatment of acute and chronic staphylococcal infections. *Cold Spring Harb. Perspect. Med.* **6**, (2016).
157. Aasen, A. J. & Jensen, S. L. Fungal carotenoids. II. The structure of the carotenoid acid neurosporaxanthin. *Acta Chem. Scand.* **19**, 1843–1853 (1965).
158. Spilsbury, J. F. & Wilkinson, S. 398. The isolation of festuclavine and two new clavine alkaloids from Aspergillus fumigatus Fres. *J. Chem. Soc.* 2085 (1961). doi:10.1039/jr9610002085
159. Youssef, F. S., Alshammari, E. & Ashour, M. L. Bioactive alkaloids from genus aspergillus: Mechanistic interpretation of their antimicrobial and potential sars-cov-2 inhibitory activity using molecular modelling. *Int. J. Mol. Sci.* **22**, 1–22 (2021).
160. Leeder, A. C., Palma-Guerrero, J. & Glass, N. L. The social network: deciphering fungal language. *Nat. Rev. Microbiol.* **9**, 440–451 (2011).
161. Fischer, M. S. & Glass, N. L. Communicate and fuse: How filamentous fungi establish and maintain an interconnected mycelial network. *Front. Microbiol.* **10**, 1–20 (2019).
162. Wei, H., Requena, N. & Fischer, R. The MAPKK kinase SteC regulates conidiophore morphology and is essential for heterokaryon formation and sexual development in the homothallic fungus Aspergillus

nidulans. *Mol. Microbiol.* **47**, 1577–1588 (2003).

163. Jun, S.-C. *et al.* The MpkB MAP kinase plays a role in post-karyogamy processes as well as in hyphal anastomosis during sexual development in Aspergillus nidulans. *J. Microbiol.* **49**, 418–30 (2011).
164. Elramli, N. *et al.* Assembly of a heptameric STRIPAK complex is required for coordination of light-dependent multicellular fungal development with secondary metabolism in Aspergillus nidulans. *PLOS Genet.* **15**, e1008053 (2019).
165. Mehmood, A. *et al.* Fungal Quorum-Sensing Molecules and Inhibitors with Potential Antifungal Activity: A Review. *Molecules* **24**, 1950 (2019).
166. Wongsuk, T., Pumeesat, P. & Luplertlop, N. Fungal quorum sensing molecules: Role in fungal morphogenesis and pathogenicity. *J. Basic Microbiol.* **56**, 1–8 (2016).
167. Hornby, J. M. *et al.* Quorum Sensing in the Dimorphic Fungus Candida albicans Is Mediated by Farnesol. *Appl. Environ. Microbiol.* **67**, 2982–2992 (2001).
168. Albuquerque, P. & Casadevall, A. Quorum sensing in fungi – a review. *Med. Mycol.* **50**, 337–345 (2012).
169. Padder, S. A., Prasad, R. & Shah, A. H. Quorum sensing: A less known mode of communication among fungi. *Microbiol. Res.* **210**, 51–58 (2018).
170. Chen, H. Tyrosol is a quorum-sensing molecule in Candida albicans. *Proc. Natl. Acad. Sci.* **101**, 5048–5052 (2004).
171. Martins, M. *et al.* Morphogenesis control in Candida albicans and Candida dubliniensis through signaling molecules produced by planktonic and biofilm cells. *Eukaryot. Cell* **6**, 2429–2436 (2007).
172. Rhome, R. & Del Poeta, M. Lipid Signaling in Pathogenic Fungi. *Annu. Rev. Microbiol.* **63**, 119–131 (2009).
173. Dichtl, K. *et al.* Farnesol misplaces tip-localized Rho proteins and

inhibits cell wall integrity signalling in Aspergillus fumigatus. *Mol. Microbiol.* **76**, 1191–1204 (2010).

174. Horowitz Brown, S., Zarnowski, R., Sharpee, W. C. & Keller, N. P. Morphological Transitions Governed by Density Dependence and Lipoxygenase Activity in Aspergillus flavus. *Appl. Environ. Microbiol.* **74**, 5674–5685 (2008).
175. Williams, H. E., Steele, J. C. P., Clements, M. O. & Keshavarz, T. γ-Heptalactone is an endogenously produced quorum-sensing molecule regulating growth and secondary metabolite production by Aspergillus nidulans. *Appl. Microbiol. Biotechnol.* **96**, 773–781 (2012).
176. Raina, S. *et al.* Is quorum sensing involved in lovastatin production in the filamentous fungus Aspergillus terreus? *Process Biochem.* **47**, 843–852 (2012).
177. Sorrentino, F., Roy, I. & Keshavarz, T. Impact of linoleic acid supplementation on lovastatin production in Aspergillus terreus cultures. *Appl. Microbiol. Biotechnol.* **88**, 65–73 (2010).
178. Fleissner, A., Leeder, A. C., Roca, M. G., Read, N. D. & Glass, N. L. Oscillatory recruitment of signaling proteins to cell tips promotes coordinated behavior during cell fusion. *Proc. Natl. Acad. Sci.* **106**, 19387–19392 (2009).
179. Bottone, E. J., Nagarsheth, N. & Chiu, K. Evidence of self-inhibition by filamentous fungi accounts for unidirectional hyphal growth in colonies. *Can. J. Microbiol.* **44**, 390–393 (1998).
180. Champe, S. P. & El-Zayat, A. A. Isolation of a sexual sporulation hormone from Aspergillus nidulans. *J. Bacteriol.* **171**, 3982–3988 (1989).
181. Tsitsigiannis, D. I., Kowieski, T. M., Zarnowski, R. & Keller, N. P. Three putative oxylipin biosynthetic genes integrate sexual and asexual development in Aspergillus nidulans. *Microbiology* **151**, 1809–1821 (2005).

182. Stark, A. & Seddon, K. R. Ionic Liquids. in *Kirk-Othmer Encyclopedia of Chemical Technology* (2007). doi:10.1002/0471238961.ionisedd.a01
183. Petkovic, M. *et al.* Exploring fungal activity in the presence of ionic liquids. *Green Chem.* **11**, 889 (2009).
184. Martins, I. *et al.* Proteomic alterations induced by ionic liquids in Aspergillus nidulans and Neurospora crassa. *J. Proteomics* **94**, 262–278 (2013).
185. Alves, P. C. *et al.* Transcriptomic and metabolomic profiling of ionic liquid stimuli unveils enhanced secondary metabolism in Aspergillus nidulans. *BMC Genomics* **17**, 284 (2016).
186. Hartmann, D. O. *et al.* Plasma membrane permeabilisation by ionic liquids: a matter of charge. *Green Chem.* **17**, 4587–4598 (2015).
187. Petkovic, M. *et al.* Novel biocompatible cholinium-based ionic liquids - Toxicity and biodegradability. *Green Chem.* **12**, 643–649 (2010).
188. Coleman, D. & Gathergood, N. Biodegradation studies of ionic liquids. *Chem. Soc. Rev.* **39**, 600 (2010).
189. Garcia, M. T., Gathergood, N. & Scammells, P. J. Biodegradable ionic liquids Part II. Effect of the anion and toxicology. *Green Chem.* (2005).
190. Hartmann, D. O., Piontkivska, D., Moreira, C. J. S. & Silva Pereira, C. Ionic Liquids Chemical Stress Triggers Sphingoid Base Accumulation in Aspergillus nidulans. *Front. Microbiol.* **10**, (2019).
191. Markham, P., Robson, G. D., Bainbridge, B. W. & Trinci, A. P. J. J. Choline: its role in the growth of filamentous fungi and the regulation of mycelial morphology. *FEMS Microbiol. Rev.* **104**, 287–300 (1993).
192. Lockman, P. R. & Allen, D. D. The Transport of Choline. *Drug Dev. Ind. Pharm.* **28**, 749–771 (2002).
193. Emri, T., Molnár, Z., Pusztahelyi, T. & Pócsi, I. Physiological and morphological changes in autolyzing Aspergillus nidulans cultures. *Folia Microbiol. (Praha).* **49**, 277–284 (2004).

194. Emri, T., Molnár, Z., Szilágyi, M. & Pócsi, I. Regulation of autolysis in aspergillus nidulans. *Appl. Biochem. Biotechnol.* (2008). doi:10.1007/s12010-008-8174-7

195. Hoffmann, B., Wanke, C., LaPaglia, S. K. & Braus, G. H. c-Jun and RACK1 homologues regulate a control point for sexual development in Aspergillus nidulans. *Mol. Microbiol.* **37**, 28–41 (2000).

196. Aguirre, J., Ríos-Momberg, M., Hewitt, D. & Hansberg, W. Reactive oxygen species and development in microbial eukaryotes. *Trends Microbiol.* **13**, 111–118 (2005).

197. Gupta, N., Balomajumder, C. & Agarwal, V. K. Enzymatic mechanism and biochemistry for cyanide degradation: A review. *J. Hazard. Mater.* **176**, 1–13 (2010).

198. Richthammer, C. *et al.* RHO1 and RHO2 share partially overlapping functions in the regulation of cell wall integrity and hyphal polarity in Neurospora crassa. *Mol. Microbiol.* **85**, 716–733 (2012).

199. Lee, B., Yoshida, Y. & Hasunuma, K. Nucleoside diphosphate kinase-1 regulates hyphal development via the transcriptional regulation of catalase in Neurospora crassa. *FEBS Lett.* **583**, 3291–3295 (2009).

200. Michán, S., Lledías, F. & Hansberg, W. Asexual Development Is Increased in Neurospora crassa cat - 3 -Null Mutant Strains. *Eukaryot. Cell* **2**, 798–808 (2003).

201. Zhang, Y.-Q., Brock, M. & Keller, N. P. Connection of Propionyl-CoA Metabolism to Polyketide Biosynthesis in Aspergillus nidulans. *Genetics* **168**, 785–794 (2004).

202. Inglis, D. O. *et al.* Comprehensive annotation of secondary metabolite biosynthetic genes and gene clusters of Aspergillus nidulans, A. fumigatus, A. niger and A. oryzae. *BMC Microbiol.* **13**, 91 (2013).

203. Degenkolb, T., Kirschbaum, J. & Brückner, H. New sequences, constituents, and producers of peptaibiotics: An updated review. *Chem. Biodivers.* **4**, 1052–1067 (2007).

Chapter II

Tailoring amphotericin B as an ionic liquid: an upfront strategy to potentiate the biological activity of antifungal drugs

This chapter is a reprint of the manuscript published in RSC Advances:

Hartmann, DO, Shimizu K, Rothkegel M, Petkovic M, Ferraz R, Petrovski Ž, Branco LC, Canongia Lopes JN and Silva Pereira C. Tailoring amphotericin B as an ionic liquid: an upfront strategy to potentiate the biological activity of antifungal drugs. RSC Adv. 11, 14441–14452 (2021).

Tailoring amphotericin B as an ionic liquid: an upfront strategy to potentiate the biological activity of antifungal drugs

Diego O. Hartmann[1], Karina Shimizu[2], Maika Rothkegel[1], Marija Petkovic[1], Ricardo Ferraz[3,4], Željko Petrovski[5], Luís C. Branco[5], José N. Canongia Lopes[2] and Cristina Silva Pereira[1*]

[1] Instituto de Tecnologia Química e Biológica António Xavier, Universidade Nova de Lisboa (ITQB NOVA), Av. da República, 2780-157, Oeiras, Portugal

[2] Centro de Química Estrutural, Instituto Superior Técnico, Universidade de Lisboa, Av. Rovisco Pais, 1049-001 Lisboa, Portugal

[3] Ciências Químicas e das Biomoléculas e Centro de Investigação em Saúde e Ambiente, Escola Superior de Saúde do Instituto Politécnico do Porto, 4400-330 Porto, Portugal.

[4] LAQV-REQUIMTE, Departamento de Química e Bioquímica, Faculdade de Ciências, Universidade do Porto, Rua do Campo Alegre 687, 4169-007 Porto, Portugal.

[5] LAQV-REQUIMTE, Departamento de Química, Faculdade de Ciências e Tecnologia da Universidade Nova de Lisboa, 2829-516 Caparica, Portugal.

Abstract

Aspergillus species are the primary cause of invasive aspergillosis, which afflicts hundreds of thousands of patients yearly, with high mortality rates. Amphotericin B is considered the gold standard in antifungal drug therapy, due to its broad-spectrum activity and rarely reported resistance. However, low solubility and permeability, as well as considerable toxicity, challenge its administration. Lipid formulations of amphotericin B have been used to promote its slow release and diminish toxicity, but these are expensive and adverse health effects of their prolonged use have been reported. In the past decades, great interest emerged on converting biologically active molecules into an ionic liquid form to overcome limitations as low solubility or polymorphisms. In this study, we evaluated the biological activity of novel ionic liquid formulations where the cholinium, cetylpyridinium or trihexyl-tetradecylphosphonium cations were combined with an anionic form of

amphotericin B. We observed that two formulations increased the antifungal activity of the drug, while maintaining its mode of action. Molecular dynamics simulations showed that higher biological activity was due to increased interaction of the ionic liquid with the fungal membrane ergosterol compared with amphotericin B alone. Increased cytotoxicity could also be observed, probably due to greater interaction of the cation with cholesterol, the main sterol in animal cells. Importantly, one formulation also displayed antibacterial activity (dual functionality), likely preserved from the cation. Collectively, the data set ground for the guided development of ionic liquid formulations that could improve the administration, efficacy and safety of antifungal drugs or even the exploitation of their dual functionality.

Introduction

Invasive fungal infections present a severe threat worldwide. The genus *Aspergillus* encloses some of the most common airborne fungi and opportunistic pathogens, allergen and mycotoxin producers[1]. *Aspergillus fumigatus* is the primary cause of invasive aspergillosis, which affects over two thousand hundred immunocompromised patients *per* year, with a mortality rate of 50% even if diagnosed and treated at early stages[1,2]. It has been demonstrated that *A. fumigatus* forms biofilms *in vivo*, i.e., a growth mode that implies tightly associated hyphae embedded in an extracellular polymeric matrix[3]. These biofilm cultures appear to be significantly more resistant to antifungal agents than free-living cultures, probably due to reduced diffusion rates of antifungal agents through the extracellular matrix, as well as an increased activity of efflux pumps and transporter proteins[3,4].

The arsenal of antifungal drugs currently in clinical use is rather limited and relays mainly on targeting ergosterol – the main fungal sterol – or its biosynthetic pathway (polyenes and azoles), fungal cell wall (echinocandins) or nucleic acids synthesis (pyrimidine analogs)[5]. Resistance to azoles (which target a 14α-demethylase in ergosterol biosynthesis)[6] and, more recently, to

echinocandins (due to mutations in cell wall biosynthetic genes)[7] have been already reported and it is assumed to be a consequence of their excessive use. The macrolide polyene amphotericin B (AmB), on the other hand, remains a gold standard in antifungal drug therapy, due to its relatively broad spectrum of action and uncommon emergence of resistance during treatment[8]. AmB preferentially binds to ergosterol, the primary sterol in the fungal cell membrane. As a consequence, there is a disruption of the osmotic integrity of the membrane, with leakage of ions and other cellular materials and, consequently, death[9]. The most commonly accepted mode of action assumes that AmB forms ion channel aggregates that are inserted in the lipid bilayer, causing its permeabilization[10]. A sterol sponge model proposed that AmB exists in the form of large extramembranous aggregates that extract ergosterol from the lipid bilayers instead[11]. Transcriptomic and proteomic analyses of *A. fumigatus* after exposure to AmB further revealed its molecular targets, mainly in the ergosterol biosynthetic pathway, cell wall maintenance, cell stress and transport proteins[12]. Oxidative stress has been implicated as critical for cell death and likely has an important role in AmB mechanism of action; however, direct proof is still lacking[13].

The amphipathic nature of AmB, along with its low solubility and permeability, has always posed as a great disadvantage in its administration. AmB itself is insoluble in saline at a physiological pH and therefore it is normally prescribed in a combination with the detergent sodium deoxycholate. The major drawback in the use of amphotericin B deoxycholate is its narrow therapeutic index, namely high toxicity manifested as acute infusion-related reactions and dose-related nephrotoxicity[14]. Since its first clinical use in 1959, three lipid formulations of AmB were commercialized (i.e. colloidal dispersion, lipid complex and liposomal AmB), as to promote slow release and diminish toxic side-effects[15]. These formulations, however, are considerably expensive, and some reports indicate adverse health effects of their prolonged use[16]. In the past years, new promising solutions to overcome

AmB limited solubility and high toxicity have emerged, such as poly(D,L-lactide-co-glycolide) nanoparticles with AmB[17]. Noteworthy is a study in which several ionic liquids were designed and used as excipients for AmB, achieving some improvement in drug solubility[18].

Ionic liquids are a class of tuneable organic salts that have been largely studied as catalysts or solvents for industrial and biotechnological applications[19,20]. In the past decade, we have witnessed the conversion of biologically active molecules to an ionic liquid form to overcome limitations such as low solubility or polymorphisms[21], e.g. ranitidine docusate[22], cholinium betulinate[23] or cholinium niflumate[24]. The strategy of transforming commonly used antibiotics[25,26], herbicides[27] or fungicides[28] to an ionic liquid form was also undertaken. As an example, the antibiotic ampicillin was combined with several cations, such as cetylpyridinium ($[C_{16}py]^+$), trihexyltetradecylphosphonium ($[P_{6\,6\,6\,14}]^+$) or cholinium ($[chol]^+$)[25]. Some of these ampicillin ionic liquids were observed to be significantly more effective against a variety of clinically relevant bacteria, especially resistant strains.

In this study, we evaluated the biological activity of new ionic liquid formulations where the $[chol]^+$, $[C_{16}py]^+$ or $[P_{6\,6\,6\,14}]^+$ cations were coupled with an anionic form of AmB ($[AmB]^-$) (Figure 1). The resulting cholinium amphotericin B ([chol][AmB]), cetylpyridinium amphotericin B ($[C_{16}py][AmB]$) and trihexyltetradecylphosphonium amphotericin B ($[P_{6\,6\,6\,14}][AmB]$) were subjected to various susceptibility assays to determine if they displayed increased antifungal activity against *Aspergillus* biofilm cultures, when compared with the parent antifungal drug, i.e., AmB. We performed gene expression analysis to confirm if the responsive genes and mode of action of AmB were kept the same. Molecular dynamics simulations studies were done to further investigate the mechanisms behind different susceptibility patterns observed between AmB and the ionic liquid formulations.

Experimental

Chemicals

Commercially available reagents were purchased from Sigma-Aldrich, BDH Laboratory Reagents, Frilabo and Solchemar (unless stated otherwise). The solvents were from Valente & Ribeiro and distilled before used. The basic anion-exchange resin Amberlite IRA-400-OH (ion-exchange capacity 1.4 Eq.mL^{-1}) was purchased from SUPELCO. The synthetized ionic liquids were characterized by IR spectroscopy (Perkin Elmer 683 spectrometer) and by ^{1}H and ^{13}C NMR spectroscopy (Bruker AMX400 spectrometer) and their purity was confirmed by Matrix Assisted Laser Desorption Ionization – Time of Flight (MALDI-TOF). 5 mM stock solutions in DMSO were prepared and kept at -20 °C. 100mM stocks were also made for [C_{16}py]Cl and [$P_{6\,6\,6\,14}$]Cl and a 2.5 M stock was made for [chol]Cl (in water).

Synthesis of amphotericin B-based ionic liquids

For the synthesis of cholinium AmB ([chol][AmB]), cetylpyridinium AmB ([C_{16}py][AmB]) and trihexyltetradecylphosphonium AmB ([$P_{6\,6\,6\,14}$][AmB]), (2-hydroxyethyl)-trimethylammonium chloride, cetylpyridinium chloride or trihexyl(tetradecyl)phosphonium chloride, respectively, was dissolved in methanol and passed through an ion-exchange Amberlite IRA-400(OH) (5 eq., flux rate 0.133 mL.min^{-1} = 8 BVh^{-1}). Each hydroxide solution formed was slowly added to AmB dissolved in 1.0 M dried triethylamine methanolic solution. Each mixture was stirred at room temperature for 1 hour. After solvent evaporation the residue was dried *in vacuum* for 24 hours to provide the desired products. Detailed data on the synthesis and characterization of each AmB ionic liquid are described in the supplementary information.

Fungal susceptibility assays

The fungal strains *Aspergillus fumigatus* Af293 and *Aspergillus terreus* NIH2624 were purchased from the Fungal Genetics Stock Centre (Table S1). Cultures were grown on Sabouraud dextrose agar at 37 °C and conidial

suspensions were prepared and stored at -20 °C in 20% glycerol until use. The method used in the susceptibility assays was a modified version of that proposed by Mowat *et al.*[4]. The cultivation medium was RPMI 1640 (Sigma-Aldrich, R0883), supplemented with glutamine (0.3 g/L), glucose (10 g/L) and 0.165 M MOPS, and buffered to pH 7.0. All procedures were carried out in an ESCO Class II Biosafety Cabinet. *Aspergillus fumigatus* and *A. terreus* biofilms were formed on sterile, polystyrene, flat-bottomed, 96-well microtiter plates (Corning). 200 µL of conidial suspension (10^5 conidia *per* mL) in MOPS-buffered RPMI 1640 was added to each well and incubated statically for 24 hours at 37°C. A minimum of five replicates was performed for each experimental parameter, plus suitable controls (DMSO control, negative control and blank wells). After 24 hours, the biofilms were formed; the medium was aspirated and replaced by serial double dilutions of the compounds. The selected concentrations varied for each compound. The range was from 0.03125 to 32 µM for AmB-based compounds, 0.098 to 200 µM for $[C_{16}py]Cl$ and $[P_{6\,6\,6\,14}]Cl$ and 1 µM to 1M for [chol]Cl. The challenged biofilm cultures were incubated for additional 24 hours at 37°C. Metabolic activity reduction was assessed using a standard MTT assay, in comparison to untreated culture. Briefly, a solution of 3-(4,5-dimethylthiazol-2-yl)-2,5-diphenyl tetrazolium bromide (MTT) was added to each well at a final concentration of 0.438 $mg \cdot mL^{-1}$, and then incubated for further 4 hours. Afterwards the supernatant medium was removed and replaced by 0.04 M HCl in isopropanol to dissolve the formed formazan crystals. MTT reduction was monitored with a micro-plate reader scoring absorbance at 570 nm. The same method was used to evaluate the interaction of $[C_{16}py]Cl$ and AmB in a checkerboard assay[29]. Each experiment was repeated on at least three separate occasions. Statistical analysis was performed using Graph Prism v7.0. Independent experiments were compared using one-way ANOVA analysis of variance and Bonferroni's multiple comparison test and no significant differences were observed. The half-minimal inhibitory

concentrations (IC_{50}, i.e., the concentration of the test substance that lowers MTT reduction by 50% when compared to the untreated control) were calculated from dose-response curves. The curves of each treatment were compared using paired Student's t-test with 95% confidence interval.

Gene expression analysis

A suspension of 10^5 *A. fumigatus* conidia *per* ml of medium was incubated in 50 ml of MOPS-buffered RPMI 1640 medium (as described above). Triplicate biofilm cultures were cultivated in 75 cm^2 surface-treated cell culture flasks. After 24 hours of growth, AmB, [chol][AmB], [C_{16}py][AmB] or [$P_{6\,6\,6\,14}$][AmB] were added to the culture media to obtain a final concentration corresponding to the IC_{50} of each compound and incubated for 4 or 24 hours. A negative control without the addition of any compound was also included. Afterwards, mycelia were recovered by filtration (0.45 µm membrane filters, Millipore) and immediately frozen in liquid nitrogen. Approximately 100 mg of frozen mycelia were ground with poly(vinylpolypyrrolidone) (0.4 mg *per* mg of mycelia) using a TissueLyser LT (QIAGEN). The final powder was used in the extraction and purification of total RNA using the RNeasy Plant Mini Kit (QIAGEN), according to the manufacturer's protocol. Genomic DNA digestion was done with the RNase-Free DNase Set (QIAGEN). Quality, integrity and quantity of the total RNA were analyzed using a NanoDrop 1000 Spectrophotometer (Thermo Scientific) and by running 2 mg of RNA into 1% agarose gels in TAE buffer. The complementary DNA (cDNA) was synthesized from 500 ng of the total RNA using an iScript cDNA Synthesis Kit (Bio-Rad) in a T100 Thermal Cycler (Bio-Rad). The reaction protocol consisted of 5 min at 25 °C, 30 min at 42 °C and 5 min at 85 °C.

For the gene expression analysis by quantitative real-time PCR (*q*RT-PCR), oligonucleotide pairs for nine specific AmB-responsive *A. fumigatus* genes (Table S2) were designed using the Gene-Fisher2 web tool (bibiserv.techfak.uni-bielefeld.de/genefisher2) and produced by STAB VIDA. The *q*RT-PCR

analysis was performed in a CFX96 Thermal Cycler (Bio-Rad), using a SsoFast EvaGreen Supermix (Bio-Rad), 250 nM of each oligonucleotide and the cDNA template equivalent to 10 ng of the total RNA, at a final volume of 10 µl *per* well, in three technical replicates. The PCR conditions were enzyme activation at 95 °C for 30 s; 40 cycles of denaturation at 95 °C for 10 s and annealing/extension at 59 °C for 10 s; and a melting curve obtained from 65 °C to 95 °C, consisting of 0.5 °C increments for 5 s. Data analyses were performed using the CFX Manager software (Bio-Rad). The expression of each gene was normalized by the expression of the glyceraldehyde-3-phosphate dehydrogenase gene (*gpdA*, internal control). Final expression values were obtained as a relative expression comparatively to the negative control, for each target gene. Three biological replicates were performed. Statistical analysis was performed in the GraphPad Prism v7.0 software. Treatments with ionic liquids formulations were compared with AmB for each time point (4 and 24 hours) by multiple Student's t-test. Differences with a P value below 0.05 were considered statistically significant.

Cytotoxicity assay

Cell line mIMCD-3 (ATCC® CRL-2123™) from mouse (*Mus musculus*) inner medulla collecting duct was kindly provided by Dr Duarte C. Barral (Chronic Diseases Research Center, NOVA Medical School, Lisbon, Portugal). Cells with a passage number between six and 21 were used. Cells were cultured in Dulbecco's Modified Eagle Medium: nutrient mixture F-12 supplemented with fetal calf serum (10% v/v) and 1% Pen Strep preparation (all from Life Technologies). 96-well micro-plates were used for MTT assays, using the two-fold dilutions of the tested compounds. Equal volumes of cell suspension and test solution in culture media were added to each well, to obtain final volume of 150 µl with 7.5×10^4 cells. The plates were incubated for 68 hours at 37 °C in a 5% CO_2 atmosphere. A solution of MTT was then added to each well to reach a final concentration of 3.6 $mg \cdot ml^{-1}$, and then incubated as before for further 4 hours. Afterwards, the supernatant media was removed

and substituted by acidified (0.02M HCl) 10% v/v SDS solution, followed by overnight incubation in the dark at room temperature. At the end of the experiment, MTT reduction was monitored with a micro-plate reader scoring absorbance at 570 nm.

Molecular dynamics simulations

The [C_{16}py][AmB] formulation was parameterized using the CL&P atomistic force field[30], an extension of the AMBER and OPLS force fields[31], specially designed to study ionic liquids and their homologous series. Water, ergosterol, cholesterol, AmB and [AmB]$^-$ anion were modeled using the SPC model[32] and the OPLS force field, respectively. Molecular dynamics simulations were carried out using the DL_POLY 2.20 package[33] and Gromacs package[34–38]. The runs in DL_POLY started from low-density configurations built with the PACKMOL package[39] and were performed using 2 fs time steps and 2 nm cut-off distances. All simulations were subjected to equilibration runs under isobaric isothermal ensemble conditions (p = 0.1 MPa and T = 300 K with Nosé−Hoover thermostats and barostats with relaxation time constants of 1 and 4 ps, respectively) for 200 ps. Therefore, Gromacs simulations were performed using 2 fs time steps and 2 nm cut-off distances, with Ewald summation corrections performed beyond the cut-offs. The isothermal-isobaric ensemble conditions used during equilibration were p = 0.1 MPa and T = 300 K with V-rescale thermostats and Berendsen barostats with relaxation time constants of 1 and 4 ps, respectively. Nine consecutive runs were carried out to conduct an annealing process. The temperature range was from 300 K to 500 K. After 10 ns, the density of each system reached constant and consistent values, indicating that equilibrium had been attained and possible ergodicity problems were overcome. Finally, 10 ns production stage was performed using 1 fs time step; the isothermal-isobaric ensemble conditions used during equilibration were p = 0.1 MPa and T = 300 K with Nosé−Hoover thermostats and Parrinello-Rahman barostats with relaxation time constants of 1 and 4 ps,

respectively. The aqueous solutions containing the ergosterol or cholesterol and AmB or [C_{16}py][AmB] were modeled using one sterol molecule and two AmB or [C_{16}py][AmB] molecules mixed with 4000 water molecules. Three different complexes were produced for each mixture. All simulations were performed as described above. The most stable complexes were chosen (Table S3). Low density initial configurations were randomly built using the packmol package, placing ten complexes mixed with 10000 water molecules, and then new simulations were performed.

The aggregation analyses of ergosterol, cholesterol, AmB and [C_{16}py][AmB] mixtures with water focused on two types of issues: (i) the evaluation of the connectivity among the ergosterol or cholesterol molecules and an estimation of their aggregate sizes; and (ii) the calculation of the connectivity between the AmB or [C_{16}py][AmB] and the ergosterol or cholesterol molecules. All these types of connectivity analyses were based on previously described algorithms[40] that generate neighbor lists for selected interaction centers, in a three-stage sequential process. First, the different types of interaction centers were defined. In type (i) analyses the selected interaction centers were all non-hydrogen atoms in the ergosterol or cholesterol molecules. Type (ii) analyses were conducted by selecting all carbon atoms of the alkyl chain of the cation or carbon atoms of the unsaturated part of the AmB or [C_{16}py][AmB], and all non-hydrogen atoms in the ergosterol or cholesterol molecules. Second, a connectivity threshold for each case was established by considering the corresponding $g_{ij}(r)$ data between the selected interaction centers[40]. In cases (i) and (ii) the threshold was set to 0.5 nm, corresponding to average intermolecular contact distances between non-hydrogen atoms evaluated from the corresponding $g(r)$ functions. Third, the use of the threshold criteria allowed the computation of closest-neighbor lists for each interaction center for all recorded configurations in the molecular dynamics' trajectories, thus ascertaining the connectivity between the selected species. When the interaction centers belonged to species of

the same type, i.e., sterol–sterol in case (i), the corresponding aggregates corresponded to clusters containing a single type of molecule. In the case of interaction centers belonging to different species, i.e. sterol–AmB or sterol-[C_{16}py][AmB] in case (ii), the analyses yielded aggregates with a built-in between species.

High-Performance Liquid Chromatography (HPLC) analyses

To mimic the conditions from the molecular dynamics simulations, ergosterol was incubated in water with either AmB, [C_{16}py][AmB] or [C_{16}py]Cl. 20 µM of ergosterol was mixed with 20, 30, 40, 50 or 60 µM of each compound in ultrapure water, at a final volume of 1 mL, at room temperature, for one hour. Ergosterol with equal concentrations of DMSO as each condition was used as control. After incubation. the mixtures were centrifuged at 25000 *g* for 10 min, the supernatant was recovered and ergosterol content was analyzed on a Waters HPLC System with a 2707 Autosampler, a 1525 Binary HPLC pump with a column oven, and a 2998 Photodiode Array Detector. A Symmetry® C18 reverse phase column (250 × 4.6 mm), packed with end capped particles (5 µm, pore size 100 Å) was used at 30°C. Data were acquired using Empower 2 software, 2006 (Waters Corporation). Sample injections of 50 µl were made using a 100 µl loop operated in partial loop mode. The mobile phase, at a flow rate of 1.2 ml·min^{-1}, consisted of 90% methanol and 10% acetonitrile. Each sample was run for 17 min. Ergosterol eluted at 13min. Ergosterol was quantified by peak area according to a calibration curve. Three replicates of each condition were performed. Ergosterol content in the supernatant of mixtures of AmB, [C_{16}py][AmB] or [C_{16}py]Cl was taken relative to the control.

Antibacterial activity assays

The ionic liquid formulation [C_{16}py][AmB] and its parental compounds AmB and [C_{16}py]Cl were assessed for their antimicrobial activity against *Staphylococcus aureus* NCTC8325 and *Escherichia coli* TOP 10 strains. The

bacteria were grown to approximately 1 to 2 × 10^8 CFU·mL^{-1} in Mueller Hinton Broth (MHB, Panreac). Two-fold serial dilutions of each compound were performed to obtain final concentrations between 0.195 and 100 µM, in 96-well plates, in triplicates. Abiotic (medium alone) and biotic controls (without addition of any compound) were included for each test. Plates were incubated statically at 37°C for 24 hours and absorbance (600 nm) was measured at the end of incubation using a Tecan Infinite 200 Microplate spectrophotometer (Männedorf, Switzerland). At least three biological replicates were performed. Statistical analysis and determination of IC_{50} values were done as described for the fungal susceptibility assays.

Results and Discussion

In this study, we investigated the biological activity of new ionic liquid formulations of AmB, which were designed as an alternative to overcome the low solubility of this antifungal drug. The anionic form of AmB was combined with three different cations, namely $[chol]^+$, $[C_{16}py]^+$ or $[P_{6\,6\,6\,14}]^+$ (Figure 1). $[chol]^+$ is a well-known nutraceutical (in the form of cholinium chloride)[41], and has been proposed in many ionic liquid formulations as a non-toxic and biodegradable cation[42]. $[C_{16}py]^+$ has been widely used, mainly in its chloride form, as an antimicrobial agent in oral hygiene products[43] and in some ionic liquids formulations combined with active pharmaceutical ingredients, e.g. aspirin[44]. Despite the considerably high toxicity of $[P_{6\,6\,6\,14}]^+$[45], this cation has already been successfully used in the development of antibiotic ionic liquid formulations, increasing the biocidal activity of ampicillin[25], amoxicillin and penicillin G[26] against resistant bacterial strains.

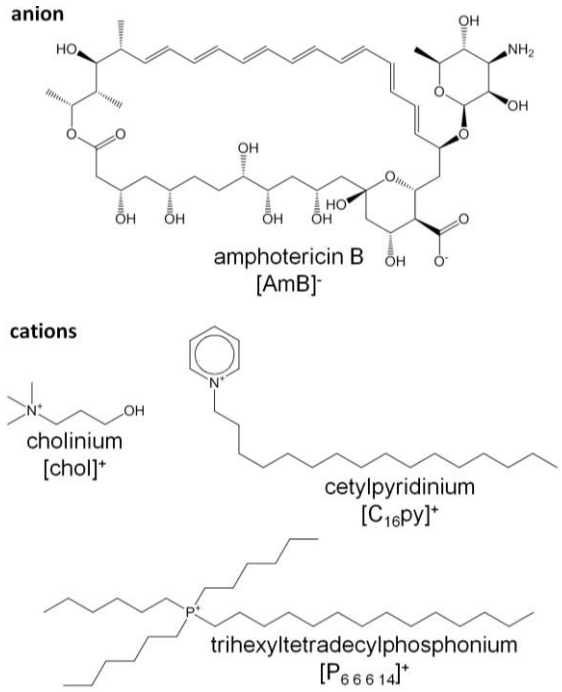

Figure 1 Anion and cations structures present in the amphotericin B-ionic liquid formulations used in this study: cholinium amphotericin B ([chol][AmB]), cetylpyridinium amphotericin B ([C16py][AmB]) and trihexyltetradecylphosphonium amphotericin B ([P6 6 6 14][AmB]).

Antifungal activity against *Aspergillus fumigatus*

We evaluated the susceptibility of *A. fumigatus* to the synthesized formulations [chol][AmB], [C_{16}py][AmB] and [$P_{6\,6\,6\,14}$][AmB], comparatively to the effect of their parental compounds. While the antifungal drug AmB presented an IC_{50} of 0.70 µM, the parental compounds [chol]Cl, [C_{16}py]Cl and [$P_{6\,6\,6\,14}$]Cl presented much lower activity against *A. fumigatus*, with IC_{50} of 880 mM (approximate value), 12.78 µM and 28.4 µM, respectively (Figure 2). An initial comparison of the dose-response curves showed that both ionic liquid formulations [chol][AmB] and [C_{16}py][AmB] appear to be more effective than AmB (Figure 2). However, the statistical analysis revealed that only [C_{16}py][AmB] presents a dose-response curve significantly different from AmB (P value: 0.0008), while the differences between the curves of [chol][AmB] and the parental compound are not statistically significant

(P value: 0.4674). Despite that, both ionic liquid formulations showed lower calculated IC_{50} values than AmB (determined in this study as 0.70 μM). [chol][AmB] and [C_{16}py][AmB] displayed IC_{50} values of 0.57 and 0.22 μM, respectively, representing an increase in the antifungal activity of *ca.* 1.2 and 3.2-fold. Interestingly, despite showing a significantly different dose-response curve compared to AmB (P value: 0.0292), the [$P_{6\,6\,6\,14}$][AmB] formulation had an opposite effect and decreased the activity of AmB, with a calculated IC_{50} of 1.62 μM (Figure 2).

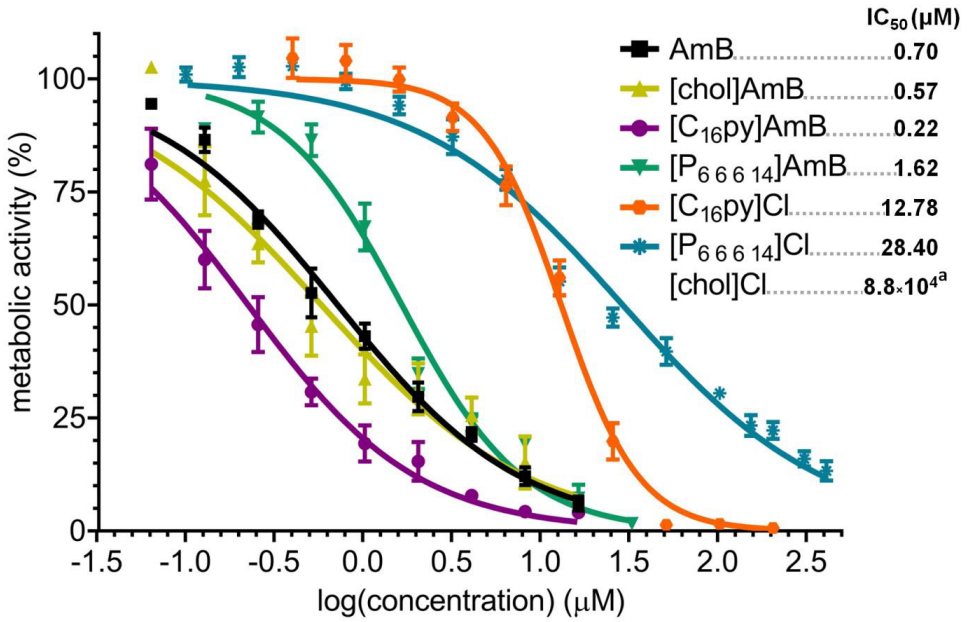

Figure 2 Dose-response curve and calculated IC50 values (in μM, upper right corner) of amphotericin B (AmB, black squares), cholinium amphotericin B ([chol][AmB], yellow triangles), cetylpyridinium amphotericin B ([C16py][AmB], purple circles), trihexyltetradecylphosphonium amphotericin B ([P6 6 6 14][AmB], green inverted triangles), cetylpyridinium chloride ([C16py]Cl, orange hexagons), trihexyltetradecylphosphonium chloride ([P6 6 6 14][AmB], blue asterisks) and cholinium chloride against Aspergillus fumigatus. The y axis represents the percentage of metabolic activity (determined by standard MTT assay) comparatively to the growth without any treatment. The x axis represents the log of the concentration of each tested compound. [a]For cholinium chloride, the curve was omitted since most tested concentrations displayed no inhibition of activity and the IC50 value is an approximate prediction based on the obtained data.

Expression analyses of AmB-responsive genes

The susceptibility data showed that the ionic liquid formulations of AmB were able to alter the dose necessary to affect the growth of *A. fumigatus*, but whether the mode of action of the antifungal drug were kept the same was still unclear. To address this question, we analyzed the expression of *A. fumigatus* genes known to be responsive to AmB. Based on transcriptomic and proteomic analyses of *A. fumigatus* after exposure to AmB[12], we selected a set of nine genes that belong to main functional groups with increased expression upon AmB exposure: ergosterol biosynthesis (sterol 24-C-methyltransferase – *erg6*; 14-α demethylase – *erg11B*; and hydroxymethyl glutaryl-coenzyme A synthase – *erg13*), cell stress (manganese superoxide dismutase – *sod3*; and putative glutathione S-transferase, "GST"), cell wall proteins (conidial cell wall hydrophobin – *rodB*) and transporter proteins (multidrug resistance protein4 – *mdr3*, plasma membrane H^+ ATPase – *pma1*; and putative GTPase-activating protein, "GTPase"). These genes have been previously reported to be up-regulated after 24 hours of exposure to AmB[12].

In our study, we analyzed the expression of these nine genes after 4 or 24 hours of exposure to AmB, [chol][AmB], [C_{16}py][AmB] and [$P_{6\,6\,6\,14}$][AmB], relatively to a negative control. We observed that, after 4 hours of exposure to AmB, all the tested genes underwent a great downregulation in their expression (Figure 3 and Table S4). Except for *mdr3* (that had a 5.5-fold increase), we did not observe a considerable increase in the expression of the genes after 24 hours of exposure to AmB relative to the negative control (Figure 3 and Table S4). However, we observe that the genes underwent an up-regulation in their expression compared to 4 hours of exposure. These results are consistent with other studies that reported major decreases in the expression of responsive genes within the first hours of AmB exposure, followed by their increase afterwards[12,46].

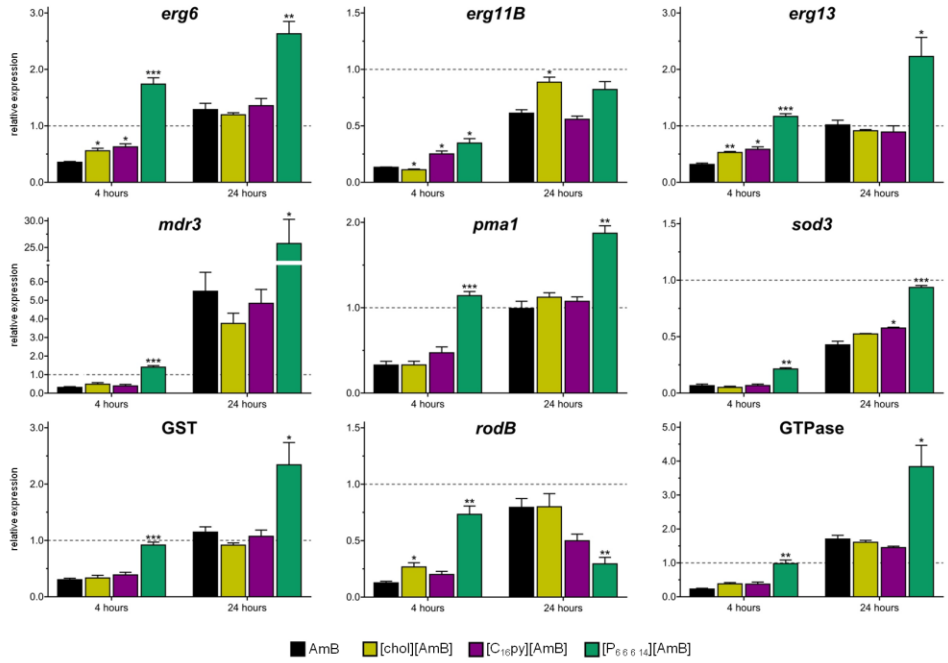

Figure 3 Gene expression analysis of nine amphotericin B-responsive genes in Aspergillus fumigatus (erg6, erg11B, erg13, mdr3, pma1, sod3, putative glutathione S-transferase gene (GST, Afu3g07930), rodB and putative GTPase gene (Afu6g12340)) after 4 or 24-hour exposure to amphotericin B (AmB, black bars), cholinium amphotericin B ([chol][AmB], yellow bars), cetylpyridinium amphotericin B ([C16py][AmB], purple bars) or trihexyltetradecylphosphonium amphotericin B ([P6 6 6 14][AmB], green bars). Glyceraldehyde 3-phosphate dehydrogenase gene (gpdA) was used as internal control. Values represent the fold-change relative to the negative (untreated) control followed by their standard deviation. Three biological replicates were performed. The asterisks mark statistically significant differences in the expression of [chol][AmB], [C16py][AmB] or [P6 6 6 14][AmB] when compared to AmB for each exposure time (= p<0.05; ** = p<0.01, *** = p <0.001).*

After 4 hours of exposure to [chol][AmB] or [C_{16}py][AmB], the majority of the responsive genes (five for [chol][AmB] and six for [C_{16}py][AmB], out of nine tested genes) displayed expression profiles with no significant differences from AmB (Figure 3 and Table S4). This similarity is even more evident after 24 hours of exposure to the ionic liquid formulations. Eight out of nine of the tested genes, either for [chol][AmB] or [C_{16}py][AmB], had expression levels with no significant differences from the AmB treatment (Figure 3 and Table S4). These results indicate that redesigning AmB as [chol][AmB] or

[C_{16}py][AmB] did not alter the molecular response of the fungus, suggesting the preservation of its mechanism of action in these ionic liquid formulations. This was not observed for the [$P_{6\,6\,6\,14}$][AmB], since all or nearly all genes had significantly different expression levels compared to AmB, either for 4 or 24 hours (Figure 3 and Table S4). Quaternary phosphonium-based ionic liquids, e.g. alkyltributylphosphonium chlorides, have been previously described to inhibit the growth and completely kill *A. nidulans* at concentrations above 10 μM, mainly by inducing damage to the fungal cell wall and plasma membrane[47,48]. In this study, although [$P_{6\,6\,6\,14}$]Cl displayed inhibition values comparable to those reported in the literature for similar compounds, its combination with AmB in an ionic liquid form decreased the activity and altered the fungal response to the parental antifungal drug. [$P_{6\,6\,6\,14}$]Cl has a strong hydrophobic nature[49]; it is possible that this, in combination with the also low solubility of AmB, decreased the bioavailability of the antifungal drug, therefore its activity. Having the lower activity of [$P_{6\,6\,6\,14}$][AmB] in consideration, the following studies focused on [chol][AmB] and [C_{16}py][AmB] formulations.

Antifungal activity against intrinsically resistant *Aspergillus terreus*

Considering their higher antifungal activity towards *A. fumigatus* and preserved mechanism of action, we asked if other fungal species would also be more susceptible to [chol][AmB] or [C_{16}py][AmB], compared to AmB. We selected *A. terreus*, which is also an important causative agent of invasive fungal infections and that, more importantly, presents an intrinsic resistance to AmB[13,50]. In our study, AmB had a calculated IC_{50} of 2.60 μM against *A. terreus* (Figure 4), almost four times higher than that determined for *A. fumigatus* (Figure 2). The parental compounds [chol]Cl and [C_{16}py]Cl displayed low antifungal activity, with IC_{50} values of 1.08 M (approximate value) and 11.85 μM, respectively (Figure 4). When testing [chol][AmB] and [C_{16}py][AmB] against *A. terreus*, we observed that both formulations showed significantly different dose-response curves when compared to AmB

(P values: 0.0133 and 0.0009, respectively) (Figure 4). [chol][AmB] had an IC_{50} of 2.11 µM, while [C_{16}py][AmB] displayed a calculated IC_{50} of 0.82 µM, which represent *ca.* 1.2 and 3.2-fold increase in AmB activity, respectively, the same levels observed for *A. fumigatus* (Figure 2).

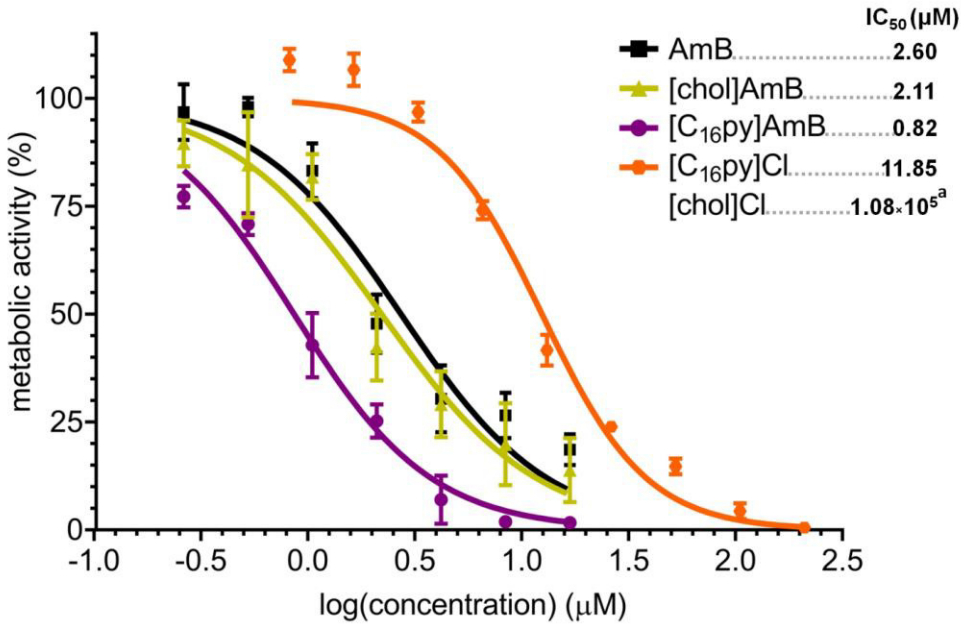

Figure 4 Dose-response curve and calculated IC50 values (in µM, upper right corner) of amphotericin B (AmB, black squares), cholinium amphotericin B ([chol][AmB], yellow triangles), cetylpyridinium amphotericin B ([C16py][AmB], purple circles), cetylpyridinium chloride ([C16py]Cl, orange hexagons) and cholinium chloride against Aspergillus terreus. The y axis represents the percentage of metabolic activity (determined by standard MTT assay) comparatively to the growth without any treatment. The x axis represents the log of the concentration of each tested compound. [a]For cholinium chloride, the curve was omitted since most tested concentrations displayed no inhibition of activity and the IC50 value is an approximate prediction based on the obtained data.

Influence of an ionic liquid form

As previously reported for ionic liquids based on ampicillin[25], amoxicillin and penicillin G[26], combination of AmB with the [C_{16}py]$^+$ cation also resulted in the most active formulation. Our data showed that [C_{16}py][AmB] displayed significant differences in dose-response curves and the highest antifungal

activity for both fungi, while likely maintaining the mode of action of AmB. For these reasons, this ionic liquid was selected to further investigate the mechanisms behind this increased biological activity. Initially, we aimed at understanding if an ionic liquid formulation, rather than a simple synergy between the parental compounds, was essential for the increased activity of [C_{16}py][AmB]. We performed a checkerboard assay[29], where we tested the susceptibility of *A. fumigatus* to combinations of different concentrations of cetylpyridinium chloride ([C_{16}py]Cl) and AmB. The equimolar combination of both compounds produced a dose-response curve that was significantly different from those of [C_{16}py]Cl (P value: 0.0105) and AmB (P value: 0.0473) alone, and also from the curve obtained for [C_{16}py][AmB] (P value: 0.0133) (Figure 5). It appears that addition of [C_{16}py]Cl to a neutral AmB actually decreases the activity of the latter, as seen by the calculated IC_{50} of 1.58 μM. This value is ca. eight times lower than the IC_{50} of [C_{16}py]Cl (12.58 μm), but more than double of that for AmB alone (0.70 uM) and more than seven times higher than the IC_{50} of [C_{16}py][AmB] (0.22 μm) (Figure 5). An ionic liquid formulation, that combines a cation such as $[C_{16}py]^+$ and the anionic form of AmB ($[AmB]^-$) anion, seems to be necessary for increased antifungal activity. Even though further evidence is necessary, the enhanced antifungal activity observed in our study could be a consequence of $[C_{16}py]^+$ and $[AmB]^-$ acting as a pair, instead of dissociated ions. This is in line with the idea of the existence of ion-pairing in ionic liquids[51], which is already believed to be behind some of the physical properties of this class of compounds[52].

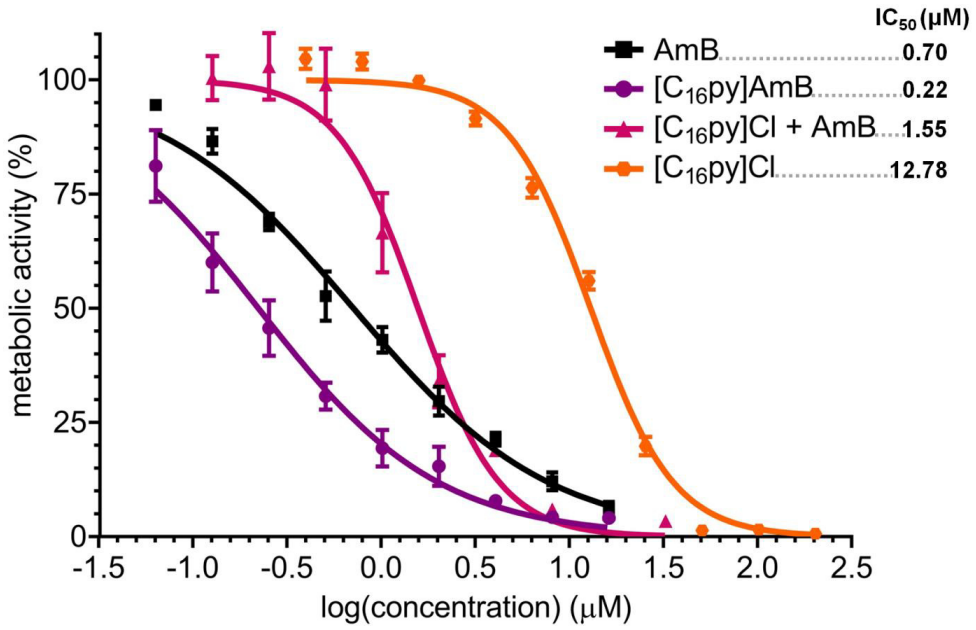

Figure 5 Dose-response curve and calculated IC50 values (in μM, upper right corner) of amphotericin B (AmB, black squares), cetylpyridinium chloride ([C16py]Cl, orange hexagons), cetylpyridinium amphotericin B ([C16py][AmB], purple circles) and a equimolar mixture of [C16py]Cl and AmB ([C16py]Cl + AmB, pink triangles), against Aspergillus fumigatus. The y axis represents the percentage of metabolic activity (determined by standard MTT assay) comparatively to the growth without any treatment. The x axis represents the log of the concentration of each tested compound.

Interactions with fungal ergosterol

The main proposed models for AmB mechanism of action, from the formation of ion channel aggregates[10] to the sterol sponge model[11], have in common the interaction of AmB with the main fungal membrane sterol, i.e. ergosterol. We performed molecular dynamics simulations to verify if there were any differences between the interaction of ergosterol with AmB or [C_{16}py][AmB]. Two types of model system were considered: (i) aqueous solutions containing ergosterol and AmB and (ii) aqueous solutions containing ergosterol and the ionic liquid formulation. Figure 6 shows relevant aggregate distribution functions along with snapshots of the equilibrated simulation boxes corresponding to the clustering of ergosterol molecules and AmB

(Figure 6A) and ergosterol molecules and [C_{16}py][AmB] (Figure 6B). The "ergo–AmB" distribution function (Figure 6A) shows that only 4% of the AmB or ergosterol molecules are not in contact with the other species, and that most of them are part of a very large cluster with maximum probability (96%) around n_a = 30 (the maximum possible aggregate size). On the other hand, the "ergo–[AmB]$^-$" distribution function of the ergosterol–[C_{16}py][AmB] system (Figure 6B) shows that only 2% of the [AmB]$^-$ anion or ergosterol molecules are not in contact with the other species and that most of them are part of very large clusters with $26 < n_a < 30$ (with a maximum probability around n_a = 30). A close behavior was observed for the "ergo–[C_{16}py]$^+$" distribution function (Figure 6B): only 1% of the [C_{16}py]$^+$ cation or ergosterol molecules are not in contact with the other species and most of them are part of very large cluster around n_a = 29. These mixed cation–ergosterol clusters are formed due to favorable interactions between the two species, i.e., the dispersion forces between their non-polar moieties (the alkyl chain of the cation and the ergosterol molecule).

The difference between the two systems is more noticeable if one compares the "ergo–ergo" distribution functions of each system. In the ergosterol–AmB system (Figure 6A), the "ergo–ergo" distribution shows only one aggregate comprising all ergosterol molecules. The "ergo–ergo" distribution function of the ergosterol–[C_{16}py][AmB] system (Fig. 6B) shows that the cluster sizes are part of a distribution of small clusters with $1 < n_a < 10$ (with a maximum probability around n_a = 6). This is due to the fact that the ergosterol is also involved in strong interactions with the [C_{16}py]$^+$ cation.

Collectively, the molecular dynamics simulations show that ergosterol interacts more with [C_{16}py][AmB] than with pure AmB. This occurs because ergosterol molecules seem to be embedded in the midst of [C_{16}py][AmB] molecules. While the interaction between sterol and the [AmB] anion exists,

the interaction between ergosterol and cation are even stronger, which would justify increased antifungal activity of [C_{16}py][AmB] compared to pure AmB.

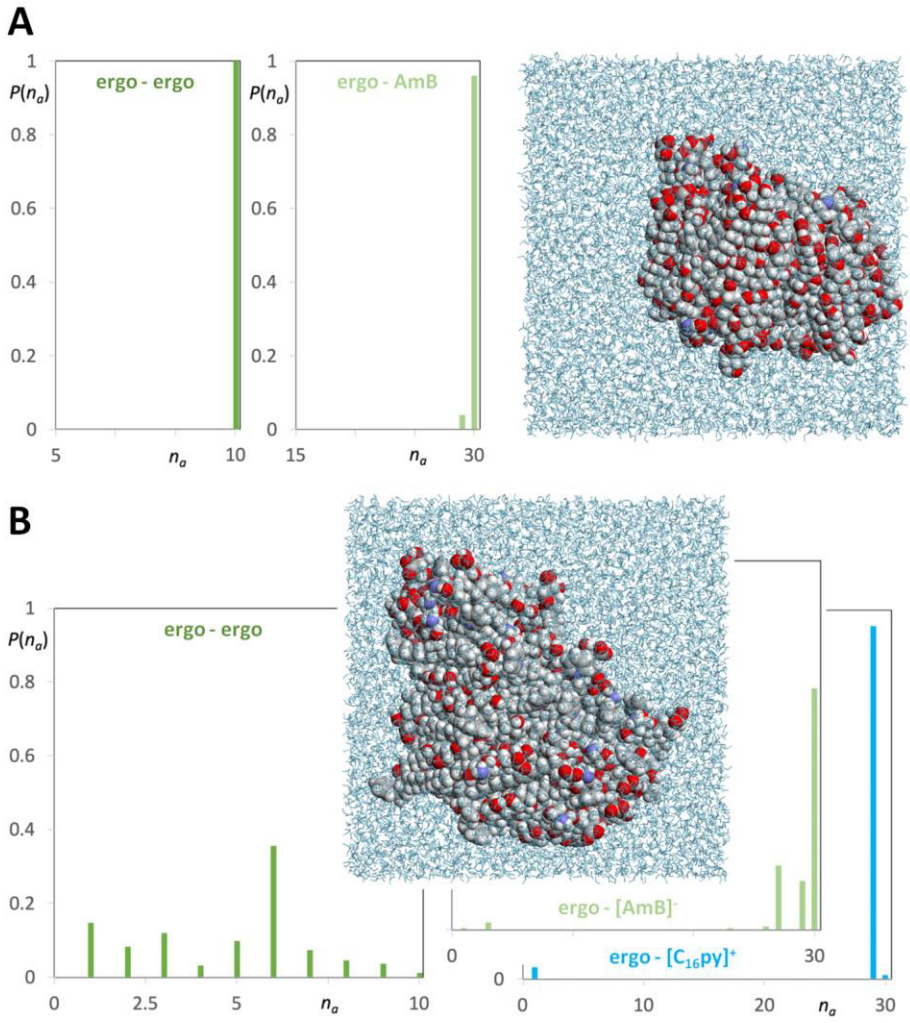

Figure 6 Molecular dynamics simulation snapshots and discrete probability distribution functions of aggregate sizes (P(na)) for different aggregate types of ergosterol (ergo), amphotericin B (AmB) and cetylpyridinium amphotericin B ([C16py][AmB]). (A) AmB–ergosterol simulations (dark green graph: ergosterol clusters; light green graph: ergosterol–AmB aggregates). (B) [C16py][AmB]–ergosterol simulations (deep green graph: ergosterol clusters; light green graph: ergosterol–[AmB]- anion aggregates; blue graph: ergosterol–[C16py]+ cation aggregates).

To further support these observations, 20 μM ergosterol was mixed in water with different concentrations of either AmB, [C_{16}py][AmB] or [C_{16}py]Cl. The mixtures were incubated for one hour to allow interaction of ergosterol with each compound, and then centrifuged at high speed to allow precipitation. It was expected that higher amounts of ergosterol would precipitate along with the compound that it has greater interaction with.

The results depicted in Table 1 show that for all tested concentrations of [C_{16}py][AmB] there was a greater decrease in ergosterol amounts in the supernatant in comparison with either AmB or [C_{16}py]Cl. Nearly 50% of ergosterol seemed to precipitate when combined with 60 μM of [C_{16}py][AmB], while the maximum precipitation observed for AmB was around 20% (50 μM of AmB). This is suggestive that ergosterol interacts more with the ionic liquid formulation than with AmB. Moreover, this does not seem to be solely an effect of the cation, since much higher decreases of ergosterol was observed for all concentrations of [C_{16}py][AmB] when compared to [C_{16}py]Cl (Table 1).

Table 1 Percentage of ergosterol in the supernatant of aqueous mixtures with 20, 30, 40, 50 or 60 μM of AmB, [C16py][AmB] or [C16py]Cl, after precipitation. 20 μM of ergosterol was mixed with of each compound in ultrapure water, incubated for one hour and centrifuged. The supernatant was analyzed by HPLC and ergosterol content was quantified. The data is presented as the percentage (followed by the standard deviation) of ergosterol present in the supernatant of each mixture relative to ergosterol alone, after precipitation by centrifugation.

Concentration (μM)	AmB	[C_{16}py][AmB]	[C_{16}py]Cl
20	98,70 ± 0,45	70,14 ± 0,35	91,70 ± 2,15
30	85,01 ± 1,78	78,91 ± 2,13	95,94 ± 1,40
40	97,97 ± 3,75	58,68 ± 5,49	92,24 ± 1,31
50	78,52 ± 2,41	72,72 ± 1,26	85,48 ± 0,91
60	99,59 ± 0,30	45,39 ± 1,02	92,67 ± 3,00

Evaluation of cytotoxicity

The interaction with membrane sterols is not only underlying the AmB antifungal activity, but it is also one of the most accepted reasons for its high toxicity. This is mainly due to the high structural similarities between ergosterol and cholesterol, the main sterol of animal cells (Figure S1). We have performed a MTT metabolic activity assay with mIMCD-3 cells, to determine and compare the cytotoxicity of [C16py][AmB] to the parental compound, AmB. While we calculated an IC50 of 42.61 μM for AmB (Table 2), the ionic liquid formulation displayed a much higher cytotoxicity, with an IC50 of 0.06 μM (over 700-times higher than AmB). These results are in accordance with previously reported higher cytotoxicity of a cetylpyridinium ampicillin ionic liquid formulation, which displayed IC_{50} values of ca. 0.03 and 0.01 μM against skin and gingival fibroblasts, respectively, while for the parental compound (i.e. sodium ampicillin) the IC_{50} was above 100 μM[53]. Furthermore, in agreement with previous studies that reported the high cytotoxicity of [C16py]Cl, we have registered an IC50 of 0.01 μM for this compound (Table 2).

Table 2 Calculated IC50 values (in μM) of amphotericin B (AmB), cetylpyridinium amphotericin B ([C16py][AmB]) and cetylpyridinium chloride ([C16py]Cl) towards mIMCD-3 cells, determined by standard MTT assays.

	IC_{50} (μM)
AmB	42.61
[C_{16}py][AmB]	0.06
[C_{16}py]Cl	0.01

Interactions with cholesterol

Altogether, the data suggest that, as seen for ergosterol, increased interactions between [C_{16}py][AmB] and cholesterol could also be occurring and that the cytotoxicity of the ionic liquid formulation could be greatly influenced by the $[C_{16}py]^+$ cation. Molecular dynamics simulations combining

cholesterol with AmB or [C_{16}py][AmB] were performed to identify the interactions between these molecules. Figure S2 shows relevant aggregate distribution functions along with snapshots of the equilibrated simulation boxes corresponding to the clustering of cholesterol molecules and AmB (Figure S2A) and cholesterol molecules and [C_{16}py][AmB] (Figure S2B). The "chol–AmB" distribution function in Fig. S2A shows that the molecules are forming a large cluster with maximum probability (99.9%) around n_a = 30 (the maximum size possible for the aggregate in the box), with a small fraction (0.1%) of AmB and cholesterol molecules not in close contact with each other. The "chol–[AmB]$^-$" distribution probability of the cholesterol–[C_{16}py][AmB] system (Figure S2B) shows that there is a large distribution of aggregate sizes, with $1 < n_a < 28$ (maximum probability around n_a = 19). For the "chol–[C_{16}py]$^+$" aggregate distribution function, on the other hand, only 0.5% of the [C_{16}py]$^+$ cation or cholesterol molecules are isolated and most of the species are forming a very large cluster around n_a = 30 (Figure S2B). As seen in the ergosterol–[C_{16}py][AmB] simulations, the dispersion interaction between the alkyl chain of [C_{16}py]$^+$ cation and cholesterol molecule is the main drive of the formation of mixed "chol–[C_{16}py]$^+$" clusters.

Comparison of "chol–chol" distribution functions shows only one large aggregate comprising all cholesterol molecules present in the system with neutral AmB (Figure S2A), while the "chol–chol" cluster sizes are distributed between $1 < n_a < 8$ (with a maximum probability around n_a = 6) in the presence of [C_{16}py][AmB] (Figure S2B). As seen for "ergo–ergo" distribution functions (Figure 6A and 6B), the reduction in "chol–chol" cluster sizes is the result of the strong interactions of the sterol molecules with the [C_{16}py]$^+$ cation (Figure S2A and S2B). Comparing the ergosterol and cholesterol simulations, it is observed that cholesterol exhibits an even bigger interaction with the [C_{16}py]$^+$ cation than ergosterol. The small differences between the structures of ergosterol and cholesterol (Figure S1) have been suggested to have little influence in their interaction with AmB[54]. However, it is possible

that these differences could in fact influence sterol–$[C_{16}py]^+$ interactions, yet to be disclosed, in ways that would explain a greater affinity of cholesterol towards the cation, compared with ergosterol. This could explain why the IC_{50} values of $[C_{16}py][AmB]$ towards animals cells are lower than those determined for the fungal strains (Figure 2, Figure 4 and Table 2). It is apparent that interaction with ergosterol or cholesterol occurs mainly between the aliphatic moieties of the cation. Deeper studies need be conducted, aiming at identifying specific modifications in the cation, e.g. double bonds, which could alter its affinity to specific regions in each sterol.

Evaluation of antibacterial activity

The potential biological activity of some ionic liquids, namely antibacterial activity, have been already reported to be strongly influenced by the cation, as seen in formulations containing long-chain imidazolium[55], quinolinium[56], pyridinium[57] and tetraalkylammonium[42,58] or tetraalkylphosphonium cations[47]. Taking their high toxicity as an advantage, some of those ionic liquids were proposed as biocides, e.g. in wood preservation[59], tissue embalming[60] and bacterial biofilm eradication[55,56]. Due to its antibacterial properties, $[C_{16}py]Cl$ has already been explored in human healthcare products[43]. It has been used in mouthwash formulations in the United States since the 1940s and, more recently, it has been investigated as a potential antiseptic in other medical applications, such as the treatment and management of chronic wounds[61].

In our study, we wanted to evaluate whether the $[C_{16}py]AmB$ formulation preserved the antibacterial activity of the $[C_{16}py]^+$ cation, using *S. aureus* and *E. coli* as gram-positive and gram-negative bacteria models, respectively. AmB did not inhibit the growth of either bacterium at the maximum concentration tested (predicted IC_{50} values above 100 μM), while $[C_{16}py]Cl$, as expected, displayed antibacterial activity against both *E. coli* and *S. aureus*, with calculated IC_{50} values of 13.2 and 3.7 μM, respectively (Table

3). The [C_{16}py][AmB] formulation displayed similar (even slightly stronger) antibacterial activity as [C_{16}py]Cl, with IC_{50} values of 10 μM for the gram-negative bacterium *E. coli* and 2.7 μM for the gram-positive *S. aureus* (Table 3). The dual nature of ionic liquids has been already explored in the development of active formulations displaying two biological functions (e.g. antimicrobial proprieties and artificial sweeteners). Our data show that the combination of $[C_{16}py]^+$ and $[AmB]^-$ results in a formulation with dual biological functionality: the increased antifungal activity, comparatively to pure AmB, combined with the preserved antibacterial properties of the $[C_{16}py]^+$ cation.

Table 3 Calculated IC_{50} values (in μM) of amphotericin B (AmB), cetylpyridinium amphotericin B ([C_{16}py][AmB]) and cetylpyridinium chloride ([C_{16}py]Cl) towards the bacteria Staphyloccoccus aureus or Escherichia coli, determined by absorbance measurement (OD_{600}).

	IC_{50}	
	S. aureus	*E. coli*
AmB	>100	>100
[C_{16}py][AmB]	2.8	10.0
[C_{16}py]Cl	3.7	13.2

Despite its high cytotoxicity, the use of [C_{16}py]Cl in oral hygiene products in concentrations up to 0.1 $mg \cdot ml^{-1}$ is approved by the U.S. Food and Drug Administration (https://www.fda.gov). Therefore, pharmacological data is already available to guide the appropriate studies and predict the recommended doses and therapeutics to explore formulations containing the $[C_{16}py]^+$ cation, including the dual activity of [C_{16}py][AmB] against mixed communities of bacteria and fungi.

Conclusions

Creating new opportunities in antifungal therapy is crucial for improving the efficacy of medications already in clinical use, defeating induced resistance and the emergence of novel pathogens. In this study, we evaluated the

biological activity of three novel ionic liquid formulations that resulted from the combination of an anionic form of the antifungal drug AmB with three distinct cations: $[chol]^+$, $[C_{16}py]^+$ or $[P_{6\,6\,6\,14}]^+$. $[P_{6\,6\,6\,14}][AmB]$ led to a decreased antifungal activity and what seems to be a mode of action distinct from the parental antifungal drug. The ionic liquid formulations [chol][AmB] and $[C_{16}py][AmB]$, however, increased AmB antifungal activity 1.2- and 3.2-fold, respectively, either for *A. fumigatus* or the intrinsically resistant *A. terreus*. Gene expression analysis seems to indicate that either ionic liquid maintained the mechanism of action of AmB. Deeper investigations on the effects of $[C_{16}py][AmB]$, revealed that an ionic liquid formulation is required for increased antifungal activity, which was not observed with an equimolar combination of the parental compounds, AmB and $[C_{16}py]Cl$. Molecular dynamics simulations further reveal that the reason behind the increased antifungal activity of $[C_{16}py][AmB]$ is the greater interaction of ergosterol, the main fungal membrane sterol, with the ionic liquid formulation, when compared to AmB. This is strongly influenced by the close interactions observed between ergosterol and the $[C_{16}py]^+$ cation. Even greater seems to be the interaction of cholesterol, the main animal sterol, with $[C_{16}py]^+$, which seems to justify the high cytotoxicity of $[C_{16}py][AmB]$, as well as of the parental compound $[C_{16}py]Cl$.

These data set ground to further exploring ionic liquid formulations as alternative solutions for enhanced administrations and antifungal activity of AmB, as well as other antifungal drugs. It emphasizes that molecular studies are crucial for the deep understanding of the interactions between ionic liquid formulations and the biological targets of AmB, i.e., membrane sterols. Our results can be used as a guide towards the fine-tuning and development of AmB-based ionic liquid formulations that selectively target ergosterol in detriment of cholesterol, resulting in effective antifungal agents with low cytotoxicity.

Furthermore, [C_{16}py][AmB] not only presented increased antifungal activity, but was also effective against the bacteria *S. aureus* and *E. coli*, indicating a preservation of the antibacterial properties of the parental compound [C_{16}py]Cl. This ionic liquid formulation is based on two pharmaceutical ingredients approved by the regulating authorities, which can guide and facilitate the necessary studies for its use. One conceived strategy for the application of this new dual functional formulation in the near future is to consider their slow release from patches for wound care of chronic wounds which frequently contain a mixed microbiota of bacteria and fungi.

Acknowledgements

This work was financially supported by Fundação para a Ciência e a Tecnologia (FCT) by Project MOSTMICRO ITQB with refs UIDB/04612/2020 and UIDP/04612/2020, and by the European Research Council through grant ERC 2014-CoG-647928. The authors thank Associate Laboratory for Green Chemistry-LAQV which is financed by national funds from FCT/MCTES (UIDB/50006/2020) and co-financed by the ERDF under the PT2020 Partnership Agreement (POCI-01-0145-FEDER – 007265), to FCT (PTDC/QUI-QOR/32406/2017) and MAR2020 (MAR-02.01.01-FEAMP-0042 – INOVA4AQUA). DOH, MR and MP are grateful for the fellowships SFRH/BPD/121354/2016, SFRH/BD/113989/2015 and SFRH/BPD/85753/2012, respectively. KS and ZP are grateful for the working contract financed by national funds under *norma transitória* D.L. n.° 57/2016.

References

1. Brown, G. D. *et al.* Hidden killers: human fungal infections. *Sci. Transl. Med.* **4**, 165rv13 (2012).
2. Kwon-Chung, K. J. & Sugui, J. A. Aspergillus fumigatus - What makes the species a ubiquitous human fungal pathogen? *PLOS Pathog.* **9**, e1003743 (2013).
3. Beauvais, A. *et al.* An extracellular matrix glues together the aerial-

grown hyphae of Aspergillus fumigatus. *Cell. Microbiol.* **9**, 1588–1600 (2007).

4. Mowat, E., Butcher, J., Lang, S., Williams, C. & Ramage, G. Development of a simple model for studying the effects of antifungal agents on multicellular communities of Aspergillus fumigatus. *J. Med. Microbiol.* **56**, 1205–1212 (2007).
5. Kathiravan, M. K. *et al.* The biology and chemistry of antifungal agents: a review. *Bioorg. Med. Chem.* **20**, 5678–5698 (2012).
6. Verweij, P. E., Snelders, E., Kema, G. H., Mellado, E. & Melchers, W. J. Azole resistance in Aspergillus fumigatus: a side-effect of environmental fungicide use? *Lancet. Infect. Dis.* **9**, 789–795 (2009).
7. Jiménez-Ortigosa, C., Moore, C., Denning, D. W. & Perlin, D. S. Emergence of echinocandin resistance due to a point mutation in the fks1 gene of Aspergillus fumigatus in a patient with chronic pulmonary aspergillosis. *Antimicrob. Agents Chemother.* **61**, e01277-17 (2017).
8. Moosa, M.-Y. S., Alangaden, G. J., Manavathu, E. & Chandrasekar, P. H. Resistance to amphotericin B does not emerge during treatment for invasive aspergillosis. *J. Antimicrob. Chemother.* **49**, 209–213 (2002).
9. Hamill, R. J. Amphotericin B formulations: a comparative review of efficacy and toxicity. *Drugs* **73**, 919–934 (2013).
10. Kamiński, D. M. Recent progress in the study of the interactions of amphotericin B with cholesterol and ergosterol in lipid environments. *Eur. Biophys. J.* **43**, 453–467 (2014).
11. Anderson, T. M. *et al.* Amphotericin forms an extramembranous and fungicidal sterol sponge. *Nat. Chem. Biol.* **10**, 400–406 (2014).
12. Gautam, P. *et al.* Proteomic and transcriptomic analysis of Aspergillus fumigatus on exposure to amphotericin B. *Antimicrob. Agents Chemother.* **52**, 4220–4227 (2008).
13. Blum, G. *et al.* Potential basis for amphotericin B resistance in

Aspergillus terreus. *Antimicrob. Agents Chemother.* **52**, 1553–1555 (2008).

14. Botero Aguirre, J. P. & Restrepo Hamid, A. M. Amphotericin B deoxycholate versus liposomal amphotericin B: effects on kidney function. *Cochrane Database Syst. Rev.* CD010481 (2015). doi:10.1002/14651858.CD010481.pub2
15. Herbrecht, R., Natarajan-Amé, S., Nivoix, Y. & Letscher-Bru, V. The lipid formulations of amphotericin B. *Expert Opin. Pharmacother.* **4**, 1277–1287 (2003).
16. Michot, J. M. *et al.* Very prolonged liposomal amphotericin B use leading to a lysosomal storage disease. *Int. J. Antimicrob. Agents* **43**, 566–569 (2014).
17. Van de Ven, H. *et al.* PLGA nanoparticles and nanosuspensions with amphotericin B: Potent in vitro and in vivo alternatives to Fungizone and AmBisome. *J. Control. Release* **161**, 795–803 (2012).
18. McCrary, P. D. *et al.* Drug specific, tuning of an ionic liquid's hydrophilic–lipophilic balance to improve water solubility of poorly soluble active pharmaceutical ingredients. *New J. Chem.* **37**, 2196–2202 (2013).
19. Plechkova, N. V. & Seddon, K. R. Applications of ionic liquids in the chemical industry. *Chemical Society Reviews* (2008). doi:10.1039/b006677j
20. Petkovic, M. & Silva Pereira, C. Pioneering biological processes in the presence of ionic liquids: the potential of filamentous fungi. in *Ionic Liquids UnCOILed: Critical Expert Overviews* (eds. Plechkova, N. V & Seddon, K. R.) 283–303 (John Wiley & Sons, Inc., 2012). doi:10.1002/9781118434987.ch9
21. Balk, A., Holzgrabe, U. & Meinel, L. 'Pro et contra' ionic liquid drugs – Challenges and opportunities for pharmaceutical translation. *Eur. J. Pharm. Biopharm.* **94**, 291–304 (2015).

22. Hough-Troutman, W. L. *et al.* Ionic liquids with dual biological function: sweet and anti-microbial, hydrophobic quaternary ammonium-based salts. *New J. Chem.* **33**, 26–33 (2009).
23. Suresh, C., Zhao, H., Gumbs, A., Chetty, C. S. & Bose, H. S. New ionic derivatives of betulinic acid as highly potent anti-cancer agents. *Bioorg. Med. Chem. Lett.* **22**, 1734–1738 (2012).
24. Araújo, J. M. M. *et al.* Cholinium-based ionic liquids with pharmaceutically active anions. *RSC Adv.* **4**, 28126–28132 (2014).
25. Ferraz, R. *et al.* Antibacterial activity of ionic liquids based on ampicillin against resistant bacteria. *RSC Adv.* **4**, 4301–4307 (2014).
26. Ferraz, R. *et al.* Synthesis and antibacterial activity of ionic liquids and organic salts based on penicillin G and amoxicillin hydrolysate derivatives against resistant bacteria. *Pharmaceutics* **12**, 221 (2020).
27. Cojocaru, O. A. *et al.* Ionic liquid forms of the herbicide dicamba with increased efficacy and reduced volatility. *Green Chem.* **15**, 2110–2120 (2013).
28. Pernak, J. *et al.* Ionic liquids with dual pesticidal function. *RSC Adv.* **4**, 39751–39754 (2014).
29. Cokol-Cakmak, M. & Cokol, M. Miniaturized checkerboard assays to measure antibiotic interactions. *Methods Mol. Biol.* **1939**, 3–9 (2019).
30. Canongia Lopes, J. N. & Pádua, A. A. H. Molecular force field for ionic liquids composed of triflate or bistriflylimide anions. *J. Phys. Chem. B* **108**, 16893–16898 (2004).
31. Jorgensen, W. L., Maxwell, D. S. & Tirado-Rives, J. Development and testing of the OPLS all-atom force field on conformational energetics and properties of organic liquids. *J. Am. Chem. Soc.* **118**, 11225–11236 (1996).
32. Praprotnik, M., Janežič, D. & Mavri, J. Temperature dependence of water vibrational spectrum: a molecular dynamics simulation study. *J. Phys. Chem. A* **108**, 11056–11062 (2004).

33. Smith, W. & Forester, T. R. The DL_POLY package of molecular simulation routines. (2006).
34. Bekker, H. *et al.* Gromacs: A parallel computer for molecular dynamics simulations. *Physics Computing ´92* **92**, 252–256 (1993).
35. Berendsen, H. J. C., van der Spoel, D. & van Drunen, R. GROMACS: A message-passing parallel molecular dynamics implementation. *Comput. Phys. Commun.* **91**, 43–56 (1995).
36. Van Der Spoel, D. *et al.* GROMACS: Fast, flexible, and free. *J. Comput. Chem.* **26**, 1701–1718 (2005).
37. Páll, S. *et al.* Tackling exascale software challenges in molecular dynamics simulations with GROMACS. *International Conference on Exascale Applications and Software 2014* **8759**, 3–27 (2015).
38. Abraham, M. J. *et al.* GROMACS: High performance molecular simulations through multi-level parallelism from laptops to supercomputers. *SoftwareX* **1**–**2**, 19–25 (2015).
39. Martinez, L., Andrade, R., Birgin, E. G. & Martinez, J. M. PACKMOL: a package for building initial configurations for molecular dynamics simulations. *J. Comput. Chem.* **30**, 2157–2164 (2009).
40. Bernardes, C. E. S., Shimizu, K., Lobo Ferreira, A. I. M. C., Santos, L. M. N. B. F. & Canongia Lopes, J. N. Structure and aggregation in the 1,3-dialkyl-imidazolium bis(trifluoromethylsulfonyl)imide ionic liquid family: 2. From single to double long alkyl side chains. *J. Phys. Chem. B* **118**, 6885–6895 (2014).
41. Markham, P., Robson, G. D., Bainbridge, B. W. & Trinci, A. P. J. J. Choline: its role in the growth of filamentous fungi and the regulation of mycelial morphology. *FEMS Microbiol. Rev.* **104**, 287–300 (1993).
42. Petkovic, M. *et al.* Novel biocompatible cholinium-based ionic liquids - Toxicity and biodegradability. *Green Chem.* **12**, 643–649 (2010).
43. Wu, C. D. & Savitt, E. D. Evaluation of the safety and efficacy of over-the-counter oral hygiene products for the reduction and control of

plaque and gingivitis. *Periodontol. 2000* **28**, 91–105 (2002).

44. Bica, K., Rijksen, C., Nieuwenhuyzen, M. & Rogers, R. D. In search of pure liquid salt forms of aspirin: ionic liquid approaches with acetylsalicylic acid and salicylic acid. *Phys. Chem. Chem. Phys.* **12**, 2011–2017 (2010).
45. Frade, R. F. M. *et al.* Toxicological evaluation on human colon carcinoma cell line (CaCo-2) of ionic liquids based on imidazolium, guanidinium, ammonium, phosphonium, pyridinium and pyrrolidinium cations. *Green Chem.* **11**, 1660–1665 (2009).
46. Zhao, Y. *et al.* Expression turnover profiling to monitor the antifungal activities of amphotericin B, voriconazole, and micafungin against Aspergillus fumigatus. *Antimicrob. Agents Chemother.* **56**, 2770 (2012).
47. Petkovic, M. *et al.* Unravelling the mechanism of toxicity of alkyltributylphosphonium chlorides in Aspergillus nidulans conidia. *New J. Chem.* **36**, 56–63 (2012).
48. Hartmann, D. O. & Silva Pereira, C. A molecular analysis of the toxicity of alkyltributylphosphonium chlorides in Aspergillus nidulans. *New J. Chem.* **37**, 1569–1577 (2013).
49. Neves, C. M. S. S., Carvalho, P. J., Freire, M. G. & Coutinho, J. A. P. Thermophysical properties of pure and water-saturated tetradecyltrihexylphosphonium-based ionic liquids. *J. Chem. Thermodyn.* **43**, 948–957 (2011).
50. Blum, G. *et al.* In vitro and in vivo role of heat shock protein 90 in amphotericin B resistance of Aspergillus terreus. *Clin. Microbiol. Infect.* **19**, 50–55 (2013).
51. Kirchner, B., Malberg, F., Firaha, D. S. & Hollóczki, O. Ion pairing in ionic liquids. *J. Phys. Condens. Matter* **27**, 463002 (2015).
52. Matsumoto, R., Thompson, M. W. & Cummings, P. T. Ion pairing controls physical properties of ionic liquid-solvent mixtures. *J. Phys.*

Chem. B **123**, 9944–9955 (2019).

53. Ferraz, R. *et al.* Antitumor activity of ionic liquids based on ampicillin. *ChemMedChem* **10**, 1480–1483 (2015).
54. Baran, M., Borowski, E. & Mazerski, J. Molecular modeling of amphotericin B–ergosterol primary complex in water II. *Biophys. Chem.* **141**, 162–168 (2009).
55. Carson, L. *et al.* Antibiofilm activities of 1-alkyl-3-methylimidazolium chloride ionic liquids. *Green Chem.* **11**, 492–497 (2009).
56. Busetti, A. *et al.* Antimicrobial and antibiofilm activities of 1-alkylquinolinium bromide ionic liquids. *Green Chem.* **12**, 420–425 (2010).
57. Pernak, J., Kalewska, J., Ksycińska, H. & Cybulski, J. Synthesis and anti-microbial activities of some pyridinium salts with alkoxymethyl hydrophobic group. *Eur. J. Med. Chem.* **36**, 899–907 (2001).
58. Pernak, J. *et al.* Long alkyl chain quaternary ammonium-based ionic liquids and potential applications. *Green Chem.* **8**, 798–806 (2006).
59. Pernak, J., Zabielska-Matejuk, J. & Urbanik, E. New quaternary ammonium chlorides - Wood preservatives. *Holzforschung* **52**, 249–254 (1998).
60. Majewski, P., Pernak, A., Grzymisławski, M., Iwanik, K. & Pernak, J. Ionic liquids in embalming and tissue preservation. Can traditional formalin-fixation be replaced safely? *Acta Histochem.* **105**, 135–142 (2003).
61. Fromm-Dornieden, C., Rembe, J.-D., Schäfer, N., Böhm, J. & Stuermer, E. K. Cetylpyridinium chloride and miramistin as antiseptic substances in chronic wound management – prospects and limitations. *J. Med. Microbiol.* **64**, 407–414 (2015).

Chapter III

Tryptoquivaline F, produced under stress by *Aspergillus fumigatus*, induces germination

The study reported here forms part of ongoing work and includes unpublished data (manuscript in preparation).

Tryptoquivaline F, produced under stress by *Aspergillus fumigatus*, induces germination

Maika Rothkegel[1], Patrícia Sequeira[1], Oscar Núñez[2], Cristina Silva Pereira[1]

[1] Applied and Environmental Mycology Laboratory, Instituto de Tecnologia Química e Biológica António Xavier, Universidade Nova de Lisboa (ITQB-NOVA), Av. da República, 2780-157, Oeiras, Portugal

[2] Department of Analytical Chemistry, University of Barcelona, Martí i Franquès 1-11, E08028 Barcelona, Spain; Institute for Nutrition and Food Safety Research, Torribera Food and Nutrition Campus, Av. Prat de la Riba, 171, 08921 Santa Coloma de Gramenet, Spain

Abstract

Microbial organisms within a community need to coordinate their growth and development to optimally exploit their ecological niche and to react to external cues and stress. In recent years, several intercellular signaling mechanisms coordinating fungal development, including quorum sensing, have been found in fungal organisms, especially in yeast such as *Candida albicans,* but also in other *Ascomycota* spp. such as *Aspergillus flavus* or *Aspergillus nidulans.* Secondary metabolites, including farnesol, tyrosol, oxylipins, some pheromones and lactones were identified as self-signaling molecules. In other fungi such as *Aspergillus fumigatus,* no such signaling molecules have been discovered thus far. Here we use medium supplementation of *Aspergillus fumigatus* cultures with the ionic liquid cholinium decanoate to stimulate cryptic secondary metabolite production and test the spent medium extract for their bioactivity on *Aspergillus fumigatus* itself. We found that those extracts induce an accelerated germination and growth and are enriched in peptidyl alkaloids. We could reproduce the phenotype with the identified pure compound tryptoquivaline F, suggesting its role as a signaling molecule involved in coordinating the germination of *Aspergillus fumigatus.*

Introduction

Aspergillus fumigatus is primarily a saprophytic filamentous fungus that can colonize diverse environments by growing on decaying matter and playing an important role in carbon and nitrogen recycling[1]. In specific cases the fungus can become pathogenic, causing life threatening diseases, mostly in immunocompromised patients[2]. There are only three classes of antifungals available for the treatment of invasive aspergillosis - polyenes, azoles and echinocandins - most of which cause severe side effects and their effectiveness is unpredictable[3,4]. It is therefore important to study mechanisms employed by the fungus that promote its growth and dissemination to eventually develop new antifungal strategies.

An interesting feature of filamentous fungi is the production of a wide spectrum of secondary metabolites with diverse bioactive properties such as antibiotics (e.g penicillin), immunosuppressants (e.g cyclosporine) and antitumor agents (*e.g.* camptothecin), among others[5,6]. There are five main classes of secondary metabolites, polyketides, non-ribosomal peptides, ribosomally synthesized and post-translationally modified peptides (RiPPs), indole alkaloids (or shikimic acid derived compounds) and terpenes, as well as some hybrid combinations like NRP-PKs, which involve more than one type of biosynthesis enzyme[7,8].

Secondary metabolites can act as intercellular signaling molecules that control fungal development. Intercellular communication can follow various secrete-and-sense mechanisms[9]. Some signaling molecules can be considered autoinducers, even following a quorum sensing mechanism. The first quorum sensing molecule (QSM) to be discovered and the best studied so far is farnesol, produced by *Candida albicans*, which has been shown to block hyphal formation, affect morphological pathways and inhibit biofilm formation; as well as to influence hyphal morphology, conidiation and germination in other fungal species[10,11]. More studies identified some

alcohols, such as tyrosol, lipids, pheromones and lactones, but overall there are relatively few QSMs discovered so far and most part of the studies focus on yeast organisms[10,12,13]. In *Aspergillus* spp. true QSMs that are cell-density dependent include oxylipins, which seem to coordinate conidium and sclerotium formation in *A. flavus*[14] and γ-heptalactone which leads to a reduction of the lag-phase in *A. nidulans*[15]. Other intercellular signaling compounds have been identified that have not been linked to a cell-density dependent production in *Aspergillus* spp. Their outward growth is controlled by the secretion of unidentified growth inhibitors just behind the growing front[16] and the two oxylipins psiA and psiB, promote fruiting body formation and inhibit conidiation in *A. nidulans,* while psiC promotes conidiation[17,18]. In *A. fumigatus,* no such self-signaling molecule has been identified to date.

The discovery of secondary metabolites and therefore new signaling compounds is hindered by the fact that the genes involved in their biosynthesis usually remain silent under standard laboratory conditions[6,19]. Moreover, if produced, those type of compounds are often present at very low quantities, making their isolation and identification a difficult task. One approach to stimulate secondary metabolite production is to supplement the medium culture with stimulating agents. The addition of ionic liquids -simple organic salts that are liquid below 100°C[20] - is a highly useful resource to activate secondary metabolite production in fungi including metabolites otherwise cryptic[21,22]. In this study we utilized choline decanoate (ChoDec) to supplement the culture medium and to study secondary metabolites secreted in response which could potentially act as autoinducers. We found that the exogenous stress provokes a growth inhibitory stress in *A. fumigatus* and the secretion of molecules that favor accelerated germination and growth of conidia. Under these conditions, mass spectrometry revealed the presence of the ergot alkaloids tryptoquivaline F, Phe-Ser-DKP and gliotoxin, of which tryptoquivaline F indeed induced accelerated germination when tested individually, suggesting a signaling role under stress conditions.

Materials & Methods

Chemicals

Commercially available reagents were purchased from Sigma Aldrich, Fisher Bioreagents unless otherwise stated. The ionic liquid choline decanoate was purchased from Ionic Liquids Technologies (IoLiTec).

MIC determination

The fungal strain *Aspergillus fumigatus* Af293 (*A. fumigatus*) was purchased from the Fungal Genetics Stock Center. The minimal inhibitory concentration (MIC) of choline decanoate (ChoDec) was determined as described previously[23]. Final concentrations of ionic liquid in growth media were in the range from 100 µM to 5 mM. Each liquid medium (1 mL) was inoculated with 10^6 conidia and divided into four wells (0.2 mL each) of a 96-well plate. Cultures were incubated at 37 °C, for seven days. Fungal growth (or lack thereof) was evaluated at the end of incubation, gauging by the naked eye the formation of mycelium (turbidity). The lowest concentration that inhibited growth was taken as the MIC. Values should not be interpreted as absolute ones, but as an indication of the inhibitory and the fungicidal upper concentration limits.

Culture conditions

For spore preparation, *A. fumigatus* cultures were grown on DG18 (Oxoid) agar at 37°C, conidial suspensions were prepared and stored at -20 °C in 20% glycerol until use. Liquid cultures were grown in minimal medium containing glucose (10 g/L), thiamine (0.01 g/L), 5 % (v/v) nitrate salts solution and 0.1 % (v/v) trace elements solution, adjusted to pH 6.5 with 1 M NaOH. Nitrate salts solution was composed of $NaNO_3$ (120.0 g/L); KCl (10.4 g/L); $MgSO_4 \cdot 7H_2O$ (10.4 g/L) and KH_2PO_4 (30.4 g/L) in distilled water. Trace elements solution was composed of $ZnSO_4 \cdot 7H_2O$ (22.0 g/L); H_3BO_3 (11.0 g/L); $MnCl_2 \cdot 4H_2O$ (5.0 g/L); $FeSO_4 \cdot 7H_2O$ (5.0 g/L); $CoCl_2 \cdot 6\ H_2O$ (1.7 g/L);

$CuSO_4 \cdot 5\ H2O$ (1.6 g/L); $Na_2MoO_4 \cdot 2\ H_2O$ (1.5 g/L) and Na_4EDTA (50.0 g/L) in distilled water, adjusted to pH 6.5 with KOH.

For liquid cultures, minimal medium (100 mL) was inoculated with 10^6 spores/mL and incubated in the dark at 37°C with orbital agitation (200 rpm). 24 hours post inoculation, cultures where either subjected to a heat shock of 1 hour at 90°C or media supplements were added to the following final concentrations: Choline Decanoate (1.7 mM), Choline Chloride (1.7 mM), Sodium Decanoate (1.7 mM), Itraconazole (0.8 µg/mL), Amphotericin B (0.8 µg/mL), Caspofungin (0.2 µg/ mL), mix of amino acids (100 µM each). The amino acid mix contained Alanine, Arginine, Aspartic acid, Cysteine, Glutamic acid, Glutamine, Glycine, Histidine, Isoleucine, Leucine, Lysine, Methionine, Phenylalanine, Proline, Serine, Threonine, Tryptophan, Tyrosine and Valine. Cultures have been incubated for another 24 hours. Abiotic (medium alone) and biotic controls (without supplementation) were included for each assay. At the end of incubation, spent media were separated from fungal mycelia using vacuum assisted filtration with miracloth. The filtrate and biomass were frozen in liquid nitrogen and lyophilized. To compare the biomass production, lyophilized mycelial pellets were weighed. For each culture condition, at least three biological replicates were analyzed.

Extraction medium supernatant

Lyophilized filtrate was extracted by adding 10 mL of MeOH (1/10 of original volume), followed by 10 minutes sonication and centrifugation at 800 g for 5 minutes. The supernatant was dried under nitrogen flow and resuspended in 1 mL H_2O (1/100 of the original volume of the spent medium). Unless otherwise stated, extracts were tested at final concentrations equivalent to the original concentration in the spent medium.

Ionic liquid quantification

The residual concentration of decanoate in culture filtrate at the end of the incubation were analyzed by ultra-performance liquid chromatography

(UPLC) using a Waters (Waters Corporation, Milford, USA) Acquity chromatographer with Photodiode Array (PDA) detector, cooling auto-sampler, and column oven, fitted with a Synergi Polar-RP column (150 × 4.6 mm) packed with polar end-capped particles (4 mm, pore size 80 Å) (Phenomenex), at 35 °C. Data acquisition was accomplished with the Empower 2 software, 2006 (Waters Corporation). All solvents were of the highest analytical grade, and water was obtained from a Milli-Q system (Millipore). Samples were injected using a 50 µL loop operated in full loop mode. The mobile phase, at a flow rate of 0.4 mL/ min, consisted of a solution of 0.1% Phosphonic Acid in water (v/v) (solvent A) and Acetonitrile (solvent B), set to a linear gradient of 90% to 5% of solvent A for 5.7 minutes, and of 5% to 0% of solvent A during another 1.3 minutes, followed by 1.5 minutes to return to the initial conditions, and additional 1.5 min to re-equilibrate the column. The chromatographic profiles of the samples were obtained at the wavelength of 212 nm with a retention time of 5.7 minutes for the decanoate anion.

Growth rate assay

Growth rates were analyzed by OD measurements in honeycomb 100-well plates (Thermo Fisher Scientific). Semi-solid minimal medium of 0.125% (w/v) agarose in minimal medium was prepared and sterilized by autoclaving. The medium was cooled down to 40°C, mixed with *A. fumigatus* spores to a final concentration of 10^5 spores/mL and 200 µl added to each well containing the test extract. Plates were incubated at 37°C for 72 hours in a Bioscreen C analyzer (Oy Growth Curves Ab Ltd), taking hourly absorbance measurements (600 nm). All tests were done in triplicate; abiotic (medium alone) and biotic controls (fungal spores without extract) were included for each replicate.

Germination rate assays

Germination rate was assessed by cell counts and D-trehalose content measurements. For cell counts, in 96-well plates, $5x10^5$ *A. fumigatus* spores/mL were incubated with the extracts in minimal medium at final concentrations equivalent to the original concentration in the spent medium. Phase contrast pictures were taken after 5-6 hours with an Eclipse Ts2-FL inverted phase contrast microscope (Nikon) and a minimum of 300 cells were counted for each condition. All tests were done in triplicate.

To analyze the germination rate by measuring D-trehalose content, conidia were grown in minimal medium in the dark at 37°C with orbital agitation (150 rpm) with or without the addition of spent medium extracts, the amino acid mix (50 µM each), gliotoxin (Sigma), Phe-Ser-DKP (Cyclo-Phe-Ser, Merck) or tryptoquivaline F, extracted from *Neosartorya* spp.[24,25] (50 µM). Around $1x10^8$ dormant conidia (0 hours) or germinating conidia (0.5 - 2.5 hours) were collected by centrifugation at 11,000×g for 5 minutes, washed once with Saline and finally resuspended in 100 µL 0.25 M Na_2CO_3. To extract the cytosolic content, spores were subjected to heating for 30 min at to 99°C, freeze dried immediately in liquid nitrogen and mechanically disintegrated by adding 3-4 glass beads and subjecting them to the Qiagen TissueLyser for 30 minutes at full speed. The level of D-trehalose in the resulting supernatant was assayed using a commercial kit (Megazyme International Ireland Ltd.), according to the manufacturers protocol, in 96-well plates. In this assay, trehalose is first hydrolyzed to D-glucose, which is further phosphorylated to glucose-6-phosphate (G-6-P). G-6-P is then oxidized to gluconate-6-phosphate with the formation of nicotinamide-adenine dinucleotide phosphate (NADPH), resulting in an increase in absorbance at 340 nm. The amounts of NADPH released in the assays were measured using a Tecan Infinite 200 Microplate (Männedorf, Switzerland). Simultaneous measurements of a D-trehalose standard provided in the kit, were used to calculate the D-trehalose content in each sample. Measurements were done

in duplicate, and all tests done in triplicate. Statistical analyses were performed with GraphPad Prism 6.

Microscopy

For morphological analyses, $2.5x10^5$ spores/ mL in minimal medium with or without extract were seeded onto coverslips placed in 24-well plates, previously washed with absolute Ethanol. After 5-6 hours, coverslips were placed inverted on a glass slide, coated with 1.7% agar containing 10µM Calcofluor-White. Picture acquisition was done on a Leica DM 6000B upright microscope equipped with an Andor iXon 885 EMCCD camera and controlled with the MetaMorph V5.8 software, using the 100x 1.4 NA oil immersion objective plus a 1.6x optovar, the fluorescence filter set DAPI and Contrast Phase optics. Microscopy images were processed by FIJI software (Fiji Is Just ImageJ).

Amino acid quantification

Extracts were analyzed using the AccQ•Tag Ultra Amino Acid Analysis Method™ (eluent concentrates, derivatization kit and standard mixture of amino acid hydrolysates, Waters) [26,27]. Briefly, the samples, standard amino acids (Aib and Acc) and the standard mixture of amino acid hydrolysates were derivatized following the manufacturer's instructions. The obtained derivatives were separated on an AccQ•Tag Ultra column (100 mm x 2.1 mm, 1.7 µm) by reversed phase ultra-performance liquid chromatography (UPLC), and detected by fluorescence (FLR), according to the following details. The column heater was set at 55 °C, and the mobile phase flow rate was maintained at 0.7 mL/min. Eluent A was 5% AccQ•Tag Ultra concentrate solvent A and eluent B was 100% AccQ•Tag Ultra solvent B. The separation gradient was 0-0.54 min (99.9% A), 5.74 min (90.9% A), 7.74 min (78.8% A), 8.04 min (40.4% A), 8.05-8.64 min (10.0% A) and 8.73-10.50 min (99.9% A). Two microliters (2 µL) of sample were injected for analysis using a 10 µL loop. The FLR detector was set at 266 nm and 473 nm of excitation and

emission wavelengths, respectively. Data were acquired using Empower 2 software, 2006 (Waters). Quantification was done according to calibration curves prepared for each standard.

HRMS analysis

Dried extracts were resuspended in methanol:water (1:1 v/v) and analyzed by ultra-high-performance liquid chromatography-electrospray-high resolution mass spectrometry (UHPLC-ESI-HRMS) using a LTQ Orbitrap Velos MS system (Thermo Fisher Scientific, Hemel Hempstead, UK) equipped with an ESI source working in both positive and negative mode. Mass spectra were acquired in profile mode with a setting of 30,000 resolution full width half maximum (FWHM) at *m*/*z* 400 and data-dependent MS/MS events acquired at a resolving power of 15,000 (FWHM). Operation parameters were as follows: source voltage, 4 kV (both, positive and negative ion mode); sheath gas, 60 (arbitrary units); auxiliary gas, 10 (arbitrary units); sweep gas, 0 (arbitrary units); and capillary temperature, 320 °C. Default values were used for most other acquisition parameters (FT Automatic gain control (AGC) target $5 \cdot 10^5$ for MS mode and $5 \cdot 10^4$ for MS^n mode). The most intense ions detected during full scan MS triggered data-dependent scanning. Data-dependent scanning was carried out without the use of a parent ion list. An isolation width of 100 amu was used and precursors were fragmented by collision-induced dissociation C-trap (CID) with a normalized collision energy of 35 V and an activation time of 10 ms. The mass range in FTMS mode was from *m*/*z* 100 to 1500. The data analysis was achieved using XCalibur software v2.0.7 (Thermo Fisher Scientific).

Chromatographic separation was carried out in an UHPLC system (Dionex; ThermoFisher Scientific) using an Ascentix Express C18 (150 × 2.1 mm, 2.7 µm particle size) column from Supelco (USA). The mobile phase, at a flow rate of 300 µL/min, consisted of a solution of 0.1% formic acid (solvent A) and a solution of acetonitrile containing 0.1% formic acid (solvent B), set as

follows: 10% B in 1 min, followed by a liner gradient of 10–95% B in 4.7 min, 1.3 min to reach 100% B, 3 min of 100% B, 0.5 min to return to the initial conditions, and 5.5 min to re-equilibrate the column.

MS data was processed by TraceFinder™ 3.3 software (Thermo Fisher) by applying a user target database list. Several parameters such as retention time, accurate mass errors and isotopic pattern matches were used to confirm the identity of metabolites. When available, standard compounds were also analyzed by UHPLC-ESI-MS to confirm the identity.

Results & Discussion

ChoDec supplemented spent medium extract accelerates germination and increases biomass

Ionic liquids have been shown to induce a stress response that includes an altered secondary metabolism[21]. Here, choline decanoate (ChoDec) has been utilized at sub-inhibitory concentrations as a growth medium supplement to induce the biosynthesis of cryptic secondary metabolites and therefore, used as a tool to study the secreted molecules. ChoDec was chosen, as it contains a relatively long alkyl chain in the anion (C10) resulting in higher toxicity towards filamentous fungi compared to shorter alkyl chain containing ionic liquids[23,28]. Therefore, less quantities are needed to induce stress, reducing secondary effects due to an additional carbon source in the growth medium. The minimal inhibitory concentration of ChoDec against *A. fumigatus* was determined to be 3.4 mM, of which half the concentration, 1.7 mM, has been added to the growth medium. In addition, choline based ionic liquids have been shown to be biodegradable[23,29]. Already 24 hours after incubation, the decanoate anion could not be detected anymore by UPLC analysis in the medium supernatant (*data not shown*). ChoDec therefore represents a good candidate to study stress induced metabolite production without side effects caused by residual ionic liquid.

Aspergillus fumigatus was exposed to the ChoDec chemical stimulus after 24h of pre-growth. Upon another 24h of incubation, fungal cultures were harvested, and the cultivation medium extracted. The aim of this study was to understand, if the ChoDec medium supplementation leads to the secretion of metabolites that exhibit bioactivity against *A. fumigatus* itself. Therefore, we determined the effect of medium extracts with or without ChoDec supplementation on *A. fumigatus* growth curves (Figure 1A). The spent medium extract (SME) of ChoDec supplemented cultures leads to an earlier onset of the exponential phase and to higher OD values in the stationary phase. This suggests that metabolites present in that extract initiate earlier germination and lead to an overall higher biomass. Germination in *A. fumigatus* follows two stages; first a swelling of the spore to almost double its size, the isotropic growth, and second the formation of a germ tube, the polarized growth. D-trehalose is stored in high amounts in resting spores and rapidly metabolized when germination sets in. To confirm the accelerated germination, we counted the spores and germlings in each phase after 6h of incubation and assessed their D-trehalose content over time (Figure 1B & C). The spore count depicted in Figure 1B shows an increased number of germlings, especially in the polarized growth stage, when spores are grown with the ChoDec SME. Figure 1C shows that D-trehalose decreases more rapidly in spores grown in presence of ChoDec SME compared to the Control (no SME addition), indicating an earlier onset of germination. Both assays therefore corroborate the presence of metabolites in the ChoDec extract with a triggering effect on spore germination.

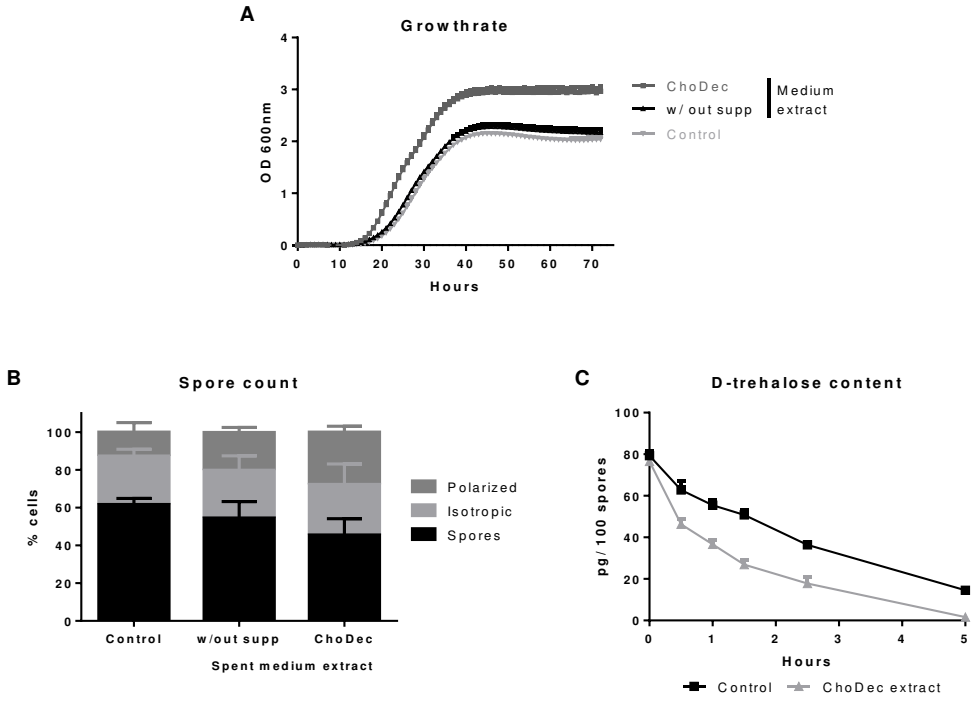

Figure 1 Effects of ChoDec supplemented spent medium extracts (SMEs) on the germination and growth of new A. fumigatus cultures. A) OD_{600} measurements for 72 hours; ChoDec SMEs induce an earlier onset of the exponential growth phase and a higher OD of the stationary phase compared to both controls. B) Microscopic cell counts of spores and germlings after 6 hours show an increased percentage of germinating cells when grown in the presence of ChoDec SME compared to controls. C) ChoDec SME leads to a faster reduction of D-trehalose in spores compared to control, indicating earlier onset of germination.

The microscopic analysis revealed morphological changes, which were examined in more detail by fluorescence microscopy (Figure 2). Spores and germlings were stained with calcofluor white, a cell wall staining, after 6 hours of incubation with or without the ChoDec SME. Figure 2 shows an increase of germinated spores grown in the presence of the ChoDec SME, as well as an enlarged swollen phenotype. The observed increase in total biomass determined by an increase in the OD (Figure 1A) could be caused by an overall higher number of spores germinating and contributing to the hyphal network or in fact by larger hyphal cell bodies.

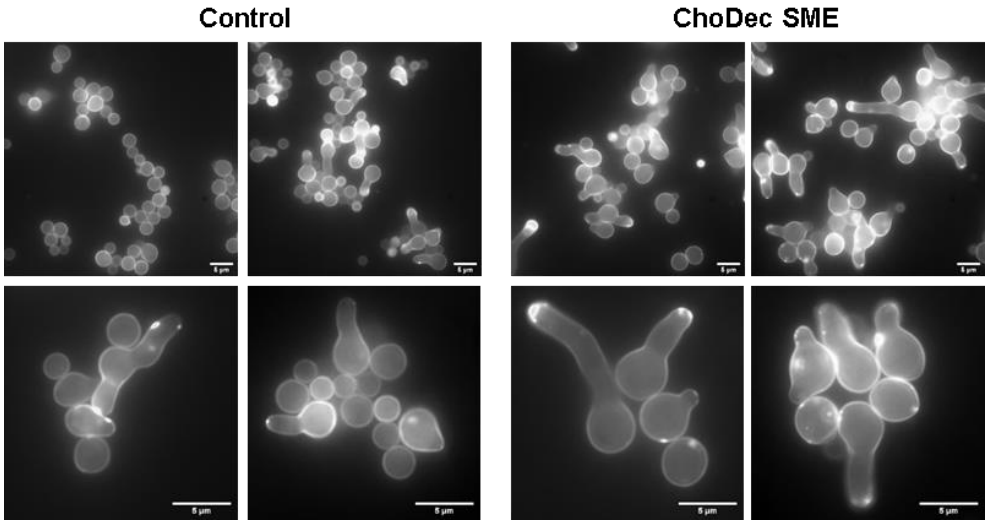

Figure 2 Morphological evaluation of germinating A. fumigatus spores after 6 hours grown with and without ChoDec SME, Calcofluor white staining of membranes, scale bar = 5µm (the lower panel shows a 2.5x magnification). Compared to spores growing under Control conditions, in the presence of ChoDec SME, more spores have started to germinate, and they appear to have a swollen phenotype.

Bioactivity is a response to stress and potentially cell death

To understand if the metabolite(s) provoking this phenotype is specific for the supplementation with ChoDec, cultures were supplemented with Choline chloride (ChoCl), Sodium decanoate (NaDec), Itraconazole (ITC) or Amphotericin B (AmB). To cover all three classes of antifungals, Caspofungin (CAS) supplementation was also attempted but residual amounts of the compound in the SMEs inhibited fungal growth and made an analysis impossible (data not shown). Antifungal drugs have been added at concentrations corresponding to 80% of their minimal inhibitory concentrations accordingly to the EUCAST MIC distribution website (for ITC and AmB) and the literature (for CAS)[30,31]. ChoCl and NaDec were added at concentrations equimolar to the initially used 1,7 mM for ChoDec. When supplementing fungal cultures with ChoDec, we observed a reduction in biomass and therefore speculated if this reduction is correlated to the production of bioactive SMEs (Figure 3).

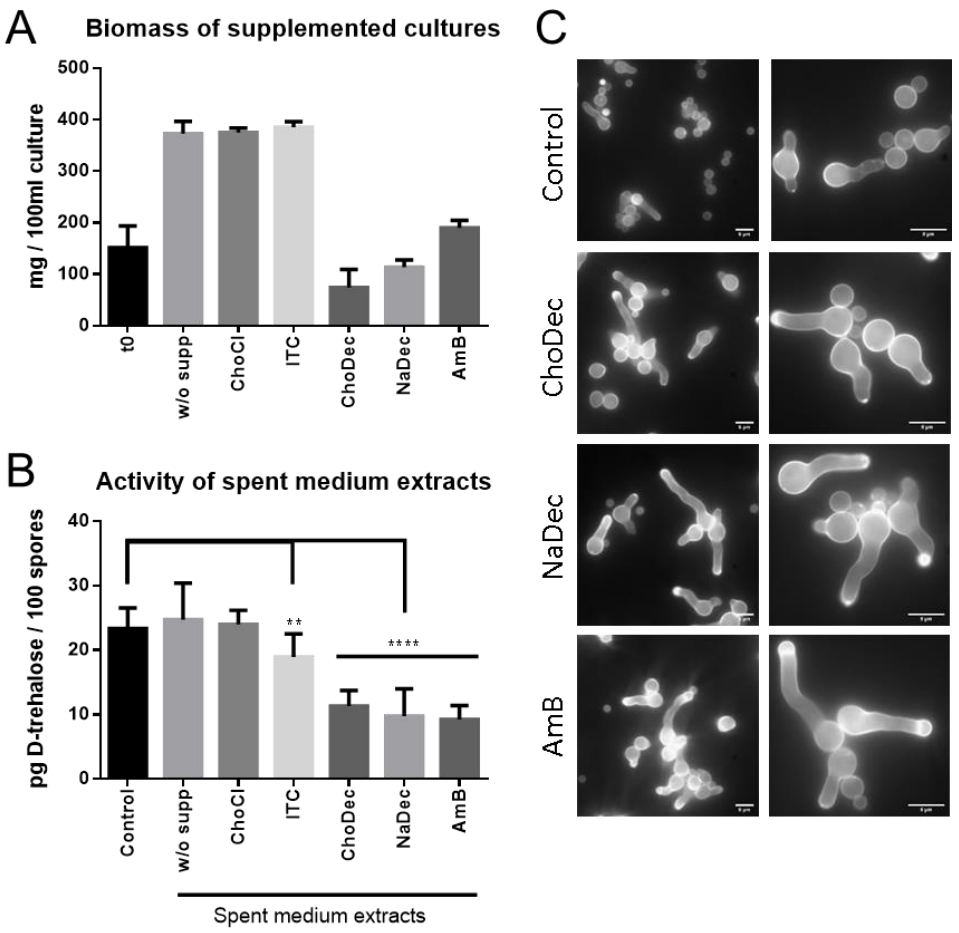

*Figure 3 Effects of different medium supplements on the biomass of A. fumigatus, the production of bioactive metabolites and cell morphology. A) Biomass of supplemented cultures after 48 hours (24 hours of pre-growth plus 24 hours with added supplements). ChoDec, ChoCl and NaDec were added at equimolar concentrations of 1,7mM. ITC and AmB were added at 80% of their reported MIC values against A. fumigatus. t0 refers to the biomass after 24h-pregrowth before addition of the supplements. B) Effect of SMEs on the A. fumigatus´germination analyzed by D-trehalose measurements after 2 hours of growth The unpaired t-test test was performed to compare each condition relative to the Control. Statistically significant differences are depicted; * P ≤ 0.05 ** P ≤ 0.01 *** P ≤ 0.001 **** P ≤ 0.0001 C) Changes of the phenotype induced by the SMEs, stained with calcofluor white, scale bar = 5µm (the right panel shows a 2.5x magnification).*

ChoDec, NaDec and AmB SMEs showed a reduction of D-trehalose after 2h of incubation compared to the control, indicating an acceleration of germination (Figure 3B). The spent medium of ITC supplemented cultures

showed some reduction of D-trehalose as well, but the effect of this extract was not as prominent as the others. All three supplements leading to the production of bioactive extracts affected fungal growth. Compared to the biomass after 24h of pre-growth, before supplementation (t0), ChoDec and NaDec supplemented cultures show a reduction of biomass suggesting cell lysis whereas the biomass of AmB supplemented cultures remained unchanged, being consistent with growth inhibition or beginning cell lysis not yet affecting overall biomass (Figure 3A). In addition to the D-trehalose assay (Figure 3B), morphological changes were analyzed as well upon treatment with NaDec and AmB SMEs, comparing them to the effects observed for ChoDec SMEs (Figure 3C). All three active SMEs show to induce an overall higher number of spores germinating as well as the swollen phenotype observed before.

Interestingly, NaDec, but not ChoCl led to the same effects as ChoDec, suggesting that the anionic moiety of the ionic liquid is responsible for inducing the production of bioactive metabolites. The high lipophilicity due to the long alkyl chain is believed to interfere with the cell membrane, but a membrane permeabilization or cell wall damage could not be confirmed[28,32]. ChoDec does activate the sphingolipid biosynthetic pathway though, which seems to be involved in the response to cell wall damage[32]. Although the mechanism of action remains to be solved, its toxicity against filamentous fungi has been shown in various studies[23,28,33]. One study observed the production of the toxic compound cyanide upon the uptake of the cholinium cation and suggested that this might cause growth inhibition[22]. This is probably true for medium supplementation with high quantities of cholinium based ionic liquids (0.2-0.7 M in the growth medium) used in this study. In contrast, our data indicate that toxicity of choline decanoate is primarily caused by the anionic moiety and the reduction of biomass suggests a mechanism leading to cell lysis (Figure 3A). AmB is fungicidal, it preferentially binds to ergosterol, the primary sterol in the fungal cell

membrane, leading to membrane leakage and cell death[34]. The biomass data suggest that 24h after addition of AmB, cell death followed by cell lysis has not been completed, but the toxicity is already exerting growth inhibition with potential membrane leaking (Figure 3A). The fungicidal activity of ITC is caused by binding to the lanosterol 14-α-demethylase (*CYP51)*, a key enzyme in the ergosterol biosynthesis pathway. Depletion of ergosterol and the accumulation of a toxic sterol activates a compensatory cell wall stress pathway that results in carbohydrate patch formation with subsequent penetration of plasma membrane and fungal killing. The ITC concentrations used were insufficient to induce an effect comparable to AmB and ChoDec after 24h. Cell death in the presence of ITC may take longer than the 24h of incubation, therefore one cannot exclude that ITC supplementation would eventually lead to the same effects of biomass reduction and comparable bioactivity of the SMEs. These data suggest that the secretion of growth enhancing molecules into the medium is a common stress response to fungicidal compounds.

Free amino acids are accumulated upon stress conditions

Upon addition of ChoDec, NaDec and AmB to the culture medium, we could observe a reduction in biomass after 24h (Figure 3), which suggests cell death due to the toxic nature of these compounds. Cell lysis can lead to the release of nutrients, such as amino acids, which have been shown to induce germination in *Aspergillus niger*[35]. In fact, preliminary isolation attempts of the bioactive metabolites, suggested the presence of small amines (data not shown). Therefore, we analyzed free amino acids in the spent medium of cultures supplemented or not with ChoDec, NaDec or AmB (Figure 4A).

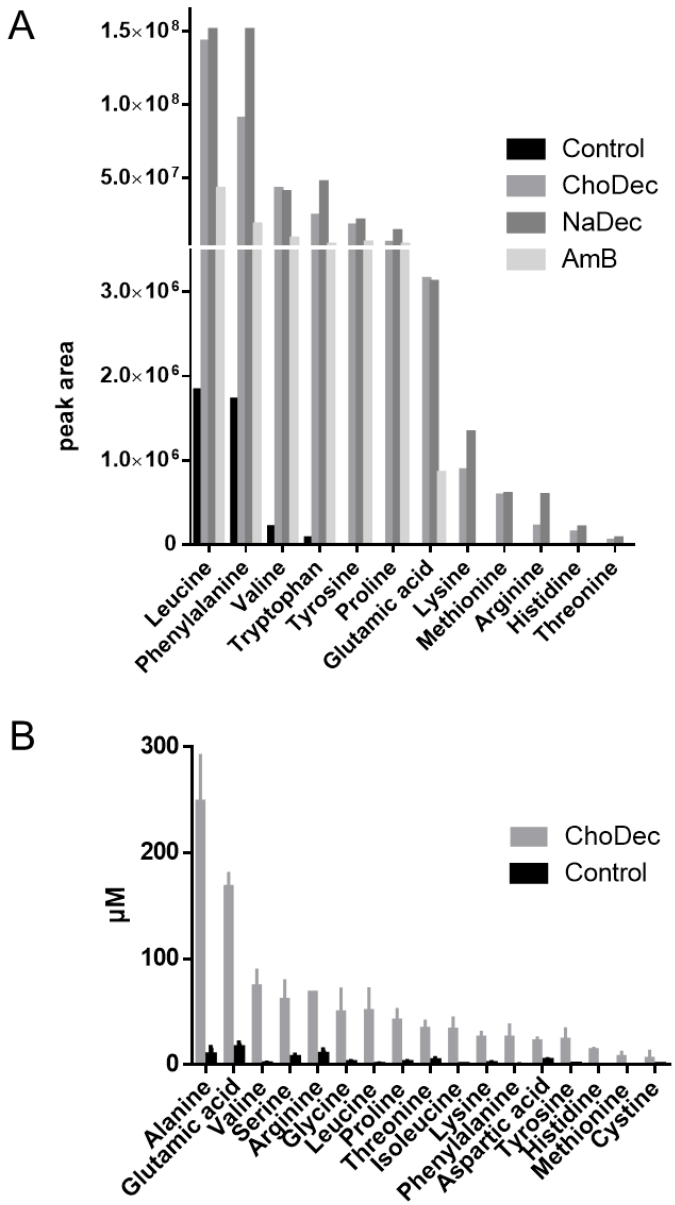

Figure 4 Analysis of free amino acids in the SMEs derived from cultures grown with supplementation of ChoDec, NaDec or AmB, and without supplementation (Control). A) Comparison of bioactive extracts for their amino acid composition analyzed by HR-MS, B) HPLC quantification of free amino acids in the SMEs supplemented with ChoDec or without supplement (Control).

Analysis by high resolution mass spectrometry (HRMS) clearly showed that the addition of any of the three compounds to the culture medium leads to an accumulation of free amino acids. Since HRMS could not reliably detect most amino acids due to the complexity of extracts, free amino acids have been quantified by HPLC analysis comparing ChoDec SMEs with non-supplemented SMEs (Figure 4B). Only glutamine, asparagine and tryptophan cannot be quantified by the applied method, as glutamine and asparagine are converted to their acidic form and tryptophan elutes too close to the end of the chromatographic run, complicating its identification. The most abundant amino acid quantified in the ChoDec SME is alanine, followed by glutamic acid, representing the sum of glutamic acid and glutamine in the sample. Overall, the quantification confirmed the increase of free amino acids in the extracts of cultures supplemented with toxic compounds.

Naturally, in a next step, amino acids were tested for their ability to induce germination in *A. fumigatus*. A mix of 19 proteinogenic amino acids at 100µM each was compared to the ChoDec SME for their ability to accelerate germination (Figure 5). In fact, the mix of amino acids induced germination to the same extent as the ChoDec SME (Figure 5A). This is an expected result and in accordance with the aforementioned study in *A. niger*[35], since amino acids, together with sugars and inorganic salts, are essential for conidial germination[36,37]. A previous work has shown, that the addition of human albumin to the growth medium of *A. fumigatus* enhances germination, hyphal growth and even antifungal resistance[38]. The authors have not analyzed the potential contribution of free amino acids released due to albumin proteolytic digestion to the observed phenomenon. Functional protein biosynthesis is required for germination, in contrast to DNA and RNA biosynthesis[39,40]. It is among the earliest detectable events of germination with large amounts of mRNA stored in resting conidia, covering up to 27% of the genes in *A. fumigatus*[41,42]. Free amino acids are therefore essential for germination and increased available amounts may accelerate the process.

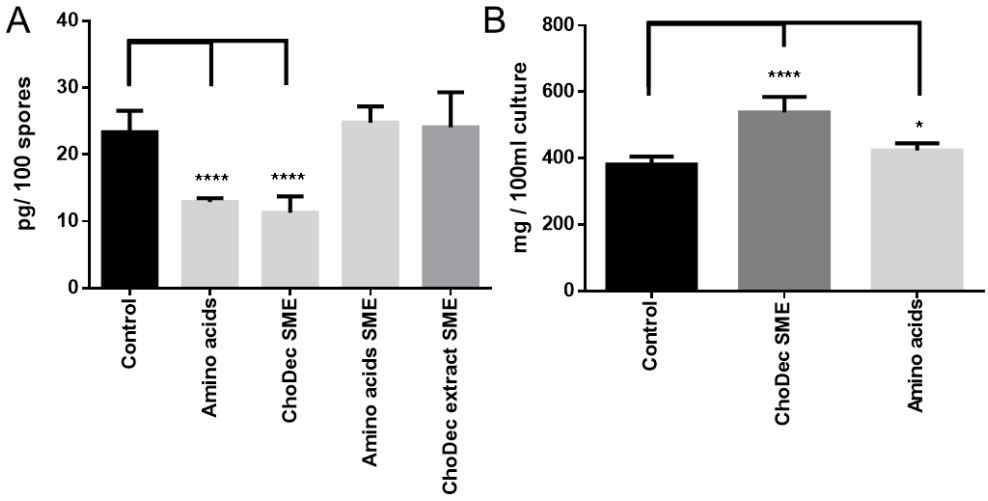

*Figure 5 Comparison of the effects induced by an artificial amino acid mix and the ChoDec SME. A) Germination inducing activity analyzed by D-trehalose content after 2 hours of growth. Both, the amino acid mix and the ChoDec SME show to significantly enhance germination compared to the control (no supplement). Extracts of cultures supplemented with either the amino acid mix or the ChoDec SME, don´t show any activity. B) Biomass of cultures grown with or without the ChoDec SME or the amino acid mix. Only the ChoDec SME shows to significantly increase overall biomass production after 24 hours. The unpaired t-test test was performed to compare each condition relative to the Control. Statistically significant differences are depicted; * P ≤ 0.05 ** P ≤ 0.01 *** P ≤ 0.001 **** P ≤ 0.0001.*

In a follow-up experiment, *A. fumigatus* cultures were supplemented with the bioactive ChoDec SME, or the amino acid mix and the spent medium extracted again. Those secondary extracts were then tested in turn on new *A. fumigatus* cultures, to understand if the ChoDec SME or the amino acids would induce the production of more bioactive metabolites. No germination inducing activities could be detected though. These results indicate, that neither the amino acids nor any other metabolite present in the ChoDec SME trigger the production of bioactive metabolites and confirms that the bioactivity results from a stress mechanism induced by toxic exogenous agents.

Supplementation of the growth medium with ChoDec SME led to the production of an overall higher biomass (Figure 1A), however the mix of free amino acids did not reproduce this effect (Figure 4-5B). The free amino acids alone are not responsible for the increased production of biomass, therefore the bioactivity of the ChoDec SME may be the result of various bioactive compounds present.

The bioactive extracts are enriched with alkaloids

To understand if in addition to the detected free amino acids, other compounds may contribute to the bioactivity of the ChoDec SME, HRMS was applied to screen for differentially secreted secondary metabolites. The bioactive SMEs of ChoDec, NaDec and AmB supplemented cultures were analyzed and compared to the Control SME without supplementation. The results are depicted in Table 1, showing three peptidyl alkaloids exclusively identified in the active extracts (Figure 6).

Table 1 HR-MS analysis of SMEs, listed are metabolites that were exclusively identified in the bioactive SMEs.

	Peak area			
	w/out supp	**ChoDec**	**NaDec**	**AmB**
Phe-Ser-DKP	-	2.15E+07	1.82E+07	2.09E+07
Gliotoxin	-	5.23E+06	5.36E+06	1.22E+06
Tryptoquivaline F/J	-	4.29E+05	6.66E+05	2.79E+05

Tryptoquivaline J is a stereoisomer of tryptoquivaline F, which is also called fumitremorgin F[43,44]. These compounds belong to the class of tremorgenic mycotoxins, which can be structurally divided into the indole-diterpenoids (e.g. penitrems and paspalitrems), the prenylated indole-diketopiperazines (e.g. fumitremorgens and verruculogens), and the quinazoline-containing indole alkaloids related to tryptoquivaline[45,46]. Tryptoquivaline F contains the quinazoline-ring and therefore belongs to the tryptoquivalines and not the fumitremorgins. Several studies have tested tryptoquivaline F against a range of cell lines, but in contrast to other tremorgenic mycotoxins no

cytotoxic activity could be detected[24,47,48]. Neither has any antimicrobial bioactivity been detected against *S. aureus*, *B. subtilis*, *P. aeruginosa* or *C. albicans*[49]. Gliotoxin, derived from the 2,5-diketopiperazine (DKP) Phe-Ser-DKP, belongs to the epipolythiodioxopiperazine (ETP) class toxins, which share a characteristic sulfur bridge responsible for their activity. Gliotoxin is produced by many fungal species, among which *A. fumigatus* may be the major producer[50] for which it has been shown to be an important virulence factor, exhibiting immunosuppressive activity in humans[51–53]. *Aspergillus fumigatus* protects itself from the toxic activity of gliotoxin by expressing GliT, a gliotoxin reductase, which catalyzes the oxidation of reactive dithiol gliotoxin to gliotoxin[54,55].

Interestingly, another study described the enhanced production and secretion of gliotoxin in response to Caspofungin treatment for 24h together with the release of free amino acids and protein and the reduction of biomass in *A. fumigatus*[56]. The authors speculated that the enhanced production of gliotoxin is a mean to restore the redox balance disrupted by the drug and/ or cell leakage. In fact, two other studies in *A. fumigatus* found that gliotoxin reduced reactive oxygen species (ROS) and growth inhibition in cells exposed to hydrogen peroxide (H_2O_2)[57,58]. The release of gliotoxin or other peptidyl alkaloids may be a general response to exogenous toxins.

Both, tryptoquivaline F and gliotoxin, are synthetized by NRPSs from amino acid precursors (Figure 6)[59]. The biosynthesis of gliotoxin production has been fully elucidated. Its biosynthetic gene cluster comprises 13 genes, which are regulated by the *gliZ* (a zinc-finger transcription factor) and *gliP* (an NRPS) genes and the global regulator LaeA[60–63]. The first step in the biosynthesis is the formation of Phe-Ser-DKP, which is catalyzed by the bimodular GliP NRPS[64,65]. 2,5-DKPs, also called cyclodipeptides (CDP) are the smallest form of cyclic peptides, mainly produced by microorganisms[66].

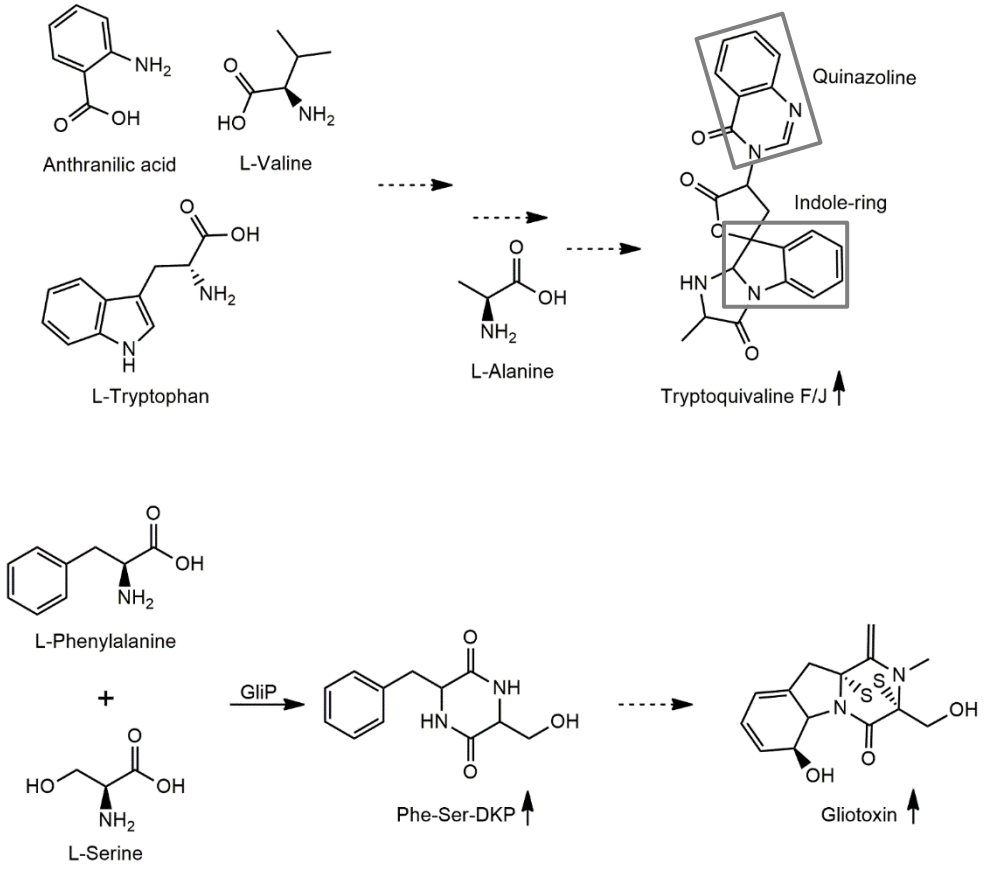

Figure 6 Structures of the peptidyl alkaloids enriched in the bioactive SMEs and their (potential) biosynthetic precursors. Tryptoquivaline F is probably derived from Anthranilic acid, valine and tryptophan with the addition of alanine in a later step, as has been suggested for the biosynthesis of tryptoquivaline. Gliotoxin is derived from phenylalanine and serine, which in a first step are synthetized to the Phe-Ser-DKP, detected in the active extracts as well.

In contrast, the biosynthesis of tryptoquivaline F or any other tryptoquivaline has not been elucidated yet. It is assumed, that it is biosynthesized from the non-proteinogenic amino acid anthranilic acid and the two proteinogenic amino acids L-tryptophan and L-valine[43,67]. Later on, the indole-ring derived from the L-tryptophan moiety is probably N-acetylated with L-alanine[43,68,69]. The biosynthesis of structurally related metabolites has been studied, such as fumiquinazoline produced by *A. fumigatus* and tryptoquialanine produced by *Penicillium aethiopicum*. Both metabolites and their derivatives are

synthesized by Ant-Trp-Ala NRPSs, thus having L-alanine as a precursor instead of L-valine like tryptoquivaline. The study investigating the fumiquinazoline biosynthesis identified the acetylation mechanism with L-alanine, which involves the oxidation of the indole by an FAD-dependent monooxygenase (Af12060), followed by the alanine coupling by a monomodular NRPS (Af12050)[68]. The same mechanism may be involved in the biosynthesis of related indole alkaloids, like tryptoquivaline[68]. In *P. aethiopicum* the *tqa* cluster is responsible for the biosynthesis of tryptoquialanine[67]. A BLAST analysis identified the putative *tqv* cluster in *Aspergillus clavatus*, which may be involved in the biosynthesis of tryptoquivaline[67]. Comparative genomics could further help to identify the biosynthetic genes of tryptoquivaline and concomitantly tryptoquivaline F in *A. fumigatus* (an according analysis is ongoing).

Tryptoquivaline F enhances germination

In a next step we wanted to understand whether the identified alkaloids contribute in fact to the observed germination inducing effect of the ChoDec SME. D-trehalose was quantified in spores grown in the presence of 50µM of gliotoxin, tryptoquivaline F or Phe-Ser-DKP. The amount of trehalose per sample was normalized to their corresponding non-treated control and the variation in % has been plotted (Figure 7). The results clearly show, that tryptoquivaline F induces germination to an equal extent as the ChoDec SME, in contrast to gliotoxin and Phe-Ser-DKP. The same assay with 100 µM of the tested compounds reproduced comparable results, but the available amounts of compounds were insufficient to produce replicates for statistical analyses (data not shown).

A possible explanation for the effects of tryptoquivaline F is that the fungus uses it as an additional nitrogen source comparable to amino acids, but in that case, some bioactivity would also be expected from gliotoxin and Phe-Ser-DKP. Hence, we hypothesize that tryptoquivaline F, a secondary

metabolite produced and secreted under stress conditions, could serve as a germination inducing signaling compound, to be further investigated.

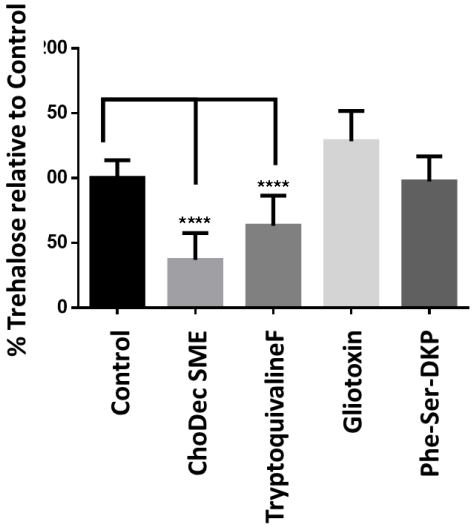

*Figure 7 Effects of the ergot alkaloids identified in the active SMEs on A. fumigatus germination analyzed by D-trehalose content after 2 hours. The D-trehalose content is depicted as the % relative to the control to minimize experimental variations. The unpaired t-test test was performed to compare each condition relative to the Control. Statistically significant differences are depicted; * P ≤ 0.05 ** P ≤ 0.01 *** P ≤ 0.001 **** P ≤ 0.0001.*

Conclusions & Future Perspectives

In this study we analyzed whether the supplementation of growth medium with the ionic liquid ChoDec leads to the production and secretion of potential intraspecies signaling molecules in *A. fumigatus* cultures. We found that the SMEs in fact had bioactivity towards *A. fumigatus* itself, by inducing germination, a swollen phenotype, and the production of overall more biomass (Figure 1 & 4-2). The effect of accelerated germination could also be observed with SMEs from cultures supplemented with NaDec and AmB, as well as to some extent with ITC (Figure 3). In all three bioactive extracts, from ChoDec, NaDec and AmB supplemented cultures, an increase of free amino acids, as well as the three peptidyl alkaloids tryptoquivaline F/J, Phe-Ser-DKP and gliotoxin were detected (Figure 4, Table 1). These findings

suggest a common survival strategy of *A. fumigatus* in response to fungicidal exogenous toxics. In fact, gliotoxin secretion has also been observed upon caspofungin treatment in another study[56]. The toxic stress leads to cell death, potentially inducing cell leakage, as indicated by the biomass reduction (Figure 3) and to the release of alkaloids, as well as free amino acids into the medium. Both, the secreted tryptoquivaline F and the amino acids accelerate germination of *A. fumigatus* spores (Figure 5, Figure 7). The availability of large amounts of free amino acids appear not to induce the production of the detected alkaloids, although these are derived from amino acid precursors (Figure 5). Both, the release of amino acids and of the alkaloids seem to be a direct response to the imposed stress.

Tryptoquivaline F may be classified as an intraspecies signaling molecule. To date, only alcohols, lipids, pheromones and lactones have been described as self-regulating signaling molecules, but no ergot alkaloids yet[12]. According to Albuquerque and Casadevall, for a self-signaling molecule to be classified as such, the compound should fulfill the following five criteria: (I) accumulation in the extracellular environment during microbial growth; (II) at a concentration proportional to cell density, restricted to a specific growth phase; (III) lead to a coordinated response across the population, which is not simply the metabolization or detoxification of the molecule itself; (IV) reproduce the QS phenotype when being added exogenously; (V) it is not merely a by-product of microbial catabolism[70,71]. Tryptoquivaline F meets criteria I and III-V, as the metabolite is accumulated extracellularly, is not simply metabolized but leads to the induction of germination, an effect that is reproduced when being added exogenously and is not a by-product of catabolism, since accumulation could not be observed under control conditions. Criterion II does not properly fit our approach, since we did not study signaling molecules that are produced upon intrinsic signals within the colony in response to cell density, but to external signals. However, quorum sensing has been shown to be linked to several stress responses in

bacteria[72–75]. Whether the secretion of self-regulating signaling molecules is always cell density dependent and restricted to a specific growth phase remains to be determined[76]. For tryptoquivaline F to be considered a quorum sensing like molecule, further experiments need to analyze its autoinducing capacity, meaning the concentration dependent, synchronized activation or repression of genes.

It is assumed that maximum biomass is equivalent to the amount of initial nutrients available, but the ChoDec SME increased biomass substantially without the addition of carbohydrates and the mix of free amino acids did not induce the same effect. This can have various explanations, such as the swollen phenotype, an optimized utilization of nutrients or reduced cell death in the stationary phase. Not all spores within a culture germinate and it has been described that in *A. niger* no more spores germinate after 14h at standard laboratory conditions[77]. It is possible, that tryptoquivaline F not only induces accelerated germination, but indeed induces a synchronized germination of the remaining spores.

Further analyses are ongoing to fully understand the potential role of tryptoquivaline F as a germination and growth inducing signaling molecule in response to stress and to determine if it may be an autoinducer. The gene *rtfA*, an orthologue to *rtf1* from *S. cerevisae*, which encodes a protein that functions as an RNA polymerase II transcription elongation factor, has been shown to be involved in the regulation of tryptoquivaline F production in *A. fumigatus*[78]. Deletion of this gene led to a substantial increase of tryptoquivaline F and may thus present a suitable target for gene regulation analyses upon medium supplementation. Furthermore, plans are ongoing to analyze the transcriptional reprograming of the wild type using RNAseq to monitor the upregulation of essential genes involved in germination, in response to tryptoquivaline F supplementation. The major current drawback is the time-consuming complex purification of tryptoquivaline F (not

commercially available), hence a *rtfA* deletion mutant will be made to ease the purification of the metabolite and to support the transcriptomic analyses. In the case of tryptoquivaline F, the biosynthetic pathway has not been described yet, and the analysis might not be straightforward. However, all 12 canonical genes involved in the biosynthesis of gliotoxin have been identified (as well as the transcription factors GliZ and GipA)[60,79–81]. Accordingly, they may help to generally confirm the production of peptidyl alkaloids under fungicidal stress conditions. Finally, the upregulation of the two enzymes involved in the N-acetylation step of fumiquinazoline and potentially of tryptoquivaline in *A. fumigatus,* Af12060 and Af12050, will be observed[68]. RNAseq followed by comparative genomics to compare upregulated genes for their homology to the *tqa* cluster in *P. aethiopicum* encoding biosynthetic enzymes for the tryptoquialanine synthesis and the putative *tqv* cluster in *A. clavatus* may identify more genes involved in the biosynthesis of tryptoquivaline and tryptoquivaline F.

Future studies could analyze the production of the metabolites herein described, prioritizing tryptoquivaline F, during an invasive infection in response to antifungal treatments. The combination of tryptoquivaline F as a growth enhancer and gliotoxin as a cytotoxin, may provide the fungus with a rescue strategy against drug treatment. The dynamics between repeated and prolonged drug administration, metabolite production and growth recovery of the fungus should be analyzed. Gaining a better understanding of *A. fumigatus´* strategies to fight exogenous toxic stress will provide knowledge to counteract such strategies in the future.

Acknowledgements

MR and PS are grateful to *Fundação para a Ciência e a Tecnologia* (FCT) for the fellowship PD/BD/113989/2015 and PD/BD/135481/2018, respectively. The authors are thankful to Maria C. Leitão (ITQB NOVA) for meaningful support in chromatographic analyses and Anake Kijjoa (Ciimar)

for kindly providing isolated tryptoquivaline F. The authors acknowledge the use of microscope at the Bacterial Imaging Cluster (ITQB-NOVA).

References

1. Tekaia, F. & Latgé, J.-P. Aspergillus fumigatus: saprophyte or pathogen? *Curr. Opin. Microbiol.* **8**, 385–392 (2005).
2. Latgé, J.-P. & Chamilos, G. Aspergillus fumigatus and Aspergillosis in 2019. *Clin. Microbiol. Rev.* **33**, (2019).
3. Patterson, T. F. *et al.* Invasive Aspergillosis Disease Spectrum, Treatment Practices, and Outcomes. *Medicine (Baltimore).* **79**, 250–260 (2000).
4. Jenks, J. D. & Hoenigl, M. Treatment of aspergillosis. *J. Fungi* **4**, (2018).
5. Fleming, A. The discovery of Penicillin. *Br Med Bull* **2**, 4–5 (1944).
6. Brakhage, A. A. Regulation of fungal secondary metabolism. *Nat. Rev. Microbiol.* **11**, 21–32 (2013).
7. Pusztahelyi, T., Holb, I. J. & PÃ^{3}csi, I. Secondary metabolites in fungus-plant interactions. *Front. Plant Sci.* **6**, (2015).
8. Bills, G. F. & Gloer, J. B. Biologically Active Secondary Metabolites from the Fungi. *Microbiol. Spectr.* **4**, (2016).
9. Doğaner, B. A., Yan, L. K. Q. & Youk, H. Autocrine Signaling and Quorum Sensing: Extreme Ends of a Common Spectrum. *Trends Cell Biol.* **26**, 262–271 (2016).
10. Wongsuk, T., Pumeesat, P. & Luplertlop, N. Fungal quorum sensing molecules: Role in fungal morphogenesis and pathogenicity. *J. Basic Microbiol.* **56**, 1–8 (2016).
11. Hornby, J. M. *et al.* Quorum Sensing in the Dimorphic Fungus Candida albicans Is Mediated by Farnesol. *Appl. Environ. Microbiol.* **67**, 2982–2992 (2001).
12. Chen, H. Tyrosol is a quorum-sensing molecule in Candida albicans. *Proc. Natl. Acad. Sci.* **101**, 5048–5052 (2004).

13. Martins, M. *et al.* Morphogenesis control in Candida albicans and Candida dubliniensis through signaling molecules produced by planktonic and biofilm cells. *Eukaryot. Cell* **6**, 2429–2436 (2007).
14. Horowitz Brown, S., Zarnowski, R., Sharpee, W. C. & Keller, N. P. Morphological Transitions Governed by Density Dependence and Lipoxygenase Activity in Aspergillus flavus. *Appl. Environ. Microbiol.* **74**, 5674–5685 (2008).
15. Williams, H. E., Steele, J. C. P., Clements, M. O. & Keshavarz, T. γ-Heptalactone is an endogenously produced quorum-sensing molecule regulating growth and secondary metabolite production by Aspergillus nidulans. *Appl. Microbiol. Biotechnol.* **96**, 773–781 (2012).
16. Bottone, E. J., Nagarsheth, N. & Chiu, K. Evidence of self-inhibition by filamentous fungi accounts for unidirectional hyphal growth in colonies. *Can. J. Microbiol.* **44**, 390–393 (1998).
17. Champe, S. P. & El-Zayat, A. A. Isolation of a sexual sporulation hormone from Aspergillus nidulans. *J. Bacteriol.* **171**, 3982–3988 (1989).
18. Tsitsigiannis, D. I., Kowieski, T. M., Zarnowski, R. & Keller, N. P. Three putative oxylipin biosynthetic genes integrate sexual and asexual development in Aspergillus nidulans. *Microbiology* **151**, 1809–1821 (2005).
19. Bok, J. W. & Keller, N. P. LaeA, a regulator of secondary metabolism in Aspergillus spp. *Eukaryot. Cell* **3**, 527–535 (2004).
20. Kirk-Othmer. Kirk-Othmer Encyclopedia of Chemical Technology. *Kirk-Othmer Encycl. Chem. Technol.* **24**, 233–250 (1997).
21. Alves, P. C. *et al.* Transcriptomic and metabolomic profiling of ionic liquid stimuli unveils enhanced secondary metabolism in Aspergillus nidulans. *BMC Genomics* **17**, 284 (2016).
22. Martins, I. *et al.* Proteomic alterations induced by ionic liquids in Aspergillus nidulans and Neurospora crassa. *J. Proteomics* **94**, 262–

278 (2013).

23. Petkovic, M. *et al.* Novel biocompatible cholinium-based ionic liquids - Toxicity and biodegradability. *Green Chem.* **12**, 643–649 (2010).
24. Buttachon, S. *et al.* Sartorymensin, a new indole alkaloid, and new analogues of tryptoquivaline and fiscalins produced by Neosartorya siamensis (KUFC 6349). *Tetrahedron* **68**, 3253–3262 (2012).
25. Zin, W. W. M. *et al.* A new meroditerpene and a new tryptoquivaline analog from the algicolous fungus Neosartorya takakii KUFC 7898. *Mar. Drugs* **13**, 3776–3790 (2015).
26. Armenta, J. M. *et al.* Sensitive and Rapid Method for Amino Acid Quantitation in Malaria Biological Samples Using AccQ•Tag Ultra Performance Liquid Chromatography-Electrospray Ionization-MS/MS with Multiple Reaction Monitoring. *Anal. Chem.* **82**, 548–558 (2010).
27. Penrose, D. M., Moffatt, B. A. & Glick, B. R. Determination of 1-aminocycopropane-1-carboxylic acid (ACC) to assess the effects of ACC deaminase-containing bacteria on roots of canola seedlings. *Can. J. Microbiol.* **47**, 77–80 (2001).
28. Hartmann, D. O. *et al.* Plasma membrane permeabilisation by ionic liquids: a matter of charge. *Green Chem.* **17**, 4587–4598 (2015).
29. Boethling, R. S., Sommer, E. & DiFiore, D. Designing Small Molecules for Biodegradability. *Chem. Rev.* **107**, 2207–2227 (2007).
30. Warn, P. A., Sharp, A., Morrissey, G. & Denning, D. W. Activity of aminocandin (IP960; HMR3270) compared with amphotericin B, itraconazole, caspofungin and micafungin in neutropenic murine models of disseminated infection caused by itraconazole-susceptible and -resistant strains of Aspergillus fumigatus. *Int. J. Antimicrob. Agents* **35**, 146–151 (2010).
31. European Committee on Antimicrobial Susceptibility Testing. Available at: http://www.eucast.org. (Accessed: 17th February 2021)
32. Hartmann, D. O., Piontkivska, D., Moreira, C. J. S. & Silva Pereira, C.

Ionic Liquids Chemical Stress Triggers Sphingoid Base Accumulation in Aspergillus nidulans. *Front. Microbiol.* **10**, (2019).

33. Petkovic, M. *et al.* Exploring fungal activity in the presence of ionic liquids. *Green Chem.* **11**, 889 (2009).
34. Gray, K. C. *et al.* Amphotericin primarily kills yeast by simply binding ergosterol. *Proc. Natl. Acad. Sci.* **109**, 2234–2239 (2012).
35. Hayer, K., Stratford, M. & Archer, D. B. Germination of Aspergillus niger conidia is triggered by nitrogen compounds related to L-amino acids. *Appl. Environ. Microbiol.* **80**, 6046–6053 (2014).
36. Carlile, M. J., Watkinson, S. C. & Gooday, G. W. The Fungi 2nd. *Sci. Acad. Press. San Diego* (2001).
37. Osherov, N. The molecular mechanisms of conidial germination. *FEMS Microbiol. Lett.* **199**, 153–160 (2001).
38. Rodrigues, A. G., Araujo, R. & Pina-Vaz, C. Human albumin promotes germination, hyphal growth and antifungal resistance by Aspergillus fumigatus. *Med. Mycol.* **43**, 711–717 (2005).
39. Osherov, N. & May, G. Conidial germination in Aspergillus nidulans requires RAS signaling and protein synthesis. *Genetics* **155**, 647–56 (2000).
40. Baltussen, T. J. H., Zoll, J., Verweij, P. E. & Melchers, W. J. G. Molecular Mechanisms of Conidial Germination in Aspergillus spp. *Microbiol. Mol. Biol. Rev.* **84**, 1–31 (2020).
41. d'Enfert, C. Fungal Spore Germination: Insights from the Molecular Genetics ofAspergillus nidulansandNeurospora crassa. *Fungal Genet. Biol.* **21**, 163–172 (1997).
42. Lamarre, C. *et al.* Transcriptomic analysis of the exit from dormancy of Aspergillus fumigatus conidia. *BMC Genomics* **9**, 1–15 (2008).
43. Yamazaki, M., Fujimoto, H. & Okuyama, E. Structure determination of six fungal metabolites, tryptoquivaline E,F,G,H,I and J from Aspergillus fumigatus. *Chem. Pharm. Bull.* **26**, 111–117 (1978).

44. National Center for Biotechnology Information. PubChem. Compound Summary for CID 181786, Tryptoquivaline F. Available at: https://pubchem.ncbi.nlm.nih.gov/compound/Tryptoquivaline-F. (Accessed: 30th September 2021)
45. Steyn, P. S. & Vleggaar, R. Tremorgenic mycotoxins. *Fortschritte der Chemie Org. Naturstoffe* **48**, 1–80 (1985).
46. D'yakonov, A. L. & Telezhenetskaya, M. V. Quinazoline alkaloids in nature. *Chem. Nat. Compd. 1997 333* **33**, 221–267 (1997).
47. Prata-Sena, M. *et al.* Cytotoxic activity of Secondary Metabolites from Marine-derived Fungus Neosartorya siamensis in Human Cancer Cells. *Phyther. Res.* **30**, 1862–1871 (2016).
48. Afiyatullov, S. S. *et al.* New Metabolites from the Marine-Derived Fungus Aspergillus Fumigatus. *Nat. Prod. Commun.* **7**, 1934578X1200700 (2012).
49. Shaaban, M. *et al.* Sulochrins and alkaloids from a fennel endophyte Aspergillus sp. FVL2. *Nat. Prod. Res.* 1–11 (2021). doi:10.1080/14786419.2021.2005054
50. Gardiner, D. M., Waring, P. & Howlett, B. J. The epipolythiodioxopiperazine (ETP) class of fungal toxins: distribution, mode of action, functions and biosynthesis. *Microbiology* **151**, 1021–1032 (2005).
51. Yamada, A., Kataoka, T. & Nagai, K. The fungal metabolite gliotoxin: immunosuppressive activity on CTL-mediated cytotoxicity. *Immunol. Lett.* **71**, 27–32 (2000).
52. Schlam, D. *et al.* Gliotoxin Suppresses Macrophage Immune Function by Subverting Phosphatidylinositol 3,4,5-Trisphosphate Homeostasis. *MBio* **7**, (2016).
53. Scharf, D. H., Brakhage, A. A. & Mukherjee, P. K. Gliotoxin - bane or boon? *Environ. Microbiol.* **18**, 1096–1109 (2016).
54. Schrettl, M. *et al.* Self-Protection against Gliotoxin—A Component of

the Gliotoxin Biosynthetic Cluster, GliT, Completely Protects Aspergillus fumigatus Against Exogenous Gliotoxin. *PLoS Pathog.* **6**, e1000952 (2010).

55. Scharf, D. H. *et al.* Transannular Disulfide Formation in Gliotoxin Biosynthesis and Its Role in Self-Resistance of the Human Pathogen Aspergillus fumigatus. *J. Am. Chem. Soc.* **132**, 10136–10141 (2010).
56. Eshwika, A., Kelly, J., Fallon, J. P. & Kavanagh, K. Exposure of Aspergillus fumigatus to caspofungin results in the release, and de novo biosynthesis, of gliotoxin. *Med. Mycol.* **51**, 121–127 (2013).
57. Gallagher, L. *et al.* The Aspergillus fumigatus protein gliK protects against oxidative stress and is essential for gliotoxin biosynthesis. *Eukaryot. Cell* **11**, 1226–1238 (2012).
58. Owens, R. A., Hammel, S., Sheridan, K. J., Jones, G. W. & Doyle, S. A proteomic approach to investigating gene cluster expression and secondary metabolite functionality in Aspergillus fumigatus. *PLoS One* **9**, e106942 (2014).
59. Walsh, C. T., Haynes, S. W., Ames, B. D., Gao, X. & Tang, Y. Short pathways to complexity generation: Fungal peptidyl alkaloid multicyclic scaffolds from anthranilate building blocks. *ACS Chem. Biol.* **8**, 1366–1382 (2013).
60. Bok, J. W. *et al.* GliZ, a Transcriptional Regulator of Gliotoxin Biosynthesis, Contributes to Aspergillus fumigatus Virulence. *Infect. Immun.* **74**, 6761–6768 (2006).
61. Bok, J. W. *et al.* LaeA, a Regulator of Morphogenetic Fungal Virulence Factors. *Eukaryot. Cell* **4**, 1574–1582 (2005).
62. Kupfahl, C. *et al.* Deletion of the gliP gene of Aspergillus fumigatus results in loss of gliotoxin production but has no effect on virulence of the fungus in a low-dose mouse infection model. *Mol. Microbiol.* **62**, 292–302 (2006).
63. Cramer, R. A. *et al.* Disruption of a Nonribosomal Peptide Synthetase

in Aspergillus fumigatus Eliminates Gliotoxin Production. *Eukaryot. Cell* **5**, 972–980 (2006).

64. Balibar, C. J. & Walsh, C. T. GliP, a Multimodular Nonribosomal Peptide Synthetase in Aspergillus fumigatus , Makes the Diketopiperazine Scaffold of Gliotoxin. *Biochemistry* **45**, 15029–15038 (2006).
65. Scharf, D. H. *et al.* Biosynthesis and function of gliotoxin in Aspergillus fumigatus. *Appl. Microbiol. Biotechnol.* **93**, 467–472 (2012).
66. Prasad, C. Bioactive cyclic dipeptides. *Peptides* **16**, 151–164 (1995).
67. Gao, X. *et al.* Fungal indole alkaloid biosynthesis: Genetic and biochemical investigation of the tryptoquialanine pathway in penicillium aethiopicum. *J. Am. Chem. Soc.* **133**, 2729–2741 (2011).
68. Ames, B. D., Liu, X. & Walsh, C. T. Enzymatic processing of fumiquinazoline F: A tandem oxidative-acylation strategy for the generation of multicyclic scaffolds in fungal indole alkaloid biosynthesis. *Biochemistry* **49**, 8564–8576 (2010).
69. Ahammad Uz Zaman, K. H., Hu, Z., Wu, X. & Cao, S. Tryptoquivalines W and X, two new compounds from a Hawaiian fungal strain and their biological activities. *Tetrahedron Lett.* **61**, (2020).
70. Mehmood, A. *et al.* Fungal Quorum-Sensing Molecules and Inhibitors with Potential Antifungal Activity: A Review. *Molecules* **24**, 1950 (2019).
71. Albuquerque, P. & Casadevall, A. Quorum sensing in fungi – a review. *Med. Mycol.* **50**, 337–345 (2012).
72. Joelsson, A., Kan, B. & Zhu, J. Quorum sensing enhances the stress response in Vibrio cholerae. *Appl. Environ. Microbiol.* **73**, 3742–3746 (2007).
73. García-Contreras, R. *et al.* Quorum sensing enhancement of the stress response promotes resistance to quorum quenching and prevents social cheating. *ISME J.* **9**, 115–125 (2015).

74. Walawalkar, Y. D., Vaidya, Y. & Nayak, V. Response of Salmonella Typhi to bile-generated oxidative stress: Implication of quorum sensing and persister cell populations. *Pathog. Dis.* **74**, (2021).
75. van Kessel, J. C. *et al.* Quorum sensing regulates the osmotic stress response in Vibrio harveyi. *J. Bacteriol.* **197**, 73–80 (2015).
76. Zhang, X. *et al.* The impact of cell structure, metabolism and group behavior for the survival of bacteria under stress conditions. *Arch. Microbiol.* **203**, 431–441 (2021).
77. Ijadpanahsaravi, M., Punt, M., Wösten, H. A. B. & Teertstra, W. R. Minimal nutrient requirements for induction of germination of Aspergillus niger conidia. *Fungal Biol.* **125**, 231–238 (2021).
78. Myers, R. R. *et al.* rtfA controls development, secondary metabolism, and virulence in Aspergillus fumigatus. *PLoS One* **12**, 1–26 (2017).
79. Gardiner, D. M. & Howlett, B. J. Bioinformatic and expression analysis of the putative gliotoxin biosynthetic gene cluster of Aspergillus fumigatus. *FEMS Microbiol. Lett.* **248**, 241–248 (2005).
80. Patron, N. J. *et al.* Origin and distribution of epipolythiodioxopiperazine (ETP) gene clusters in filamentous ascomycetes. *BMC Evol. Biol.* **7**, 1–15 (2007).
81. Schoberle, T. J. *et al.* A Novel C2H2 Transcription Factor that Regulates gliA Expression Interdependently with GliZ in Aspergillus fumigatus. *PLoS Genet.* **10**, e1004336 (2014).

Chapter IV

Untargeted metabolomics shed light on the secondary metabolism of fungi triggered by choline-based ionic liquids

This chapter is a reprint of the manuscript published in Frontiers in Microbiology: Sequeira P, Rothkegel M, Domingos P, Martins I, Leclercq CC, Renaut J, Goldman GH and Silva Pereira C. Untargeted metabolomics sheds light on the secondary metabolism of fungi triggered by choline-based ionic liquids. Front. Microbiol. 13, 946286 (2022)

Untargeted metabolomics shed light on the secondary metabolism of fungi triggered by choline-based ionic liquids

Patrícia Sequeira[1,#], Maika Rothkegel[1,#], Patrícia Domingos[1], Isabel Martins[1], Celine C. Leclercq[2], Jenny Renaut[2], Gustavo H. Goldman[1,3], Cristina Silva Pereira[1*]

[1]Applied and Environmental Mycology Laboratory, Instituto de Tecnologia Química e Biológica António Xavier, Universidade Nova de Lisboa (ITQB-NOVA), Av. da República, 2780-157, Oeiras, Portugal

[2]Integrative biology platform, Environmental Research and Technology Platform, Luxembourg Institute of Science and Technology, Belvaux, Luxembourg

[3]Faculdade de Ciências Farmacêuticas de Ribeirão Preto, Universidade de São Paulo, Ribeirão Preto, Brazil

[#]Equally contributing authors

Abstract

Fungal secondary metabolites constitute a rich source of yet undiscovered bioactive compounds. Their production is often silent under standard laboratory conditions, but production of some compounds can be triggered simply by altering the cultivation conditions. The usage of an organic salt - ionic liquid – as growth medium supplement can greatly impact the biosynthesis of secondary metabolites, leading to higher diversity of compounds accumulating extracellularly. This study examines if such supplements, specifically cholinium-based ionic liquids, can support discovery of bioactive secondary metabolites across three model species: *Neurospora crassa, Aspergillus nidulans* and *Aspergillus fumigatus.* Enriched organic extracts obtained from medium supernatant revealed high diversity in metabolites. The supplementation led apparently to increased levels of either 1-aminocyclopropane-1-carboxylate or α-aminoisobutyric acid. The extracts where bioactive against two major foodborne bacterial strains: *Staphylococcus aureus* and *Escherichia coli*. In particular, those retrieved from *N. crassa* cultures showed greater bactericidal potential

compared to control extracts derived from non-supplemented cultures. An untargeted mass spectrometry analysis using the Global Natural Product Social Molecular Networking tool enabled to capture the chemical diversity driven by the ionic liquid stimuli. Diverse macrolides, among other compounds, were putatively associated with *A. fumigatus*; whereas an unexpected richness of cyclic (depsi)peptides with *N. crassa*. Further studies are required to understand if the identified peptides are the major players of the bioactivity of *N. crassa* extracts, and to decode their biosynthesis pathways as well.

Introduction

Microbial infections and antimicrobial resistance constitute a major threat to human health, globally. The last was recognized by the World Health Organization, in 2019, as one of the top 10 global public health threats facing humanity. It is estimated that *ca.* 700,000 people die every year from drug-resistant infections[1]. To fight this threat, the development of new drugs that target microbial virulence and/or pathogenicity is a priority[2]. Microorganisms constitute a diverse and resourceful source for bioactive natural products discovery, which can be used as drug leads or therapeutics itself[3]. In particular, filamentous fungi are considered gifted producers of structurally diverse low-molecular weight secondary metabolites. These compounds are synthesized by using precursors derived from primary metabolism and, generally, are not essential for the growth and development of the producer organism[4–6]. Secondary metabolites are, however, often critical for the survival and growth of the fungus in its ecological niche[5,7], with roles identified for example in nutrient acquisition, interaction with other organisms and growth inhibition of competitors[4,8–10].

Fungal secondary metabolites classes comprise polyketides (PKs), non-ribosomal peptides (NRPs), PK-NRPs hybrids, indole alkaloids, and terpenes[11,12]. PKs, the most abundant class, use acetyl-CoA and malonyl-

CoA units, and biosynthesis is simply achieved by the elongation of carboxylic acid building blocks. The scaffold is further modified by oxygenases, glycosyltransferase and other transferases leading to a high degree of structural diversity[4,13]. NRPs, the second largest class, are synthesized by the modular assembly of short carboxylic acids and/or amino acids[14]. They are constituted of both proteinogenic and non-proteinogenic amino acids and show high diversity in terms of length, variation in their functional domains and whether they are cyclized or not[15]. Other units such as fatty acids, α-hydroxy acids, α-keto acids, heterocycles, and others, can also be incorporated[16]. Terpenes(oids) are made up of several C5 isoprene units, which are synthesized from acetyl-CoA through the mevalonate pathway. They are found to be linear or cyclic, saturated or unsaturated. Their classification is based on the number of isoprene units, among others, triterpenes (steroids) and tetraterpenes (carotenoids)[17]. Compounds of pharmacological interest are for example griseofulvin - PKS[18] and echinocandin B - NRP[19], both with antibiotic properties, and fumagillin – terpenoid, with potential antifungal and antitumoral properties[20].

The first biosynthesis step is catalyzed by a multidomain (backbone) enzyme that defines the produced class: PKs synthases, NRP synthases, hybrid NRP–PK synthases, prenyltransferases (or dimethylallyl tryptophan synthases), or terpene cyclases[21]. Genes encoding for biosynthesis of a secondary metabolite are often arranged in gene clusters that are co-regulated under certain conditions; usually silent under standard laboratory conditions[4]. Many backbone genes already identified have not yet been matched to the produced compound, and *vice versa*[4,22]. To stimulate the production of a rich diversity of secondary metabolites, several strategies have been used, for example co-cultivation with other fungi or genome engineering[6,23,24]. The simplest is, however, the one strain-many compounds (OSMAC) approach that explores modification of the cultivation conditions to activate those metabolic pathways[25]. Ionic liquids, organic salts with a

melting point below 100°C, represent a promising class of chemical stimuli that can profoundly impact fungi metabolism[26–29]. When used as growth media supplements, many backbone genes underwent upregulation, accordingly a higher diversity of secondary metabolites, including cryptic ones, were biosynthesized[27,28]. The stimuli caused by the ionic liquid supplements differ from that of a simple inorganic salt[30].

This study examines if ionic liquids supplements can support discovery of bioactive secondary metabolites in fungi. Three model fungi – *Neurospora crassa, Aspergillus nidulans and Aspergillus fumigatus*, and two choline-based ionic liquids - choline chloride (ChoCl) and choline decanoate (ChoDec), were tested. Specifically, we focused on compounds accumulating extracellularly. The antibacterial activity of the ensuing crude extracts was evaluated against two major foodborne bacterial strains, *Staphylococcus aureus* and *Escherichia coli*. To characterize the chemical landscape of the extracts, their amino acid composition and an untargeted mass spectrometry analysis using the online platform Global Natural Product Social Molecular Networking - GNPS - were applied. An unexpected richness of peptide-based structures could be putatively associated with *N. crassa*.

Material & Methods

Chemicals

Compounds used in preparation of minimal media were purchased from Sigma-Aldrich, except for NaCl and $MgSO_4 \cdot 7H_2O$ (Panreac), phosphoric acid (Fisher Scientific) and $NaNO_3$ (ACROS organics). The standard chemicals (1-aminocyclopropane-1-carboxylate – ACC; and α-aminoisobutyric acid - Aib) and chromatographic solvents were of highest analytical grade and purchased from Sigma Aldrich and Fisher Scientific, respectively. Water was obtained from a Milli-Q system (Millipore). Choline Chloride (>98 %) was purchased from Sigma Aldrich and Choline Decanoate (>95 %) from Iolitec.

Fungal strains

A. fumigatus AF293 (FGSC A1100), *A. nidulans* (FGSC A4) and *N. crassa* (FGSC 2489) were obtained from the Fungal Genetics Stock Center. All strains were cultivated on DG18 (Oxoid) agar plates. Cultures were incubated in the dark, for 6–7 days, at 30°C (*A. nidulans* and *N. crassa*) or 37°C (*A. fumigatus*). Asexual spores (conidia) were harvested using a NaCl (0.85% w/v) and Tween-20 (0.1% w/v) sterile solution and collected after passing through three layers of miracloth. The harvested spores were washed twice with a sterile NaCl solution (0.85% w/v) and finally resuspended in the NaCl solution (0.85% w/v), to be used immediately, or in a cryoprotective saline solution containing 10% (v/v) glycerol, to be stored at -20°C or -80°C.

Growth Media

A. fumigatus and *A. nidulans* were cultivated in liquid minimal medium containing glucose (10.0 $g \cdot L^{-1}$), thiamine (0.01 $g \cdot L^{-1}$), 5 % (v/v) nitrate salts solution [$NaNO_3$ (120.0 $g \cdot L^{-1}$), KCl (10.4 $g \cdot L^{-1}$), $MgSO_4 \cdot 7H_2O$ (10.4 $g \cdot L^{-1}$) and KH_2PO_4 (30.4 $g \cdot L^{-1}$)] and 0.1% (v/v) trace elements solution [$ZnSO_4 \cdot 7H_2O$ (22.0 $g \cdot L^{-1}$), H_3BO_3 (11.0 $g \cdot L^{-1}$), $MnCl_2 \cdot 4H_2O$ (5.0 $g \cdot L^{-1}$), $FeSO_4 \cdot 7H_2O$ (5.0 $g \cdot L^{-1}$), $CoCl_2 \cdot 6H_2O$ (1.7 $g \cdot L^{-1}$), $CuSO_4 \cdot 5H_2O$ (1.6 $g \cdot L^{-1}$), $Na_2MoO_4 \cdot 2H_2O$ (1.5 $g \cdot L^{-1}$) and Na_4EDTA (50.0 $g \cdot L^{-1}$)]. The pH was adjusted to 6.5 with NaOH and the medium sterilized in an autoclave (15 minutes; 110 °C).

N. crassa was cultivated in liquid minimal medium containing K_2PO_4 (1 $g \cdot L^{-1}$) and glucose (10 $g \cdot L^{-1}$) dissolved in distilled water. The pH was adjusted to 7 with 10% phosphoric acid and the medium sterilized in an autoclave (10 minutes; 110°C). Filter sterilized salts [1% (v/v), *per* 100 mL: $NaNO_3$ (30 g), $MgSO_4.7H_2O$ (5 g), KCl (5 g), $ZnSO_4.H_2O$ (100 mg), $CuSO_4.5H_2O$ (50 mg), HCl 37% (10 µL) and $FeSO_4.7H_2O$ (100 mg)] were added after autoclaving.

Minimal inhibitory concentrations (MICs) of ionic liquids

The minimal inhibitory concentrations (MICs) were determined as described previously[31]. Final concentrations of ionic liquids in growth media ranged from 100 µM up to maximum solubility. Each liquid medium (1 mL) was inoculated with 10^6 spores and divided into four wells (0.2 mL each) of a 96 well microtiter plate. Cultures were incubated in the dark, at 30°C (*A. nidulans* and *N. crassa*) or 37°C (*A. fumigatus*) for 7 days. Fungal growth (or lack thereof) was determined at the end of incubation gauging by eye the formation of mycelium (turbidity). The lowest concentration that inhibited the formation of mycelium was defined as the MIC. Values should not be interpreted as absolute ones, but as an indication of the inhibitory and the fungicidal upper concentration limits.

Metabolite production

Fungal cultures (100 mL) were initiated from 10^6 spores *per* mL in the respective minimal medium. Liquid cultures were incubated in the dark at 30°C (*N. crassa*, *A. nidulans*) or 37°C (*A. fumigatus*) with orbital agitation of 200 rpm. After 24 hours, the ionic liquid supplement was added at 50% (i.e., 1.7 mM ChoDec for *A. fumigatus*) or 80% of the MIC (i.e., 0.96 M and 1.76 M ChoCl for *N. crassa* and *A. nidulans*, respectively, and 2.7 mM ChoDec for *A. fumigatus*); (see Results & Discussion section). Negative conditions (without ionic liquid supplement) were prepared in parallel. Cultures were grown for 10 more days under agitation (100 rpm). At the end of incubation, the media supernatants were separated from mycelia using vacuum assisted filtration with miracloth (Merck Millipore Calbiochem). *N. crassa* filtrates required the use of protease inhibitors (cOmplete™ Protease Inhibitor Cocktail, Waters) as preliminary tests showed degradation of untreated extracts (data not shown). The mycelia and filtrates were frozen immediately in liquid nitrogen and lyophilized.

Metabolite extraction

Lyophilized filtrates were homogenized in 10 mL Milli-Q water, extracted three times with ethyl acetate (1:1) and the combined ethyl acetate fractions dried under soft nitrogen flow. Peptide enrichment was achieved using the Sep-Pak plus C18 cartridge (Waters) as previously described[32]. The samples were re-dissolved in 10 mL of MeOH/H_2O (1/2, v/v) and loaded with a syringe onto a conditioned cartridge. The cartridge was washed with 10 mL of MilliQ water and 10 mL MeOH/H_2O (1/2, v/v). The retained compounds were eluted with 10 mL of MeOH to a pre-weighed glass tube and dried under soft nitrogen flow (crude extracts). Conditioning of the cartridge was done successively with 10 mL of MeOH, MilliQ water and MeOH/H_2O (1/2, v/v).

Chromatographic analysis

The crude extracts in 10% (w/v) MeOH, were chromatographically separated using a Waters Acquity chromatographer with Photodiode Array (PDA) detector, cooling auto-sampler and column oven. A Symmetry® C18 column (250 × 4.6 mm), packed with end-capped particles (5 µm, pore size 100 Å) (Waters Corporation), was used at 26 °C. Data were acquired using Empower 2 software, 2006 (Waters Corporation). Samples were injected using a 10 µL loop operated in full loop mode. The mobile phase, at a flow rate of 0.9 mL·min^{-1}, consisted of a solution of 0.1% TFA in water (v/v) (solvent A) and Acetonitrile (solvent B), set to a linear gradient of 99.5% to 0% of solvent A during 30 minutes, followed by 100% of solvent B for 10 minutes, 2 minutes to return to the initial conditions, and additional 10 minutes to re-equilibrate the column. The chromatographic profiles of the samples were obtained at the wavelength of 205 nm. Sample fractionation was performed with a Fraction collector III (Waters) connected to the Acquity chromatographer (Waters) using the same conditions described above. The collected fractions were dried under nitrogen flow and kept at 4°C (short term) or -20 °C (long term) until further analysis.

Total amino acid hydrolysis and analysis

Total hydrolysis of the crude extracts (approximately 100 µg) was performed using 6 N HCl for 24 hours at 110 °C under inert atmosphere (nitrogen flushed). The fractions were also hydrolyzed for 1 hour at 150 ºC under inert atmosphere (nitrogen/vacuum cycles) in a Workstation Pico-Tag (Waters). Hydrolyzed samples were further analyzed using the AccQ•Tag Ultra Amino Acid Analysis Method™ (eluent concentrates, derivatization kit and standard mixture of amino acid hydrolysates, Waters)[33,34]. Briefly, the hydrolyzed samples, the standards of Aib and ACC, and the standard mixture of amino acid hydrolysates were derivatized following the manufacturer's instructions. The obtained derivatives were separated on an AccQ•Tag Ultra column (100 mm x 2.1 mm, 1.7 µm) by reversed phase ultra-performance liquid chromatography (UPLC), and detected by fluorescence (FLR), according to the following details. The column heater was set at 55 °C, and the mobile phase flow rate was maintained at 0.7 $mL \cdot min^{-1}$. Eluent A was 5% AccQ•Tag Ultra concentrate solvent A and eluent B was 100% AccQ•Tag Ultra solvent B. The separation gradient was 0-0.54 minutes (99.9% A), 5.74 minutes (90.9% A), 7.74 minutes (78.8% A), 8.04 minutes (40.4% A), 8.05-8.64 minutes (10.0% A) and 8.73-10.50 minutes (99.9% A). Two microliters (2 µL) of sample were injected for analysis using a 10 µL loop. The FLR detector was set at 266 nm and 473 nm of excitation and emission wavelengths, respectively. Data were acquired using Empower 2 software, 2006 (Waters). Calibration curves of each standard were used to quantify amino acids, the values are represented as the relative % of total amount of amino acids. The total area of peaks was used to determine the overall % of identification.

Antibiotic evaluation of peptide-based metabolites

The extracts were assessed for their antimicrobial activity against gram-positive bacteria *Staphylococcus aureus* NCTC8325 and gram-negative bacteria *Escherichia coli* TOP 10, following the standard methodology implemented by the Clinical and Laboratory Standards Institute[35]. First,

bacteria were grown until approximately 1 to 2 × 10^8 CFU·mL^{-1} in Mueller Hinton Broth (MHB, Panreac). Then, two-fold serial dilutions were performed to obtain final extracts concentrations between 1000 and 62.5 µg·mL^{-1}. Plates were incubated at 37°C for 24 hours in a Bioscreen C analyzer (Oy Growth Curves Ab Ltd), taking hourly absorbance measurements (600 nm). All tests were done in triplicate; abiotic (medium alone) and biotic controls (each bacterium without extract) were included for each replicate.

After incubation with the crude extracts, 100 µl of each sample were mixed with 10 µl of 5 mg·mL^{-1} 3-(4,5-dimethylthiazol-2-yl)-2,5-diphenyl tetrazolium bromide (MTT) (Sigma Aldrich) in PBS (96-well microtiter plates) and incubated (dark, 37ºC, 30 minutes). Then, 100 µl 10% SDS in 0.01 M HCl were added to each well and plates incubated for 2 hours in the dark at room temperature. Absorbance was measured at 560 nm and 700 nm using Tecan Infinite 200 Microplate (Männedorf, Switzerland). For quantification, values at 560 nm were subtracted from the values at 700 nm. A second aliquot of 50µl was used to label the cells with propidium iodide (20 µM PI, Biotium) and SYTO9 (3 µM; Alfagene) and further incubated for 15 minutes at room temperature with agitation. Fluorescence intensity was measured with a FLUOstar OPTIMA Microplate Reader (BMG·Labtech) using a 488/20 nm excitation filter (for both SYTO9 and PI), and a 528/20 nm (SYTO9 emission wavelength) and 645/40 nm (PI emission wavelength) emission filter. The signal from the staining solution (SYTO9/PI) was subtracted from all data to minimize cross-signal background. Microscopy assessment of the live/dead staining was done on a Leica DM 6000B upright microscope equipped with an Andor iXon 885 EMCCD camera and controlled with the MetaMorph V5.8 software, using the 100x 1.4 NA oil immersion objective plus a 1.6x optovar, the fluorescence filter sets FTIC + TX2 and Contrast Phase optics. Images were analyzed by FIJI software (Fiji Is Just ImageJ). IC_{50} (half maximal inhibitory concentration of a compound) values were calculated from dose response curves constructed by plotting cell viability (MTT data) versus

extract concentration (µg·mL^{-1}) using the Logit regression model (dose effect analysis tool of XLSTAT).

LC-MS/MS analysis

NanoLC-MS/MS analysis was performed using an Eksigent Nano-LC 425 System (Eksigent, SCIEX) coupled TripleTOF® 6600+ mass spectrometer (SCIEX). Samples (<1 µg·mL^{-1}; 4 µL each) were analyzed as follows. *N. crassa* samples were loaded on a C18 PepMap trap column (5µm, 300 µm x 5mm) (Thermo Scientific) at a flow rate of 2 µL min^{-1} for 10 minutes using 2% (v/v) ACN + 0.05% (v/v) TFA as mobile phase[36]; then peptides were separated at a flow rate of 300 nL·min^{-1} into a C18 PepMap 100 column (75µm x 150mm, 3µm, 100Å) (Thermo Scientific) using a linear binary gradient of 0.1% formic acid (v/v) in water (solvent A) and 0.1% formic acid (v/v) in ACN (solvent B) for a total running time of 100 minutes. Gradient program was 3%-60% B in 60 minutes, then 40% B from 60 to 70 minutes, increasing again to 80% B to wash the column and finally re-equilibrating to the initial conditions (3% B) for 20 minutes. For *A. fumigatus* samples, the initial step of pre-concentration was the same as for *N. crassa*. Running gradient was different and adapted from Marik *et al.*[37]. Briefly, samples were separated at a flow rate of 300 nL·min^{-1} using a linear gradient of 0.05% (v/v) TFA in water (Solvent A) and 0.05% (v/v) TFA in ACN/MeOH (1:1, v/v) (solvent B). Gradient program for solvent B was 65% for 5 minutes, 65%-80% from 5 to 45 minutes, then 100% until 75 minutes and last 65% from 76 to 81 minutes. MS data was acquired in positive mode over a mass range 300-1250 m/z (for *N. crassa*) and 100-2000 m/z (for *A. fumigatus*), with 250 ms of accumulation time. The 30 most intense ions were selected to perform fragmentation with high sensitivity mode using the automatically adjusted system of rolling collision energy. MS/MS scans were acquired over a mass range 100-1500 m/z with an accumulation time set at 50 ms; raw data files.

Molecular networking and Compound dereplication on GNPS platform

Raw data files (.wiff) were converted to open format mzXML using ProteoWizard MSConvert version 3.0.10051 (http://proteowizard.sourceforge.net)[38] to transform spectra from profile to centroid mode. Data files were uploaded on GNPS through WinSCP (version 5.17.3) to generate a molecular network (http://gnps.ucsd.edu) according to guidelines[39], which can be openly accessed. To create the network, first all MS/MS spectra were aligned. Data were then filtered by removing all MS/MS peaks within +/- 17 Da of the precursor m/z. MS/MS spectra were window filtered by choosing only the top six peaks in the +/- 50 Da window throughout the spectrum. The precursor ion mass tolerance was set to 2.0 Da and a MS/MS fragment ion tolerance of 0.5 Da. A network was then created where edges were filtered to have a cosine score >0.7 and more than 6 matched peaks. Cosine score ranges from 0 (different parent ions) to 1 (structurally similar compounds)[40]. Edges between two nodes were kept in the network only if each of the nodes appeared in each other's respective top 10 most similar nodes. The maximum size of a molecular family was set to 100, and the lowest scoring edges were removed until the size was below this threshold. Self-loop nodes indicate that there is no structurally related molecule present in the sample. The spectra in the network were then searched against GNPS' spectral libraries (e.g., MassBank, ReSpect, and NIST) to assign a putative identification[41]. The library spectra were filtered in the same manner as the input data. All matches kept between network spectra and library spectra were again required to have a score >0.7 and at least 6 matched peaks. The resulting molecular network was visualized using Cytoscape software v3.7.2[42]. The molecular network is comprised by nodes (specific consensus spectrum) connected with edges (significant pairwise alignment between nodes). Nodes were labeled with putative identification and colored according to the group where the precursor was detected; edges thickness is proportional to cosine score. Complementary to library matching,

DEREPLICATOR+ workflow allow to predict fragmentation spectra *in silico* from known structures and to search for candidate structures in chemical databases[43]. MS/MS data were used as input. The output table with potential candidates was integrated into the molecular network using Cytoscape. Manual validation of putative identifications was done through removal of hits from negative mode MS (not acquired herein) or after mirror plots (library compounds *vs.* input spectra) inspection. According to Sumner et al. 2007, putative annotations of compound and molecular families based on GNPS correspond to level 2[44]. Herein, no standards were used to validate identifications. Complementary analysis of the MS spectra of the fractions was done using the NRPro database (https://web.expasy.org/) that is not represented in the GNPS databases; hits were validated (p-value<0.05) upon further inspection of the number of scored peaks *vs* annotated peaks.

Statistical analysis

Data were analyzed using standard statistical software (Origin v8.5 Software, San Diego, CA, USA, and GraphPad Software Prism v7, San Diego, CA, USA). Three biological replicates were executed. Results are expressed as mean value ± standard deviation. The statistical significance of values between conditions was evaluated by One-Way ANOVA test. Differences were considered significant when the p-value ≤ 0.05.

Results & Discussion

Ionic liquid supplements triggered a metabolic shift in the fungal cultures

It has been observed that culture conditions greatly impact secondary metabolism[45]. This explains the rationale behind the OSMAC approach to alter secondary metabolism in fungi[46], and the usage of ionic liquids supplements as well[26,28]. In the present study, two choline based ionic liquids were chosen, namely choline chloride (ChoCl) and choline decanoate (ChoDec). The first that has been previously reported to boost differential

metabolic responses in fungi[27,28]. ChoDec because longer alkyl chains in the anion have higher toxicity towards fungi, thus less quantities are needed to induce stress[31,47]. The MIC values for each fungus - *A. nidulans*, *A. fumigatus* and *N. crassa* - are listed in Table 1. Choline based ionic liquids have been shown to be biodegradable, specifically the choline cation was observed to be partially degraded after fifteen days of incubation with either *A. nidulans* and *N. crassa*[27]. The decanoate anion was herein undetectable in the medium supernatant (chromatographic analysis) after 5 days of incubation (data not shown). Similar degradation yields have been previously reported for other filamentous fungi[31,48].

Table 1 Minimal inhibitory concentrations of the cholinium-based ionic liquids (Choline chloride, ChoCl and Choline decanoate, ChoDec) used as media supplements for each fungal strain.

	ChoCl [M]	**ChoDec [mM]**
A. fumigatus	1,7	3,4
A. nidulans	2,2	2,6
N. crassa	1,2	-

Upon 10 days of incubation, fungal cultures were harvested, and the cultivation media were extracted. Secondary metabolites were enriched by liquid-liquid extraction with ethyl acetate, followed by solid-phase extraction resulting in peptide enriched fractions[32]. The metabolic footprints (i.e., pool of metabolites produced at a given point under certain culture conditions) of the crude extracts were investigated by liquid chromatography (Figure 1). *A. nidulans* and *A. fumigatus,* in contrast to *N. crassa,* show high basal diversity of metabolites. In general, the profiles are distinct in cultures grown in the supplemented media compared to the negative control (without supplementation).

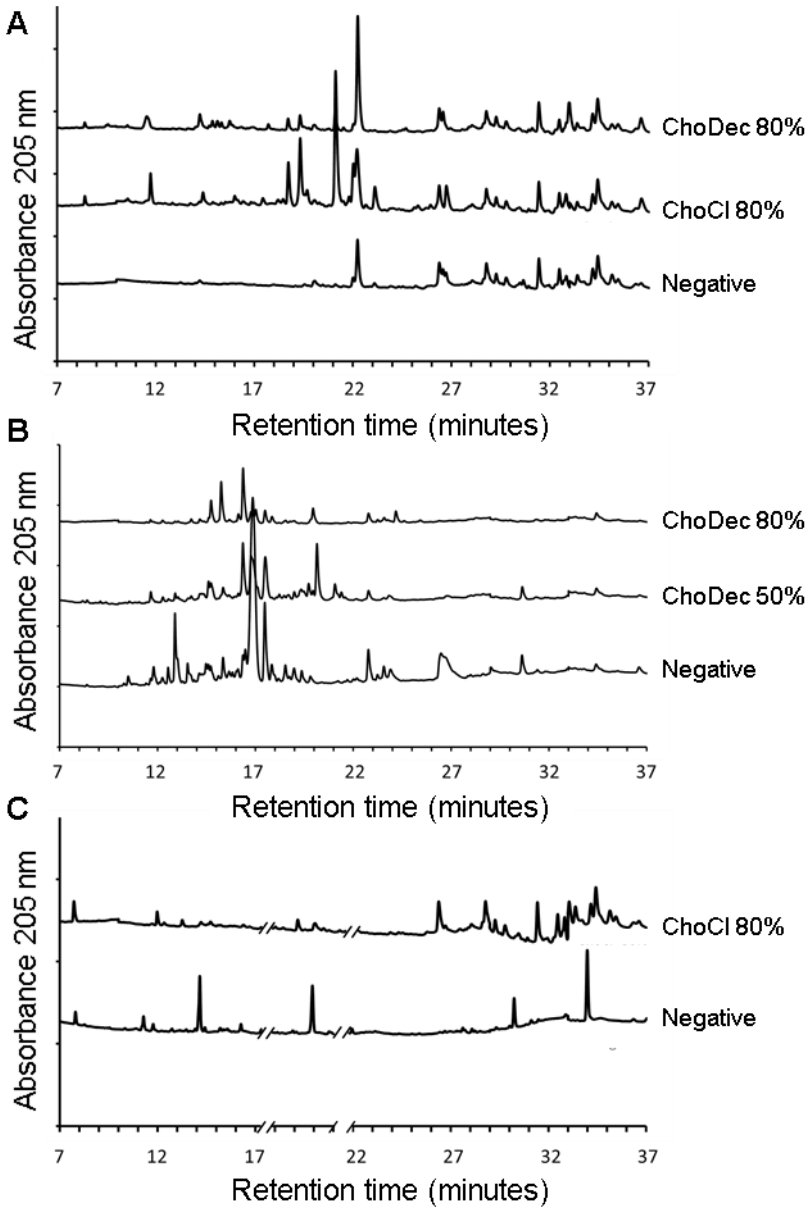

Figure 1 Ionic liquid supplements triggered a metabolic shift in the fungal cultures. Chromatographic analyses of the metabolic footprint of A. nidulans (A), A. fumigatus (B) and N. crassa (C) crude extracts. Crude extracts are from cultures grown for ten days in either choline chloride (ChoCl) or choline decanoate (ChoDec) supplemented media, at 50% or 80% of the MIC, and from cultures without ionic liquid supplementation (negative controls). Truncated parts of the chromatogram from N. crassa cultures (panel C) correspond to the elution of protease inhibitors.

The observed metabolic footprints depend on the ionic liquid supplement (Figure 1A) and of its concentration as well (*viz,* 50% and 80% of the MIC of ChoDec) (Figure 1B). This result corroborates preceding observations that distinct ionic liquids induced distinct metabolic alterations on the fungal metabolism, increasing, in general, the diversity of synthesized low molecular-weight molecules[26–28]. Using a similar approach, monodictyphenone and orsellinic acid, otherwise cryptic metabolites, accumulated (in a pool of *ca.* 40 ion masses) in cultures of *A. nidulans* grown in medium supplemented with 1-ethyl-3-methylimidazolium chloride[28]. Proteomic analyses of *A. nidulans* and *N. crassa* cultures, showed that several biological processes and pathways were affected upon supplementation with ChoCl, provoking also an accumulation of stress-responsive proteins and osmolytes[27].

Total amino acid hydrolysis discloses the presence of non-proteinogenic residues in *N. crassa* and *A. fumigatus* extracts

Fungi are able to use both proteogenic and non-proteinogenic amino acids (NPAAs) for incorporation in NRPs; NPAAs may positively impact the stability, potency, permeability, oral bioavailability, and immunogenicity of peptides as they do not occur naturally in humans[49]. In fact, an important feature of many fungal antimicrobial peptides is the presence of NPAAs or other α-hydroxy and carboxylic acids[50]. A previous study has shown that ChoCl supplementation of *N. crassa* growth medium led to the increased expression of the 1-aminocyclopropane-1-carboxylate (ACC) deaminase, which mediates the formation of ACC[27]. In some fungi, the presence of ACC has been linked to the peptaibiotics neofrapeptins and acretocins, isolated from *Geotrichum candidum* SID 22780 and *Acremonium crotocinigenum* cultures, respectively[51,52]. Peptaibiotics show a unique structure varying from 5-21 amino acid residues, including numerous NPAAs, mainly α-aminoisobutyric acid (Aib), and/or lipoamino acids[53,54]. Aib has been found to

correlate to specific types of secondary structures, namely helical structures, improving peptide functioning and increasing enzymatic resistance[55].

To verify if the ionic liquid-supplements have induced the production of peptides containing NPAAs, specifically ACC and Aib, the total amino acid content of extracts (upon hydrolysis) were chromatographically analyzed. Both NPAAs could be detected, most evident in *N. crassa* and *A. fumigatus* (Figure 2). In *N. crassa* ACC levels show an increasing trend upon ChoCl supplementation, consistent with the accumulated levels of ACC deaminase described before[27]. *A. fumigatus* control extracts show low levels of Aib with a slight, but not statistically significant, increase when the culture is supplemented with ChoDec (at 80% of MIC). In *A. nidulans*, an increasing trend in either NPAA upon ChoDec supplementation was observed, but the overall amounts of Aib and ACC are substantially lower compared to the other two fungi.

Ionic liquid-exposure altered the pattern of the overall amino acid content, suggestive of an altered peptidome profile (Table S1). Nonetheless, no meaningful alterations were found (pairwise, ANOVA) in the detected amounts of each amino acid with or without media supplementation, possibly a consequence of high variability between the biological replicates. For *A. fumigatus* around 30% and for *N. crassa* 45-65% of the peaks could not be assigned to any of the amino acid standards. For *A. nidulans*, the values were lower: 4-7 % (negative and ChoCl supplemented extracts) and 27% (ChoDec supplemented extracts). Despite these inherent technical fragilities, this analysis provides an estimation of the amino acid profiles of each sample, and excitingly point to the existence of peptides containing ACC and/or Aib in either crude extract from ionic liquid supplemented cultures. Based on these results, *N. crassa* and *A. fumigatus* extracts were selected for subsequent analyses focusing antibacterial efficacy and compositional signature (LC-MS/MS).

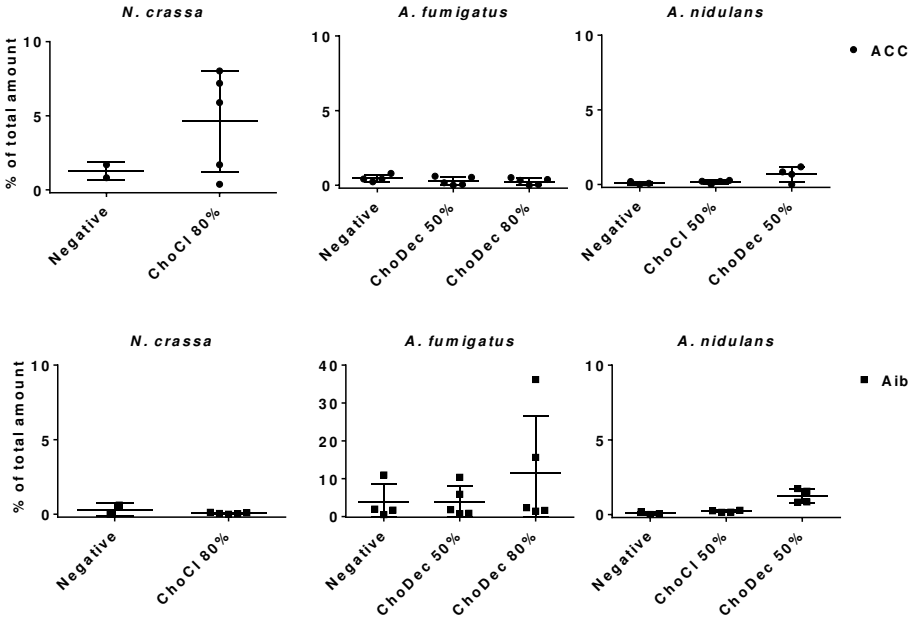

Figure 2 Total amino acid hydrolysis discloses the presence of two non-proteinogenic residues in N. crassa and A. fumigatus extracts. Scatter plot depicting individual values of percentage (%) of total amount of ACC (•) and Aib (■) obtained from total hydrolysis of the crude extracts derived from cultures grown in media with or without (negative) supplementation.

N. crassa and *A. fumigatus* crude extracts depict antibacterial activity

The antibacterial activity of *N. crassa* and *A. fumigatus* extracts against *S. aureus* and *E. coli* was assessed using the broth dilution method. For each crude extract, two-fold dilutions of an initial concentration of 1000 $\mu g \cdot mL^{-1}$ were performed. Bacterial growth, inferred by the medium turbidity (600 nm), was measured for 24 hours. Bacterial viability was evaluated via measurements of the metabolic activity (MTT) and the live/dead cell ratio obtained from fluorescent staining quantifications. After 24 hours, cell viability decreased significantly relative to the control, reflected in the MTT and live/dead cell ratio quantifications (Figure 3). Microscopic snapshots show major cell lysis upon exposure to extracts derived from ionic liquid-supplemented cultures compared to the control (no extract) (Figure 4).

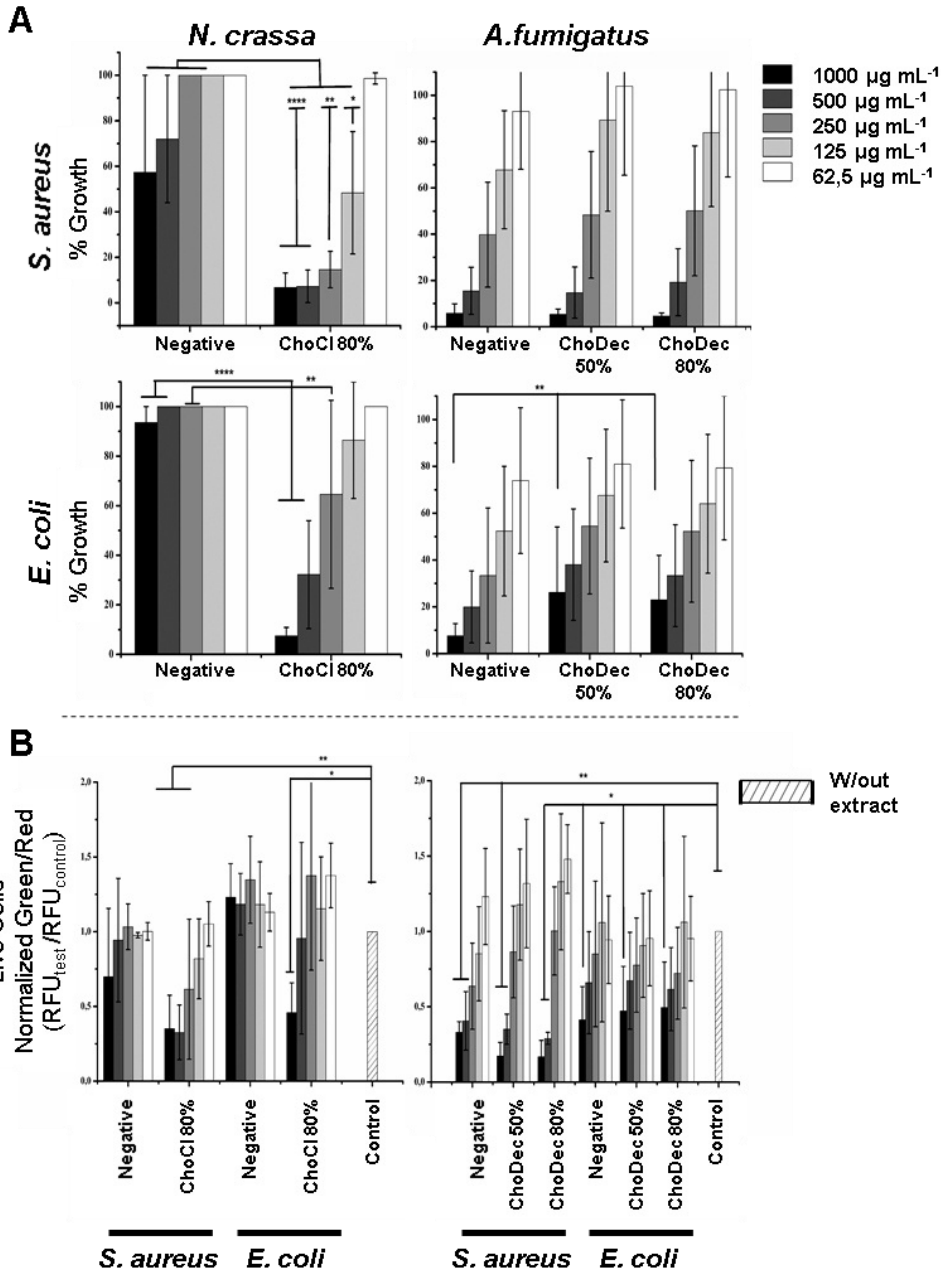

*Figure 3 N. crassa and A. fumigatus crude extracts depict antibacterial activity against S. aureus and E. coli. A) Cell viability measured by MTT assay of extracts derived from cultures grown in media with or without (negative) supplementation; B) Quantification of bacterial viability through the normalized green/red ratio (i.e. SYTO9 (green, live cells)/PI (red, dead cells) staining). Statistically significant differences are depicted; * p ≤ 0.05 ** p ≤ 0.01 *** p ≤ 0.001 **** p ≤ 0.0001.*

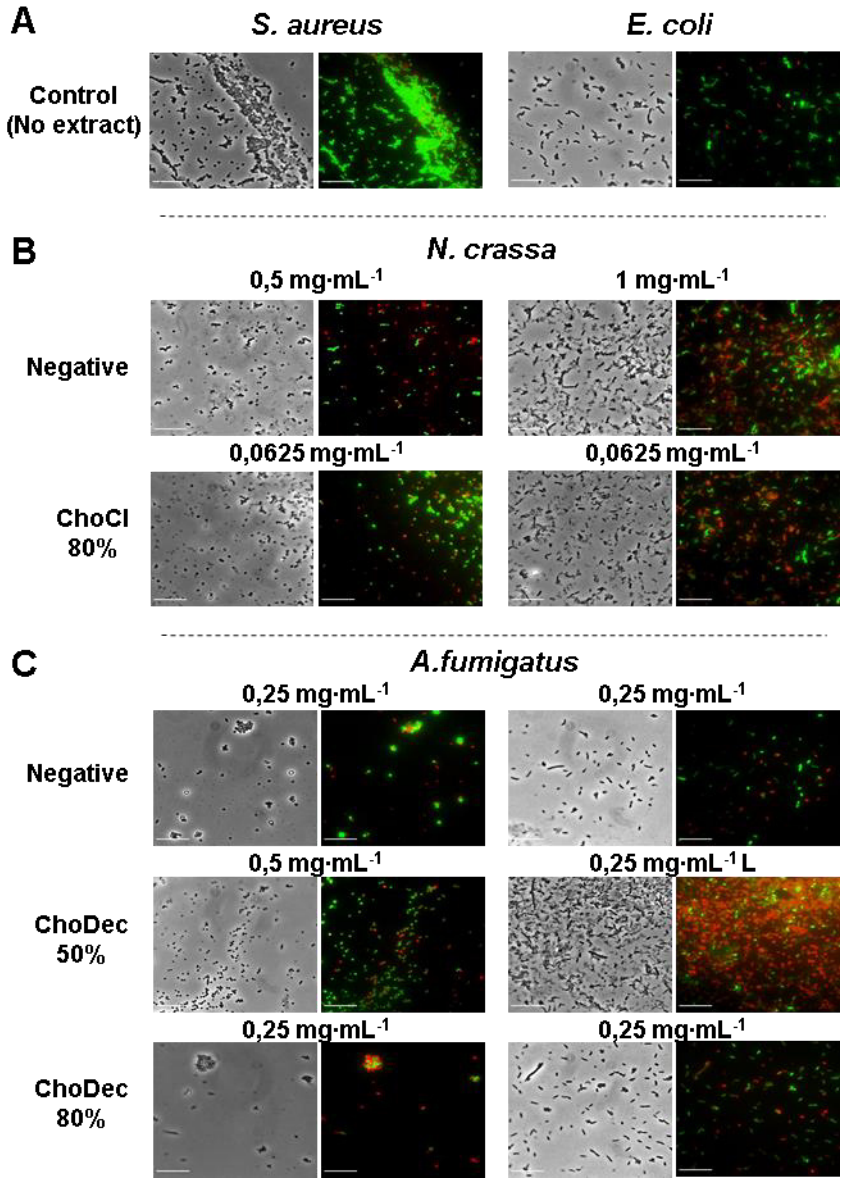

Figure 4 N. crassa and A. fumigatus crude extracts led to significant lysis of S. aureus and E. coli cells. Microscopic snapshots of E. coli and S. aureus grown in the absence of extract (A) and in the presence of crude extracts derived from cultures grown in media with or without (negative) supplementation: (B) N. crassa and (C) A. fumigatus. Images of bacteria at concentrations near the measured IC_{50} for each crude extract are shown. Cells were stained with SYTO9 (green) and PI (red) denoting live and dead cells, respectively. Scale bar, 10 µm

The IC_{50} values were calculated from MTT measurements for each extract derived from cultures supplemented or not with an ionic liquid (Table 2). All extracts from the supplemented cultures showed activity against both bacterial strains in a dose-dependent manner, more pronounced against *S. aureus* than *E. coli*. *N. crassa* extracts from ChoCl supplemented cultures depicted the highest bactericidal efficacy against either bacterium at concentrations of 125 – 250 $\mu g \cdot mL^{-1}$ (Figure 3 and Figure 4B). Their IC_{50} values are nearly five to ten-fold lower than that of the control extract (Table 2). All *A. fumigatus* extracts from the supplemented cultures showed also antibacterial activity against the two bacteria in the range of 250 – 500 $\mu g \cdot mL^{-1}$ (Figure 3 and Figure 4C). However, the control extract also showed activity, with the lowest IC_{50} values. Varying the supplement concentration did not affect the antibacterial activity levels of the derived extracts against *E. coli;* contrary to *S. aureus* where decreasing its concentration resulted in more active extracts.

Table 2 IC_{50} values determined for A. fumigatus and N. crassa crude extracts from media supplemented or not (negative control) with ChoCl or ChoDec, at 50% or 80% of the MICs. IC_{50} represents the crude extract concentration that inhibits bacterial activity by 50% and were calculated from curves constructed by plotting cell viability (MTT data) vs extract concentration ($\mu g \cdot mL^{-1}$).

Fungal Strain	Bacterial strain	Extract tested	IC_{50} ($\mu g \cdot mL^{-1}$)
N. crassa	*E. coli*	Negative	1280
		ChoCl 80%	103
	S. aureus	Negative	310
		ChoCl 80%	70
A. fumigatus	*E. coli*	Negative	120
		ChoDec 50%	310
		ChoDec 80%	350
	S. aureus	Negative	310
		ChoDec 50%	260
		ChoDec 80%	470

The results show the production of antimicrobial compounds in *N. crassa* cultures under ionic liquid supplementation, likely associated to production of metabolites otherwise cryptic. The hypothesis that these antimicrobial compounds support *N. crassa* competitiveness in specific niches deserves further consideration. However, contrary to that observed for *N. crassa*, the supplementation did not increase the antibacterial activity of *A. fumigatus* derived extracts. Regardless of these contrasting results, the chemical landscape of either extract was further analyzed using an untargeted MS metabolomics approach.

LC-MS/MS analyses of *A. fumigatus* extracts derived from ionic liquid supplemented cultures, suggests the accumulation of macrolides, among other metabolites

The MS spectra collected for the *A. fumigatus* extracts derived from the ionic liquid supplemented cultures were subjected to a molecular networking analysis on the web-based platform GNPS. This platform relies on the principle that structurally similar compounds will have similar MS/MS fragmentation patterns, and hence allows deconvolution of large MS datasets, annotation, and discovery of novel and/or analog compounds. This automated annotation belongs to a class 2 classification[44], therefore all compound identifications discussed below remain putative, requiring further validation for targeted compounds in the near future.

The metabolic footprints of *A. fumigatus* extracts grown in media supplemented with 50% (G1) or 80% (G2) of the ChoDec MIC concentration were analyzed. Of 1471 nodes, 684 nodes were clustered into 135 molecular families and the remaining 787 did not share any connection (full dataset hyperlink in Table S3). In total, 18 metabolites were putatively identified, 8 by spectral match in GNPS databases (black border nodes) and 10 by *in silico* DEREPLICATOR+ tool (red border nodes) (Figure 5B, Table S4).

Most of the nodes correspond to metabolites produced in both conditions. Only compounds with signal intensity >$1.5 \cdot 10^7$ in the total ion chromatogram (with a clear separation from baseline values) will be discussed in greater detail (Table 3, bottom panel in Figure 5B). Half of these compounds belong to the class of polyketides, some of which were found only in G2 (80% MIC). In either sample, G1 and G2, the most frequently found polyketide compounds are macrolides; a class of antibiotics composed of a large lactone ring with an attached sugar. The macrolides putatively identified were dolabelide C, efomycin G, roflamycoin, and antibiotic A 59770A. The first has been reported in a sea hare[57], while the last three are known as bacterial metabolites[58–60]. Macrolides are mostly produced by actinomycetes, but the production in fungi has been reported before; e.g. phaeospelide A in *Aspergillus oryzae*[61,62]. These extracts showed a more pronounced effect over *S. aureus* (Figure 3), consistent with the putative identification of macrolides. This class of compounds is usually bacteriostatic, most efficient against Gram-positive bacteria but can also be active against several Gram-negative bacteria[63]. In particular, efomycin is active against a number of drug-resistant pathogens (e.g. methicillin-resistant *S. aureus*)[64], and roflamycoin exerts activity against a broad spectrum of organisms[65].

Apart from macrolides, in either sample, 7α,27-dihydroxycholesterol was identified, which belongs to the terpen(oid) class. It derives from cholesterol, and has been reported before in the *A. fumigatus* metabolome[66]. It is functionally relevant, supporting the fungus to counteract the effects of antifungals targeting ergosterol[67]; therefore presenting a potential new drug target. Finally, PK-terpene hybrids[21], two pregnane glycosides specifically, were identified in either extract. They show broad spectrum activity (e.g. anticancer, analgesic, anti-inflammatory and antimicrobial) and to date only few have been reported in fungi, for example in *Aspergillus versicolor* cultures grown in rich medium for 15 days[68] and *Cladosporium* spp. grown in rice-based medium for 45 days[69]. A single peptide was putatively identified,

namely the cyclohexapeptide aeruclynamide D, a ribosomal metabolite that has been previously described in a cyanobacterium as a new antiparasitic compound[70].

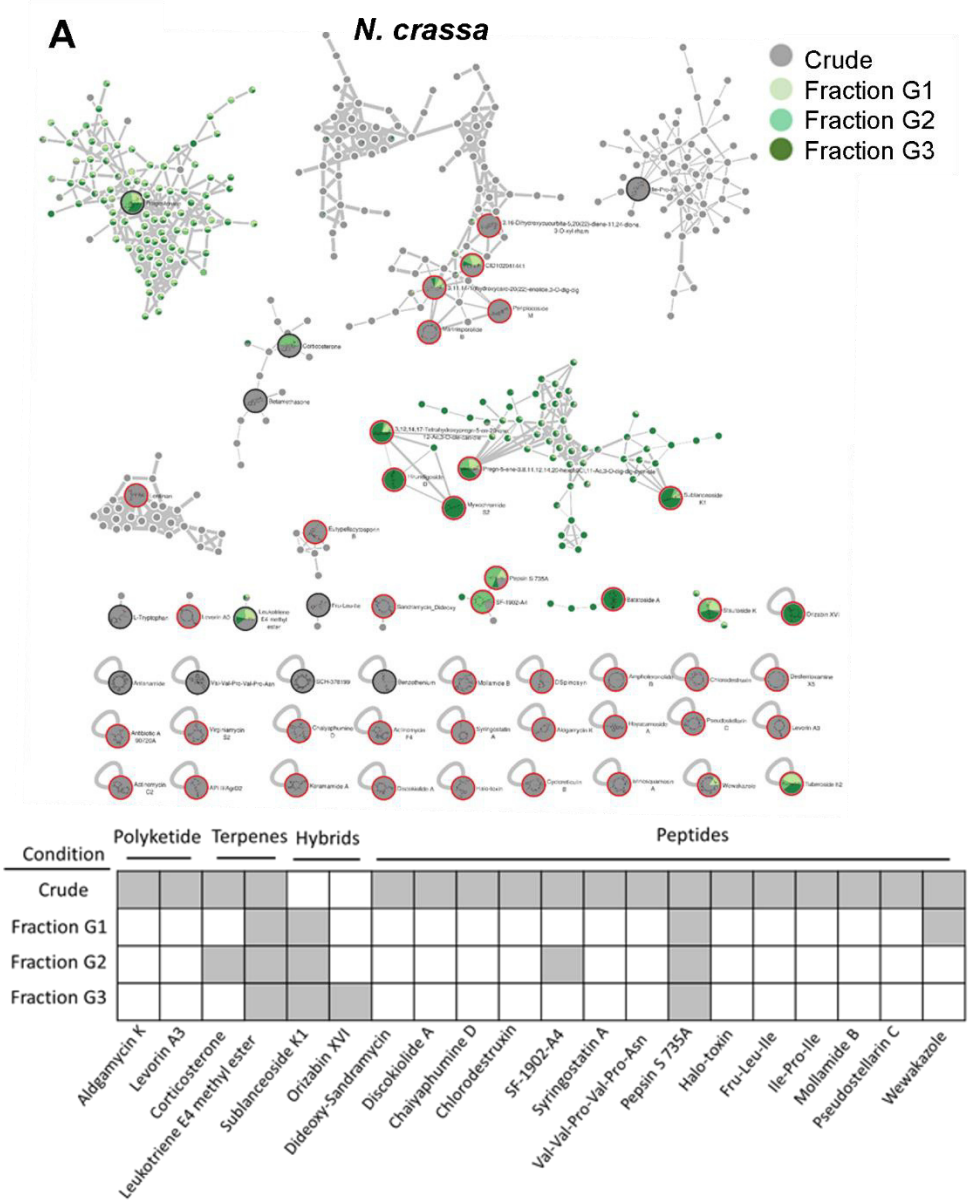

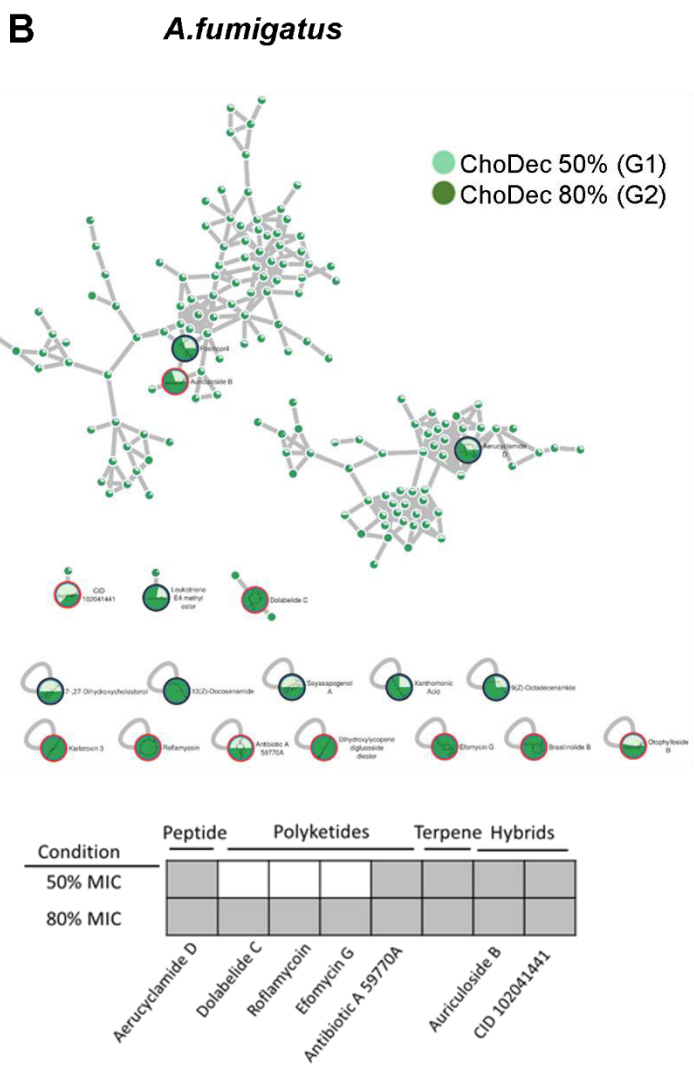

Figure 5 The molecular network generated by the GNPS tool using the MS data acquired for N. crassa and A. fumigatus extracts derived from ionic liquid supplemented cultures, considering the putatively identified compounds the accumulation, among other metabolites of macrolides and peptides, respectively. Putative identifications retrieved by using molecular networking analysis and compound dereplication in GNPS, from spectral match (*) and in silico tool DEREPLICATOR+. For N. crassa, isolated fractions (G1, G2 and G3) as well as crude (G4) extracts were analyzed, whereas for A. fumigatus, extracts from cultures supplemented with ChoDec at 50% (G1) and 80% (G2) of the MIC. Only peaks with signal intensity >1.5·107 (for A. fumigatus: G1 and G2) and >3·107 (for N. crassa: G4) in the total ion chromatogram are depicted (Full list in Table S4). For N. crassa fractions, G1 to G3, the two most intense peaks in the total ion chromatogram are depicted.

LC-MS/MS analyses of *N. crassa* extracts derived from ionic liquid supplemented cultures, suggests the accumulation of several cyclic (depsi)peptides, among other metabolites

Neurospora crassa extracts derived from ChoCl supplemented cultures were chromatographically fractionated at the retention times of 15.6, 17.3, 19.6 min, corresponding to G1, G2 and G3, respectively. The peptidome of each fraction was analyzed as previously described (including the NPAAs ACC and Aib) (Figure S1). G1 contains ACC; G2 contains Aib and ACC, and G3 contains none. Accordingly, G2 might comprise peptaibiotics. To determine the complete amino acid sequence of these fractions, Edman sequencing was attempted but failed, possibly due to a blocked N-terminal[50]. Overall, these observations further support the hypothesis that growth medium supplementation with ChoCl triggered production of peptaibiotics in *N. crassa*, otherwise cryptic.

The chemical landscape of these 3 samples and of the corresponding crude extract (G4) were analyzed, similarly to that done for *A. fumigatus*. A total of 5249 nodes were obtained, 1514 nodes clustered into 247 molecular families, and the remaining are self-loop nodes (full dataset hyperlink in Table S3). To simplify, only clusters with putative hits are shown. In total, 11 compounds were putatively identified by comparison against GNPS databases (black border nodes) and 41 compounds by using the DEREPLICATOR+ tool (red border nodes) (Figure 5A Table S4). To focus the discussion, for G4 only the compounds presenting signal intensity $>3.0 \cdot 10^7$ in the total ion chromatogram are further considered, whereas for G1-G3 the two highest intensity signals are detailed if absent in G4 (Table 3, bottom panel in Figure 5A). G4 shows, as expected, the highest diversity of compounds. Like that found in *A. fumigatus* extracts, macrolides were the only polyketide compounds identified, specifically aldgamycin K and levorin A3. A single terpene, corticosterone, and one lipid-based metabolite, leukotriene E4 methyl ester, were putatively identified as well. Leukotrienes

are eicosanoids produced by pathogenic fungi, suggested to act as virulence factors[95]. They are a subset of oxylipins, a class of metabolites that act mainly as lipid mediators, signaling spore development, metabolites production and virulence in fungi[96].

Table 3 Untargeted LC-MS/MS analyses of A. fumigatus and N. crassa extracts derived from ionic liquid supplemented cultures suggests the accumulation, among other metabolites of macrolides and peptides, respectively. Putative identifications retrieved by using molecular networking analysis and compound dereplication in GNPS, from spectral match (*) and in silico tool DEREPLICATOR+. For N. crassa, isolated fractions (G1, G2 and G3) as well as crude (G4) extracts were analyzed, whereas for A. fumigatus, extracts from cultures supplemented with ChoDec at 50% (G1) and 80% (G2) of the MIC. Only peaks with signal intensity >1.5·107 (for A. fumigatus: G1 and G2) and >3·107 (for N. crassa: G4) in the total ion chromatogram are depicted (Full list in Table S3). For N. crassa fractions, G1 to G3, the two most intense peaks in the total ion chromatogram are depicted. [G]In-house library from GNPS

Putative identification	**Exact mass**	**Condi-tion**	**Class**	**Reported activity**
Aspergillus fumigatus				
Dolabelide C[57]	796.497	G2	Macrolide	Antitumor
Roflamycoin[65,71]	738.455	G2	Macrolide	Antifungal; antiprotozoaric
Efomycin G[64,72,73]	1010.58	G2	Macrolide	Antibacterial; antitumor
Antibiotic A 59770A[58]	1000.63	G1, G2	Macrolide	Pesticidal
Aerucyclamide D*[70]	603.06	G1, G2	Cyclic peptide	Antiparasite
7α,27-Dihydroxy-cholesterol*[74]	401.342	G1, G2	Steroid	Not reported
Auriculoside B[75]	1214.64	G1, G2	Pregnane glycoside	Antitumor
CID 102041441[76]	810.477	G1, G2	Pregnane glycoside	Not reported

Neurospora crassa				
Levorin A3[77,78]	1092.58	G4	Macrolide	Antifungal
Dideoxy-Sandramycin[79]	1188.56	G4	Cyclic depsipeptide	Antitumor
Discokiolide A[80]	1026.51		Cyclic depsipeptide	Antitumor
Chaiyaphumine D[81]	644.296	G4	Cyclic depsipeptide	Not reported
Chlorodestruxin[82]	629.319	G4	Cyclic depsipeptide	Anti-insecticidal
SF-1902-A4	667.452	G2, G4	Cyclic lipo-depsipeptide	Antibacterial
Syringostatin A[83]	1178.59	G4	Cyclic lipo-depsipeptide	Antifungal
Val-Val-Pro-Val-Pro-Asn*[G]	651.396	G4	Peptide	Not reported
Pepsin S 735A[84,85]	685.463	G1-G4	Peptide	Protease inhibitor
Halo-toxin[86]	626.343	G4	Peptide	Not reported
Fru-Leu-Ile*[G]	407.239		Peptide	Not reported
Ile-Pro-Ile*[G]	342.239	G4	Peptide	Not reported
Mollamide B[87]	696.367	G4	Cyclic peptide	Antimalarial, antivirus, antitumor
Pseudostellarin C[88]	812.443	G4	Cyclic peptide	Tyrosinase inhibitor; antitumor
Wewakazole[89,90]	1140.54	G1, G4	Cyclic peptide	Antitumor
Corticosterone*[91]	347.222	G2, G4	Terpene	Not reported
Leukotriene E4 methyl ester*[92]	459.22	G1-G4	Lipid	Immuno-modulation
Orizabin XIV[93]	1120.6	G3	Glycolipid	Antitumor, antibacterial
Sublanceoside K1[94]	1082.57	G1-G3	Terpene glycoside	Not reported

Remarkably, *N. crassa* seems to be an abundant producer of NRPs, including peptides (linear and cyclic, 7 distinct compounds) and depsipeptides (5 distinct compounds) when grown in medium supplemented with ChoCl. Specifically, two cyclic peptides were identified: pseudostellarin C and mollamide B, and five linear peptides: pepsin S 735A, halo-toxin, two peptide fragments (Fru-Leu-Ile and Ile-Pro-Ile) and one hexapeptide (Val-Val-Pro-Val-Pro-Asn). Pepsin is the only linear peptide identified in all samples, possibly an artefact of the protease inhibitors herein used. The tri/hexapeptides identified here have never been reported before, questioning if these compounds are hydrolyzed products or are precursors of larger peptides. Besides, four cyclic depsipeptides were also putatively identified: discokiolide A, dideoxy-sandramycin, chlorodestruxin and chaiyaphumine D, all of which, except the last, have been reported before and related to either antitumor or anti-insecticidal activities. Syringostatin A, a lipodepsinonapeptide, has reported antifungal activity[83]. In cyclic depsipeptides at least one amino acid is replaced by a hydroxylated carboxylic acid (α-hydroxy acid), resulting in a mix of amide and ester bonds in the core ring, conferring high stability (X. Wang et al. 2018; Taevernier et al. 2017). α-Hydroxy acids structural similarity to α-amino acids, ensures that depsipeptides can interact with numerous proteins yet showing higher resistance against hydrolyzing enzymes due to cyclization[97,98]. The higher resistance is expected to result in enhanced oral bioavailability (Sivanathan and Scherkenbeck 2014). Several known depsipeptides contain NPAAs, for example 2-hydroxy-3-methyl-pentanoic acid, tiglic acid, α-aminobutyric acid, picolinic acid; constituents of compounds putatively identified in the extracts yet below the defined threshold of peak intensity, e.g., SCH-378199 and virginiamycin S5 (Table S4). This observation is consistent with the presence of many non-identified amino acids in the *N. crassa* extracts (nearly half of the chromatographic peak area could not be assigned, Table S1). The presence of Aib in this class of compounds remains to be seen. On the

contrary, ACC is known to be a building block of depsipeptides, for example of BZR-cotoxin II, a metabolite of *Bipolaris zeicola*, and of CBS 154-94A, a metabolite of *Streptomyces* spp[52]. The last has antibiotic activity, acting as protein farnesyl transferase inhibitor. Finally, the cyclic lipodepsipeptide SF-1902-A4 was also identified (present also in G2); previously reported to be antibacterial[99]. As above mentioned, most compounds were only found in the crude extract, except in the denoted cases. Looking at the two most intense peaks of G1-G3 fractions revealed the presence of wewakazole (G1, also in G4 but below the defined intensity threshold), orizabin XIV (G3), and sublanceoside K1 (in all fractions). The first compound, a cyclic dodecapeptide, has been reported to exhibit cytotoxicity against H460 human lung cancer cell line[90]. The second is a glycolipid that inhibits the activity of 1,3-β-glucan synthase, required for cell wall synthesis in fungi[100]; a target of clinically approved antifungal drugs[101]. The last, a terpene glucoside, has no reported bioactivity to date. Apart from these compounds, the remaining hits correspond to clusters containing spectra from all samples (G1 to G3), and include compounds belonging to resin glycosides, fatty acids, terpenoids and cyclic peptides. The chromatographic elution of the fractions (with close retention times) did not result in a clean separation, explaining why these clustered together in the molecular network. Since the NRPro database (https://web.expasy.org/) that is specific for NRPs is not included in the GNPS platform, the MS spectra of the fractions were also queried in this database. Putative identifications were found only for G1 and G2 (Table S5) revealing five additional cyclic peptide candidates. Specifically, G1 showed matches to guangomide A (depsipeptide), arbumelin and a cyclohexapeptide. The first two compounds have been previously identified in fungal strains, namely in *Trichothecium sympodiale*[102] and *Calcarisporium arbuscular* (upon target inactivation of H3 deacetylase)[103], respectively. In G2, cyclotheonamide E3 and nostophycin were found, compounds identified before in a marine sponge[104] and in a

cyanobacterium[105], respectively. In addition, the fractions were analyzed by NMR but their chemical complexity and low abundance of each constituent of the mixture hindered stringent spectral assignments (data not shown).

Conclusions & Future perspectives

The aim of this study was to examine if ionic liquids supplements, specifically choline-based ones, can support discovery of bioactive secondary metabolites in three distinct fungi – *N. crassa, A. nidulans* and *A. fumigatus*. The usage of ionic liquid-based supplements has been shown before to greatly impact fungal metabolism, leading to upregulation of the expression of genes coding in secondary metabolism, including some backbone genes, and altering the ensuing extracellular metabolic footprint. Building on this past evidence, choline-based ionic liquids were used as growth media supplements (at concentrations below their MIC, Table 1), testing different anions and concentrations as well. In either fungus, the media supplementation altered the diversity of compounds accumulating extracellularly (Figure 1). The peptidome composition of the obtained crude extracts (inferred by the abundance/diversity of amino acids in the corresponding hydrolysates) was also impacted by the supplementation (Table S1). Specifically, ACC and Aib levels showed an increasing trend in *N. crassa* and *A. fumigatus*, respectively (Figure 2). Moreover, these metabolite extracts reduced the metabolic activity of bacterial cells, in some cases leading to cell lysis (Figure 3 and 4). Based on the estimated IC_{50} values (Table 2), the supplementation compared to control conditions, greatly increased the bactericidal activity of the *N. crassa* extracts, but not of the *A. fumigatus* extracts. At this stage, the observed activity cannot be linked to a specific compound. To pinpoint potential candidates, untargeted MS analyses using the GNPS platform were applied. A total of 52 and 18 compounds were identified in *N. crassa* and *A. fumigatus* extracts derived from the ionic-liquid supplemented cultures, respectively (Figure 5, Table S4). By eliminating compounds of low signal intensity, the most

promising candidates potentially produced by *A. fumigatus* are macrolides and terpenes and by *N. crassa* cyclic peptides, including five depsipeptides; which are structurally of high pharmacological interest (Table 3). Fractionation of the *N. crassa* extract added another cyclic peptide to the pool of compounds annotated through the GNPS tool, likely of low abundance in the crude extract. Analysis of their whole chemical landscape highlighted, however, a weak sample deconvolution with many compounds present in the three fractions. Through direct query of intense spectra in the NRPro database, five additional hits of cyclic peptides (including one depsipeptide) were found (Table S5).

The usage of GNPS as a dereplication strategy clearly showed that a rich diversity of structures can be generated under an ionic liquid stimulus. It allowed for a rapid comparison of the collected MS data, to obtain a "holistic" view of the chemical space of the fungal extracts, getting one step closer to the identification of novel bioactive metabolites. Its effectiveness can be illustrated by two related examples: diversity of secondary metabolites in *Botryosphaeria mamani* upon medium supplementation with histone deacetylase inhibitors[106], and in *Penicillium nordicum*, which, completed with isotope labelling analyses, led to the identification of 69 unknown metabolites[107]. The tool is subject to the availability of similar structures in the GNPS databases (as highlighted by additional identifications in the fractions when using NRPro); all the identifications proposed herein remain putative and further confirmation is therefore required. Database search tools, e.g., Mascot, usually used for the MS/MS identification of linear peptides are not directly applicable to cyclopeptides or depsipeptides that generate very complex fragmentation patterns. In addition, >300 NPAAs can be incorporated into fungal NRPs, further enlarging the associated chemical space. None of the compounds putatively identified (Table S4 and S5) contain either ACC or Aib, irrespectively of their detection in the hydrolysates of the crude extracts/fractions. This is likely due to the lack of similar

structures in the GNPS and NRPro databases. Besides, it reveals that the chemical space of either extract remains to be fully disclosed. Despite these limitations, specifically the GNPS tool exposed the most promising candidates - cyclic (depsi)peptides of *N. crassa*, setting foundations for their isolation and identification in the near future.

The data obtained highlight the capacity of *N. crassa* to generate a rich portfolio of cyclic peptide-based metabolites, with high pharmacological interest. In the genome of *N. crassa*, only four putative NRPS genes have been assigned, none however has been linked to the produced metabolite to date. Preliminary tests suggest that three of these genes were upregulated in the supplemented medium compared to the control (data not shown). Due to the scarcity of NRPS genes in the *N. crassa* genome, ionic-liquid supplementation shows matchless potential to link each NRPS to its peptide-product(s), deserving a focused analysis soon.

Acknowledgments

MR, PS and IM are grateful to FCT for the fellowship PD/BD/113989/2015, PD/BD/135481/2018 and for the working contract financed by national funds under Norma Transitória D.L. no. 57/2016, respectively. The authors acknowledge the use of microscope at the Bacterial Imaging Cluster (ITQB-NOVA). The authors are thankful to Pedro Lamosa and Maria C. Leitão (ITQB NOVA) for support with the NMR and chromatographic analyses, respectively. Finally, the authors acknowledge Paula Alves (ITQB alumni) for collection of preliminary data that inspired this study.

References

1. Global antimicrobial resistance and use surveillance system (GLASS) report 2021. *World Health Organization.* 180 (2021). Available at: https://www.who.int/publications/i/item/9789240027336. (Accessed: 20th March 2022)
2. Meyer, V. *et al.* Current challenges of research on filamentous fungi in

relation to human welfare and a sustainable bio-economy: a white paper. *Fungal Biol. Biotechnol.* **3**, 6 (2016).

3. Newman, D. J. & Cragg, G. M. Natural Products as Sources of New Drugs over the Nearly Four Decades from 01/1981 to 09/2019. *Journal of Natural Products* **83**, 770–803 (2020).
4. Brakhage, A. A. Regulation of fungal secondary metabolism. *Nat. Rev. Microbiol.* **11**, 21–32 (2013).
5. Fox, E. M. & Howlett, B. J. Secondary metabolism: regulation and role in fungal biology. *Curr. Opin. Microbiol.* **11**, 481–487 (2008).
6. Netzker, T. *et al.* Microbial communication leading to the activation of silent fungal secondary metabolite gene clusters. *Front. Microbiol.* **6**, 1–13 (2015).
7. Rodrigues, A. G. Secondary Metabolism and Antimicrobial Metabolites of Aspergillus. in *New and Future Developments in Microbial Biotechnology and Bioengineering: Aspergillus System Properties and Applications* (2016). doi:10.1016/B978-0-444-63505-1.00006-3
8. Calvo, A. M., Wilson, R. A., Bok, J. W. & Keller, N. P. Relationship between Secondary Metabolism and Fungal Development. *Microbiol. Mol. Biol. Rev.* **66**, 447–459 (2002).
9. Macheleidt, J. *et al.* Regulation and Role of Fungal Secondary Metabolites. *Annu. Rev. Genet.* **50**, 371–392 (2016).
10. Khaldi, N. *et al.* SMURF: Genomic mapping of fungal secondary metabolite clusters. *Fungal Genet. Biol.* **47**, 736–741 (2010).
11. Pusztahelyi, T., Holb, I. J. & PÃ³csi, I. Secondary metabolites in fungus-plant interactions. *Front. Plant Sci.* **6**, (2015).
12. Bills, G. F. & Gloer, J. B. Biologically Active Secondary Metabolites from the Fungi. *Microbiol. Spectr.* **4**, (2016).
13. Hertweck, C. The Biosynthetic Logic of Polyketide Diversity. *Angew. Chemie Int. Ed.* **48**, 4688–4716 (2009).

14. Maddah, F. El, Nazir, M. & König, G. M. The Rare Amino Acid Building Block 3-(3-furyl)-Alanine in the Formation of Non-ribosomal Peptides. *Nat. Prod. Commun.* **12**, 147–150 (2017).
15. Keller, N. P., Turner, G. & Bennett, J. W. Fungal Secondary Metabolism - From Biochemistry to Genomics. *Nat. Rev. Microbiol.* **3**, 937–947 (2005).
16. McErlean, M., Overbay, J. & Van Lanen, S. Refining and expanding nonribosomal peptide synthetase function and mechanism. *J. Ind. Microbiol. Biotechnol.* **46**, 493–513 (2019).
17. Bhattarai, K., Kabir, M. E., Bastola, R. & Baral, B. Fungal natural products galaxy: Biochemistry and molecular genetics toward blockbuster drugs discovery. in *Advances in Genetics* **107**, 193–284 (Academic Press, 2021).
18. Cacho, R. A., Chooi, Y.-H., Zhou, H. & Tang, Y. Complexity Generation in Fungal Polyketide Biosynthesis: A Spirocycle-Forming P450 in the Concise Pathway to the Antifungal Drug Griseofulvin. *ACS Chem. Biol.* **8**, 2322–2330 (2013).
19. Cacho, R. A., Jiang, W., Chooi, Y.-H., Walsh, C. T. & Tang, Y. Identification and Characterization of the Echinocandin B Biosynthetic Gene Cluster from Emericella rugulosa NRRL 11440. *J. Am. Chem. Soc.* **134**, 16781–16790 (2012).
20. Lin, H. C. *et al.* The fumagillin biosynthetic gene cluster in Aspergillus fumigatus encodes a cryptic terpene cyclase involved in the formation of β-trans-bergamotene. *J. Am. Chem. Soc.* **135**, 4616–4619 (2013).
21. Keller, N. P. Fungal secondary metabolism: regulation, function and drug discovery. *Nat. Rev. Microbiol.* **17**, 167–180 (2019).
22. Bergmann, S. *et al.* Genomics-driven discovery of PKS-NRPS hybrid metabolites from Aspergillus nidulans. *Nat. Chem. Biol.* **3**, 213–217 (2007).
23. Begani, J., Lakhani, J. & Harwani, D. Current strategies to induce

secondary metabolites from microbial biosynthetic cryptic gene clusters. *Ann. Microbiol.* **68**, 419–432 (2018).

24. Liu, Z., Zhao, Y., Huang, C. & Luo, Y. Recent Advances in Silent Gene Cluster Activation in Streptomyces. *Front. Bioeng. Biotechnol.* **9**, 88 (2021).
25. Bode, H. B., Bethe, B., Höfs, R. & Zeeck, A. Big Effects from Small Changes: Possible Ways to Explore Nature's Chemical Diversity. *ChemBioChem* **3**, 619 (2002).
26. Petkovic, M. *et al.* Exploring fungal activity in the presence of ionic liquids. *Green Chem.* **11**, 889 (2009).
27. Martins, I. *et al.* Proteomic alterations induced by ionic liquids in Aspergillus nidulans and Neurospora crassa. *J. Proteomics* **94**, 262–278 (2013).
28. Alves, P. C. *et al.* Transcriptomic and metabolomic profiling of ionic liquid stimuli unveils enhanced secondary metabolism in Aspergillus nidulans. *BMC Genomics* **17**, 284 (2016).
29. Hartmann, D. O., Piontkivska, D., Moreira, C. J. S. & Silva Pereira, C. Ionic Liquids Chemical Stress Triggers Sphingoid Base Accumulation in Aspergillus nidulans. *Front. Microbiol.* **10**, (2019).
30. Petkovic, M. *et al.* Novel biocompatible cholinium-based ionic liquids—toxicity and biodegradability. *Green Chem.* **12**, 643 (2010).
31. Petkovic, M. *et al.* Novel biocompatible cholinium-based ionic liquids - Toxicity and biodegradability. *Green Chem.* **12**, 643–649 (2010).
32. Krause, C., Kirschbaum, J. & Brückner, H. Peptaibiomics: An advanced, rapid and selective analysis of peptaibiotics/peptaibols by SPE/LC-ES-MS. *Amino Acids* **30**, 435–443 (2006).
33. Armenta, J. M. *et al.* Sensitive and Rapid Method for Amino Acid Quantitation in Malaria Biological Samples Using AccQ•Tag Ultra Performance Liquid Chromatography-Electrospray Ionization-MS/MS with Multiple Reaction Monitoring. *Anal. Chem.* **82**, 548–558 (2010).

34. Penrose, D. M., Moffatt, B. A. & Glick, B. R. Determination of 1-aminocycopropane-1-carboxylic acid (ACC) to assess the effects of ACC deaminase-containing bacteria on roots of canola seedlings. *Can. J. Microbiol.* **47**, 77–80 (2001).
35. Wayne, P. CLSI. Performance Standards for Antimicrobial Susceptibility Testing. 28th ed. CLSI. in *Performance Standards for Antimicrobial susceptibility Testing* (2018).
36. Ribeiro, D. M. *et al.* The effects of improving low dietary protein utilization on the proteome of lamb tissues. *J. Proteomics* **223**, 103798 (2020).
37. Marik, T. *et al.* New 19-residue peptaibols from trichoderma clade viride. *Microorganisms* **6**, (2018).
38. Kessner, D., Chambers, M., Burke, R., Agus, D. & Mallick, P. ProteoWizard: Open source software for rapid proteomics tools development. *Bioinformatics* **24**, 2534–2536 (2008).
39. Aron, A. T. *et al.* Reproducible molecular networking of untargeted mass spectrometry data using GNPS. *Nat. Protoc.* **15**, 1954–1991 (2020).
40. Watrous, J. *et al.* Mass spectral molecular networking of living microbial colonies. *Proc. Natl. Acad. Sci. U. S. A.* **109**, 10150 (2012).
41. Wang, M. *et al.* Sharing and community curation of mass spectrometry data with Global Natural Products Social Molecular Networking. *Nature Biotechnology* **34**, 828–837 (2016).
42. Shannon, P. *et al.* Cytoscape: A software Environment for integrated models of biomolecular interaction networks. *Genome Res.* **13**, 2498–2504 (2003).
43. Mohimani, H. *et al.* Dereplication of microbial metabolites through database search of mass spectra. *Nat. Commun. 2018 91* **9**, 1–12 (2018).
44. Sumner, L. W. *et al.* Proposed minimum reporting standards for

chemical analysis: Chemical Analysis Working Group (CAWG) Metabolomics Standards Initiative (MSI). *Metabolomics* **3**, 211–221 (2007).

45. Mathew Valayil, J. Activation of Microbial Silent Gene Clusters: Genomics Driven Drug Discovery Approaches. *Biochem. Anal. Biochem.* **5**, 2–5 (2016).
46. Chiang, Y.-M., Lee, K.-H., F.Sanchez, J., Keller, N. P. & Wang, C. C. C. Unlocking Fungal Cryptic Natural Produts. *Nat. Prod. Commun.* **11**, 1505–1510 (2009).
47. Hartmann, D. O. *et al.* Plasma membrane permeabilisation by ionic liquids: a matter of charge. *Green Chem.* **17**, 4587–4598 (2015).
48. Boethling, R. S., Sommer, E. & DiFiore, D. Designing Small Molecules for Biodegradability. *Chem. Rev.* **107**, 2207–2227 (2007).
49. Ding, Y. *et al.* Impact of non-proteinogenic amino acids in the discovery and development of peptide therapeutics. *Amino Acids* **52**, 1207–1226 (2020).
50. Mootz, H. D., Schwarzer, D. & Marahiel, M. A. Ways of Assembling Complex Natural Products on Modular Nonribosomal Peptide Synthetases. *ChemBioChem* **3**, 490–504 (2002).
51. Brückner, H., Fox, S. & Degenkolb, T. Sequences of Acretocins, Peptaibiotics Containing the Rare 1-Aminocyclopropanecarboxylic Acid, from Acremonium crotocinigenum CBS 217.70. *Chem. Biodivers.* **16**, e1900276 (2019).
52. Fredenhagen, A., Molleyres, L.-P., Böhlendorf, B. & Laue, G. Structure Determination of Neoefrapeptins A to N:Peptides with Insecticidal Activity Produced bythe Fungus Geotrichum candidum. *J. Antibiot.* **59**, 267–280 (2006).
53. Degenkolb, T., Berg, A., Gams, W., Schlegel, B. & Gräfe, U. The occurrence of peptaibols and structurally related peptaibiotics in fungi and their mass spectrometric identification via diagnostic fragment

ions. *J. Pept. Sci.* **9**, 666–678 (2003).

54. Degenkolb, T. & Brückner, H. Peptaibiomics: towards a myriad of bioactive peptides containing C(alpha)-dialkylamino acids? *Chem. Biodivers.* **5**, 1817–1843 (2008).
55. Niu, X., Thaochan, N. & Hu, Q. Diversity of linear non-ribosomal peptide in biocontrol fungi. *J. Fungi* **6**, 61 (2020).
57. Suenaga, K., Nagoya, T., Shibata, T., Kigoshi, H. & Yamada, K. Dolabelides C and D, cytotoxic macrolides isolated from the sea hare Dolabella auricularia. *J. Nat. Prod.* **60**, 155–157 (1997).
58. Hoehn, M. M., Michel, K. H. & Yao, R. C.-F. Europaisches Patentamt European Patent Office. (1990).
59. Klassen, J. L., Lee, S. R., Poulsen, M., Beemelmanns, C. & Kim, K. H. Efomycins K and L from a termite-associated Streptomyces sp. M56 and their putative biosynthetic origin. *Front. Microbiol.* **10**, 1739 (2019).
60. Schlegel, R., Thrum, H., Zielinski, J. & Borowski, E. The structure of roflamycoin, a new polyene macrolide antifungal antibiotic. *J. Antibiot. (Tokyo).* **34**, 122–123 (1981).
61. Katz, L. & Mankin, A. S. Macrolides. in *Encyclopedia of Microbiology* 529–558 (Academic Press, 2009). doi:10.1016/B978-012373944-5.00041-9
62. Morishita, Y., Zhang, H., Taniguchi, T., Mori, K. & Asai, T. The Discovery of Fungal Polyene Macrolides via a Postgenomic Approach Reveals a Polyketide Macrocyclization by trans-Acting Thioesterase in Fungi. *Org. Lett.* **21**, 4788–4792 (2019).
63. Arslan, I. Trends in Antimicrobial Resistance in Healthcare-Associated Infections: A Global Concern. in *Encyclopedia of Infection and Immunity* 652–661 (Elsevier, 2022). doi:10.1016/b978-0-12-818731-9.00111-7
64. Wu, C. *et al.* Identification of elaiophylin derivatives from the marine-

derived actinomycete Streptomyces sp. 7-145 using PCR-based screening. *J. Nat. Prod.* **76**, 2153–2157 (2013).

65. Han, X. *et al.* Identification and Predictions Regarding the Biosynthesis Pathway of Polyene Macrolides Produced by Streptomyces roseoflavus Men-myco-93-63. *Appl. Environ. Microbiol.* **87**, 1–13 (2021).
66. Gil-De-la-fuente, A. *et al.* Aspergillus metabolome database for mass spectrometry metabolomics. *J. Fungi* **7**, 387 (2021).
67. Xiong, Q. *et al.* Cholesterol import by Aspergillus fumigatus and its influence on antifungal potency of sterol biosynthesis inhibitors. *Antimicrob. Agents Chemother.* **49**, 518–524 (2005).
68. Ding, J. H. *et al.* A new pregnane steroid from cultures of Aspergillus versicolor. *Nat. Prod. Res.* **33**, 1885–1890 (2019).
69. Yu, M. L., Guan, F. F., Cao, F., Jia, Y. L. & Wang, C. Y. A new antiviral pregnane from a gorgonian-derived Cladosporium sp. fungus. *Nat. Prod. Res.* **32**, 1260–1266 (2018).
70. Portmann, C. *et al.* Isolation of aerucyclamides C and D and structure revision of microcyclamide 7806A: Heterocyclic ribosomal peptides from Microcystis aeruginosa PCC 7806 and their antiparasite evaluation. *J. Nat. Prod.* **71**, 1891–1896 (2008).
71. Schlegel, R. & Thrum, H. A new polyene antibiotic, flavomycoin structural investigations. I. *J. Antibiot. (Tokyo).* **24**, 360–367 (1971).
72. Supong, K. *et al.* Antimicrobial compounds from endophytic Streptomyces sp. BCC72023 isolated from rice (Oryza sativa L.). *Res. Microbiol.* **167**, 290–298 (2016).
73. Gui, M., Zhang, M. xue, Wu, W. hui & Sun, P. Natural occurrence, bioactivity and biosynthesis of elaiophylin analogues. *Molecules* **24**, 3840 (2019).
74. Brown, A. J. & Jessup, W. Oxysterols and atherosclerosis. *Atherosclerosis* **142**, 1–28 (1999).

75. Teng, H. L., Lu, Y., Li, J., Yang, G. Z. & Mei, Z. N. Two new steroidal glycosides from the root of Cynanchum auriculatum. *Chinese Chem. Lett.* **22**, 77–80 (2011).
76. Deng, Y. R., Wei, Y. P., Yin, F., Yang, H. & Wang, Y. A new cardenolide and two new pregnane glycosides from the root barks of Periploca sepium. *Helv. Chim. Acta* **93**, 1602–1609 (2010).
77. Pawlak, J., Sowinski, P., Bieszczad, T. & Borowski, E. Structure of Levorin A3, a Minor Component of Levorin Complex. *ChemInform* **37**, 1667–1672 (2006).
78. Szczeblewski, P. *et al.* Analytical studies on ascosin, candicidin and levorin multicomponent antifungal antibiotic complexes. the stereostructure of ascosin A2. *Sci. Rep.* **7**, 40158 (2017).
79. Boger, D. L. & Chen, J. H. An exceptionally potent analog of sandramycin. *Bioorganic Med. Chem. Lett.* **7**, 919–922 (1997).
80. Tada, H., Tozyo, T., Terui, Y. & Hayashi, F. Discokiolides. Cytotoxic Cyclic Depsipeptides from the Marine Sponge Discodermia kiiensis. *Chem. Lett.* **21**, 431–434 (1992).
81. Grundmann, F. *et al.* Antiparasitic chaiyaphumines from entomopathogenic xenorhabdus sp. PB61.4. *J. Nat. Prod.* **77**, 779–783 (2014).
82. Gupta, S., Roberts, D. W. & Renwick, J. A. A. Insecticidal cyclodepsipeptides from Metarhizium anisopliae. *J. Chem. Soc. Perkin Trans. 1* 2347–2357 (1989). doi:10.1039/p19890002347
83. Sorensen, K. N., Kim, K. H. & Takemoto, J. Y. In vitro antifungal and fungicidal activities and erythrocyte toxicities of cyclic lipodepsinonapeptides produced by Pseudomonas syringae pv. syringae? *Antimicrob. Agents Chemother.* **40**, 2710–2713 (1996).
84. Morishima, H., Takita, T., Aoyagi, T., Takeuchi, T. & Umezawa, H. The structure of pepstatin. *J. Antibiot. (Tokyo).* **23**, 263–265 (1970).
85. Omura, S. *et al.* Ahpatinins, new acid protease inhibitors containing 4-

amino-3-hydroxy-5-phenylpentanoic acid. *J. Antibiot. (Tokyo).* **39**, 1079–1085 (1986).

86. Kajimoto, T. *et al.* Structure of Halo-toxin Produced by Phytopathogenic Bacterium, Pseudomonas syringae pv. mori. *Chem. Lett.* **18**, 679–680 (1989).
87. Donia, M. S. *et al.* Mollamides B and C, cyclic hexapeptides from the indonesian tunicate Didemnum molle. *J. Nat. Prod.* **71**, 941–945 (2008).
88. Morita, H. *et al.* Pseudostellarins A - C, new tyrosinase inhibitory cyclic peptides from Pseudostellaria heterophylla. *Tetrahedron* **50**, 6797–6804 (1994).
89. Nogle, L. M., Marquez, B. L. & Gerwick, W. H. Wewakazole, a novel cyclic dodecapeptide from a papua new guinea Lyngbya majuscula. *Org. Lett.* **5**, 3–6 (2003).
90. Gogineni, V. & Hamann, M. T. Marine natural product peptides with therapeutic potential: Chemistry, biosynthesis, and pharmacology. *Biochimica et Biophysica Acta - General Subjects* **1862**, 81–196 (2018).
91. Steiger, M. & Reichstein, T. Chemical structure of corticosterone [6]. *Nature* **141**, 202 (1938).
92. Cohen, N. *et al.* Enantiospecific Syntheses of Leukotrienes C4, D4, and E4 and [14,15-3 H2]Leukotriene E4 Dimethyl Ester. *J. Am. Chem. Soc.* **105**, 3661–3672 (1983).
93. Pereda-Miranda, R. & Hernández-Carlos, B. HPLC Isolation and structural elucidation of diastereomeric niloyl ester tetrasaccharides from Mexican scammony root. *Tetrahedron* **58**, 3145–3154 (2002).
94. Warashina, T. & Noro, T. Glycosides of 14,15-seco and 13,14:14,15-disecopregnanes from the roots of Cynanchum sublanceolatum. *Chem. Pharm. Bull.* **54**, 1551–1560 (2006).
95. Noverr, M. C., Toews, G. B. & Huffnagle, G. B. Production of

prostaglandins and leukotrienes by pathogenic fungi. *Infect. Immun.* **70**, 400–402 (2002).

96. Tsitsigiannis, D. I. & Keller, N. P. Oxylipins as developmental and host-fungal communication signals. *Trends in Microbiology* **15**, 109–118 (2007).
97. Stone, T. A. & Deber, C. M. Therapeutic design of peptide modulators of protein-protein interactions in membranes. *Biochimica et Biophysica Acta - Biomembranes* **1859**, 577–585 (2017).
98. Gentilucci, L., De Marco, R. & Cerisoli, L. Chemical Modifications Designed to Improve Peptide Stability: Incorporation of Non-Natural Amino Acids, Pseudo-Peptide Bonds, and Cyclization. *Curr. Pharm. Des.* **16**, 3185–3203 (2010).
99. Omoto, S., Ogino, H. & Inouye, S. Studies On SF-1902 A2~A5, minor components of SF-1902 (GLOBOMYCIN). *J. Antibiot. (Tokyo).* **34**, 1416–1423 (1981).
100. Castelli, M. V. *et al.* In vitro inhibition of 1,3-β-Glucan synthase by glycolipids from convolvulaceous species. *Planta Med.* **68**, 739–742 (2002).
101. Lima, S. L., Colombo, A. L. & de Almeida Junior, J. N. Fungal Cell Wall: Emerging Antifungals and Drug Resistance. *Front. Microbiol.* **10**, 2573 (2019).
102. Sy-Cordero, A. A. *et al.* Cyclodepsipeptides, sesquiterpenoids, and other cytotoxic metabolites from the filamentous fungus Trichothecium sp. (MSX 51320). *J. Nat. Prod.* **74**, 2137–2142 (2011).
103. Mao, X. M. *et al.* Epigenetic genome mining of an endophytic fungus leads to the pleiotropic biosynthesis of natural products. *Angew. Chemie - Int. Ed.* **54**, 7592–7596 (2015).
104. Nakao, Y., Oku, N., Matsunaga, S. & Fusetani, N. Cyclotheonamides E2 and E3, new potent serine protease inhibitors from the marine sponge of the genus Theonella. *J. Nat. Prod.* **61**, 667–670 (1998).

105. Fujii, K., Sivonen, K., Kashiwagi, T., Hirayama, K. & Harada, K. I. Nostophycin, a novel cyclic peptide from the toxic Cyanobacterium Nostoc sp. 152. *J. Org. Chem.* **64**, 5777–5782 (1999).
106. Triastuti, A. *et al.* How Histone Deacetylase Inhibitors Alter the Secondary Metabolites of Botryosphaeria mamane, an Endophytic Fungus Isolated from Bixa orellana. *Chem. Biodivers.* **16**, e1800485 (2019).
107. Hautbergue, T. *et al.* Combination of Isotope Labeling and Molecular Networking of Tandem Mass Spectrometry Data to Reveal 69 Unknown Metabolites Produced by Penicillium nordicum. *Anal. Chem.* **91**, 12191–12202 (2019).

Chapter V

Final Discussion

The following section presents a critical and integrated discussion of data presented in the previous chapters, as well as future perspectives

Final discussion

Microbial pathogens, despite centuries of research, are still posing a great threat, mostly due to the increase of multi-resistant fungal and bacterial strains. According to the World Health Organization, antimicrobial resistance is one of the top 10 global public health threats facing humanity[1]. The occurrence of invasive fungal infections is only a fraction compared to bacterial infections, although the death rate is alarming due to inadequate treatment options. Additionally, the number of life threatening invasive fungal infections is increasing as medical treatments involving the suppression of the immune system are advancing. Due to the lack of interest and adequate actions, fungal infections have even been referred to as “hidden killers” and the “neglected epidemic”[2,3]. Several new antibiotic and antifungal[4] drugs are currently in development or in clinical trials, some exhibiting novel mode of actions. Nevertheless, increasing our toolbox of strategies to develop antimicrobial solutions, is essential to effectively fight microbial infections. Not only are bacteria and fungi believed to eventually develop resistance against any newly introduced drug, but the antimicrobial drugs currently in the pipelines, are not even targeting some of the most dangerous microbial organisms already threatening lives[5].

This work describes several approaches to design strategies to fight microbial human infections combining fungal biology and ionic liquids, with a focus on invasive fungal infections caused by *Aspergillus fumigatus*. Ionic liquids have been the subject of several studies in our laboratory, investigating their toxicity and effects towards filamentous fungi. In fact, our laboratory was the first to systematically describe cholinium alkanoates, the class of ionic liquids which has mainly been utilized in the subsequent studies of our laboratory, including studies on fungal biology, secondary metabolism and the extraction of functional polymers from the plant cell-wall macromolecules cutin and suberin[6–11]. In this work, ionic liquids have been used in diverse functions. On one hand, they served as medium supplements

to study stress responses of *A. fumigatus* and to stimulate the production of secondary metabolites with antimicrobial properties in *A. fumigatus, Aspergillus nidulans* and *Neurospora crassa*. On the other hand, ionic liquids have been studied as antimicrobial drugs themselves.

We investigated a novel formulation of Amphotericin B ([AmB]) (Chapter II), coupling an anionic form of the antifungal drug with the cation cholinium ($[chol]^+$), cetylpyridinium ($[C16py]^+$) or trihexyltetradecylphosphonium ($[P6\ 6\ 6\ 14]^+$) to form ionic liquids. We showed that the formulations [chol][AmB] and [C16py][AmB] compared to AmB alone, increased antifungal activity 1.2 - and 3.2 - fold, respectively, for both *A. fumigatus* and *Aspergillus terreus*. Either ionic liquid seemed to maintain the mechanism of action of AmB, but molecular dynamic simulations showed an enhanced interaction of [C16py][AmB] with ergosterol, the main fungal membrane sterol, probably causing the increased antifungal activity. Interestingly, [C16py][AmB] additionally showed antibiotic activity against *Staphylococcus aureus* and *Escherichia coli*. [C16py]Cl is an approved antiseptic, mainly utilized in dental care. The ionic liquid formulation of both drugs therefore combined their individual activity which can be further optimized by fine-tuning the components. Higher cytotoxicity of the AmB formulation, due to simultaneously enhanced cholesterol interactions, poses a drawback for the application of [C16py][AmB] specifically. Nevertheless, the study emphasizes a general use of ionic liquid formulations to extend antimicrobial properties of existing drugs, while potentially improving their administration due to higher solubility. Large-scale screenings could lead to the development of improved antimicrobial formulations.

Chapter III and Chapter IV focused on the utilization of ionic liquids as medium supplements to study fungal biology, specifically supporting the discovery of novel antifungal targets and antimicrobial compounds. Filamentous fungi have the capacity to synthesize a great variety of

secondary metabolites, but most of them remain cryptic under standard laboratory conditions[12,13]. Previous work from our laboratory has shown, that medium supplementation with ionic liquids alters the overall metabolism in fungi, including secreted secondary metabolites, as their biosynthetic backbone genes are activated[7,8]. Considering the vast array of secondary metabolites, their potential activation by the addition of sub-lethal concentrations of ionic liquids to the growth medium, provides ground for diverse interesting study approaches. In this thesis, cholinium based ionic liquids were utilized, as they are biodegradable by the fungus, avoiding any interference of residual ionic liquids in spent medium extracts in bioactivity assays.

Previous studies involving ionic liquids and their effects on filamentous fungi mainly involved the model organisms *N. crassa* and *A. nidulans*, as well as some studies on soil communities and *Penicillium* spp[14–16]. This work put a special focus on *A. fumigatus,* a pathogenic fungus capable of provoking life threatening invasive fungal infections. The initial motivation was to utilize ionic liquids to trigger the production of signaling molecules not yet described for *A. fumigatus* (Chapter III). As we continue to unravel quorum sensing in bacteria, there is increasing evidence that fungi have developed equally sophisticated communication systems[17]. Understanding this chemical language and how it influences fungal growth, dissemination, and resilience, may prove advantageous for the development of novel antifungal drugs. Fungal specific metabolic pathways and stress mechanisms are promising research areas for targeted drug development[18–20].

ChoDec was employed to trigger the production of these potential signaling molecules by *A. fumigatus* (Chapter III). Spent medium extracts of cultures supplemented with sub-inhibitory concentrations of ChoDec showed to induce germination and enhance growth in *A. fumigatus*, an effect that could be recapitulated when supplementing cultures with NaDec or AmB. Mass

spectrometry analysis pointed to the production of alkaloid metabolites under these conditions, specifically tryptoquivaline F, gliotoxin and its precursor Phe-Ser-DKP. Tryptoquivaline F, in contrast to the other two secondary metabolites, showed to induce germination in *A. fumigatus* like the spent medium extracts. It should be noted that the identification by mass spectrometry was performed by comparison to a database of known secondary metabolites. Hence it cannot be excluded, that the extracts contain additional bioactive metabolites not yet described. The role of tryptoquivaline F for the survival and germination of *A. fumigatus*, as well as its specific production under stress conditions must be further elucidated by additional studies, such as RNAseq and the investigation of appropriate mutant strains.

Some studies suggested that the production of gliotoxin is a stress response to the exposure of *A. fumigatus* to reactive oxygen species, restoring the redox balance provoked by external agents and/ or cell leakage[21–23]. It is still unclear how ChoDec exerts its toxicity on filamentous fungi[24]. The reduction of fungal biomass 24h after its addition to the growth medium suggests some cell death though, potentially including leakage of cells. ChoDec seems to induce cell death potentially involving the production of reactive oxygen species, which in turn leads to the production of gliotoxin, explaining its appearance. Since medium supplementation with NaDec and AmB produced the same effects and one of the studies mentioned above detected gliotoxin upon Caspofungin treatment[22], the production of gliotoxin as well as tryptoquivaline F may be a general survival mechanism of *A. fumigatus.* Future studies should concentrate on understanding this mechanism under infection conditions. It should be investigated whether the treatment of invasive fungal infections with antifungals lead to the production of tryptoquivaline F and gliotoxin, which in turn promote germination and counteract cell death. Additionally, it has been described that the generation of an oxidative stress environment is an important line of host defense

against *A. fumigatus* infections, which could also provoke the production of these metabolites[25,26]. The development of supplementary drugs targeting their production or removal could prove beneficial for improved treatment options.

Apart from the alkaloids, the results also showed the presence of an excess of free amino acids in the spent medium extracts after ChoDec, NaDec and AmB supplementation. Elevated amounts of free amino acids in turn also led to accelerated germination in *A. fumigatus*. Amino acid homeostasis is a determining factor during early stages of infection[27]. One of the innate defenses against fungal lung infections, is host-imposed nitrogen starvation[28,29]. However, the highly adapted *A. fumigatus* disposes of a great variety of proteases with redundant activities, which the fungus utilizes to acquire carbon and nitrogen from protein degradation[30]. In addition to acquisition of host nutrients, it has been suggested that *A. fumigatus* can recycle nutrients via autophagy under stress or starvation situations[31,32]. Another study reported, that an excess of amino acids, specifically aromatic amino acids, can be utilized by the fungus to be integrated into secondary metabolites, that influence pathogenicity[18]. The release of amino acids by the fungus itself upon cell death due to antifungal treatment, may therefore provide additional advantages for the surviving fungal cells and complicate complete fungal removal.

While the short-term exposure (24 hours) of *A. fumigatus* to sub-lethal concentrations of ChoDec led to the above-described stress response, long-term culturing after the ionic liquid exposure (up to 10 days) led to an altered profile of peptide secondary metabolites, putatively including some with antibacterial properties (Chapter IV). Following previous studies of our laboratory, we systematically investigated the activation of antimicrobial peptides production by three fungal organisms, *N. crassa*, *A. nidulans* and *A. fumigatus,* in response to ionic liquid medium supplementation[7,8].

Secondary metabolite enriched extracts of the spent medium of *N. crassa* and *A. fumigatus* in fact revealed antimicrobial activity against *E. coli* and *S. aureus*. Chemical characterization of the extracts by untargeted mass spectrometry analysis and total amino acid content suggested the presence of metabolites containing non-proteinogenic amino acids. These rare amino acids are of special interest, as they are not produced by humans and can influence certain properties such as enhanced stability, potency, permeability, oral bioavailability, and immunogenicity, which is advantageous for drug development[33].

Putatively identified compounds by the MS analysis showed a wide variety of compounds being produced, including polyketides, nonribosomal peptides, terpenes, and hybrids (PKs-terpenes and PKs-NRPs). Especially noteworthy is the detection of several macrolides in *A. fumigatus* extracts and of nonribosomal peptides, particularly depsipeptides, in *N. crassa* extracts. Both classes of compounds are of pharmacological interest. Macrolides are known for their antimicrobial activity and depsipeptides, some of which are cyclized, exhibit enhanced stability, due to the cyclization and/ or the incorporation of hydroxy acids, making them promising targets for the development of novel drugs[34–36]. With the MS analysis it was possible to putatively identify only a fraction of the detected compounds - none of which contain ACC and/or Aib, indicating the presence of yet uncharacterized compounds in the extracts. The optimization of the extraction protocol, tailored to the isolation of cyclic peptides and depsipeptides followed by an in-depth structural characterization harbors a great potential to discover new bioactive peptides as a basis for drug development. Our data already showed antibacterial potential, but many natural peptides have already been described for their antifungal properties as well and cyclic depsipeptides are known for diverse pharmaceutical activities[37,38].

The extracts obtained from *A. fumigatus* cultures without ionic liquid supplementation, in contrast to *N. crassa*, already exhibited antibacterial activity similar to extracts from supplemented cultures. While *N. crassa* is described as a low producer of secondary metabolites with only 10 predicted biosynthetic gene clusters encoded in its genome[39], *A.fumigatus* Af293, the strain used in this work, contains 35 biosynthetic gene clusters[40]. It is not surprising, that *A. fumigatus* already produces some bioactive compounds without any stimulation. Nevertheless, the ionic liquid supplementation led to an altered secondary metabolite profile, meaning a different set of metabolites was produced, including some still uncharacterized. The extracts activity in this study were only tested against *S. aureus* and *E. coli*. Extending the screening to other microbial pathogens, bacteria and as well as fungi, may exhibit differential activities of the extracts.

Ionic liquids come in a great variety of ion compositions, influencing toxicity, degradability and naturally their effect on fungal organisms. Further screenings employing diverse ionic liquids may therefore be performed to systematically identify cryptic bioactive compounds from different fungal strains. At the same time, as shown here and in other studies of the laboratory, ionic liquids can be utilized to study fungal stress responses[9]. Thus far in these studies ChoDec has been utilized, nevertheless, different types of ionic liquids might prove valuable in studying diverse fungal strategies to cope with stress.

Apart from filamentous fungi, many other organisms are being investigated for their potential to produce antimicrobial compounds, such as bacteria and plants. All antimicrobial drugs on the market are derived from terrestrial resources though, while marine sources have remained unexplored for a long time[41]. Now they are increasingly recognized for their potential to produce compounds with a wide range of bioactive properties, with structures and characteristics distinct from terrestrial compounds[42]. Among those,

seaweeds such as the Rhodophyta *Asparagopsis armata*, have repeatedly attracted attention as biotechnological and pharmacological resources[43]. Crude extracts from *A. armata* have shown potent antimicrobial, as well as antifouling, antioxidant and antitumor activities[43,44].

In another project, under non-disclosure agreement, and hence not described in detail within the experimental chapters, we studied an extract from an alga that does not involve biomass milling or use of harsh solvents. Compared to common extraction methods, the result is an extract composition of lower complexity, enabling the identification of molecules that are usually present at low abundance and may otherwise be masked by more prominent compounds. The crude extracts show strong activity not only against the pathogenic bacteria *E. coli* and *S. aureus,* but also against the pathogenic fungi *Candida albicans* and *A. fumigatus* (Figure 1). The methods used were similar to those reported in the Chapter IV.

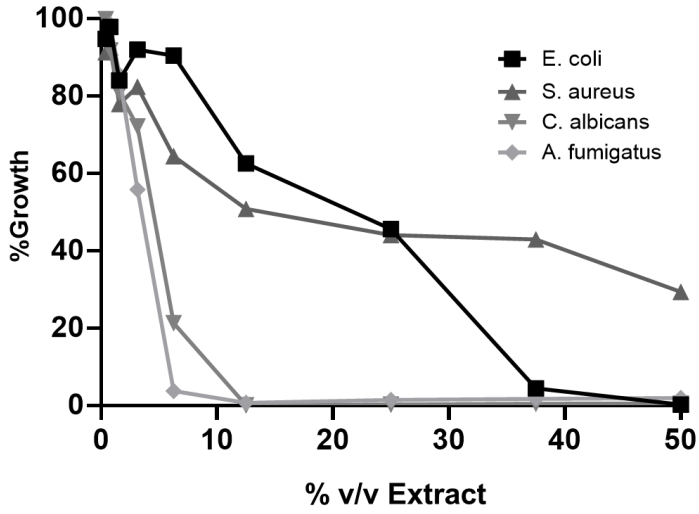

Figure 1 Extract inhibitory activity against all four test organisms, determined by microbroth dilution assay followed by MTT analysis.

We could show that, in contrast to a previous study, the activity is not based on the presence of bromoform[45]. NMR quantification and subsequent

exposure of all four organisms to the concentrations detected, demonstrated that bromoform does not provoke the same inhibitory effects as the extract (data not shown). Rhodophyta are known to produce a great variety of volatile halogenated organic compounds (VHOCs) with a wide range of bioactive properties, whereas in terrestrial organisms they are rather uncommon[46–48]. Although bromoform has been shown to possess antimicrobial activity, it is not a suitable pharmacological candidate due to its toxicity[49–51]. Studies to identify the active compound(s) are ongoing, including NMR and GC-MS analyses. Preliminary results indicate aliphatic acids to be the principal components of the extract (data not shown).

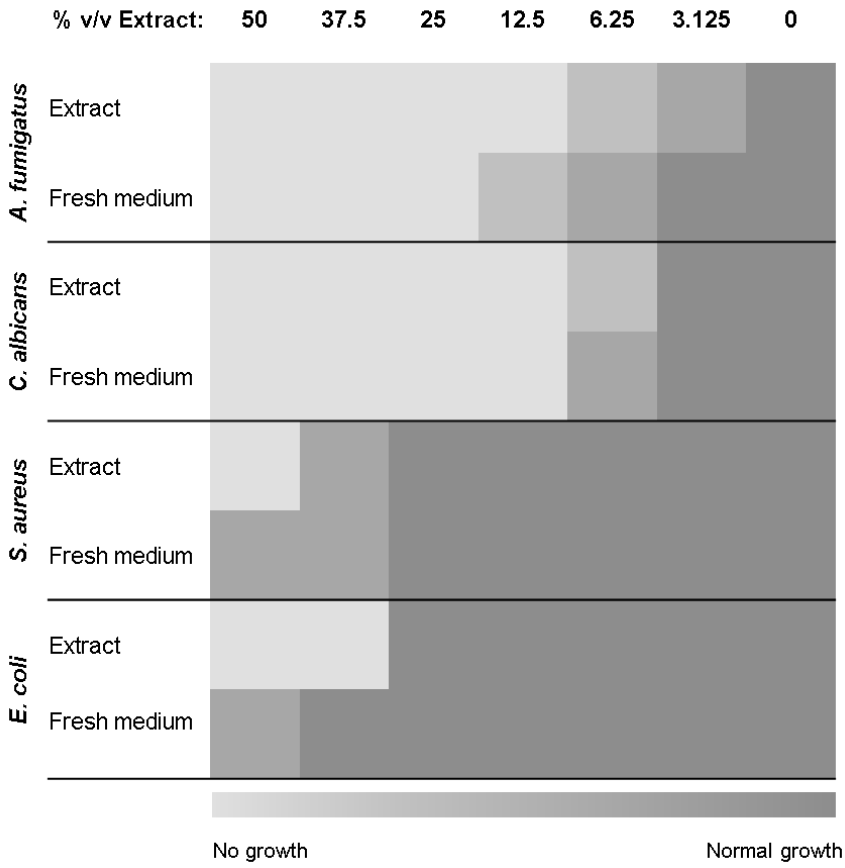

Figure 2 Medium exchange assay, microscopic analysis of growth restoration after exchange of the extract dilutions with fresh medium.

To combat (multi-)resistant pathogens, it is essential to develop antimicrobials with novel modes of action. Most antibiotics in the pipeline have the same targets as existing drugs and all antifungals target the fungal cell wall and membrane. Therefore, ongoing studies are investigating the mode of action of the extract against all four model organisms. In a first experiment, medium exchange assays were employed to understand if the extract is leading to cell death or growth inhibition. 24h after incubation with the extract, the spent medium was exchanged for fresh medium but without addition of extract and the growth or lack thereof checked microscopically (Figure 2). Both fungal organisms show only slight growth restoration when grown with low amounts of the extract, whereas high amounts of it seem to have fungicidal activity, since no growth can be observed after the medium exchange. Both bacterial organisms, however, seem to recover after the medium exchange with growth restored almost to control conditions.

Further studies will compare the mode of action of diverse antimicrobials with the algal extract. These studies include fluorescence microscopy, applying differential staining targeting different cell components, as well as the utilization of appropriate mutant strains. These studies need to be constantly adapted in accordance with the results of each step, therefore a more detailed study approach cannot be described at this point. One possibility is to perform an untargeted MS approach as that optimized in Chapter IV to pinpoint the most relevant candidates, supporting a definition of the best isolation strategy.

In conclusion, the results presented in this thesis, provide the basis for the development of diverse antimicrobial strategies. Continuous research, including creative study approaches, are of great importance to counteract the increasing emergence of multi-resistant microbial pathogens. Ionic liquid formulations of antimicrobial drugs with enhanced properties, the isolation of structurally novel secondary metabolites from filamentous fungi and yet

unexplored marine organisms, and the identification of pathogen specific stress and signaling mechanisms as promising drug targets; applying and extending these study designs will prove essential for the discovery of antimicrobials with effective new mode of actions.

References

1. World Health Organization, Antimicrobial Resistance. Available at: https://www.who.int/news-room/fact-sheets/detail/antimicrobial-resistance.
2. Stop neglecting fungi. *Nat. Microbiol.* **2**, 17120 (2017).
3. Armstrong-James, D., Meintjes, G. & Brown, G. D. *A neglected epidemic: Fungal infections in HIV/AIDS*. *Trends in Microbiology* **22**, 120–127 (Trends Microbiol, 2014).
4. Gintjee, T. J., Donnelley, M. A. & Thompson, G. R. Aspiring Antifungals: Review of Current Antifungal Pipeline Developments. *J. Fungi* **6**, 28 (2020).
5. Butler, M. S. & Paterson, D. L. Antibiotics in the clinical pipeline in October 2019. *J. Antibiot. (Tokyo).* **73**, 329–364 (2020).
6. Petkovic, M. *et al.* Novel biocompatible cholinium-based ionic liquids - Toxicity and biodegradability. *Green Chem.* **12**, 643–649 (2010).
7. Martins, I. *et al.* Proteomic alterations induced by ionic liquids in Aspergillus nidulans and Neurospora crassa. *J. Proteomics* **94**, 262–278 (2013).
8. Alves, P. C. *et al.* Transcriptomic and metabolomic profiling of ionic liquid stimuli unveils enhanced secondary metabolism in Aspergillus nidulans. *BMC Genomics* **17**, 284 (2016).
9. Hartmann, D. O., Piontkivska, D., Moreira, C. J. S. & Silva Pereira, C. Ionic Liquids Chemical Stress Triggers Sphingoid Base Accumulation in Aspergillus nidulans. *Front. Microbiol.* **10**, (2019).
10. Correia, V. G. *et al.* The molecular structure and multifunctionality of the cryptic plant polymer suberin. *Mater. Today Bio* **5**, (2020).

11. Moreira, C. J. S. *et al.* An ionic liquid extraction that preserves the molecular structure of cutin shown by nuclear magnetic resonance. *Plant Physiol.* **184**, 592–606 (2020).
12. Bok, J. W. & Keller, N. P. LaeA, a regulator of secondary metabolism in Aspergillus spp. *Eukaryot. Cell* **3**, 527–535 (2004).
13. Brakhage, A. A. Regulation of fungal secondary metabolism. *Nat. Rev. Microbiol.* **11**, 21–32 (2013).
14. Petkovic, M. *et al.* Exploring fungal activity in the presence of ionic liquids. *Green Chem.* **11**, 889 (2009).
15. Singer, S. W. *et al.* Enrichment, isolation and characterization of fungi tolerant to 1-ethyl-3-methylimidazolium acetate. *J. Appl. Microbiol.* **110**, 1023–1031 (2011).
16. Hartmann, D. O., Petkovic, M. & Pereira, C. S. Ionic liquids as unforeseen assets to fight life-threatening mycotic diseases. *Front. Microbiol.* **7**, 1–5 (2016).
17. Albuquerque, P. & Casadevall, A. Quorum sensing in fungi – a review. *Med. Mycol.* **50**, 337–345 (2012).
18. Choera, T., Zelante, T., Romani, L. & Keller, N. P. A multifaceted role of tryptophan metabolism and indoleamine 2,3-dioxygenase activity in Aspergillus fumigatus-host interactions. *Front. Immunol.* **8**, 1–11 (2018).
19. Scott, J. *et al.* Targeting methionine synthase in a fungal pathogen causes a metabolic imbalance that impacts cell energetics, growth, and virulence. *MBio* **11**, 1–23 (2020).
20. Amich, J. Sulfur Metabolism as a Promising Source of New Antifungal Targets. *Journal of Fungi* **8**, 295 (2022).
21. Gallagher, L. *et al.* The Aspergillus fumigatus protein gliK protects against oxidative stress and is essential for gliotoxin biosynthesis. *Eukaryot. Cell* **11**, 1226–1238 (2012).
22. Eshwika, A., Kelly, J., Fallon, J. P. & Kavanagh, K. Exposure of

Aspergillus fumigatus to caspofungin results in the release, and de novo biosynthesis, of gliotoxin. *Med. Mycol.* **51**, 121–127 (2013).

23. Owens, R. A., Hammel, S., Sheridan, K. J., Jones, G. W. & Doyle, S. A proteomic approach to investigating gene cluster expression and secondary metabolite functionality in Aspergillus fumigatus. *PLoS One* **9**, e106942 (2014).
24. Hartmann, D. O. *et al.* Plasma membrane permeabilisation by ionic liquids: a matter of charge. *Green Chem.* **17**, 4587–4598 (2015).
25. Dagenais, T. R. T. & Keller, N. P. Pathogenesis of Aspergillus fumigatus in invasive aspergillosis. *Clin. Microbiol. Rev.* **22**, 447–465 (2009).
26. Shibuya, K. *et al.* Catalases of Aspergillus fumigatus and inflammation in aspergillosis. *Japanese J. Med. Mycol.* **47**, 249–255 (2006).
27. Beattie, S. R. *et al.* Filamentous fungal carbon catabolite repression supports metabolic plasticity and stress responses essential for disease progression. *PLOS Pathog.* **13**, e1006340 (2017).
28. McDonagh, A. *et al.* Sub-telomere directed gene expression during initiation of invasive aspergillosis. *PLoS Pathog.* **4**, (2008).
29. Lee, I. R., Morrow, C. A. & Fraser, J. A. Nitrogen regulation of virulence in clinically prevalent fungal pathogens. *FEMS Microbiol. Lett.* **345**, 77–84 (2013).
30. Sriranganadane, D. *et al.* Aspergillus Protein Degradation Pathways with Different Secreted Protease Sets at Neutral and Acidic pH. *J. Proteome Res.* **9**, 3511–3519 (2010).
31. Richie, D. L. *et al.* Unexpected Link between Metal Ion Deficiency and Autophagy in Aspergillus fumigatus. *Eukaryot. Cell* **6**, 2437–2447 (2007).
32. Palmer, G. E., Askew, D. S. & Williamson, P. R. The diverse roles of autophagy in medically important fungi. *Autophagy* **4**, 982–988 (2008).
33. Ding, Y. *et al.* Impact of non-proteinogenic amino acids in the

discovery and development of peptide therapeutics. *Amino Acids* **52**, 1207–1226 (2020).

34. Gentilucci, L., De Marco, R. & Cerisoli, L. Chemical Modifications Designed to Improve Peptide Stability: Incorporation of Non-Natural Amino Acids, Pseudo-Peptide Bonds, and Cyclization. *Curr. Pharm. Des.* **16**, 3185–3203 (2010).
35. Stone, T. A. & Deber, C. M. Therapeutic design of peptide modulators of protein-protein interactions in membranes. *Biochimica et Biophysica Acta - Biomembranes* **1859**, 577–585 (2017).
36. Wang, X., Gong, X., Li, P., Lai, D. & Zhou, L. Structural Diversity and Biological Activities of Cyclic Depsipeptides from Fungi. *Mol. 2018, Vol. 23, Page 169* **23**, 169 (2018).
37. Ciociola, T. *et al.* Natural and synthetic peptides with antifungal activity. *Future Med. Chem.* **8**, 1413–1433 (2016).
38. Sivanathan, S. & Scherkenbeck, J. Cyclodepsipeptides: A Rich Source of Biologically Active Compounds for Drug Research. *Molecules* **19**, 12368–12420 (2014).
39. Khaldi, N. *et al.* SMURF: Genomic mapping of fungal secondary metabolite clusters. *Fungal Genet. Biol.* **47**, 736–741 (2010).
40. Steenwyk, J. L. *et al.* Variation among biosynthetic gene clusters, secondary metabolite profiles, and cards of virulence across aspergillus species. *Genetics* **216**, 481–497 (2020).
41. Hayashi, M. A., Bizerra, F. C. & Da Silva, P. I. Antimicrobial compounds from natural sources. *Front. Microbiol.* **4**, (2013).
42. Murray, P. M. *et al.* Sustainable production of biologically active molecules of marine based origin. *N. Biotechnol.* **30**, 839–850 (2013).
43. Pinteus, S. *et al.* Marine invasive macroalgae: Turning a real threat into a major opportunity - the biotechnological potential of Sargassum muticum and Asparagopsis armata. *Algal Res.* **34**, 217–234 (2018).
44. Salvador, N., Gómez Garreta, A., Lavelli, L. & Ribera, M. A.

Antimicrobial activity of Iberian macroalgae. *Sci. Mar.* **71**, 101–114 (2007).

45. Paul, N. A., Nys, R. De & Steinberg, P. D. Chemical defence against bacteria in the red alga. *Mar. Ecol. Prog. Ser.* **306**, 87–101 (2006).
46. McConnell, O. & Fenical, W. Halogen chemistry of the red alga Asparagopsis. *Phytochemistry* **16**, 367–374 (1977).
47. Kladi, M., Vagias, C. & Roussis, V. Volatile halogenated metabolites from marine red algae. *Phytochem. Rev.* **3**, 337–366 (2004).
48. Güven, K. C. *et al.* Volatile Oils from Marine Macroalgae. in *Natural Products* 2883–2912 (Springer Berlin Heidelberg, 2013). doi:10.1007/978-3-642-22144-6_128
49. von Oettingen, W. F. Bromoform. In: The Halogenated Aliphatic, Olefinic, Cyclic, Aromatic, and Aliphatic-Aromatic Hydrocarbons Including the Halogenated Insecticides, their Toxicity and Potential Dangers. *U.S. Dep. Heal. Educ. Welfare, Public Heal. Serv. Washington, DC.* (1955).
50. U.S. Environmental Protection Agency. Integrated Risk Information System (IRIS) on Bromoform. *Natl. Environ. Assessment, Off. Res. Dev. Washington, D.C* (1999).
51. Toxicological Profile for Bromoform and Chlorodibromomethane. in *ATSDR's Toxicological Profiles* (2002). doi:10.1201/9781420061888_ch46

Supplementary Material

Chapter II - Supplementary Information

Tailoring amphotericin B as an ionic liquid: an upfront strategy to potentiate the biological activity of antifungal drugs

Supplementary Methods

Synthesis of cholinium amphotericin B [chol][AmB]:

(2-Hydroxyethyl)-trimethylammonium chloride (0.0355g; 0.254 mmol) was dissolved in methanol and passed through an ion-exchange Amberlite IRA-400(OH) (5 eq., flux rate 0.133 mL.min^{-1} = 8 BVh^{-1}). Then, the hydroxide solution formed was slowly added to amphotericin B (0.249 g; 0.269 mmol) dissolved in 1.0 M dried triethylamine methanolic solution. The mixture was stirred at room temperature for 1 h. After solvent evaporation the residue was dried *in vacuum* for 24 h to provide the desired product as an orange solid (0.1335 g; 51.1 %).

$[\alpha]_D^{25}$ = 50.0 ± 5.8 (c = 1 mg.mL^{-1} in MeOH);

^{1}H-NMR (400.13 MHz, $(CD_3)_2SO$) δ = 6.47-5.97 (m, 14H), 5.68 (bs, 1H), 5.46-5.40 (m, 1H), 5.35-5.32 (m, 1H), 5.24-5.20 (m, 1H), 4.98-4.74 (m, 1H), 4.63 (bs, 1H) 4.34 (bs, 1H), 4.37-4.32 (m, 1H), 4.26-4.24 (m, 1H), 4.08-4.04 (m, 1H), 3.84-3.83 (m, 6H), 3.61-3.64 (m, 4H), 3.60-3.38 (m, 10H), 3.10 (s, 9H), 2.33-2.27 (m, 3H), 2.15 (d, 1H, *J* = 5.8 Hz), 1.91-1.70 (m, 1H), 1.65-1.31 (m, 10H), 1.23 (s, 3H), 1.14 (d, 3H, *J* = 5.6 Hz), 1.10 (d, 3H, *J* = 6.1 Hz), 1.03 (d, 3H, *J* = 6.0 Hz), 0.91 (d, 3H, *J* = 7.0 Hz), 0.83 (t, 3H, *J* = 6.7 Hz) ppm;

IR (KBr): υ = 3398, 3018, 2917, 2077, 1638, 1577, 1559, 1506, 1460, 1401, 1387, 1324, 1270, 1183, 1130, 1110, 1073, 1035, 982, 956, 851, 721 cm^{-1}.

MALDI-TOF-MS analysis in the positive ion mode: *m/z* calcd for $[C_5H_{14}NO]^+$: 104.1070, found 104.1080; MALDI-TOF-MS analysis in negative ion mode: *m/z* calcd for $[C_{47}H_{72}NO_{17}]^-$ 922.4806, found $[M-2H]^-$ 920.6717.

Synthesis of cetylpyridinium amphotericin B [C_{16}py][AmB]:

Cetylpyridinium chloride (0.088g; 0.246 mmol) was dissolved in methanol and passed through an ion-exchange Amberlite IRA-400(OH) (5 eq., flux rate 0.133 mL.min^{-1} = 8 BVh^{-1}). The hydroxide solution formed was slowly added to amphotericin B (0.250 g; 0.271 mmol) dissolved in 1.0 M dried triethylamine methanolic solution. The mixture was stirred at room temperature for 1 h. After solvent evaporation the residue was dried in vacuum for 24 h to provide the product as an orange solid (0.215 g; 71.3 %).

$[\alpha]_D^{25}$ = 49.7 ± 5.8 (c = 0.2 mg.mL^{-1} in MeOH);

^{1}H-NMR (400.13 MHz, $(CD_3)_2SO$) δ = 9.10 (d, 2H, *J* = 5.6 Hz), 8.60 (t, 1H, *J* = 7.6 Hz), 8.16 (t, 2H, *J* = 6.7 Hz), 6.47-5.97 (m, 14H), 5.65 (bs, 1H), 5.51-5.40 (m, 1H), 5.33-5.31 (m, 1H), 5.21-5.20 (m, 1H), 4.79-4.78 (m, 3H), 4.59 (t, 3H, *J* = 7.4 Hz) 4.34 (bs, 1H), 4.24-4.23 (m, 2H), 4.17-4.12 (m, 1H), 4.07-4.05 (m, 1H), 3.74-2.81 (m, 12H), 2.41-2.25 (m, 3H), 2.15 (d, 1H, *J* = 5.7 Hz), 1.91-1.89 (m, 2H), 1.82-1.37 (m, 16H), 1.27-1.23 (m, 28H), 1.14 (d, 3H, *J* = 5.8 Hz), 1.11 (d, 3H, *J* = 6.1 Hz), 1.03 (d, 3H, *J* = 5.9 Hz), 0.90 (d, 3H, *J* = 6.9 Hz), 0.85 (t, 3H, *J* = 6.7 Hz) ppm;

^{13}C-NMR (150 MHz, $(CD_3)_2SO$) δ = 170.45, 145.37, 144.64, 133.66, 133.63, 133.61, 133.47, 133.17, 132.70, 132.66, 132.25, 132.20, 131.99, 131.90, 131.84, 131.80, 127.99, 99.28, 96.65, 79.10, 78.88, 78.66, 73.50, 72.87, 69.18, 68.75, 67.70, 66.15, 60.68, 44.65, 44.29, 44.27, 41.96, 35.08, 31.20, 30.61, 28.95, 28.91, 28.81, 28.68, 28.61, 28.28, 25.31, 22.00, 18.41, 18.00, 16.91, 13.87, 11.99 ppm;

IR (KBr): υ = 3435, 3010, 2920, 2852, 1638, 1579, 1563, 1488, 1456, 1401, 1383, 1340, 1324, 1272, 1181, 1130, 1108, 1069, 1037, 1009, 982, 908, 887, 853, 772, 719, 683 cm^{-1}.

MALDI-TOF-MS analysis in the positive ion mode: *m/z* calcd for $[C_{21}H_{38}N]^+$: 304.2999 found 304.3117; MALDI-TOF-MS analysis in negative ion mode: *m/z* calcd for $[C_{47}H_{72}NO_{17}]^-$ 922.4806, found $[M-2H]^-$ 920.5183.

Synthesis of trihexyltetradecylphosphonium amphotericin B $[P_{6\,6\,6\,14}]$[AmB]:

Trihexyl(tetradecyl)phosphonium (0.127 g; 0.246 mmol) was dissolved in methanol and passed through an ion-exchange Amberlite IRA-400(OH) (5 eq., flux rate 0.133 mL.min^{-1} = 8 BVh^{-1}). The hydroxide solution formed was slowly added to amphotericin B (0.251 g; 0.270 mmol) dissolved in 1.0 M dried triethylamine methanolic solution. The mixture was stirred at room temperature for 1 h. After solvent evaporation the residue was dried in vacuum for 24 h to provide the product as orange solid. (0.1953 g; 75.0 %).

$[\alpha]_D^{25}$ = 95.0 ± 3.8 (c = 1 mg.mL^{-1} in MeOH);

^{1}H-NMR (400.13 MHz, $(CD_3)_2SO$) δ = , 6.35-6.02 (m, 16H), 5.71 (bs, 1H), 5.53-5.21(m, 6H), 4.79-3.89 (m, 24H), 2.12 (t, 12H, *J* = 14.3 Hz), 1.47- 137 (m, 24H), 1.29-1.24 (m, 47H), 1.13 (dd, 2H, *J* = 16.5, J = 5.9 Hz), 1.06-0.99(m, 3H), 0.87 (t, 12H, *J* = 7.3 Hz) ppm;

IR (KBr): υ = 3435, 2921, 2848, 1656, 1648, 1579, 1561, 1490, 1480, 1456, 1385, 1322, 1262, 1179, 1130, 1106, 1069, 1039, 1009, 901, 853, 776, 719, 685 cm^{-1}

MALDI-TOF-MS analysis in the positive ion mode: *m/z* calcd for $[C_{32}H_{68}P]^+$: 483.51, found 483.4919; MALDI-TOF-MS analysis in negative ion mode: *m/z* calcd for $[C_{47}H_{72}NO_{17}]^-$ 922.4806, found $[M-2H]^-$ 920.6147.

Supplementary Tables & Figures

Table S 1 Fungal strains used in this study. [a]Fungal Genetics Stock Center.

Strains	Genotype	Source	Catalog Number
Aspergillus fumigatus Af293	wild type	FGSC[a]	A1100
Aspergillus terreus NIH2624	wild type	FGSC[a]	A1156

Table S 2 List of Aspergillus fumigatus primers used in qRT-PCR analyses

Gene (Code)	Strand	Sequence 5´ – 3´
Afu4g03630 (*erg6*)	Forward	TGGACGAGTACTTCAAGCATTGGG
	Reverse	TAAAGATCCGTGGCCAGGTTGT
Afu7g03740 (*erg11B*)	Forward	GGTGCATTGGCGAGCAATTT
	Reverse	AGCGGTTTGGAGAACAGAGAAG
Afu3g10660 (*erg13*)	Forward	ACTGCGTGACTTGGATTACGA
	Reverse	TGGCCGTGTACATGTTACCA
Afu3g03500 (*mdr3*)	Forward	AAAGTACGGCACCAGTAGAGCA
	Reverse	GTAGTGGACGCAGGGAAGGAGATA
Afu3g07640 (*pma1*)	Forward	CGTGAGCTGGTCACTGGTGATATT
	Reverse	TTGAGGGTGTCATCGTTGGCA
Afu1g14550 (*sod3*)	Forward	GGTGGATATGTGGGAGCATGCTT
	Reverse	TGTCACCCGCTATGTACCGATTCT
Afu3g07930	Forward	ATCTCAAGCACACCAGTACGAC
	Reverse	GGGGACCATGATTTTGACGAAC
Afu1g17250 (*rodB*)	Forward	AAGTTCCTCGCTGTTGTCTCTC
	Reverse	GCATTGCTTGTTGAGGAGGT

Afu6g12340	Forward	CTGTCCAGCAATCCTGAATCCA
	Reverse	GGTTCCATCCACGGCTCTTTAT
Afu5g01970 (*gpdA*)	Forward	CTCTCCAACGCCTCTTGCA
	Reverse	CTTGTTGGAGGGAGCATCGA

Table S 3 Energies of the different complexes generated for the molecular dynamics simulations of this study. The aqueous solutions containing the ergosterol or cholesterol and amphotericin B (AmB) or cetylpyridiniym amphotericin B ([C16py][AmB]) were modelled using 1 sterol molecule and 2 AmB or [C_{16}py][AmB] molecules mixed with 4000 water molecules. Three different complexes (at least) were produced for each mixture. All simulations were performed as described in materials and methods. The most stable complex for each combination was chosen (bold). Low density initial configurations were randomly built using the packmol package, placing 10 complexes mixed with 10000 water molecules.

System	**Energy kJ/mol**	**Diff kJ/mol**
AmB + ergosterol – complex 1	-133619	3
AmB + ergosterol – complex 2	-133604	18
AmB + ergosterol – complex 3	**-133622**	**0**
AmB + ergosterol – complex 4	-133612	10
[C_{16}py][AmB] + ergosterol – complex 1	-133646	43
[C_{16}py][AmB] + ergosterol – complex 2	-133683	6
[C_{16}py][AmB] + ergosterol – complex 3	**-133689**	**0**
AmB + cholesterol – complex 1	**-133601**	**0**
AmB + cholesterol – complex 2	-133592	9
AmB + cholesterol – complex 3	-133593	8
[C_{16}py][AmB] + cholesterol – complex 1	**-133665**	**0**
[C_{16}py][AmB] + cholesterol – complex 2	-133650	15
[C_{16}py][AmB] + cholesterol – complex 3	-133653	12

Table S 4 Gene expression analysis (qRT-PCR) of amphotericin B-responsive genes in Aspergillus fumigatus after 4 or 24-hour exposure to amphotericin B (AmB), cholinium amphotericin B ([chol][Amb]), cetylpyridinium amphotericin B ([C_{16}py][AmB]) or trihexyltetradecylphosphonium amphotericin B ([$P_{6\,6\,6\,14}$][AmB]). Glyceraldehyde 3-phosphate dehydrogenase gene (gpdA) was used as internal control. Values represent the fold-change relative to the negative control followed by their standard deviation. Three biological replicates were performed. The asterisks mark significant differences in expression when compared to AmB for each exposure time (= p<0.05; ** = p<0.01, *** = p <0.001).*

	4 hours			
	AmB	**[chol][AmB]**	**[C_{16}py][AmB]**	**[$P_{6\,6\,6\,14}$][AmB]**
erg6	-2.81 ± 0.03	**-1.79 ± 0.08***	**-1.59 ± 0.09***	**1.74 ± 0.19*****
erg11B	-7.52 ± 0.01	**-8.99 ± 0.01***	**-3.98 ± 0.04***	**-2.88 ± 0.07***
erg13	-3.16 ± 0.04	**-1.89 ± 0.03****	**-1.71 ± 0.08***	**1.17 ± 0.08*****
mdr3	-3.19 ± 0.07	-2.06 ± 0.15	-2.56 ± 0.15	**1.40 ± 0.15*****
pma1	-3.05 ± 0.08	-3.03 ± 0.08	-2.12 ± 0.12	**1.14 ± 0.08*****
sod3	-15.14 ± 0.02	-19.80 ± 0.02	-14.91 ± 0.02	**-4.68 ± 0.02****
GST	-3.30 ± 0.05	-2.99 ± 0.08	-2.57 ± 0.08	**-1.09 ± 0.09*****
rodB	-7.91 ± 0.02	**-3.74 ± 0.06***	-4.98 ± 0.05	**-1.36 (± 0.13****
GTPase	-4.39 ± 0.04	-2.62 ± 0.07	-2.68 ± 0.11	**0.98 ± 0.18****

	24 hours			
	AmB	**[chol][AmB]**	**[C_{16}py][AmB]**	**[$P_{6\,6\,6\,14}$][AmB]**
erg6	1.29 ± 0.19	1.20 ± 0.06	1.36 ± 0.22	**2.63 ± 0.38****
erg11B	-1.63 ± 0.05	**-1.13 ± 0.08***	-1.79 ± 0.05	-1.22 ± 0.12
erg13	1.02 ± 0.14	-1.10 ± 0.04	-1.12 ± 0.19	**2.23 ± 0.58***
mdr3	5.49 ± 1.77	3.76 ± 0.95	4.84 ± 1.29	**25.75 ± 7.84***
pma1	-1.01 ± 0.15	1.12 ± 0.09	1.08 ± 0.09	**1.87 ± 0.15****
sod3	-2.34 ± 0.06	-1.91 ± 0.01	**-1.74 ± 0.01***	**-1.07 ± 0.03****

GST	1.15 ± 0.16	-1.09 ± 0.07	1.07 ± 0.19	**2.34 ± 0.69***
rodB	-1.26 ± 0.14	-1.25 ± 0.20	-2.00 ± 0.10	**-3.39 ± 0.10****
GTPase	1.70 ± 0.19	1.61 ± 0.10	1.45 ± 0.07	**3.84 ± 1.08***

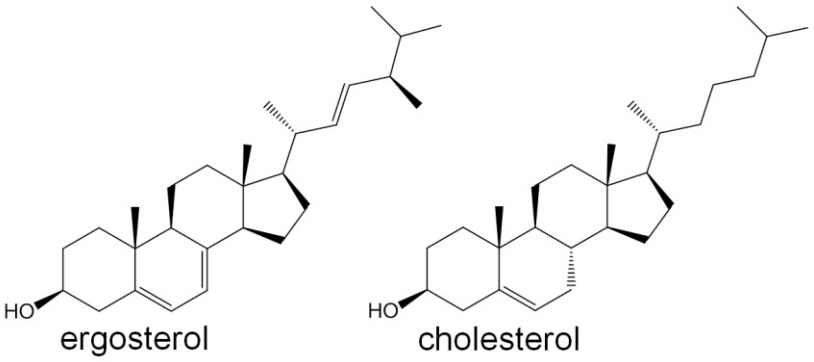

Figure S 1 The structure of ergosterol (main fungal sterol) and cholesterol (main animal sterol).

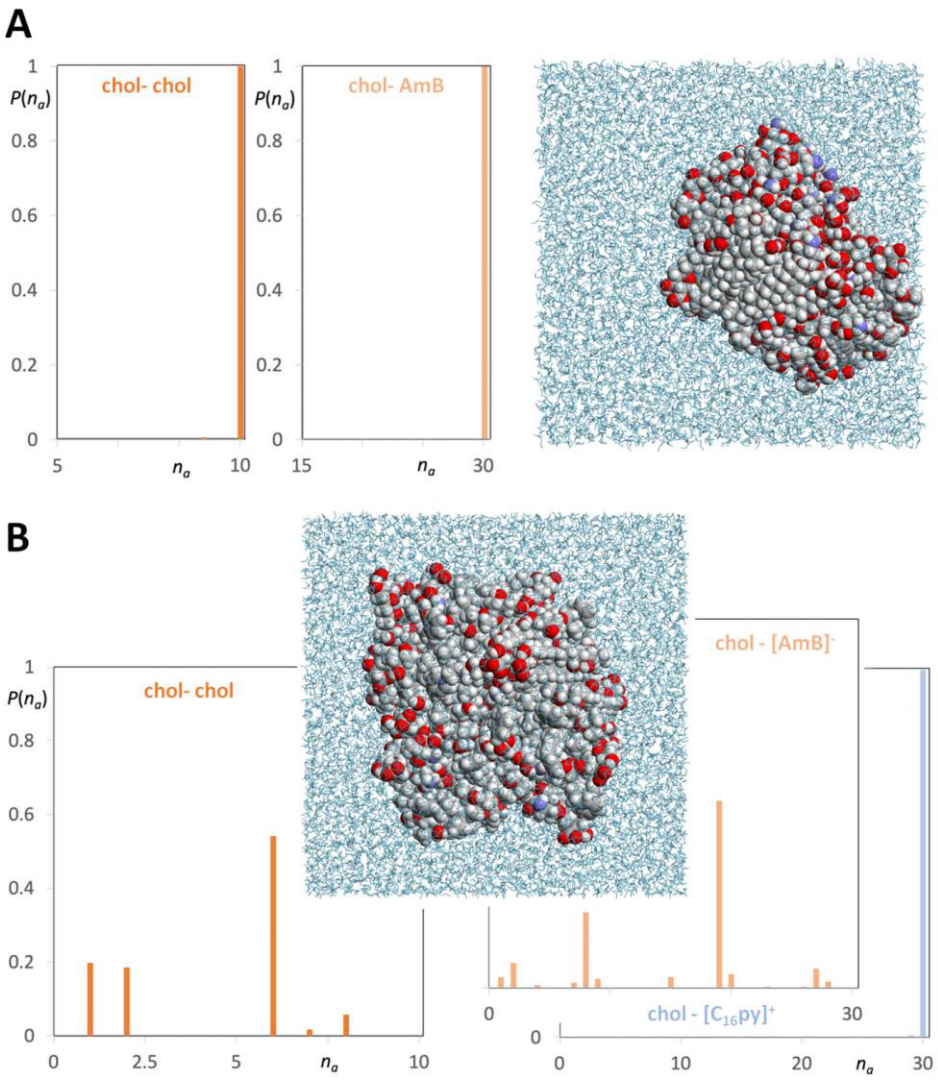

Figure S 2 Molecular dynamics simulation snapshots and discrete probability distribution functions of aggregate sizes ($P(n_a)$) for different aggregate types of cholesterol (chol), amphotericin B (AmB) and cetylpyridinium amphotericin B ([C_{16}py][AmB]). ***(A)*** *AmB–cholesterol simulations (dark orange graph: cholesterol clusters; light orange graph: cholesterol–AmB aggregates).* ***(B)*** *[C_{16}py][AmB]–cholesterol simulations (dark orange graph: cholesterol clusters; light orange graph: cholesterol–$[AmB]^-$ anion aggregates; blue graph: cholesterol–$[C_{16}py]^+$ cation aggregates).*

Chapter IV - Supplementary Information

Untargeted metabolomics shed light on the secondary metabolism of fungi triggered by choline-based ionic liquids

Supplementary Tables & Figures

Table S 1 Amino acid content analysis of A. nidulans, A. fumigatus and N. crassa crude extracts derived from cultures grown in media with or without (Neg) supplementation, choline chloride (ChoCl) or choline decanoate (ChoDec) at 50% or 80% of the MIC. Values depict the percentage (%) of each amino acid relative to the total amino acid amount, presented as Mean ± SD. ND – not detected; ACC - 1-aminocyclopropane-1-carboxylic acid; Aib - α-aminoisobutyric acid

	N. crassa		**A. fumigatus**			**A. nidulans**		
	Neg	**ChoCl**	**Neg**	**ChoDec 50%**	**ChoDec 80%**	**Neg**	**ChoCl 80%**	**ChoDec 80%**
ACC	1.3±0.6	7.0±1.1	0.5±0.2	0.3±0.3	0.2±0.2	0.1±0.1	0.2±0.1	0.9±0.3
Aib	0.3±0.4	0.1±0.0	3.8±4.8	3.9±4.2	11.4±15.1	0.1±0.1	0.2±0.1	1.4±0.5
Ala	20.2±5.8	28.7±1.7	24.7±12.1	17.5±9.5	16.5±10.8	31.8±1.6	29.3±4.4	8.5±3.9
Gly	3.7±2.5	0.9±0.2	9.4±7.8	1.9±1.3	4.2±5.0	21.7±8.0	31.8±6.6	20.0±4.5
Iso	6.1±2.1	3.8±3.2	0.5±0.9	ND	ND	0.5±0.7	ND	1.6±0.3
Leu	19.0±5.6	4.8±2.8	1.2±2.4	0.1±0.2	0.2±0.3	15.7±1.9	13.1±2.8	4.9±1.5
Met	ND	ND	2.3±2.6	0.8±1.0	1.2±2.0	ND	0.3±0.7	ND
Phe	0.1±0.2	0.5±0.0	1.0±0.9	3.2±1.8	2.2±1.3	1.4±1.1	0.5±0.3	4.2±1.9
Pro	ND	0.1±0.2	6.6±8.8	4.4±5.6	7.3±9.4	0.0±0.1	0.3±0.2	0.7±0.7
Val	38.8±10.7	51.0±3.9	4.6±2.8	2.5±2.6	4.0±3.1	18.7±2.9	18.9±1.0	12.9±5.2
Cys	1.5±2.1	ND	0.3±0.6	0.2±0.4	ND	ND	0.1±0.1	ND
Ser	1.9±1.5	0.6±0.2	3.4±5.6	1.3±1.7	1.0±1.7	1.2±0.6	0.3±0.3	6.2±2.4

Thr	ND	0.1±0.1	0.9±1.8	0.1±0.2	0.1±0.3	ND	ND	0.8±0.6
Tyr	3.8±0.2	1.5±0.1	27.2±9.9	24.1±9.0	21.3±12.2	6.7±3.7	3.6±2.6	24.9±12.7
Asp	2.0±1.0	0.6±0.2	10.1±5.0	39.7±12.5	30.0±5.9	1.8±0.7	0.9±0.1	9.3±0.7
Glu	1.0±1.2	0.4±0.2	2.3±4.6	0.0±0.1	0.3±0.6	0.3±0.4	0.2±0.2	3.4±0.6
Arg	0.3±0.4	0.1±0.1	0.7±1.5	ND	0.0±0.1	ND	0.2±0.5	0.4±0.2
His	ND	ND	0.1±0.3	ND	ND	ND	ND	ND
Lys	ND	ND	0.4±0.9	ND	ND	ND	ND	ND
	% peak area assigned to standards							
	35.9±7.4	54.0±5.7	67.6±9.0	70.6±5.4	69.1±6.1	93.1±2.8	95.7±1.3	73.0±4.3
	& peak area not assigned to standards							
	64.1±7.4	46.0±5.7	32.4±9.0	29.4±5.4	30.9±6.1	6.9±2.8	4.3±1.3	27.0±4.3

*Table S 2 Comparison of significant differences of MTT measurements from bacteria grown in the presence of different concentrations of the crude extracts from N. crassa and A. fumigatus cultures grown in media with or without (i.e. negative) supplementation. The one-way ANOVA test was performed to each condition relative to control (bacteria grown with no extract) and in the between different conditions at same concentration. * p ≤ 0.05 ** p ≤ 0.01 *** p ≤ 0.001 **** p ≤ 0.0001; ns p > 0.05. [a] ns, non-significant.*

Fungal Strain	Bacterial Strain	Condition *vs* control	*p*-value (One-way ANOVA test)	Condition vs negative	*p*-value (one-way ANOVA test)
N. crassa	*E. coli*	**ChoCl 80%**		**ChoCl 80%**	
		[1 mg·mL^{-1}]****	6,86E^{-8}	[1 mg·mL^{-1}]****	2,82E^{-11}
		[0.5 mg·mL^{-1}]****	2,69E^{-6}	[0.5 mg·mL^{-1}]****	2,50E^{-5}
		[0.25 mg·mL^{-1}]**	0,0021	[0.25 mg·mL^{-1}]**	0,0037
	S. aureus	**Negative control**			
		[1 mg/mL]**	0,00342		
		ChoCl 80%		**ChoCl 80%**	
		[1 mg·mL^{-1}]****	6,01E^{-6}	[1 mg·mL^{-1}]****	6,45E^{-9}
		[0.5 mg·mL^{-1}]****	6,04E^{-6}	[0.5 mg·mL^{-1}]****	9,30E^{-5}
		[0.25 mg·mL^{-1}]****	1,67E^{-5}	[0.25 mg·mL^{-1}]**	2,77E^{-9}
		[0.125 mg·mL^{-1}]**	0,0026	[0.125 mg·mL^{-1}]*	0,024
A. fumigatus	*E. coli*	**Negative Control**			
		[1 mg·mL^{-1}]****	1,02E^{-6}		
		[0.5 mg·mL^{-1}]****	1,59E^{-5}		
		[0.25 mg·mL^{-1}]***	1,78E^{-4}		
		[0.125 mg·mL^{-1}]**	0,0025		
		ChoDec 50%		**ChoDec 50%**	
		[1 mg·mL^{-1}]****	8,09E^{-5}	[1 mg·mL^{-1}]**	0,0095
		[0.5 mg·mL^{-1}]***	4,37E^{-4}		
		[0.25 mg·mL^{-1}L]**	0,0067		
		ChoDec 80%			
		[1 mg·mL^{-1}]****	7,29E^{-5}	**ChoDec 80%**	0,0026
		[0.5 mg·mL^{-1}]***	5,41E^{-4}	[1 mg·mL^{-1}]**	
		[0.25 mg·mL^{-1}]*	0,041		
	S. aureus	**Negative control**			
		[1 mg·mL^{-1}]***	6,05E^{-4}		
		[0.5 mg·mL^{-1}]**	0,0019		
		[0.25 mg·mL^{-1}]*	0,023		
		ChoDec 50%			
		[1 mg·mL^{-1}]***	2,81E^{-4}	ns	ns
		[0.5 mg·mL^{-1}]**	0,0013		
		[0.25 mg·mL^{-1}]*	0,019		
		ChoDec 80%			
		[1 mg·mL^{-1}]**	0,0039		
		[0.5 mg·mL^{-1}]*	0,019		

Table S 3 Accession hyperlinks for N. crassa and A. fumigatus jobs in GNPS platform, specifically Molecular networking and in silico DEREPLICATOR+ tool.

	Link
A. fumigatus	Molecular network: https://gnps.ucsd.edu/ProteoSAFe/status.jsp?task=3ad96b8f862649f7b093b108c1b830d6
	DEREPLICATOR+: https://gnps.ucsd.edu/ProteoSAFe/status.jsp?task=e4fc67fa7f934ef59f641332e29d51b0
N. crassa	Molecular network: https://gnps.ucsd.edu/ProteoSAFe/status.jsp?task=90a9e46b3366476da0c0be310bec167a
	DEREPLICATOR+: https://gnps.ucsd.edu/ProteoSAFe/status.jsp?task=f2c4cc99f6514113afccf8655c3b34e0

Table S 4 Putative identifications retrieved by using molecular networking analysis and compound dereplication in GNPS, from spectral match (*) and in silico tool DEREPLICATOR+. For N. crassa, isolated fractions (G1, G2 and G3) as well as crude (G4) extracts, whereas for A. fumigatus, extracts from cultures supplemented with Choline Decanoate at 50% (G1) and 80% (G2) of the MIC were analyzed. GIn house library from GNPS

Putative identification	RT (sec)	Exact mass	m/z found	Adduct	Class	Reported activity
Aspergillus fumigatus						
Antibiotic A 59770A[1]	2334	1000.63	501.321	M+2H	Macrolide	Pesticidal
Dolabelide C[2]	4340.22	796.497	797.508	M+H	Macrolide	Antitumor
Roflamycoin[3,4]	3104.03	738.455	370.236	M+2H	Macrolide	Antifungal; antiprotozoaric
Brasilionolide B[5]	4159.99	1180.7	591.356	M+2H	Macrolide	Antifungal
Efomycin G[6–8]	1878.16	1010.58	506.297	M+2H	Macrolide	Antibacterial; antitumor
Karlotoxin 3[9]	3807.66	1324.85	663.43	M+2H	Polyketide	Hemolytic
Aeruclynamide D[10]	2809.06	603.06	604.774	M+OH	Cyclohexa-peptide	Antiparasite
Dihydroxylycopene diglucoside diester[11]	1101.17	790.538	396.275	M+2H	Carotenoids	Not reported
Leukotriene E4 methyl ester*[12]	3872.23	459.22	459.313	M+H	Eicosanoid	Immunomodulation

Soyasapogenol A[13,14]	1657.02	475.378	474.339	M+H	Triterpenoid	Antitumor
Xanthomonic acid[15]	1266.77	468.31	467.312	M+H	Terpenoid	Antitumor
7α,27-Dihydroxycholesterol*[16]	787.783	401.342	399.367	M+H-H2O	Steroid	Not reported
9-(Z)-Octadecenamide[17,18]	3893.79	563.55	563.325	2M+H	Fatty acid	Hypolipidemic; antibacterial; antifungal
13-(Z)-Docosenamide[18]	1371.23	338.34	339.24	M+H	Fatty acid	Antifungal; antibacterial
Auriculoside B[19]	2807	1214.64	608.328	M+2H	Pregnane glycoside	Antitumor
CID 102041441[20]	3361.29	810.477	406.244	M+2H	Pregnane glycoside	Not reported
Otophylloside B[21]	4153.65	922.529	462.27	M+2H	Pregnane glycoside	Antiepiletic
Fosinopril[22]	2757.34	564.308	564.331	M+H	Synthetic compound	Angiotensin-converting enzyme inhibitor
Neurospora crassa						
Amphoteronolide B[23]	894.328	778.414	390.212	M+2H	Macrolide	Not reported
Marinisporolide B[24]	3025.43	692.414	347.216	M+2H	Macrolide	Not reported

Aldgamycin K[25]	1667.11	696.367	349.19	M+2H	Macrolide	Antibacterial (*S.aureus*)
Levorin A0[26]	1371.81	1110.59	556.301	M+2H	Macrolide	Not reported
Levorin A3[27,28]	3210.69	1092.58	547.296	M+2H	Macrolide	Antifungal
Antibiotic A 59770A[1]	2334	1000.63	501.321	M+2H	Macrolide	Pesticidal
Spinosyn D[29]	2679	618	31.198	M+2H	Macrolide	Pesticidal
Dideoxy-Sandramycin[30]	1806.18	1188.56	595.289	M+2H	Cyclic depsipeptide	Antitumor
Myxochromide S2[31]	2679.72	736.416	369.216	M+2H	Cyclic depsipeptide	Not reported
Discokiolide A[32]	1682.41	1026.51	514.263	M+2H	Cyclic depsipeptide	Antitumor
Chaiyaphumine D[33]	3385.91	644.296	645.3	M+H	Cyclic depsipeptide	Not reported
Chlorodestruxin[34]	1524.11	629.319	315.666	M+2H	Cyclic depsipeptide	Anti-insecticidal
Virginiamycin S2[35]	1396.4	811.354	812.36	M+H	Cyclic depsipeptide	Antibacterial
SF-1902-A4[36]	4248.2	667.452	334.735	M+2H	Cyclic lipo-depsipeptide	Antibacterial

SCH-378199[37]	3062.28	562.819	562.885	M+2H	Depsipeptide	Not reported
Syringostatin A[38]	1259.88	1178.59	590.3	M+2H	Cyclic lipo-depsipeptide	Antifungal
Val-Val-Pro-Val-Pro-Asn*[G]	1797.39	651.396	326.705	M+2H	Peptide	Not reported
Actinomycin C2[39]	2184.16	1284.64	643.329	M+2H	Peptide	Not reported
Annosquamosin A[40]	803.485	848.41	425.212	M+2H	Peptide	Not reported
Pepsin S 735A[41,42]	4211.02	685.463	343.737	M+2H	Peptide	Protease inhibitor
Actinomycin F4[43]	3819.11	1256.64	629.327	M+2H	Peptide	Not reported
Keramamide A[44]	966.764	942.441	472.228	M+2H	Peptide	Not reported
Desferrioxamine X5[45]	920.406	598.369	300.193	M+2H	Peptide	Not reported
Halo-toxin[46]	2558.88	626.343	314.178	M+2H	Peptide	Not reported
API II/AgrD2[47]	2175.6	744.348	373.181	M+2H	Peptide	Autoinducing peptide
Antamanide*[48,49]	3397	573.85	573.5	M+2H	Peptide	Antidote
Fru-Leu-Ile*[G]	1087.43	407.239	407.192	M+H	Peptide	Not reported
Ile-Pro-Ile*[G]	1554.93	342.239	342.266	M+H	Peptide	Not reported
Mollamide B[50]	1667.11	696.367	349.19	M+2H	Cyclic peptide	Antimalarial, antivirus, antitumor
Wewakazole[51,52]	3484.76	1140.54	571.278	M+2H	Cyclic peptide	Antitumor

Cycloreticulin B[53]	3439.96	834.395	418.204	M+2H	Cyclic peptide	Not reported-
Pseudostellarin C[54]	725.799	812.443	407.23	M+2H	Cyclic peptide	Tyrosinase inhibitor; antitumor
L-Tryptophan[G]	1091.51	204.09	409.17	2M+H	Amino acid	Building block
Pregn-5-ene-3,8,11,12,14,20-hexol, 9Cl, 11-Ac,3-O-dig-dig-cym-ole	3117.61	1000.56	501.28	M+2H	Terpene glycoside	Not found
3,12,14,17-Tetrahydroxypregn-5-en-20-one, 12-Ac,3-O-ole-can-ole	2908.46	824.456	413.233	M+2H	Terpene glycoside	Not found
3,16-Dihydroxycucurbita-5,20(22)-diene-11,24-dione, 3-O-xyl-rham	3337.38	748.44	375.225	M+2H	Terpene glycoside	Not found
3,11,14-Trihydroxycard-20(22)-enolide, 3-O-dig-dig	3034.65	678.398	340.207	M+2H	Terpene glycoside	Not found
Periplocoside M[55]	2798.55	604.361	303.189	M+2H	Terpene glycoside	Not reported
Stauntoside K[56]	3029.26	762.419	382.215	M+2H	Terpene glycoside	Not reported

Batatoside A[57]	4929.79	1268.66	635.335	M+2H	Terpene glycoside	Not reported
Orizabin XIV[58]	4948.15	1120.6	561.308	M+2H	Glycolipid	Antitumor; β-1-3-glucan synthase inhbitor; antibacterial
Sublanceoside K1[59]	4950.56	1082.57	542.29	M+2H	Terpene glycoside	Not reported
Tuberoside h2[60]	2759	780.43	391.222	M+2H	Terpene glycoside	Not reported
CID 102041441[20]	3361.29	810.477	406.244	M+2H	Terpene glycoside	Not reported
Hirundigoside D[61]	3154.49	978.525	490.272	M+2H	Terpene glycoside	Anti-inflammatory
Lentinan[62]	876.36	1134.37	1135.38	M+H	Glycoside	Not reported
Eutypellacytosporin B[63]	3044.43	714.398	358.204	M+2H	Terpene	Not reported
Hoyacarnoside A[64]	3126.63	956.534	479.274	M+2H	Terpene	Not reported
Betamethasone*[65]	3343.06	393.208	391.212	M+H	Terpene	Not reported
Corticosterone*[66]	4894.41	347.222	347.215	M+H	Terpene	Not reported
Progesterone[67]	916.55	315.232	313.852	M+H	Terpene	Not reported
Leukotriene E4 methyl ester*[12]	3872.23	459.22	459.313	M+H	Eicosanoid	Immunomudulation

Table S5 Putative identifications retrieved by the NRPro tool for N. crassa most intense MS/MS spectra obtained for the fractions G1, G2 and G3.

Putative identification	RT (sec)	Exact mass	m/z found	Class	Reported activity	Special amino acid	*p*-value
Fraction G1							
Guangomide A[68]	1094.38	618.326	310.165	Cyclodepsi-peptide	Weakly antibacterial	LNMeAla and D-NMePhe	6.20E-5
Cyclo(Leu-Ser-Glu-Thr-Thr-D-Leu)	1379.11	644.338	323.184	cyclic peptide	Not reported	D-leucine	1.07E-4
Arbumelin[69]	1775.52	909.460	455.731	cyclic peptide	Not reported	D-amino acids	0.019
Fraction G2							
Cyclotheonamide E3[70]	2894.53	857.4874	413.241	cyclic peptide	Serine protease inhibitor	D-alloisoleucine	0.004
Nostophycin[71,72]	1680.82	888.474	445.247	cyclic peptide	Weakly cytotoxic; antimicrobial	novel amino acid Ahoa	0.008

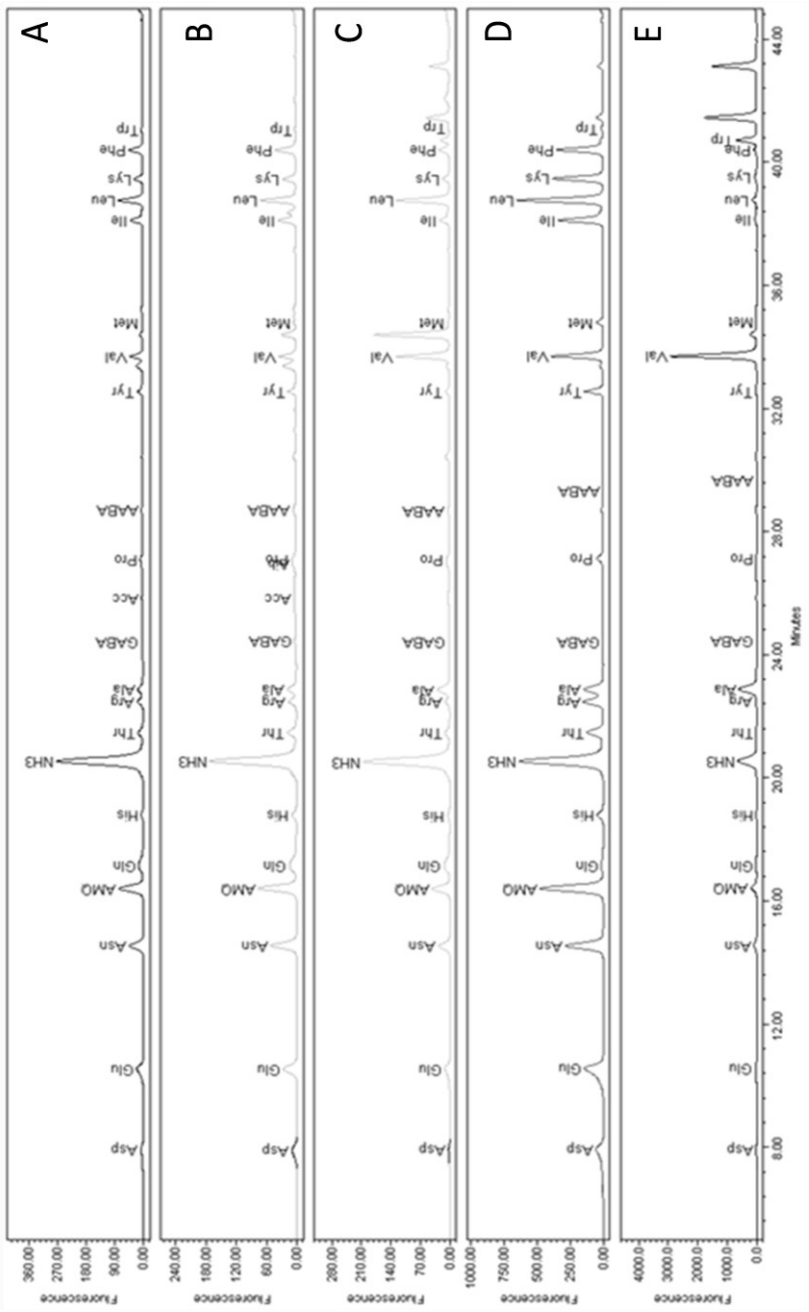

Figure S1 Chromatographic analyses of hydrolysates of the fractions obtained from the N. crassa crude extract derived from cultures grown in media containing the Choline chloride supplement, and collected at retention times of A) 15.6, B) 17.3, C) 19.6, D) 29.7 and E) 33.6 minutes.

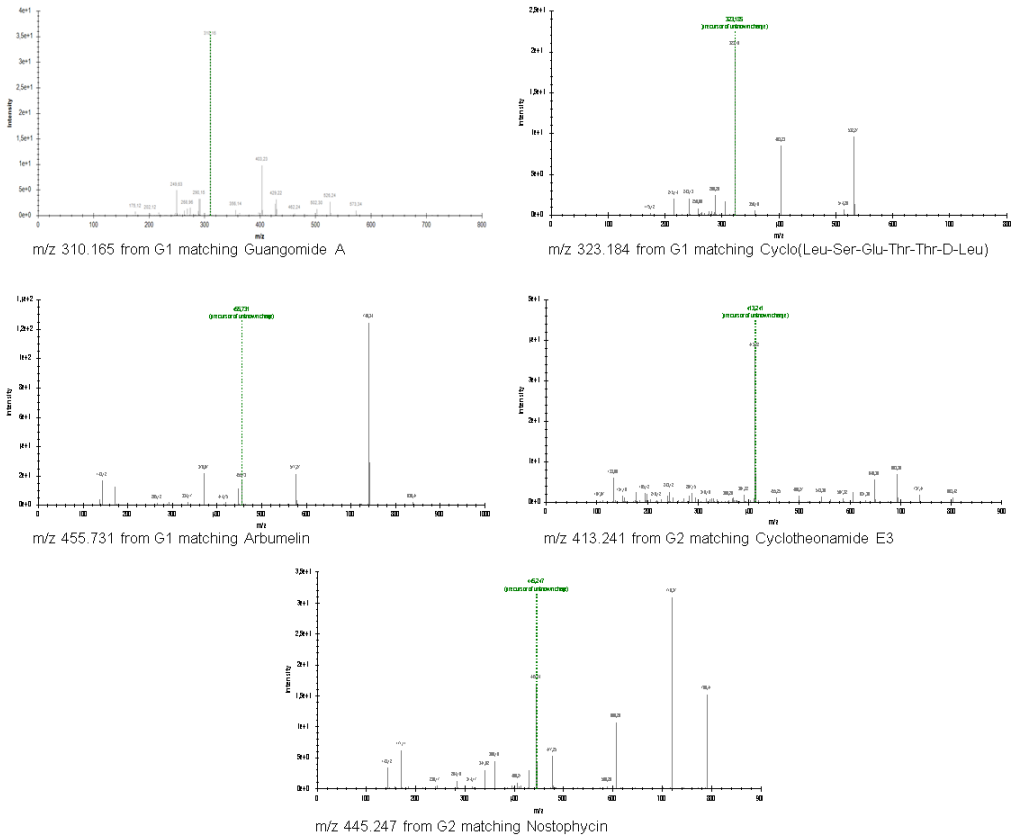

Figure S2 Spectra matching the putative identification matches found in the NRPro.

References

1. Hoehn, M. M., Michel, K. H. & Yao, R. C.-F. Europaisches Patentamt European Patent Office. (1990).
2. Suenaga, K., Nagoya, T., Shibata, T., Kigoshi, H. & Yamada, K. Dolabelides C and D, cytotoxic macrolides isolated from the sea hare Dolabella auricularia. *J. Nat. Prod.* **60**, 155–157 (1997).
3. Schlegel, R. & Thrum, H. A new polyene antibiotic, flavomycoin structural investigations. I. *J. Antibiot. (Tokyo).* **24**, 360–367 (1971).
4. Han, X. *et al.* Identification and Predictions Regarding the Biosynthesis Pathway of Polyene Macrolides Produced by Streptomyces roseoflavus Men-myco-93-63. *Appl. Environ. Microbiol.*

87, 1–13 (2021).

5. Chiu, H. T., Weng, C. P., Lin, Y. C. & Chen, K. H. Target-specific identification and characterization of the putative gene cluster for brasilinolide biosynthesis revealing the mechanistic insights and combinatorial synthetic utility of 2-deoxy-l-fucose biosynthetic enzymes. *Org. Biomol. Chem.* **14**, 1988–2006 (2016).
6. Supong, K. *et al.* Antimicrobial compounds from endophytic Streptomyces sp. BCC72023 isolated from rice (Oryza sativa L.). *Res. Microbiol.* **167**, 290–298 (2016).
7. Gui, M., Zhang, M. xue, Wu, W. hui & Sun, P. Natural occurrence, bioactivity and biosynthesis of elaiophylin analogues. *Molecules* **24**, 3840 (2019).
8. Wu, C. *et al.* Identification of elaiophylin derivatives from the marine-derived actinomycete Streptomyces sp. 7-145 using PCR-based screening. *J. Nat. Prod.* **76**, 2153–2157 (2013).
9. Van Wagoner, R. M. *et al.* Structure and relative potency of several karlotoxins from Karlodinium veneficum. *J. Nat. Prod.* **73**, 1360–1365 (2010).
10. Portmann, C. *et al.* Isolation of aerucyclamides C and D and structure revision of microcyclamide 7806A: Heterocyclic ribosomal peptides from Microcystis aeruginosa PCC 7806 and their antiparasite evaluation. *J. Nat. Prod.* **71**, 1891–1896 (2008).
11. Takaichi, S., Maoka, T., Hanada, S. & Imhoff, J. F. Dihydroxylycopene diglucoside diesters: A novel class of carotenoids from the phototrophic purple sulfur bacteria Halorhodospira abdelmalekii and Halorhodospira halochloris. *Arch. Microbiol.* **175**, 161–167 (2001).
12. Cohen, N. *et al.* Enantiospecific Syntheses of Leukotrienes C4, D4, and E4 and [14,15-3 H2]Leukotriene E4 Dimethyl Ester. *J. Am. Chem. Soc.* **105**, 3661–3672 (1983).

13. Kitagawa, I., Saito, M., Taniyama, T. & Yoshkawa, M. Saponin and Sapogenol. XXXVIII.1) Structure of Soyasaponin A2, a Bisdesmoside of Soyasapogenol A, from Soybean, the Seeds of Glycine max Merrill. *Chem. Pharm. Bull.* **33**, 598–608 (1985).
14. Zhang, W. & Popovich, D. G. Effect of soyasapogenol A and soyasapogenol B concentrated extracts on Hep-G2 cell proliferation and apoptosis. *J. Agric. Food Chem.* **56**, 2603–2608 (2008).
15. Saleh, H. *et al.* Deuterium-Labeled Precursor Feeding Reveals a New pABA-Containing Meroterpenoid from the Mango Pathogen Xanthomonas citri pv. mangiferaeindicae. *J. Nat. Prod.* **79**, 1532–1537 (2016).
16. Brown, A. J. & Jessup, W. Oxysterols and atherosclerosis. *Atherosclerosis* **142**, 1–28 (1999).
17. Cheng, M. C. *et al.* Chemical synthesis of 9(Z)-octadecenamide and its hypolipidemic effect: A bioactive agent found in the essential oil of mountain celery seeds. *J. Agric. Food Chem.* **58**, 1502–1508 (2010).
18. dos Reis, C. M. *et al.* Antifungal and antibacterial activity of extracts produced from Diaporthe schini. *J. Biotechnol.* **294**, 30–37 (2019).
19. Teng, H. L., Lu, Y., Li, J., Yang, G. Z. & Mei, Z. N. Two new steroidal glycosides from the root of Cynanchum auriculatum. *Chinese Chem. Lett.* **22**, 77–80 (2011).
20. Deng, Y. R., Wei, Y. P., Yin, F., Yang, H. & Wang, Y. A new cardenolide and two new pregnane glycosides from the root barks of Periploca sepium. *Helv. Chim. Acta* **93**, 1602–1609 (2010).
21. Yang, J. *et al.* Otophylloside B Protects Against Aβ Toxicity in Caenorhabditis elegans Models of Alzheimer's Disease. *Nat. Products Bioprospect.* **7**, 207–214 (2017).
22. Sica, D. A., Gehr, T. W. B., Kelleher, N. & Blumenthal, M. Fosinopril: Emerging considerations and implications for angiotensin-converting

enzyme inhibitor therapy. *Cardiovasc. Drug Rev.* **16**, 319–345 (1998).

23. MASAMUNE, S. Amphotericin B: Synthesis of Its Aglycone (Amphoteronolide B) and Degradation. *Ann. N. Y. Acad. Sci.* **544**, 168–179 (1988).
24. Kwon, H. C., Kauffman, C. A., Jensen, P. R. & Fenical, W. Marinisporolides, polyene-polyol macrolides from a marine actinomycete of the new genus marinispora. *J. Org. Chem.* **74**, 675–684 (2009).
25. Wang, C. X. *et al.* Aldgamycins J-O, 16-membered macrolides with a branched octose unit from streptomycetes sp. and their antibacterial activities. *J. Nat. Prod.* **79**, 2446–2454 (2016).
26. Szwarc, K., Szczeblewski, P., Sowiński, P., Borowski, E. & Pawlak, J. The structure, including stereochemistry, of levorin A1. *Magn. Reson. Chem.* **53**, 479–484 (2015).
27. Pawlak, J., Sowinski, P., Bieszczad, T. & Borowski, E. Structure of Levorin A3, a Minor Component of Levorin Complex. *ChemInform* **37**, 1667–1672 (2006).
28. Szczeblewski, P. *et al.* Analytical studies on ascosin, candicidin and levorin multicomponent antifungal antibiotic complexes. the stereostructure of ascosin A2. *Sci. Rep.* **7**, 40158 (2017).
29. Oliver, M. P., Crouse, G. D., Demeter, D. A. & Sparks, T. C. Synthesis and Insecticidal Activity of Spinosyns with C9-O-Benzyl Bioisosteres in Place of the 2',3',4'-Tri-O-methyl Rhamnose. *J. Agric. Food Chem.* **63**, 5571–5577 (2015).
30. Boger, D. L. & Chen, J. H. An exceptionally potent analog of sandramycin. *Bioorganic Med. Chem. Lett.* **7**, 919–922 (1997).
31. Wenzel, S. C. *et al.* Structure and biosynthesis of myxochromides S1-3 in Stigmatella aurantiaca: Evidence for an iterative bacterial type I polyketide synthase and for module skipping in nonribosomal peptide

biosynthesis. *ChemBioChem* **6**, 375–385 (2005).

32. Tada, H., Tozyo, T., Terui, Y. & Hayashi, F. Discokiolides. Cytotoxic Cyclic Depsipeptides from the Marine Sponge Discodermia kiiensis. *Chem. Lett.* **21**, 431–434 (1992).
33. Grundmann, F. *et al.* Antiparasitic chaiyaphumines from entomopathogenic xenorhabdus sp. PB61.4. *J. Nat. Prod.* **77**, 779–783 (2014).
34. Gupta, S., Roberts, D. W. & Renwick, J. A. A. Insecticidal cyclodepsipeptides from Metarhizium anisopliae. *J. Chem. Soc. Perkin Trans. 1* 2347 (1989). doi:10.1039/p19890002347
35. Mukhtar, T. A. & Wright, G. D. Streptogramins, oxazolidinones, and other inhibitors of bacterial protein synthesis. *Chem. Rev.* **105**, 529–542 (2005).
36. Omoto, S., Ogino, H. & Inouye, S. Studies On SF-1902 A2~A5, minor components of SF-1902 (GLOBOMYCIN). *J. Antibiot. (Tokyo).* **34**, 1416–1423 (1981).
37. Hegde, V. R. *et al.* A family of depsi-peptide fungal metabolites, as selective and competitive human tachykinin receptor (NK2) antagonists: Fermentation, isolation, physico-chemical properties, and biological activity. *J. Antibiot. (Tokyo).* **54**, 125–135 (2001).
38. Sorensen, K. N., Kim, K. H. & Takemoto, J. Y. In vitro antifungal and fungicidal activities and erythrocyte toxicities of cyclic lipodepsinonapeptides produced by Pseudomonas syringae pv. syringae? *Antimicrob. Agents Chemother.* **40**, 2710–2713 (1996).
39. Nam, J. Y. *et al.* Actinomycin D, C2 and VII, inhibitors of Grb2-Shc interaction produced by Streptomyces. *Bioorganic Med. Chem. Lett.* **8**, 2001–2002 (1998).
40. Li, X., Chen, X. L., Chen, J. W. & Sun, D. D. Annonaceous acetogenins from the seeds of Annona squamosa. *Chem. Nat.*

Compd. **46**, 101–105 (2010).

41. Morishima, H., Takita, T., Aoyagi, T., Takeuchi, T. & Umezawa, H. The structure of pepstatin. *J. Antibiot. (Tokyo).* **23**, 263–265 (1970).
42. Omura, S. *et al.* Ahpatinins, new acid protease inhibitors containing 4-amino-3-hydroxy-5-phenylpentanoic acid. *J. Antibiot. (Tokyo).* **39**, 1079–1085 (1986).
43. Kanchanasin, P. *et al.* Actinomycins produced by streptomyces lichenis lcr6-01t and its antibacterial activity. *Chiang Mai J. Sci.* **47**, 864–871 (2020).
44. Kobayashi, J. *et al.* Keramamide A, a novel peptide from the okinawan marine sponge theonella sp. *J. Chem. Soc. Perkin Trans. 1* 2609–2611 (1991). doi:10.1039/p19910002609
45. Konetschny-Rapp, S., Jung, G., Raymond, K. N., Meiwes, J. & Zähner, H. Solution Thermodynamics of the Ferric Complexes of New Desferrioxamine Siderophores Obtained by Directed Fermentation. *J. Am. Chem. Soc.* **114**, 2224–2230 (1992).
46. Kajimoto, T. *et al.* Structure of Halo-toxin Produced by Phytopathogenic Bacterium, Pseudomonas syringae pv. mori. *Chem. Lett.* **18**, 679–680 (1989).
47. M., C. C. *et al.* Regulation of Neurotoxin Production and Sporulation by a Putative agrBD Signaling System in Proteolytic Clostridium botulinum. *Appl. Environ. Microbiol.* **76**, 4448–4460 (2010).
48. Wieland, T. *et al.* The Discovery, Isolation, Elucidation of Structure, and Synthesis of Antamanide. *Angew. Chemie Int. Ed. English* **7**, 204–208 (1968).
49. Azzolin, L. *et al.* Antamanide, a derivative of amanita phalloides, is a novel inhibitor of the mitochondrial permeability transition pore. *PLoS One* **6**, e16280 (2011).
50. Donia, M. S. *et al.* Mollamides B and C, cyclic hexapeptides from the

indonesian tunicate Didemnum molle. *J. Nat. Prod.* **71**, 941–945 (2008).

51. Gogineni, V. & Hamann, M. T. Marine natural product peptides with therapeutic potential: Chemistry, biosynthesis, and pharmacology. *Biochimica et Biophysica Acta - General Subjects* **1862**, 81–196 (2018).
52. Nogle, L. M., Marquez, B. L. & Gerwick, W. H. Wewakazole, a novel cyclic dodecapeptide from a papua new guinea Lyngbya majuscula. *Org. Lett.* **5**, 3–6 (2003).
53. Wélé, A. *et al.* Sequence and three-dimensional structure of cycloreticulins A and B, new cyclooctapeptides from the seeds of Annona reticulata. *Tetrahedron* **64**, 154–162 (2008).
54. Morita, H. *et al.* Pseudostellarins A - C, new tyrosinase inhibitory cyclic peptides from Pseudostellaria heterophylla. *Tetrahedron* **50**, 6797–6804 (1994).
55. Itokawa, H., Xu, J. & Takeya, K. Studies on Chemical Constituents of Antitumor Fraction from Periploca sepium. IV. Structures of New Pregnane Glycosides, Periplocosides D, E, L, and M. *Chem. Pharm. Bull.* **36**, 2084–2089 (1988).
56. Yu, J. Q., Deng, A. J. & Qin, H. L. Nine new steroidal glycosides from the roots of Cynanchum stauntonii. *Steroids* **78**, 79–90 (2013).
57. Yin, Y., Li, Y. & Kong, L. Pentasaccharide glycosides from the tubers of sweet potato (Ipomoea batatas). *J. Agric. Food Chem.* **56**, 2363–2368 (2008).
58. Pereda-Miranda, R. & Hernández-Carlos, B. HPLC Isolation and structural elucidation of diastereomeric niloyl ester tetrasaccharides from Mexican scammony root. *Tetrahedron* **58**, 3145–3154 (2002).
59. Warashina, T. & Noro, T. Glycosides of 14,15-seco and 13,14:14,15-disecopregnanes from the roots of Cynanchum sublanceolatum.

Chem. Pharm. Bull. **54**, 1551–1560 (2006).

60. Warashina, T., Umehara, K., Miyase, T. & Noro, T. 8,12;8,20-Diepoxy-8,14-secopregnane glycosides from roots of Asclepias tuberosa and their effect on proliferation of human skin fibroblasts. *Phytochemistry* **72**, 1865–1875 (2011).
61. Lai, C. Z. *et al.* Hirundigenin type C21 steroidal glycosides from Cynanchum stauntonii and their anti-inflammatory activity. *RSC Adv.* **6**, 59257–59268 (2016).
62. Zong, A., Cao, H. & Wang, F. Anticancer polysaccharides from natural resources: A review of recent research. *Carbohydrate Polymers* **90**, 1395–1410 (2012).
63. Zhang, Y.-X. *et al.* Eutypellacytosporins A–D, Meroterpenoids from the Arctic Fungus Eutypella sp. D-1. *J. Nat. Prod.* **82**, 3089–3095 (2019).
64. Abe, F. *et al.* Pregnanes and pregnane glycosides from Hoya carnosa. *Chem. Pharm. Bull.* **47**, 1128–1133 (1999).
65. Takeoka, G., Dao, L., Wong, R. Y., Lundin, R. & Mahoney, N. Identification of benzethonium chloride in commercial grapefruit seed extracts. *J. Agric. Food Chem.* **49**, 3316–3320 (2001).
66. Steiger, M. & Reichstein, T. Chemical structure of corticosterone [6]. *Nature* **141**, 202 (1938).
67. Salhanick, H. A., Noall, M. W., Zarrow, M. X. & Samuels, L. T. The isolation of progesterone from human placentae. *Science (80-.).* **115**, 708–709 (1952).
68. Sy-Cordero, A. A. *et al.* Cyclodepsipeptides, sesquiterpenoids, and other cytotoxic metabolites from the filamentous fungus Trichothecium sp. (MSX 51320). *J. Nat. Prod.* **74**, 2137–2142 (2011).
69. Mao, X. M. *et al.* Epigenetic genome mining of an endophytic fungus leads to the pleiotropic biosynthesis of natural products. *Angew.*

Chemie - Int. Ed. **54**, 7592–7596 (2015).

70. Maryanoff, B. E. *et al.* Molecular basis for the inhibition of human α-thrombin by the macrocyclic peptide cyclotheonamide A. *Proc. Natl. Acad. Sci. U. S. A.* **90**, 8048–8052 (1993).
71. Fujii, K., Sivonen, K., Kashiwagi, T., Hirayama, K. & Harada, K. I. Nostophycin, a novel cyclic peptide from the toxic Cyanobacterium Nostoc sp. 152. *J. Org. Chem.* **64**, 5777–5782 (1999).
72. Gupta, V. & Vyas, D. Antimicrobial effect of a cyclic peptide Nostophycin isolated from wastewater cyanobacteria, Nostoc calcicola. *Curr. Bot.* **12**, 94–101 (2021).

ITQB NOVA, Avenida da República, 2780-157 Oeiras, Portugal | Tel +351 214 469 100 | itqb.unl.pt